frontiers | Research Topics

Molecular and cytogenetic research advances in human reproduction

Edited by
Ihtisham Bukhari, Shi Qinghua and Rick Francis Thorne

Published in
Frontiers in Endocrinology
Frontiers in Physiology

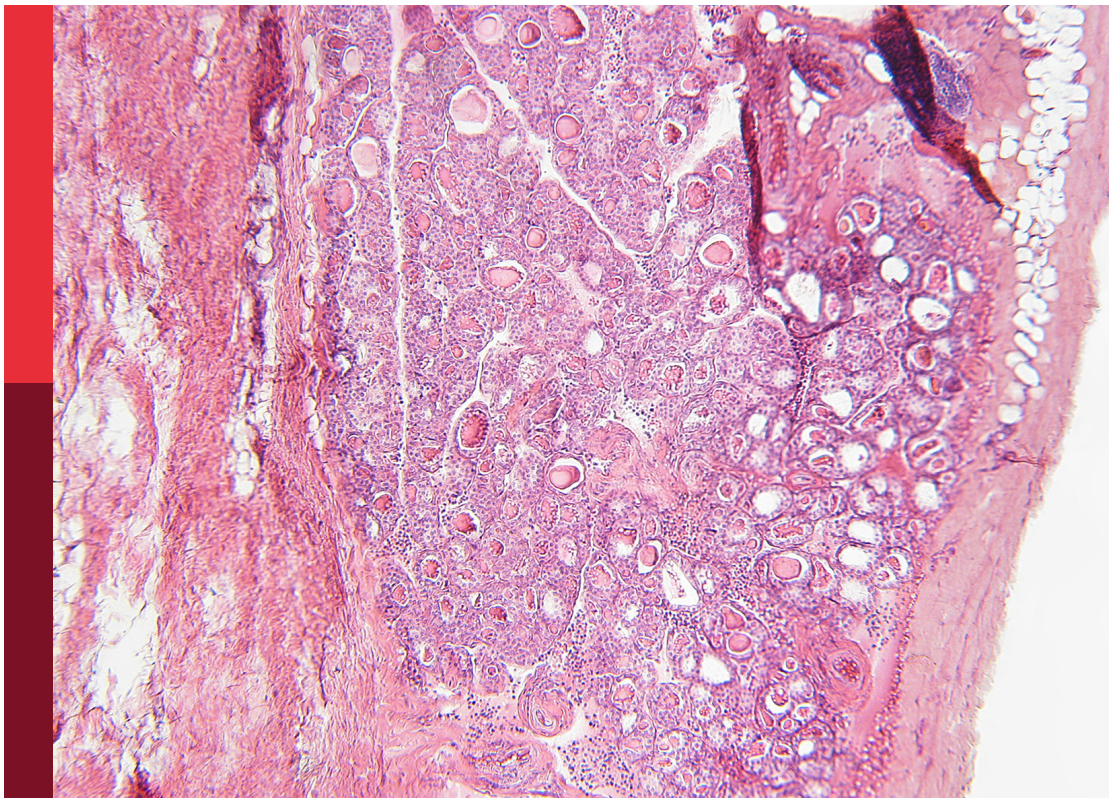

FRONTIERS EBOOK COPYRIGHT STATEMENT

The copyright in the text of individual articles in this ebook is the property of their respective authors or their respective institutions or funders. The copyright in graphics and images within each article may be subject to copyright of other parties. In both cases this is subject to a license granted to Frontiers.

The compilation of articles constituting this ebook is the property of Frontiers.

Each article within this ebook, and the ebook itself, are published under the most recent version of the Creative Commons CC-BY licence. The version current at the date of publication of this ebook is CC-BY 4.0. If the CC-BY licence is updated, the licence granted by Frontiers is automatically updated to the new version.

When exercising any right under the CC-BY licence, Frontiers must be attributed as the original publisher of the article or ebook, as applicable.

Authors have the responsibility of ensuring that any graphics or other materials which are the property of others may be included in the CC-BY licence, but this should be checked before relying on the CC-BY licence to reproduce those materials. Any copyright notices relating to those materials must be complied with.

Copyright and source acknowledgement notices may not be removed and must be displayed in any copy, derivative work or partial copy which includes the elements in question.

All copyright, and all rights therein, are protected by national and international copyright laws. The above represents a summary only. For further information please read Frontiers' Conditions for Website Use and Copyright Statement, and the applicable CC-BY licence.

ISSN 1664-8714
ISBN 978-2-8325-3486-1
DOI 10.3389/978-2-8325-3486-1

About Frontiers

Frontiers is more than just an open access publisher of scholarly articles: it is a pioneering approach to the world of academia, radically improving the way scholarly research is managed. The grand vision of Frontiers is a world where all people have an equal opportunity to seek, share and generate knowledge. Frontiers provides immediate and permanent online open access to all its publications, but this alone is not enough to realize our grand goals.

Frontiers journal series

The Frontiers journal series is a multi-tier and interdisciplinary set of open-access, online journals, promising a paradigm shift from the current review, selection and dissemination processes in academic publishing. All Frontiers journals are driven by researchers for researchers; therefore, they constitute a service to the scholarly community. At the same time, the *Frontiers journal series* operates on a revolutionary invention, the tiered publishing system, initially addressing specific communities of scholars, and gradually climbing up to broader public understanding, thus serving the interests of the lay society, too.

Dedication to quality

Each Frontiers article is a landmark of the highest quality, thanks to genuinely collaborative interactions between authors and review editors, who include some of the world's best academicians. Research must be certified by peers before entering a stream of knowledge that may eventually reach the public - and shape society; therefore, Frontiers only applies the most rigorous and unbiased reviews. Frontiers revolutionizes research publishing by freely delivering the most outstanding research, evaluated with no bias from both the academic and social point of view. By applying the most advanced information technologies, Frontiers is catapulting scholarly publishing into a new generation.

What are Frontiers Research Topics?

Frontiers Research Topics are very popular trademarks of the *Frontiers journals series*: they are collections of at least ten articles, all centered on a particular subject. With their unique mix of varied contributions from Original Research to Review Articles, Frontiers Research Topics unify the most influential researchers, the latest key findings and historical advances in a hot research area.

Find out more on how to host your own Frontiers Research Topic or contribute to one as an author by contacting the Frontiers editorial office: frontiersin.org/about/contact

Molecular and cytogenetic research advances in human reproduction

Topic editors

Ihtisham Bukhari — Fifth Affiliated Hospital of Zhengzhou University, China
Shi Qinghua — University of Science and Technology of China, China
Rick Francis Thorne — The University of Newcastle, Australia

Citation

Bukhari, I., Qinghua, S., Thorne, R. F., eds. (2023). *Molecular and cytogenetic research advances in human reproduction*. Lausanne: Frontiers Media SA. doi: 10.3389/978-2-8325-3486-1

Table of contents

frontiers | Frontiers in Endocrinology

TYPE Editorial
PUBLISHED 09 December 2022
DOI 10.3389/fendo.2022.1107903

Check for updates

OPEN ACCESS

EDITED AND REVIEWED BY
Richard Ivell,
University of Nottingham,
United Kingdom

*CORRESPONDENCE
Qinghua Shi
qshi@ustc.edu.cn
Rick Francis Thorne
rickfthorne@gmail.com

SPECIALTY SECTION
This article was submitted to Reproduction, a section of the journal Frontiers in Endocrinology

RECEIVED 25 November 2022
ACCEPTED 30 November 2022
PUBLISHED 09 December 2022

CITATION
Bukhari I, Thorne RF and Shi Q (2022) Editorial: Molecular and cytogenetic research advances in human reproduction. *Front. Endocrinol.* 13:1107903. doi: 10.3389/fendo.2022.1107903

COPYRIGHT
© 2022 Bukhari, Thorne and Shi. This is an open-access article distributed under the terms of the Creative Commons Attribution License (CC BY). The use, distribution or reproduction in other forums is permitted, provided the original author(s) and the copyright owner(s) are credited and that the original publication in this journal is cited, in accordance with accepted academic practice. No use, distribution or reproduction is permitted which does not comply with these terms.

Editorial: Molecular and cytogenetic research advances in human reproduction

Ihtisham Bukhari[1], Rick Francis Thorne[2,3]* and Qinghua Shi[4]*

[1]Henan Key Laboratory of Helicobacter pylori, Microbiota and Gastrointestinal Cancers, Marshall Medical Research Center, Fifth Affiliated Hospital of Zhengzhou University, Zhengzhou, China, [2]Translational Research Institute, Henan Provincial and Zhengzhou City Key Laboratory of Non-coding RNA and Cancer Metabolism, Henan International Join Laboratory of Non-coding RNA and Metabolism in Cancer, Henan Provincial People's Hospital, Academy of Medical Sciences, Zhengzhou University, Zhengzhou, Henan, China, [3]School of Environmental and Life Sciences, University of Newcastle, Callaghan, NSW, Australia, [4]Division of Reproduction and Genetics, First Affiliated Hospital of USTC, Hefei National Laboratory for Physical Sciences at Microscale, School of Basic Medical Sciences, Division of Life Sciences and Medicine, Biomedical Sciences and Health Laboratory of Anhui Province, University of Science and Technology of China, Hefei, China

KEYWORDS

molecular reproduction, human reproduction, male infertility, female infertility, reproductive diseases

Editorial on the Research Topic
Molecular and cytogenetic research advances in human reproduction

Infertility is a frequently diagnosed medical condition affecting over 15% of couples worldwide (1–3). It has diverse causes, including genetic and environmental factors (4, 5) with dozens of molecular and cytogenetic factors being identified associated with male and/or female infertility. Mainly, male infertility is caused by chromosomal abnormalities including an abnormal number or structure of sex chromosomes or autosomes (6, 7). Other than such gross chromosomal changes, single-gene mutations have recently received attention as a cause of infertility (8–11). Indeed, hundreds of mutations have been identified in men suffering from reproductive defects (12, 13), and more or less a similar number of mutations have been identified in infertile women (14, 15). Such mutations occur in genes responsible for germ cell development and other reproductive processes (16–19).

Animal models mimicking human mutations have been generated to study the mechanisms underlying the effects of the gene mutation (20). Different studies reveal their contribution at various stages of the spermatogenesis or oogenesis (21). Nevertheless, thousands of functionally relevant genes are expressed in human testes and ovaries, and malfunctioning even a single gene can potentially cause infertility (22). Moreover, routine testing for male infertility is limited to chromosome aberrations and Y-chromosome microdeletions (23, 24). However, more and more attention is paid to DNA mutations including the roles of gene expression regulators such as 3'UTR sequences (25–27). Since the impact of mutations in gene 3'UTR sequences may not

be adequately recognized in current sequencing analyses, a potentially massive gap between fertility genetics and its clinical applications has arisen.

The current Research Topic aimed to collect clinical and basic research studies reporting advancement in cytogenetic, molecular, and clinical aspects of human reproduction. After rigorously reviewing submitted articles, the current volume presents an authoritative collection of nine articles exploring new dimensions of human reproduction.

Firstly, Gao et al. introduces the role of KCNQ1 in sperm development and maturation. KCNQ1 is predominantly expressed and localized to the head and tail of sperm; its silencing causes male infertility by significantly reducing sperm motility and acrosome reaction. Alongside sperm motility, sperm morphology has long been known to be critical for successful fertilization. The study by Khan et al. presented an analysis of multiple morphological abnormalities of sperm flagella (MMAF) in two Pakistani families with several infertile brothers. Intriguingly, they found that the spermatozoan fibrous sheaths were disorganized and the central singlet of microtubules was missing. Extensive analyses revealed that the cause of MMAF involved DNAH1 mutations. Galdon et al. successfully isolated the cells from the testicular tissues of individuals with Klinefelter Syndrome (KS) and maintained the culture over 110 days. Cells with abnormal and normal karyotypes were found in testicular cells after culture. These findings could be helpful in the diagnosis and development of fertility therapies for KS patients, such as *in vitro* spermatogenesis or transplantation of SSC *in vivo*.

Testes are essential for male reproduction; different genes and signaling pathways control testes' cellular physiology and morphology. Wang et al. reviewed the role of androgen receptor signaling in spermatogenesis. As known, the androgen receptor signaling regulates biological processes in Sertoli cells and germ cells. Functionally, the androgen receptor helps in the proliferation and maturation of Sertoli cells, self-renewal, and differentiation of spermatogonia stem cells. Additionally, it maintains the integrity of the blood-testis barrier to smoothen the overall process of spermatogenesis. Similarly, Yu et al. compiled the functions of estrogen receptors in female endometrium. Mainly, estrogen induces the proliferation of endometrium mucosa through interacting with estrogen receptors, an essential step in normal menstruation and pregnancy. The abnormal expression of estrogens or their receptors could cause endometriosis (EMT), endometrial hyperplasia (EH), endometrial cancer (EC), and infertility. Therefore, it is suggested that future studies focus on evaluating new therapeutic strategies that target specific ERs and their related growth factor signaling pathways. Liu et al. investigated increases in ApoE in follicular fluid (FF) and the possible relationship between ApoE and EMT in 217 Chinese women (111 healthy controls and 106 EMT patients). Higher expression of ApoE was detected in the FF of EMT patients; however, ApoE affected the quality of blastocysts while did not change levels of fertility hormones. Thus, ApoE levels could only be used as a predictor of EMT, but further details studies are advised. On the other hand, Yu et al. determined that the HOXA10 substantially overexpressed in the ovarian endometriotic cysts stromal cell (OESC) and further uncovered that HOXA10 and its interacting genes are critical for cholesterol biosynthesis in endometrial stromal cells. To find the genetic difference in natural and IVF-ET conceived pregnancies, Yang et al. used placental tissues from both pregnancies for genetic profiling. They identified 12 differentially expressed miRNAs and 258 genes in IVF-ET placental tissues significantly enriched in angiogenesis, pregnancy, PI3K-Akt, and Ras signaling pathways. These findings provide a resource of potential molecular markers to assess the association between placental function and safety in IVF-ET offspring. Finally, Tan et al. explored the relationship between recurrent miscarriages and ovarian reserves. For this purpose, they recruited women with a history of one miscarriage, two and three, or more miscarriages. They found that with the increased number of recurrent miscarriages, the levels of anti-Müllerian hormone, antral follicle counts, and ovarian reserves significantly decreased.

Conclusion

Recent advances in next-generation sequencing (NGS) technologies have brought a paradigm shift in investigating rare and common human disorders. The ability cost-effectively to generate genome-wide sequencing data with in-depth coverage in a short time frame is replacing approaches that focus on specific regions for gene discovery and clinical testing. Articles included in the current Research Topic enlighten us about various aspects of human reproduction, such as the roles of different genes, hormones, and technologies. Isolation of normal testicular cells from Klinefelter syndrome could bring the hope of conceiving a child. However, it is too early to predict, but it is an essential step toward developing infertility cures.

Author contributions

All authors listed have made a substantial, direct, and intellectual contribution to the work and approved it for publication.

Conflict of interest

The authors declare that the research was conducted in the absence of any commercial or financial relationships that could be construed as a potential conflict of interest.

Publisher's note

All claims expressed in this article are solely those of the authors and do not necessarily represent those of their affiliated organizations, or those of the publisher, the editors and the reviewers. Any product that may be evaluated in this article, or claim that may be made by its manufacturer, is not guaranteed or endorsed by the publisher.

References

1. Leeners B, Tschudin S, Wischmann T, Kalaitzopoulos DR. Sexual dysfunction and disorders as a consequence of infertility: A systematic review and meta-analysis. *Hum Reprod Update* (2022) 28:dmac030. doi: 10.1093/humupd/dmac030

2. Basile G, Greco ME, Lauria F, Leone MC. Update on fertility preservation: New opportunities and challenges in the fight against infertility. *Clin Ter* (2022) 173:226–7. doi: 10.7417/CT.2022.2424

3. Agarwal A, Baskaran S, Parekh N, Cho CL, Henkel R, Vij S, et al. Male Infertility. *Lancet* (2021). 397:319–33 doi: 10.1016/S0140-6736(20)32667-2

4. Muffone A, De Oliveira Lubke PDP, Rabito EI. Mediterranean Diet and infertility: A systematic review with meta-analysis of cohort studies. *Nutr Rev* (2022) 8:nuac087. doi: 10.1093/nutrit/nuac087

5. Alahmar AT, Singh R, Palani A. Sperm DNA fragmentation in reproductive medicine: A review. *J Hum Reprod Sci* (2022) 15:206–218.

6. Saeed S, Hassan J, Javed SM, Shan S, Naz M. A familial case of robertsonian translocation 13;14: Case report. *Cureus* (2022) 14:E29430. doi: 10.7759/cureus.29430

7. Wu C, Wang L, Iqbal F, Jiang X, Bukhari I, Guo T, et al. Preferential y-y pairing and synapsis and abnormal meiotic recombination in a 47,Xyy man with non obstructive azoospermia. *Mol Cytogenet* (2016) 9:9. doi: 10.1186/s13039-016-0218-z

8. Yin H, Ma H, Hussain S, Zhang H, Xie X, Jiang L, et al. A homozygous fancm frameshift pathogenic variant causes Male infertility. *Genet Med* (2019) 21:62–70. doi: 10.1038/s41436-018-0015-7

9. Zhang B, Ma H, Khan T, Ma A, Li T, Zhang H, et al. A Dnah17 missense variant causes flagella destabilization and asthenozoospermia. *J Exp Med* (2020) 217(2):e20182365. doi: 10.1084/jem.20182365

10. Fan S, Jiao Y, Khan R, Jiang X, Javed AR, Ali A, et al. Homozygous mutations in C14orf39/Six6os1 cause non-obstructive azoospermia and premature ovarian insufficiency in humans. *Am J Hum Genet* (2021) 108:324–36. doi: 10.1016/j.ajhg.2021.01.010

11. Ma H, Li T, Xie X, Jiang L, Ye J, Gong C, et al. Rad51ap2 is required for efficient meiotic recombination between X and y chromosomes. *Sci Adv* (2022) 8: Eabk1789. doi: 10.1126/sciadv.abk1789

12. Li Y, Wu YF, Jiang HW, Khan R, Han QQ, Iqbal F, et al. The molecular control of meiotic double-strand break (Dsb) formation and its significance in human infertility. *Asian J Androl* (2021) 23:555–61. doi: 10.4103/aja.aja_5_21

13. Jiang H, Zhang Y, Ma H, Fan S, Zhang H, Shi Q. Identification of pathogenic mutations from nonobstructive azoospermia patientsdagger. *Biol Reprod* (2022) 107:85–94. doi: 10.1093/biolre/ioac089

14. Jiang S, Xu Y, Qiao J, Wang Y, Kuang Y. Reproductive endocrine characteristics and *In vitro* fertilization treatment of female patients with partial 17alpha-hydroxylase deficiency: Two pedigree investigations and a literature review. *Front Endocrinol (Lausanne)* (2022) 13:970190. doi: 10.3389/fendo.2022.970190

15. Fei CF, Zhou LQ. Gene mutations impede oocyte maturation, fertilization, and early embryonic development. *Bioessays* (2022) 44:E2200007. doi: 10.1002/bies.202200007

16. Sotillos S, Von Der Decken I, Domenech Mercade I, Srinivasan S, Sirokha D, Livshits L, et al. Human Dlc3 and drosophila cv-c function in testis development: Using a model organism to analyse variations in sex development. *Elife* (2022) 3:11. doi: 10.7554/eLife.82343

17. Roos K, Rooda I, Keif RS, Liivrand M, Smolander OP, Salumets A, et al. Single-cell rna-seq analysis and cell-cluster deconvolution of the human preovulatory follicular fluid cells provide insights into the pathophysiology of ovarian hyporesponse. *Front Endocrinol (Lausanne)* (2022) 13:945347. doi: 10.3389/fendo.2022.945347

18. Xie X, Khan M, Zubair M, Khan A, Khan R, Zhou J, et al. A homozygous missense variant in Dnd1 causes non-obstructive azoospermia in humans. *Front Genet* (2022) 13:1017302. doi: 10.3389/fgene.2022.1017302

19. de la Iglesia A, Jodar M, Oliva R, Castillo J. Insights into the sperm chromatin and implications for Male infertility from a protein perspective. *Wires Mech Dis* (2022) 1:E1588. doi: 10.1002/wsbm.1588

20. Ahn J, Kim DH, Park MR, Suh Y, Lee H, Hwang S, et al. A novel testis-enriched gene, Samd4a, regulates spermatogenesis as a spermatid-specific factor. *Front Cell Dev Biol* (2022) 10:978343. doi: 10.3389/fcell.2022.978343

21. Liu YJ, Zhuang XJ, An JT, Jiang H, Li R, Qiao J, et al. Identification of risk genes in Chinese nonobstructive azoospermia patients based on whole-exome sequencing. *Asian J Androl* (2022). doi: 10.4103/aja202275.

22. del Pilar Contreras-Marciales A, Lopez-Guzman SF, Benitez-Hess ML, Oviedo N, Hernandez-Sanchez J. Characterization of the promoter region of the murine Catsper2 gene. *FEBS Open Bio* (2022) 12(12):2236–49. doi: 10.1002/2211-5463.13518

23. Gao S, Yang X, Xiao X, Yin S, Guan Y, Chen J, et al. Outcomes and affecting factors for icsi and microtese treatments in nonobstructive azoospermia patients with different etiologies: A retrospective analysis. *Front Endocrinol (Lausanne)* (2022) 13:1006208. doi: 10.3389/fendo.2022.1006208

24. Huang IS, Chen WJ, Li LH, Brannigan RE, Huang WJ. The predictive factors of successful sperm retrieval for men with y chromosome azfc microdeletion. *J Assist Reprod Genet* (2022) 39:2395–401. doi: 10.1007/s10815-022-02601-1

25. Cai H, Lang J. Long noncoding rna Linc01960201 hinders decidualization of endometrial stromal cell in endometriosis: Relevance to endometrial receptivity. *Mol Med Rep* (2022) 26(6):366 doi: 10.3892/mmr.2022.12883

26. Xiong X, Min X, Yu H, Fei X, Zhu Y, Pan B, et al. Microrna-34b-5p targets Ppp1r11 to inhibit proliferation and promote apoptosis in cattleyak sertoli cells by regulating specific signaling pathways. *Theriogenology* (2022) 194:46–57. doi: 10.1016/j.theriogenology.2022.09.026

27. Liu M, Liu P, Chang Y, Xu B, Wang N, Qin L, et al. Genome-wide dna methylation profiles and small noncoding rna signatures in sperm with a high dna fragmentation index. *J Assist Reprod Genet* (2022) 39:2255–74. doi: 10.1007/s10815-022-02618-6

frontiers in Physiology

ORIGINAL RESEARCH
published: 22 October 2021
doi: 10.3389/fphys.2021.761910

KCNQ1 Potassium Channel Expressed in Human Sperm Is Involved in Sperm Motility, Acrosome Reaction, Protein Tyrosine Phosphorylation, and Ion Homeostasis During Capacitation

Tian Gao[1], Kun Li[1,2], Fei Liang[1,2], Jianmin Yu[1,2], Ajuan Liu[1], Ya Ni[1,2] and Peibei Sun[1,2]**

[1]School of Pharmacy, Hangzhou Medical College, Hangzhou, China, [2]Zhejiang Provincial Laboratory of Experimental Animal's & Nonclinical Laboratory Studies, Hangzhou Medical College, Hangzhou, China

OPEN ACCESS

Edited by:
Shi Qinghua,
University of Science and Technology of China, China

Reviewed by:
Luciana Bordin,
University of Padua, Italy
Yi Zheng,
Northwest A and F University, China

***Correspondence:**
Peibei Sun
peibeisun@hmc.edu.cn
Ya Ni
niya99@126.com

Specialty section:
This article was submitted to Reproduction, a section of the journal Frontiers in Physiology

Received: *20 August 2021*
Accepted: *29 September 2021*
Published: *22 October 2021*

Citation:
Gao T, Li K, Liang F, Yu J, Liu A, Ni Y and Sun P (2021) KCNQ1 Potassium Channel Expressed in Human Sperm Is Involved in Sperm Motility, Acrosome Reaction, Protein Tyrosine Phosphorylation, and Ion Homeostasis During Capacitation. Front. Physiol. 12:761910. doi: 10.3389/fphys.2021.761910

Potassium channels are involved in membrane hyperpolarization and ion homeostasis regulation during human sperm capacitation. However, the types of potassium channels in human sperm remain controversial. The voltage-gated ion channel KCNQ1 is ubiquitously expressed and regulates key physiological processes in the human body. In the present study, we investigated whether KCNQ1 is expressed in human sperm and what role it might have in sperm function. The expression and localization of KCNQ1 in human sperm were evaluated using Western blotting and indirect immunofluorescence. During capacitation incubation, human sperm were treated with KCNQ1- specific inhibitor chromanol 293B. Sperm motility was analyzed using a computer-assisted sperm analyzer. The acrosome reaction was studied using fluorescein isothiocyanate-conjugated *Pisum sativum* agglutinin staining. Protein tyrosine phosphorylation levels and localization after capacitation were determined using Western blotting and immunofluorescence. Intracellular K^+, Ca^{2+}, Cl^-, pH, and membrane potential were analyzed using fluorescent probes. The results demonstrate that KCNQ1 is expressed and localized in the head and tail regions of human sperm. KCNQ1 inhibition reduced sperm motility, acrosome reaction rates, and protein tyrosine phosphorylation but had no effect on hyperactivation. KCNQ1 inhibition also increased intracellular K^+, membrane potential, and intracellular Cl^-, while decreasing intracellular Ca^{2+} and pH. In conclusion, the KCNQ1 channel plays a crucial role during human sperm capacitation.

Keywords: KCNQ1 potassium channel, sperm capacitation, acrosome reaction, hyperactivation, ion homeostasis, protein tyrosine phosphorylation

INTRODUCTION

Freshly ejaculated human sperm cannot immediately fuse with an oocyte but must undergo a series of physiological and biochemical events known as capacitation, inside the female reproductive tract before they can fertilize an egg (De Jonge, 2017). This process is essential for natural fertilization. Sperm capacitation is accompanied by the removal of cholesterol from

the membrane, membrane potential (V_m) hyperpolarization, and intracellular alkalization, while increasing membrane permeability, intracellular calcium concentration ($[Ca^{2+}]_i$), and protein tyrosine phosphorylation levels (Battistone et al., 2013; Bernecic et al., 2019). After capacitation, sperm exhibit hyperactive motility and can undergo the acrosome reaction (AR). Hyperactive motility is a sperm swimming pattern with deep and asymmetrical flagellar bends, which helps sperm to progress toward and then penetrate an oocyte. The AR is a single-vesicle exocytotic event that facilitates sperm-oocyte fusion (Lopez-Torres and Chirinos, 2017). However, the mechanisms underlying capacitation remain unclear.

Ion channels play important roles in capacitation by regulating sperm membrane potential (V_m), Ca^{2+} levels, and intracellular pH (pH_i), which then affect AR, sperm motility, and other essential physiological processes involved in successful fertilization (Lishko et al., 2012; Brown et al., 2019). Potassium channels are crucial for sperm membrane potential hyperpolarization, ion homeostasis, and fertility (Vyklicka and Lishko, 2020). In mice, the principal K^+ channel that mediates sperm membrane hyperpolarization during capacitation is Slo3, an intracellular alkalization-activated K^+ channel, which is localized in the principal piece of the sperm tail region (Martinez-Lopez et al., 2009; Santi et al., 2010; Brenker et al., 2014). Mutations and deletions in *Slo3* affect male fertility (Zeng et al., 2011). In recent years, differences between human and mouse sperm K^+ currents have been reported. The human sperm K^+ current is activated by Ca^{2+} and is only weakly regulated by intracellular alkalization (Mannowetz et al., 2013). Mannowetz et al. proposed that Slo1 is the main K^+ channel in human sperm, as the Slo1 channel is activated by Ca^{2+}. They found that Slo1 is expressed and localized in the tail region of human sperm. K^+ currents in human sperm can be inhibited by Slo1-specific inhibitors (Mannowetz et al., 2013). In addition, Brenker et al. suggested that Slo3 mediates human K^+ currents. They found that as in case of Slo1, Slo3 is also expressed and localized in the tail region of human sperm and Slo3-specific inhibitors suppress human sperm K^+ currents (Brenker et al., 2014). Lopez-Gonzalez et al. suggested that both Slo1 and Slo3 contribute to capacitation-mediated hyperpolarization based on pharmacological methods (Lopez-Gonzalez et al., 2014). However, Brown et al. reported an infertile patient whose sperm showed deficient K^+ currents but still had intact *Slo1* and *Slo3* genes (Brown et al., 2016). Impaired assembly or localization of the Slo1/Slo3 channel could be an explanation, but the existence of other critical K^+ channels in human sperm cannot be ruled out at this time. Taken together, current literature suggests that K^+ channels in human sperm have not yet been fully elucidated.

KCNQ1 (also known as Kv7.1 or KvLQT1) is the pore-forming subunit (α subunit) of a voltage-gated K^+ channel. It contains six transmembrane helices (S1-S6) and four intracellular C-terminal helices (HA-HD; Börjesson and Elinder, 2008; Catterall, 2010; Sun and MacKinnon, 2017). The S1-S4 segments constitute the voltage-sensing domain (VSD), which controls the opening of the channel. The S5-S6 segments constitute the pore domain (PD), which has K^+ selectivity (Dixit et al., 2020) KCNQ1 forms a tetramer and performs its important physiological functions by interacting with auxiliary subunits, including KCNE family members (KCNE1-5; Nakajo and Kubo, 2015; Sun and MacKinnon, 2020). KCNQ1 is expressed in a wide range of human tissues, including the heart, kidney, colon, cochlea, stomach, and small intestine (Bett et al., 2006; Dixit et al., 2020). In different tissues, KCNQ1 interacts with different auxiliary subunits and performs different functions. For example, in the human heart, KCNQ1 interacts with KCNE1 and mediates a delayed rectifier K^+ current, which is critical for cardiac action potential repolarization (Wu and Larsson, 2020). In the human stomach, KCNQ1 forms a functional channel with KCNE2 and regulates gastric acid secretion (Roepke et al., 2006). Previous studies have shown that KCNQ1 and KCNE1 are expressed in rat testes and germ cells (Tsevi et al., 2005). The auxiliary subunit KCNE1 is also expressed and localized in the tail region of human sperm (Yeung and Cooper, 2008), suggesting that its pore-forming subunit KCNQ1 may also be expressed in human sperm. KCNQ1 C-terminal intracellular helices, HA and HB, can interact with calmodulin (CAM), a cytosolic Ca^{2+}-binding protein that affects KCNQ1 function. Reduced $[Ca^{2+}]_i$ causes inactivation of the KCNQ1 channel (Sun and MacKinnon, 2017). Therefore, we hypothesized that KCNQ1 exists in human sperm and plays a role in sperm function. The findings of this research will help in further understanding the role of K^+ channels in human sperm capacitation.

MATERIALS AND METHODS

Chemicals and Reagents

Percoll was obtained from GE Healthcare BioSciences (Little Chalfont, UK). Lysis buffer and other reagents for sodium dodecyl sulfate-polyacrylamide gel electrophoresis (SDS-PAGE) were purchased from the Beyotime Institute of Biotechnology (Shanghai, China). Dimethyl sulfoxide (DMSO) was acquired from Merck (Darmstadt, Germany). Enhanced chemiluminescence (ECL) Plus Chemiluminescence Kit, protein loading buffer, and pre-dyed protein markers were acquired from Thermo Fisher Scientific (Burlington, NC, United States). Polyvinylidene fluoride (PVDF) membranes were obtained from Millipore Corporation (Bedford, MA, United States). Fluorescein isothiocyanate-conjugated *Pisum sativum* agglutinin (PSA-FITC), KCNQ1 inhibitor chromanol 293B, and carbonyl cyanide m-chlorophenylhydrazone (CCCP) were obtained from Sigma-Aldrich (St. Louis, MO, United States). Complete mini EDTA-free protease inhibitor cocktail and phosphatase inhibitor cocktail (broad-spectrum phosphatase inhibitor, including Ser/Thr and Tyr phosphatase inhibitors) were obtained from Roche (Mannheim, Germany). The antibodies used in this study were as follows: KCNQ1 (ab84819), KCNE1 (ab65795), rabbit anti-β-tubulin (ab6046), Alexa Fluor 555-conjugated goat anti-mouse antibody (ab150118), Alexa Fluor 488-conjugated goat anti-rabbit antibody (ab150077), and Alexa Fluor 488-conjugated goat anti-mouse antibody (ab150113) were purchased from Abcam (Cambridge, UK); p-Tyr (sc-7,020) and KCNQ1

(sc-365,764) were obtained from Santa Cruz Biotechnology Inc (Dallas, Texas, United States). KCNE1 (31195A31) and horseradish peroxidase-conjugated goat antibodies were purchased from Invitrogen (Carlsbad, CA, United States). Fluo3-AM and MQAE were obtained from Beyotime Institute of Biotechnology (Shanghai, China). BCECF-AM, DisC3(5), and PBFI-AM were purchased from Invitrogen (Carlsbad, CA, United States).

Sperm Incubation Medium

Human tubal fluid (HTF) medium was prepared as previously described (Li et al., 2021; Sun et al., 2021). The HTF medium comprised 5.06 mM KCl, 90 mM NaCl, 25.3 mM $NaHCO_3$, 1.17 mM KH_2PO_4, 1.8 mM $CaCl_2$, 1.01 mM $MgSO_4$, 0.27 mM sodium pyruvate, 5.56 mM glucose, 21.6 mM sodium lactate, 20 mM HEPES, 4 g/L bovine serum album, 5 mg/L phenol red and 60 mg/L penicillin. The pH was adjusted to 7.4. All chemicals were obtained from Sigma-Aldrich.

Semen Collection and Sample Preparation

This study was approved by the Medical Ethics Committee of Hangzhou Medical College (no. 2018004). Written informed consent was obtained from 15 healthy male donors (aged 25–35 years). Sperm preparation was performed as previously described (Sun et al., 2021). The donors abstained from sexual intercourse for 3 days before sample collection. Fresh semen were obtained *via* masturbation, collected in sterile containers, and subsequently liquefied at 37°C for 1 h. According to the World Health Organization (WHO) requirements, semen samples in this study met the following criteria: sperm viability ≥85%, sperm motility ≥50%, morphologically normal sperm ≥15%, and sperm concentration $\geq 20 \times 10^6$ sperm/mL. To remove dead sperm and cell debris, semen samples were centrifuged with 40 and 80% discontinuous Percoll gradients at $750 \times g$ for 15 min and the precipitate was resuspended in HTF medium. Sperm collected from at least three donors were mixed, washed, adjusted to a density of approximately 20×10^6 sperm/mL, and analyzed in the following experiments. The prepared samples were incubated in a 5% CO_2 incubator at 37°C.

Protein Extraction and Western Blotting

According to our previously reported method (Sun et al., 2021), sperm samples were washed with phosphate-buffered saline (PBS) and resuspended in lysis buffer (P0013G, Beyotime Institute of Biotechnology, Shanghai, China) containing protease inhibitors (protease inhibitor cocktail and phosphatase inhibitor cocktail, Roche, Mannheim, Germany) and 1 mM phenylmethylsulfonyl fluoride (PMSF). After ultrasonication and centrifugation, the supernatant was collected. Protein sample concentrations were determined using a bicinchoninic acid assay (BCA) kit (Beyotime Institute of Biotechnology, Shanghai, China). For different treatment groups, equal amounts of sperm protein (20 μg) were denatured *via* incubation with protein loading buffer at 100°C for 5 min and separated by 10% SDS-PAGE with a pre-stained protein marker. Proteins, transferred to PVDF membranes, were blocked with 5% skim milk (m/v). The PVDF membranes were incubated with primary antibodies at 4°C overnight and then washed three times with TBS buffer supplemented with 0.01% Tween-20 (v/v). The membrane was incubated with appropriate secondary antibodies at room temperature for 2 h. After washing with TBS buffer three times, protein blots were detected by an ECL kit (Thermo Fisher Scientific) using a gel imaging system (Amersham Imager 600; General Electric Company, United States). For loading control, the membranes were stripped and probed with β-tubulin antibodies. Gray intensity was analyzed using the ImageJ software.

Indirect Immunofluorescence Staining

After fixation in 4% paraformaldehyde for 30 min, the sperm were mounted on Silane-Prep slides and airdried. Sperm were permeabilized with 0.1% Triton X-100 and blocked with 10% goat serum. The sperm were then incubated with primary antibodies (mouse anti-KCNQ1, rabbit anti-KCNE1 or mouse anti-p-Tyr) or normal IgG (negative control) overnight at 4°C. After washing three times with PBS, Alexa Fluor 555-conjugated anti-mouse IgG secondary antibody and Alexa Fluor 488-conjugated anti-rabbit IgG secondary antibody were applied for 1 h at 37°C. Following incubation with DAPI and washing with PBS, the sperm were examined using fluorescence microscopy (Nikon Eclipse 80i; Nikon Inc., Tokyo, Japan). For the immunofluorescence studies of KCNQ1, KCNE1 and p-Tyr, both non-capacitation and capacitation for 3 h samples were used.

Evaluation of Sperm Capacitation and Sperm Viability

Because only capacitated sperm undergo exocytosis, human sperm capacitation was assessed indirectly using progesterone-induced AR. Different sperm groups were treated with different reagents for 3 h during capacitation, followed by treatment with 15 μM progesterone for 15 min to induce the AR. According to the WHO Laboratory Manual for the Examination and Processing of Human Semen (5th ed.), the AR was evaluated by PSA-FITC staining. After fixing with 95% ethanol for 30 min, sperm were mounted on Silane-Prep slides, air dried, and incubated overnight at 4°C with 25 mg/L PSA-FITC in the dark. Sperm were washed with PBS and analyzed by fluorescence microscopy. At least 200 sperm were counted for each sample. To detect spontaneous AR, sperm were stained with PSA-FITC immediately after discontinuous Percoll gradient centrifugation and washing.

To evaluate sperm viability, propidium iodide (PI) was used to detect dead cells. Sperm were stained with 12 μM PI for 10 min at 37°C before or after capacitation for 3 h. After washing with PBS three times, the sperm were mounted on Silane-Prep slides, air dried, and analyzed by fluorescence microscopy. Sperm with red fluorescence at the head was considered dead sperm. At least 200 sperm were counted for each sample. The percentage of non-viable cells (NVC%) was calculated.

Sperm Motility Analysis

Sperm motility was analyzed using a computer-assisted sperm analyzer (CASA; IVOS, Hamilton-Thorne Bio-Sciences, Beverly,

MA, United States) with the following parameters: acquisition frame, 30; frame rate, 60 Hz; minimum cell size, 3 pixels; minimum contrast, 80; cell intensity, 40; magnification, 1.73 ×; temperature, 37°C; illumination intensity, 2,164; path velocity, 25.0 μm/s; straightness threshold, 80%; slow cell, average path velocity (VAP) and straight line velocity (VSL) of less than 5.0 μm/s and 11 μm/s, respectively; and chamber depth, 20 μm ($n > 200$ motile sperm per sample). Briefly, a 5 μL sperm sample was loaded into a 20 μm deep slide chamber warmed to 37°C. The following parameters were assessed for each sample: VSL, VAP, curvilinear velocity (VCL), straightness (STR), linearity (LIN), amplitude of lateral head displacement (ALH), beat-cross frequency (BCF), and percentage of motile, progressive, and hyperactivation. Hyperactivated sperm met the following criteria: VCL ≥ 150 μm/s, ALH ≥ 7.0 μm, and LIN ≤ 50%.

Intracellular K^+ Measurement in Human Sperm

$[K^+]_i$ in sperm was measured using PBFI-AM. Sperm were loaded with 10 μM PBFI-AM in a 5% CO_2 incubator in the dark at 37°C for 30 min. Excess dye in the medium was removed by washing five times with HTF. PBFI-AM-loaded sperm were resuspended in HTF and incubated at 37°C for further 20 min. Sperm aliquots (10^6 cells/mL) were exposed to vehicle control (DMSO) and chromanol 293B (20, 100, or 200 μM). The K^+ fluorescence signal was then recorded using a Synergy 2 Multi-Function Microplate Reader (Bio-Tek Instruments, Winooski, United States) with excitation at 340/380 nm and emission wavelengths of 500 nm. The data were acquired at 3 min intervals for 30 min during capacitating incubation because the effect of chromanol 293B on ion homeostasis may be compensated for by other potassium channels over time. After capacitation for 3 h, a fluorescence signal was acquired. The ratio (340:380) of the two signals is directly proportional to $[K^+]_i$. First recorded raw intensity values were used to normalize the other raw intensity values.

Intracellular Ca^{2+} Measurement in Human Sperm

The $[Ca^{2+}]_i$ levels in human sperm were measured using Fluo3-AM according to a previously described method (Li et al., 2014). Briefly, the prepared sperm were loaded with 10 μM Fluo3-AM in a 5% CO_2 incubator at 37°C for 30 min in the dark and then washed five times with HTF to remove free Fluo3-AM. Fluo3-AM-loaded sperm were resuspended in HTF and incubated at 37°C for another 20 min. Sperm aliquots (10^6 cells/mL) were then exposed to vehicle control (DMSO) and chromanol 293B (20, 100, or 200 μM). The Ca^{2+} fluorescence signal was then recorded using a Synergy 2 Multi-Function Microplate Reader, at 485 nm excitation and 528 nm emission wavelengths. The data were acquired at 3 min intervals for 30 min during the capacitating incubation. After capacitation for 3 h, a fluorescence signal was acquired. Fluorescence intensity is directly proportional to $[Ca^{2+}]_i$. First recorded raw intensity values were used to normalize the other raw intensity values.

Intracellular Cl^- Measurement in Human Sperm

The $[Cl^-]_i$ levels in sperm were measured using a Cl^-- specific fluorescence probe (MQAE). Prepared sperm were loaded with 5 μM MQAE in a 5% CO_2 incubator in the dark at 37°C for 30 min and were then washed five times with HTF to remove free MQAE. MQAE-loaded sperm were resuspended in HTF and incubated at 37°C for another 20 min. MQAE-loaded sperm aliquots (10^6 cells/mL) were exposed to vehicle control (DMSO) and chromanol 293B (20, 100, or 200 μM). The Cl^- fluorescence signal was recorded using a Synergy 2 Multi-Function Microplate Reader at 355 nm excitation and 460 nm emission wavelengths. The data were acquired at 3 min intervals for 30 min during the capacitating incubation. After capacitation for 3 h, a fluorescence signal was acquired. Fluorescence intensity was inversely proportional to $[Cl^-]_i$. First recorded raw intensity values were used to normalize the other raw intensity values.

Intracellular pH Measurement in Human Sperm

Sperm sample pH was evaluated using BCECF-AM. The prepared sperm were loaded with 10 μM BCECF-AM in a 5% CO_2 incubator in the dark at 37°C for 30 min and were then washed five times with HTF to remove free BCECF-AM. BCECF-AM-loaded sperm were resuspended in HTF and incubated at 37°C for another 20 min. BCECF-AM-loaded sperm aliquots (10^6 cells/mL) were exposed to vehicle control (DMSO) and chromanol 293B (20, 100, or 200 μM). To determine pH_i, fluorescence signals were recorded using a Synergy 2 Multi-Function Microplate Reader at 490/440 nm excitation and 535 nm emission wavelengths. The data were acquired at 3 min intervals for 30 min during the capacitating incubation. After capacitation for 3 h, a fluorescence signal was acquired. The ratio (490:440) of the two signals was directly proportional to the pH_i. The first recorded raw intensity values were used to normalize the other raw intensity values.

Assessment of Sperm Membrane Potential Changes

Sperm membrane potential changes were evaluated using the potential-sensitive fluorescence probe DiSC3(5), as previously described (Xu et al., 2007). Before measurement, the prepared sperm were loaded with 1 μM DisC3(5) in a 5% CO_2 incubator in the dark at 37°C for 5 min. CCCP was added to a final concentration of 1 μM. Sperm were incubated for 2 min. Sperm aliquots (10^6 cells/mL) were exposed to vehicle control (DMSO) and chromanol 293B (20, 100, or 200 μM). The membrane potential fluorescence signal was then recorded using a Synergy 2 Multi-Function Microplate Reader, with 620 nm excitation and 670 nm emission wavelengths. The data were acquired at 3 min intervals for 30 min during the capacitating incubation. After capacitation for 3 h, a fluorescence signal was acquired. The fluorescence intensity was directly proportional to V_m. The first recorded raw intensity values were used to normalize the other raw intensity values.

Statistical Analysis

The Statistical Package for the Social Sciences software (SPSS, version 23; IBM Corporation, Armonk, NY, United States) was used for statistical analyses. Results are expressed as the means ± standard error of the mean (SEM). One-way analysis of variance was used to determine differences between the groups. When tests for the homogeneity of variance were not significant, the least significant difference test was used; otherwise, the data were analyzed using Dunnett's T3 test; and $p < 0.05$ was considered statistically significant (two-sided).

RESULTS

Expression and Localization of KCNQ1 and KCNE1 in Human Sperm

We studied the expression of KCNQ1 and KCNE1 in human sperm using Western blotting. The results showed the presence of a KCNQ1-specific band at approximately 70 kDa and nonspecific band at approximately 48 kDa, in addition to a KCNE1-specific band at 15 kDa (**Figure 1A**). We examined the immunofluorescence of KCNQ1 and KCNE1 in human sperm before and after capacitation (**Figure 1B**). The results showed that KCNQ1 was localized mainly in the head and tail regions of human sperm, while KCNE1 was localized mainly in the neck and tail regions, which is in accordance with previous studies (Yeung and Cooper, 2008). The merging of both proteins showed that they were partially co-localized. The localization of KCNQ1 and KCNE1 in human sperm before and after capacitation was not significantly different. These results show that both KCNQ1 and KCNE1 are expressed in human sperm.

Chromanol 293B Affects AR During Human Sperm Capacitation

The effect of chromanol 293B on the human sperm AR was detected using a PSA-FITC staining assay. This method can easily distinguish sperm with acrosome integrity (AI) from those with AR (**Figure 2A**). For the AI pattern, bright and uniform fluorescence was observed in most regions of sperm heads, whereas for the AR pattern, no fluorescent staining was observed in the acrosomal zone, or only fluorescence bands in the equatorial zone were observed. The spontaneous AR (control 0 h) ratio was approximately 12.1 ± 1.4%, which was determined before capacitation incubation. After capacitation for 3 h, the AR ratio of vehicle control (DMSO) was approximately 35.1 ± 1.7%. When human sperm were treated with 100 μM chromanol 293B during capacitation, the ratio of AR was significantly lower than that of the vehicle control (29.7 ± 1.4% vs. 35.1 ± 1.7%, $p = 0.017$; **Figure 2B**). However, chromanol 293B did not affect the sperm viability. As shown in **Figure 2B**, before capacitation, the number of NVC% was approximately 13.0 ± 1.1%. After capacitation for 3 h, there were no significant differences in NVC% between the vehicle control group and the 100 μM chromanol 293B-treated group (12.6 ± 1.3% vs. 14.7 ± 1.3%). These results suggest that the KCNQ1 channel is involved in human sperm capacitation.

Chromanol 293B Changes Human Sperm Motility Parameters During Capacitation

CASA was used to analyze the effects of chromanol 293B on human sperm motility. As shown in **Table 1**, no significant differences were observed in human sperm hyperactivation between the chromanol 293B-treated groups and vehicle control (DMSO) for 3 h capacitation. However, most sperm motility parameters in the 200 μM chromanol 293B group were significantly lower than those in the vehicle control group, including sperm motility, progressive sperm, VAP, VSL, VCL, BCF, STR, and LIN ($p < 0.05$). When sperm were treated with 100 μM chromanol 293B, only sperm motility and progressive sperm showed significant differences compared to the vehicle control. These results suggest that KCNQ1 plays a role in human sperm motility during capacitation.

Chromanol 293B Changes Protein Tyrosine Phosphorylation Level and Localization During Human Sperm Capacitation

To further verify that the KCNQ1 potassium channel plays a role in human sperm during capacitation, we examined the effect of chromanol 293B on protein tyrosine phosphorylation levels, because capacitated sperm show high levels of protein tyrosine phosphorylation (Visconti et al., 2011). The effect of chromanol 293B on protein tyrosine phosphorylation levels was assessed by Western blotting. As shown in **Figure 3A**, protein tyrosine phosphorylation levels increased during human sperm capacitation. After 3 h of sperm capacitation, the 100 μM chromanol 293B group showed a significant decrease in protein tyrosine phosphorylation. We analyzed the ratio of protein tyrosine phosphorylation levels to that of the loading control, β-tubulin (**Figure 3B**). Protein tyrosine phosphorylation was enhanced over time during capacitation. The effect of 30 min treatment of chromanol 293B on capacitation was negligible. However, after capacitation for 3 h, chromanol 293B reduced protein tyrosine phosphorylation levels in a dose-dependent manner. The addition of 100 μM chromanol 293B significantly decreased tyrosine phosphorylation, with bands at 120, 90, and 70 kDa compared to the DMSO control ($p = 0.005$, 0.012, and 0.032, respectively). We also examined the effect of chromanol 293B on phosphorylated tyrosine localization using indirect immunofluorescence. Before capacitation, phosphorylated tyrosine was localized in the head and tail regions of the sperm, and the fluorescence intensity was weak. After capacitation for 3 h, the phosphorylated tyrosine was mainly localized in the equatorial and tail regions of the sperm, and the fluorescence intensity became intense. However, when the sperm were treated with 100 μM chromanol 293B, phosphorylated tyrosine only localized in the tail region (**Figure 3C**).

Chromanol 293B Increases Intracellular K^+ Concentration During Human Sperm Capacitation

To determine whether the KCNQ1 channel mediates K^+ currents during human sperm capacitation, the effect of

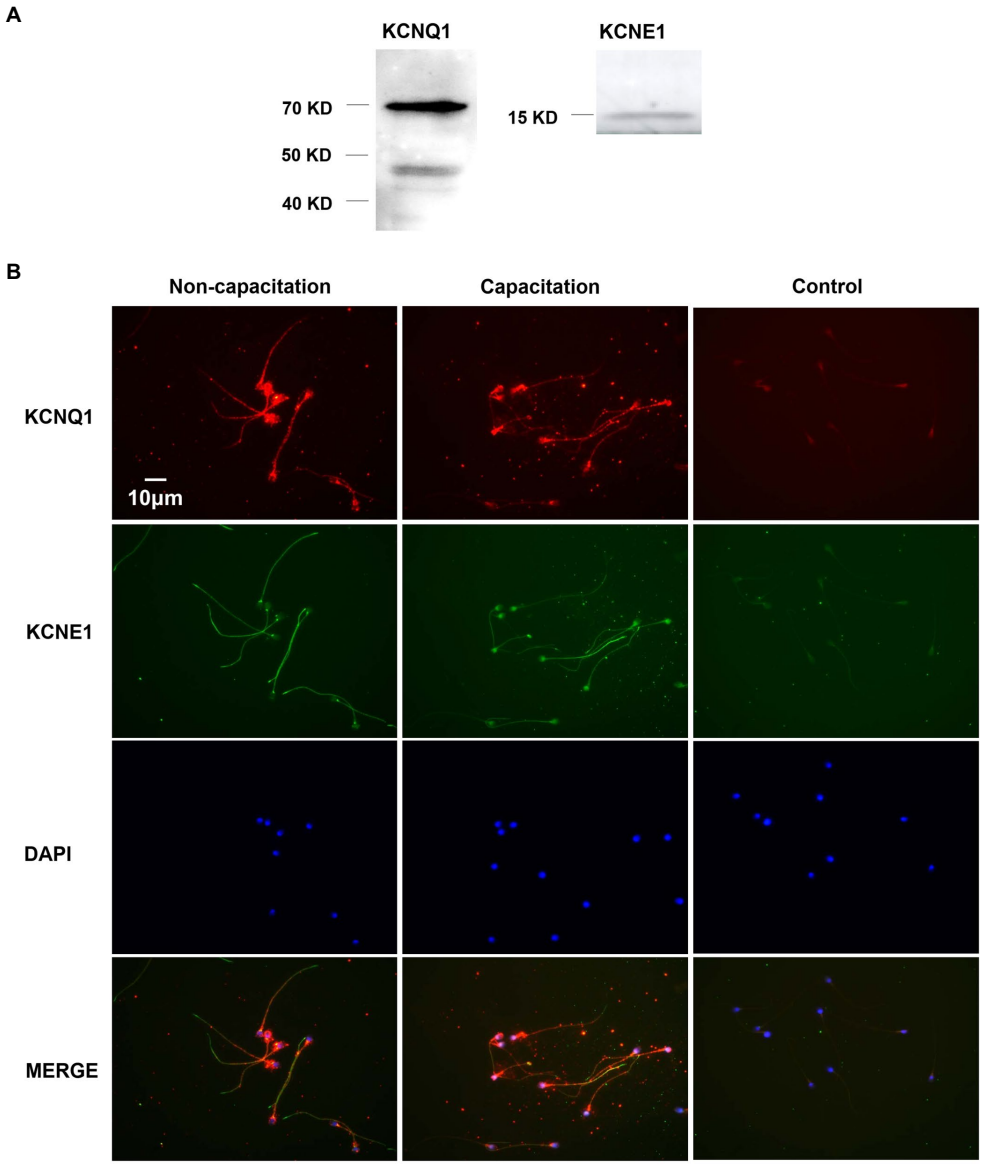

FIGURE 1 | Expression and localization of KCNQ1 and KCNE1 in human sperm. **(A)** Human sperm were lysed after capacitation for 3 h. Sperm proteins were separated and analyzed using 10% SDS-PAGE and Western blotting, using antibodies for KCNQ1 (Abcam) and KCNE1 (Abcam). The figure is representative of 3 separate experiments. The full uncropped immunoblots was provided in the supplementary data (**Supplementary Figure 1**). **(B)** Indirect immunofluorescence of KCNQ1 (Santa Cruz) and KCNE1 (Invitrogen) in human sperm before and after capacitation. KCNQ1 (red), KCNE1 (green), and co-localization of KCNQ1 and KCNE1 (merge). The negative control cells were incubated with normal IgG as the primary antibodies. The nuclei of spermatozoa were stained blue with DAPI. The figure is representative of 3 separate experiments.

chromanol 293B on intracellular K^+ concentration ($[K^+]_i$) was examined. $[K^+]_i$ was analyzed at 3 min intervals over 30 min and once after sperm were capacitated for 3 h. The intracellular K^+ concentration was detected using the K^+ fluorescence probe PBFI-AM, and the fluorescence intensity was directly proportional to $[K^+]_i$. As shown in **Figure 4A**, $[K^+]_i$ decreased during human sperm capacitation in the vehicle control (DMSO), suggesting that potassium channels open and result in K^+ efflux. However, $[K^+]_i$ increased when sperm were treated with chromanol 293B. The results showed dose-dependent changes, suggesting that chromanol 293B inhibits the KCNQ1 potassium channel, blocks K^+ efflux through KCNQ1, and increases $[K^+]_i$.

Chromanol 293B Depolarizes Membrane Potential During Human Sperm Capacitation

Because KCNQ1 inhibition increases $[K^+]_i$ in sperm and potassium channels are always involved in the regulation of membrane potential (V_m), we further examined whether the membrane was depolarized when treated with chromanol 293B.

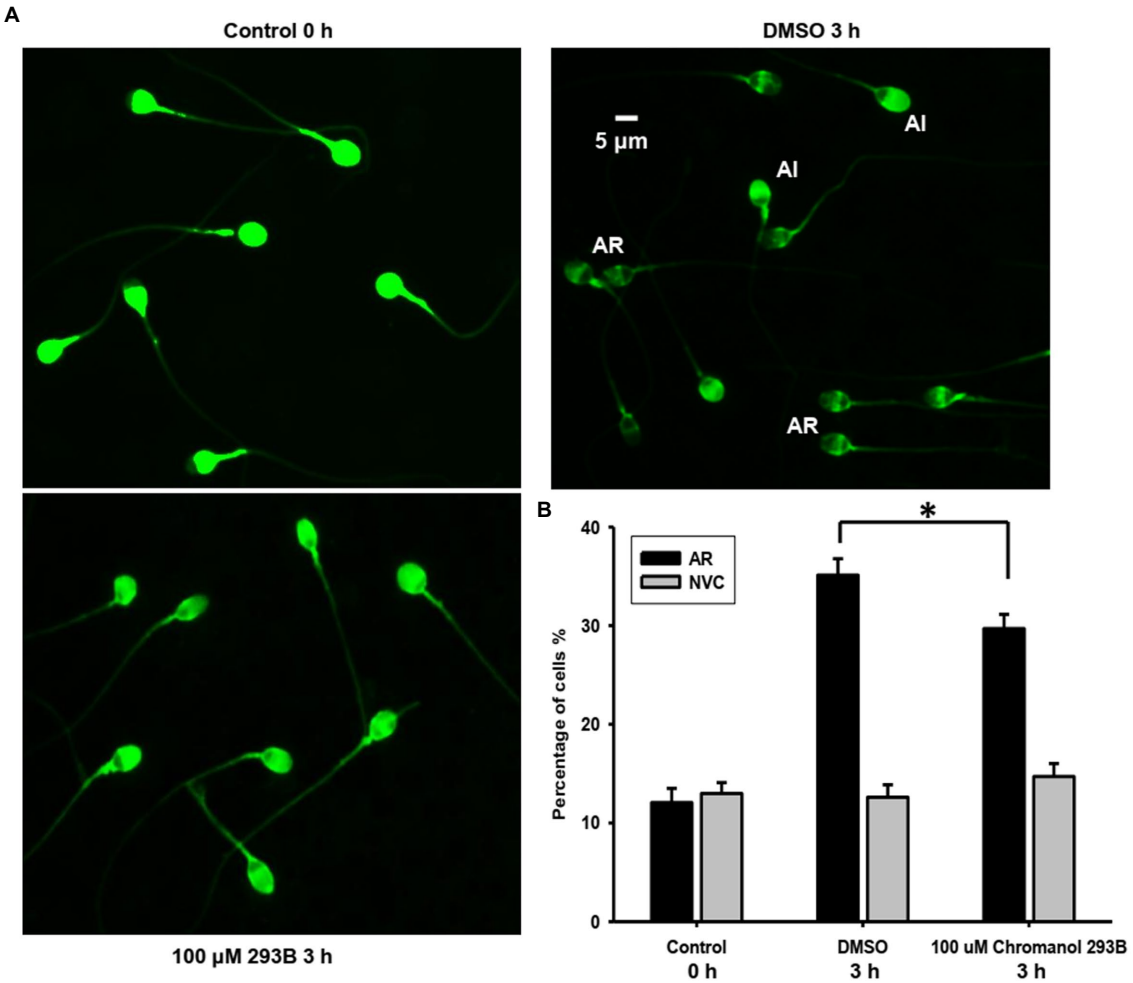

FIGURE 2 | Chromanol 293B effect on human sperm AR and viability. **(A)** The human sperm AR was evaluated using PSA-FITC staining. Sperm were treated with different reagents (DMSO or 100 μM chromanol 293B) for 3 h during capacitation, and the sperm were then treated with 15 μM progesterone for 15 min to induce AR. To detect spontaneous AR before capacitation, sperm were stained with PSA-FITC immediately after discontinuous Percoll gradient centrifugation and washing. AR indicates acrosome-reacted sperm, while acrosome integrity (AI) indicates uncapacitated sperm. **(B)** After PSA-FITC staining, sperm were examined by fluorescence microscopy. The AR ratio is calculated by dividing the number of AR sperm with the total number of sperm. For 100 μM chromanol 293B group compared to vehicle control group, $^{*}p < 0.05$. Propidium iodide (PI) is used to stain dead sperm. Percentage of not viable cells (NVC%) was calculated. Values represent the means ± SEM of at least 6 experiments.

V_m was detected using the fluorescence probe DisC3(5). The fluorescence intensity was directly proportional to V_m. As shown in **Figure 4B**, V_m of the chromanol 293B-treated groups increased during human sperm capacitation. The depolarized sperm V_m values for the groups treated with 100 and 200 μM chromanol 293B were much higher than those for the vehicle control group ($p < 0.05$). These results suggest that chromanol 293B increases $[K^+]_i$ and depolarizes V_m in human sperm.

Chromanol 293B Decreases Intracellular Ca^{2+} Concentration During Human Sperm Capacitation

To explore whether the KCNQ1 channel indirectly influences other intracellular ion homeostasis, the effect of chromanol 293B on intracellular Ca^{2+} concentration ($[Ca^{2+}]_i$) was detected using the Ca^{2+} fluorescence probe Fluo3-AM, fluorescence intensity of which was directly proportional to $[Ca^{2+}]_i$. When human sperm were treated with chromanol 293B, the $[Ca^{2+}]_i$ decreased compared to the vehicle control at the beginning of 25 min ($p < 0.05$; **Figure 4C**). The effect of 200 μM chromanol 293B on $[Ca^{2+}]_i$ decrease was negligible compared to that of 100 μM chromanol 293B. However, both 100 and 200 μM chromanol 293B groups showed a significant decrease in $[Ca^{2+}]_i$ compared to the vehicle control group ($p < 0.05$). These results indicate that KCNQ1 indirectly regulates $[Ca^{2+}]_i$ during human sperm capacitation. After capacitation for 3 h, $[Ca^{2+}]_i$ increased significantly compared to the beginning of the experiment. However, there were no statistically significant differences between the groups at 3 h. The

TABLE 1 | Effect of chromanol 293B on motility parameters during human sperm capacitation. Values represent the means ± SEM of 5 experiments.

	DMSO	100 μM Chromanol 293B	200 μM Chromanol 293B
Motility (%)	67.06 ± 1.33	63.26 ± 0.80*	34.30 ± 1.24*
Progressive motility (%)	46.76 ± 1.13	42.89 ± 0.89*	21.90 ± 0.66*
VAP (μm/s)	81.81 ± 1.64	78.52 ± 1.40	70.17 ± 1.07*
VSL (μm/s)	72.25 ± 1.62	69.01 ± 1.33	59.46 ± 0.95*
VCL (μm/s)	130.33 ± 2.66	126.99 ± 2.78	118.95 ± 1.91*
ALH (μm)	5.65 ± 0.14	5.52 ± 0.14	5.91 ± 0.07
BCF (Hz)	31.48 ± 0.29	32.01 ± 0.31	25.67 ± 0.29*
STR (%)	85.12 ± 0.42	84.50 ± 0.38	81.90 ± 0.31*
LIN (%)	54.06 ± 0.44	53.10 ± 0.38	49.30 ± 0.45*
Hyperactivation(%)	7.00 ± 0.54	7.01 ± 0.82	7.70 ± 0.68

*$p < 0.05$.

VAP, average path velocity; VSL, straight line velocity; VCL, curvilinear velocity; ALH, amplitude of lateral head displacement; BCF, beat-cross frequency; STR, straightness (VSL/VAP multiplied by 100); LIN, linearity (VSL/VCL multiplied by 100); Hyperactivation, VCL ≥ 150 μm/s, ALH ≥ 7.0 μm, and LIN ≤ 50%.

explanation for this result may be that chromanol 293B initially inhibits KCNQ1, while other potassium channels compensate over time.

Chromanol 293B Increases Intracellular Cl^- Concentration During Human Sperm Capacitation

The intracellular Cl^- concentration ($[Cl^-]_i$) was analyzed using the Cl^- fluorescence probe MQAE. The fluorescence intensity is inversely proportional to $[Cl^-]_i$. As shown in **Figure 4D**, within the first 25 min, treatment with 200 μM chromanol 293B significantly decreased the fluorescence intensity of Cl^-, which indicating that $[Cl^-]_i$ increased ($p < 0.05$; **Figure 4D**). Although there were no significant differences between all the groups when sperm were capacitated for 3 h, the groups treated with 100 and 200 μM chromanol 293B groups tended to have higher $[Cl^-]_i$. These results indicate that KCNQ1 indirectly regulates $[Cl^-]_i$ during human sperm capacitation.

Chromanol 293B Decreases Intracellular pH During Human Sperm Capacitation

The intracellular pH (pH_i) of human sperm during capacitation was measured using the pH fluorescence probe BCECF-AM. The fluorescence intensity was directly proportional to pH_i. The chromanol 293B-treated groups showed a decrease in pH_i compared to that of the vehicle control group (**Figure 4E**).

DISCUSSION

Potassium channels play an essential role in sperm function. The membrane potential of sperm becomes hyperpolarized during capacitation, which is mainly due to the outflow of K^+ currents (Lopez-Gonzalez et al., 2014). Patients lacking efflux K^+ currents in sperm show reduced fertility (Brown et al., 2016). It is known that the K^+ current characteristics in human sperm are different from those in mouse sperm. The K^+ channel type in human sperm remains controversial (Mannowetz et al., 2013; Brenker et al., 2014). To identify the critical K^+ channel types in sperm, gene knockout studies provide direct and credible evidence. However, this strategy cannot be used for studying human sperm. Other approaches, such as pharmacological assessment, immunolocalization, and patch clamp electrophysiology methods can be used to study K^+ channels in human sperm (Mansell et al., 2014). Here, by using immunoblot, immunolocalization, and pharmacological methods, we first report that the KCNQ1 channel is expressed and localized in the head and tail regions of human sperm. Moreover, the KCNQ1 channel was observed to play a role in regulating human sperm motility, AR, protein tyrosine phosphorylation, and ion homeostasis during capacitation.

The human KCNQ1 pore-forming subunit contains 676 amino acids with a molecular weight of approximately 74.6 kDa (Yang et al., 1997). Our Western blotting experiment using KCNQ1-specific antibodies showed a clear band at approximately 70 kDa (**Figure 1A**), demonstrating that KCNQ1 is expressed in human sperm. Using RT-PCR, Yeung et al. found that one of the KCNQ1 auxiliary subunits, KCNE1, is expressed in human sperm. Immunofluorescence showed that this subunit localized in the tail regions and cytoplasmic droplets of human sperm (Yeung and Cooper, 2008). Human KCNE1 contains 129 amino acids with a molecular weight of approximately 14.6 kDa (Tian et al., 2007). Evaluation of KCNE1 expression in human sperm by Western blotting revealed a specific band at approximately 15 kDa (**Figure 1A**), indicating that KCNE1 was expressed in human sperm. We found that KCNQ1 is localized in the head, neck, and tail regions of human sperm, while KCNE1 is localized in the neck and tail regions, as previously reported (Yeung and Cooper, 2008; **Figure 1B**). KCNQ1 and KCNE1 showed partial co-localization in the human sperm. The distribution of the two proteins showed no obvious differences between the non-capacitation and capacitation groups. These results suggest that KCNQ1 may form a functional channel in human sperm.

Because KCNQ1 is expressed in human sperm, we further investigated its role in sperm capacitation using pharmacological assessments. Chromanol 293B is a specific inhibitor of KCNQ1 which can electrostatically interact with the selectivity filter of KCNQ1 and block the channel (Lerche et al., 2007). The half-maximal inhibitory concentration (IC50) of chromanol 293B on KCNQ1 is approximately 65 μM. The KCNE family of auxiliary subunits enhances this block. The IC50 of chromanol 293B on KCNQ1/KCNE1 is approximately 15 μM (Bett et al., 2006). Here, we treated human sperm with 20, 100, or 200 μM chromanol 293B to examine the role of KCNQ1 in human sperm capacitation.

We analyzed the AR, hyperactivation, and protein tyrosine phosphorylation in human sperm treated with chromanol 293B because these phenomena occur during sperm capacitation. The results show that 100 μM chromanol 293B significantly reduced the AR ratio of human sperm after capacitation for 3 h (29.7 ± 1.4% vs. 35.1 ± 1.7%, $p = 0.017$), with no influence on sperm viability (**Figure 2**). In addition to KCNQ1 potassium channels, there are other potassium channels in human sperm, such as Slo1 and Slo3. These may play a compensatory role when KCNQ1 potassium

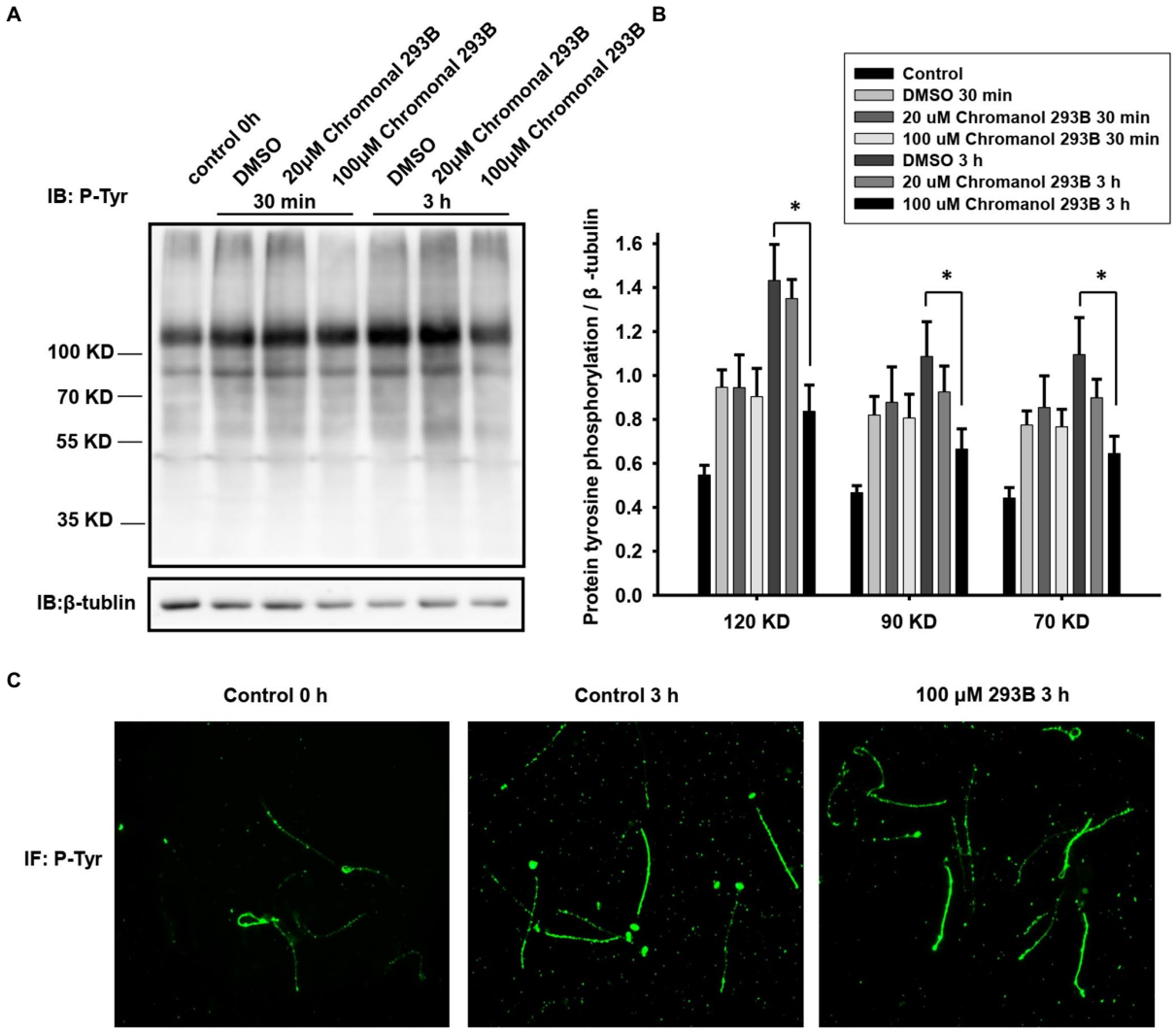

FIGURE 3 | Effect of chromanol 293B on protein tyrosine phosphorylation during human sperm capacitation. **(A)** Western blotting results showing the effect of chromanol 293B on protein tyrosine phosphorylation during human sperm capacitation. Sperm before capacitation incubation were used as the control group. Other sperm were treated with the vehicle control (DMSO), 20 μM chromanol 293B, and 100 μM chromanol 293B under capacitated conditions for 30 min and 3 h. Thereafter, sperm were lysed and then the proteins were resolved using 10% SDS-PAGE. Protein tyrosine phosphorylation was detected using a primary anti-phosphotyrosine antibody by Western blotting. Subsequently, the blot was stripped and probed with an anti-β-tubulin antibody as a loading control. The figure is representative of 6 separate experiments. The full uncropped immunoblots was provided in the supplementary data (**Supplementary Figure 2**). **(B)** The ratio of protein tyrosine phosphorylation levels to that of the loading control, β-tubulin. Values represent the means ± SEM of 6 experiments. For 100 μM chromanol 293B group compared to vehicle control group, $^{*}p < 0.05$. **(C)** Indirect immunofluorescence of protein tyrosine phosphorylation in human sperm before and after capacitation for 3 h. The figure is representative of 3 separate experiments.

channels are inhibited. Sperm treated with 100 μM chromanol 293B showed lower sperm motility and progressive motility. Treatment with 200 μM chromanol 293B significantly reduced sperm motility parameters, including sperm motility, progressive motility, VAP, VSL, VCL, BCF, STR, and LIN. However, the hyperactivation of human sperm in the chromanol 293B-treated groups and vehicle control was not significantly different (**Table 1**). This may also be because Slo1 or Slo3 potassium channels in human sperm play compensatory roles when KCNQ1 is inhibited. Many researchers have found that protein tyrosine phosphorylation is associated with sperm capacitation (Varano et al., 2008; Dona et al., 2011; Vyklicka and Lishko, 2020). Our research showed that protein tyrosine phosphorylation levels in the vehicle control group increased significantly after capacitation for 3 h. However, chromanol 293B decreased protein tyrosine phosphorylation levels in a dose-dependent manner after capacitation for 3 h (**Figure 3B**), suggesting that KCNQ1 is involved in human sperm function regulation. Chromanol 293B also changed the localization of phosphorylated tyrosine, reducing its levels in the equatorial region of human sperm (**Figure 3C**). Recently, Dona et al. found that the Cl^{-}/HCO_3^{-} exchanger SLC4A1(AE1) can be directly phosphorylated by Src family kinases, and the SLC4A1-Tyr-phosphorylation level in the apical region of sperm is involved in sperm capacitation. The inhibitors of SLC4A1 reduced

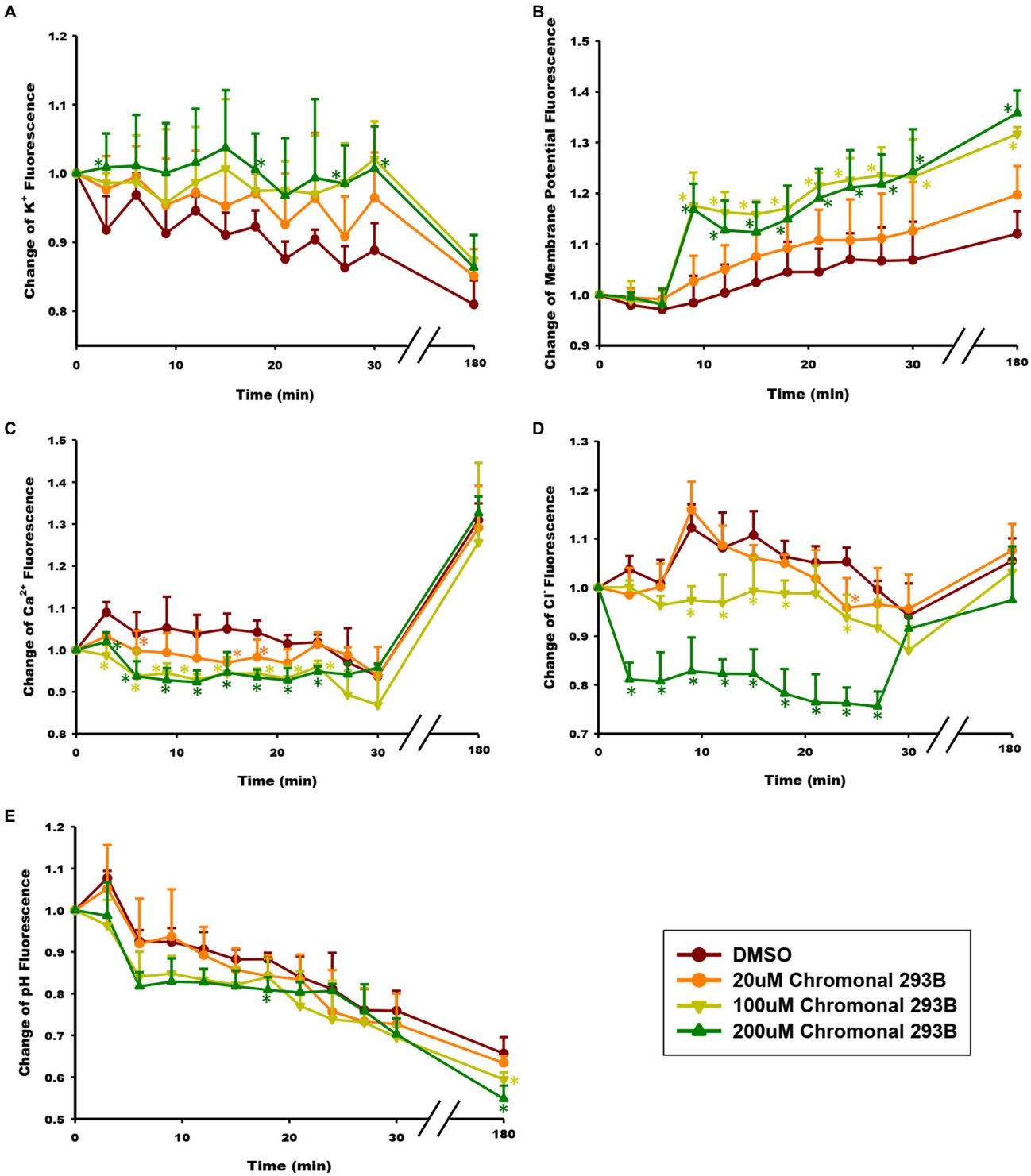

FIGURE 4 | Effect of chromanol 293B on ion homeostasis during human sperm capacitation. **(A)** Intracellular K^+ concentration ($[K^+]_i$) was detected using the K^+ fluorescence probe PBFI-AM. The fluorescence intensity was directly proportional to $[K^+]_i$. **(B)** Human sperm membrane potential (V_m) was analyzed using the fluorescence probe DisC3(5). The fluorescence intensity was directly proportional to V_m. **(C)** Intracellular Ca^{2+} concentration ($[Ca^{2+}]_i$) was detected using the Ca^{2+} fluorescence probe Fluo3-AM. The fluorescence intensity was directly proportional to $[Ca^{2+}]_i$. **(D)** Intracellular Cl^- concentration ($[Cl^-]_i$) was detected using the Cl^- fluorescence probe MQAE. The fluorescence intensity was inversely proportional to $[Cl^-]_i$. **(E)** Intracellular pH (pH_i) was analyzed using the pH fluorescence probe BCECF-AM. The fluorescence intensity was directly proportional to pH_i. All the data were acquired at 3 min intervals for 30 min during capacitating incubation. After capacitation for 3 h, the fluorescence signal was acquired again. Asterisks indicate the significant differences between samples and vehicle control at the same time point ($^*p < 0.05$). The exact P value were provided in the supplementary data (**Table S1**). Values represent the means ± SEM of 3 experiments.

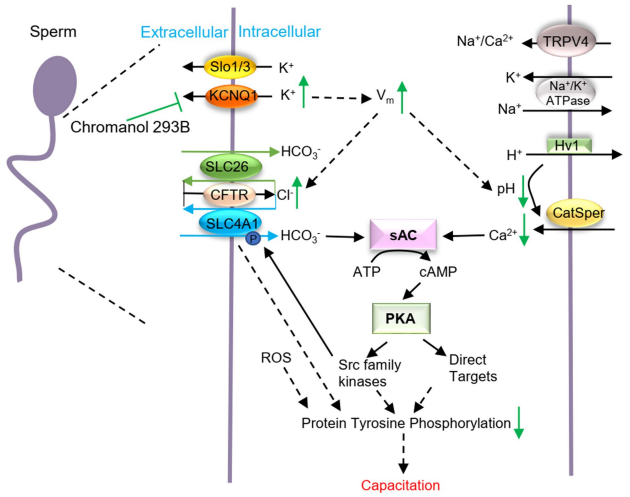

FIGURE 5 | Schematic representation of how KCNQ1 potassium channel regulates human sperm function. When human sperm are treated with chromanol 293B, the K^+ outflow currents mediated by KCNQ1 are inhibited, which causes a $[K^+]_i$ increase and the membrane depolarization. V_m changes regulate other voltage-gated channels and affect the electrical driving force for ions. Thus, $[Cl^-]_i$ increases, while the pH_i and $[Ca^{2+}]_i$ decreases. It is generally known that during capacitation, Ca^{2+} and HCO_3^- activate soluble adenylate cyclase (sAC) which converts ATP into cAMP. Then PKA can be activated. PKA subsequently activates target proteins and protein tyrosine phosphorylation levels increase. KCNQ1 in human sperm participates in ion homeostasis regulation and affects capacitation.

phosphorylated tyrosine levels in the head of human sperm, which is critical for AR (Dona et al., 2020). Other researchers have also found that protein tyrosine phosphorylation in the sperm head region is relevant to AR (Dona et al., 2011; Andrisani et al., 2015). Therefore, chromanol 293B changed the level and localization of protein tyrosine phosphorylation, which influenced the function of human sperm; however, the specific mechanisms remain unknown.

K^+ is involved in V_m regulation and its retention in sperm causes the $[K^+]_i$ to increase. During human sperm capacitation, V_m is always hyperpolarized, which is mainly due to the efflux of K^+ (Lopez-Gonzalez et al., 2014). We found that chromanol 293B depolarized human sperm V_m (**Figure 4B**), demonstrating that it inhibits KCNQ1 and increases $[K^+]_i$ and V_m (**Figure 5**). V_m then regulates ion homeostasis, as some channels in sperm are voltage-gated, and ions are also regulated by potential and chemical driving forces.

Ca^{2+} is the most important ion in sperm function during capacitation. During human sperm capacitation, $[Ca^{2+}]_i$ increases (Correia et al., 2015). We found that chromanol 293B decreased the $[Ca^{2+}]_i$ (**Figure 4C**). This may be because KCNQ1 inhibition causes V_m to increase, which then reduces the electrical driving force for Ca^{2+} influx (Clapham, 2013). Notably, Ca^{2+} is critical for sperm motility (Nowicka-Bauer and Szymczak-Cendlak, 2021), because it can bind to the motor protein dynein ATPase and regulate flagellar curvature (Wang et al., 2020). Thus, KCNQ1 inhibition decreases $[Ca^{2+}]_i$ and reduces sperm motility parameters. It is generally known that $[Ca^{2+}]_i$ and pH_i increase during human sperm capacitation. Ca^{2+} and HCO_3^- activate soluble adenylate cyclase (sAC), which converts ATP into cAMP. Protein kinase A (PKA) is subsequently activated and regulates its target proteins, and protein tyrosine phosphorylation levels increase (Allouche-Fitoussi and Breitbart, 2020; **Figure 5**). The decrease in $[Ca^{2+}]_i$ induced by chromanol 293B may explain the decrease in protein tyrosine phosphorylation levels during capacitation.

Furthermore, our results indicate that KCNQ1 inhibition increased $[Cl^-]_i$ (**Figure 4D**). This may be because chromanol 293B depolarizes sperm membrane and then increases the electrical driving force for Cl^-. The increasing of $[Cl^-]_i$ in our study indicates that Cl^- influx is greater than Cl^- efflux. In human sperm, the anion channel cystic fibrosis transmembrane conductance regulator (CFTR) mediates the influx of Cl^- (Xu et al., 2007). Solute carrier 26 (SLC26) family and SLC4A1 in human sperm are Cl^-/HCO_3^- exchangers. Chan et al. proposed that SLC26 family members take up HCO_3^- and export Cl^- with the interaction of CFTR. CFTR can provide the Cl^- through a recycling pathway (Chan et al., 2009; Chan and Sun, 2014; Puga Molina et al., 2018). Therefore, less Cl^- outflow accompanies less HCO_3^- influx, which leads to decreasing of intracellular pH and also disturbs sperm capacitation through sAC/cAMP/PKA pathway (**Figure 5**). Bachmann et al. found that chromanol 293B also blocked CFTR, with the IC50 fivefold higher than inhibition of KCNQ1/KCNE1 (Bachmann et al., 2001). However, some researchers observed no effect of chromanol 293B on Cl^- currents mediated by CFTR (Alzamora et al., 2011; Shimizu et al., 2014). CFTR inhibition theoretically reduces Cl^- influx and decreases $[Cl^-]_i$; however, our experiment showed that chromanol 293B increases $[Cl^-]_i$. These results suggest that chromanol 293B inhibits the KCNQ1 channel and indirectly regulates $[Cl^-]_i$ in human sperm. Others have also found that KCNQ1 indirectly regulates Cl^- secretion *via* CFTR in colonic cells by changing the electrical driving force, which is in accordance with our research (Preston et al., 2010; Alzamora et al., 2011).

Cytoplasmic alkalinization is another characteristic of sperm capacitation (Matamoros-Volante and Treviño, 2020). When human sperm were treated with chromanol 293B, the pH_i of the sperm decreased (**Figure 4E**), and such a decrease is not conducive to capacitation. In human sperm, the most important Ca^{2+} channel, CatSper, is activated by progesterone, membrane potential depolarization and cytoplasmic alkalinization (Sun et al., 2017). Chromanol 293B- mediated reduction in pH_i may further inhibit Ca^{2+} influx through CatSper and cause a decrease in $[Ca^{2+}]_i$, as observed in the present study.

In summary, we found that KCNQ1 is expressed in human sperm, localized in the head and tail regions and is partially co-localized with KCNE1. KCNQ1 participates in the regulation of ion homeostasis and affects the AR, sperm motility, and protein tyrosine phosphorylation during human sperm capacitation. It is likely that when KCNQ1 is inhibited in human sperm, the K^+ efflux is blocked, and the membrane potential is depolarized. The increase in membrane potential changes the electrical potential driving force of other ions and may influence other voltage-gated ion channels. Thus, ion homeostasis in human sperm is altered, including $[Ca^{2+}]_i$ and pH_i which are critical for capacitation (**Figure 5**). KCNQ1

is not the only potassium channel expressed in human sperm; there are many other important potassium channels, such as Slo1 and Slo3. These potassium channels may be able to help compensate if KCNQ1 is not fully functional. To verify the activity of the KCNQ1 channel in human sperm, its role in genetic male infertility should be studied in the future.

DATA AVAILABILITY STATEMENT

The raw data supporting the conclusions of this article will be made available by the authors, without undue reservation.

ETHICS STATEMENT

The studies involving human participants were reviewed and approved by Ethics committee of Hangzhou Medical College. The patients/participants provided their written informed consent to participate in this study.

AUTHOR CONTRIBUTIONS

PS designed the study. TG, KL, FL, JY, AL, YN, and PS performed the experiments. PS and TG analyzed the data and drafted the paper. All authors read and approved the submitted and final versions.

FUNDING

This research was funded by National Natural Science Foundation of China (Nos. 81801525 and 81771647), Health Sci&Tech Plan Project of Zhejiang Province (Nos. 2018KY039 and 2019KY363), Natural Science Foundation of Zhejiang Province (No. LQ17H040004), Special Project for the Research Institutions of Zhejiang Province (Nos. YS2021014, C11920D-04 and YS2021011), Zhejiang Province Program for the Cultivation of High-level innovative Health Talents (Year 2018).

ACKNOWLEDGMENTS

We thank all the donors who participated in this study. We thank Hanchen Ni for the helping in experiments.

SUPPLEMENTARY MATERIAL

The Supplementary Material for this article can be found online at: https://www.frontiersin.org/articles/10.3389/fphys.2021.761910/full#supplementary-material

REFERENCES

Allouche-Fitoussi, D., and Breitbart, H. (2020). The role of zinc in male fertility. *Int. J. Mol. Sci.* 21:7796. doi: 10.3390/ijms21207796

Alzamora, R., O'Mahony, F., Ko, W. H., Yip, T. W., Carter, D., Irnaten, M., et al. (2011). Berberine reduces cAMP-induced chloride secretion in T84 human colonic carcinoma cells through inhibition of basolateral KCNQ1 channels. *Front. Physiol.* 2:33. doi: 10.3389/fphys.2011.00033

Andrisani, A., Dona, G., Tibaldi, E., Brunati, A. M., Sabbadin, C., Armanini, D., et al. (2015). Astaxanthin improves human sperm capacitation by inducing Lyn displacement and activation. *Mar. Drugs* 13, 5533–5551. doi: 10.3390/md13095533

Bachmann, A., Quast, U., and Russ, U. (2001). Chromanol 293B, a blocker of the slow delayed rectifier K+ current (IKs), inhibits the CFTR cl- current. *Naunyn Schmiedeberg's Arch. Pharmacol.* 363, 590–596. doi: 10.1007/s002100100410

Battistone, M. A., Da Ros, V. G., Salicioni, A. M., Navarrete, F. A., Krapf, D., Visconti, P. E., et al. (2013). Functional human sperm capacitation requires both bicarbonate-dependent PKA activation and down-regulation of Ser/Thr phosphatases by Src family kinases. *Mol. Hum. Reprod.* 19, 570–580. doi: 10.1093/molehr/gat033

Bernecic, N. C., Gadella, B. M., Leahy, T., and de Graaf, S. P. (2019). Novel methods to detect capacitation-related changes in spermatozoa. *Theriogenology* 137, 56–66. doi: 10.1016/j.theriogenology.2019.05.038

Bett, G. C. L., Morales, M. J., Beahm, D. L., Duffey, M. E., and Rasmusson, R. L. (2006). Ancillary subunits and stimulation frequency determine the potency of chromanol 293B block of the KCNQ1 potassium channel. *J. Physiol.* 576, 755–767. doi: 10.1113/jphysiol.2006.116012

Börjesson, S. I., and Elinder, F. (2008). Structure, function, and modification of the voltage sensor in voltage-gated ion channels. *Cell Biochem. Biophys.* 52, 149–174. doi: 10.1007/s12013-008-9032-5

Brenker, C., Zhou, Y., Muller, A., Echeverry, F. A., Trotschel, C., Poetsch, A., et al. (2014). The Ca2+−activated K+ current of human sperm is mediated by Slo3. *elife* 3:e01438. doi: 10.7554/eLife.01438

Brown, S. G., Publicover, S. J., Barratt, C. L. R., and Martins da Silva, S. J. (2019). Human sperm ion channel (dys)function: implications for fertilization. *Hum. Reprod. Update* 25, 758–776. doi: 10.1093/humupd/dmz032

Brown, S. G., Publicover, S. J., Mansell, S. A., Lishko, P. V., Williams, H. L., Ramalingam, M., et al. (2016). Depolarization of sperm membrane potential is a common feature of men with subfertility and is associated with low fertilization rate at IVF. *Hum. Reprod.* 31, 1147–1157. doi: 10.1093/humrep/dew056

Catterall, W. A. (2010). Ion channel voltage sensors: structure, function, and pathophysiology. *Neuron* 67, 915–928. doi: 10.1016/j.neuron.2010.08.021

Chan, H. C., Ruan, Y. C., He, Q., Chen, M. H., Chen, H., Xu, W. M., et al. (2009). The cystic fibrosis transmembrane conductance regulator in reproductive health and disease. *J. Physiol.* 587, 2187–2195. doi: 10.1113/jphysiol.2008.164970

Chan, H. C., and Sun, X. (2014). SLC26 anion exchangers in uterine epithelial cells and spermatozoa: clues from the past and hints to the future. *Cell Biol. Int.* 38, 1–7. doi: 10.1002/cbin.10183

Clapham, D. E. (2013). Sperm BerserKers. *elife* 2:e01469. doi: 10.7554/eLife.01469

Correia, J., Michelangeli, F., and Publicover, S. (2015). Regulation and roles of Ca2+ stores in human sperm. *Reproduction* 150, R65–R76. doi: 10.1530/REP-15-0102

De Jonge, C. (2017). Biological basis for human capacitation-revisited. *Hum. Reprod. Update* 23, 289–299. doi: 10.1093/humupd/dmw048

Dixit, G., Dabney-Smith, C., and Lorigan, G. A. (2020). The membrane protein KCNQ1 potassium ion channel: functional diversity and current structural insights. *Biochim. Biophys. Acta Biomembr.* 1862:183148. doi: 10.1016/j.bbamem.2019.183148

Dona, G., Fiore, C., Tibaldi, E., Frezzato, F., Andrisani, A., Ambrosini, G., et al. (2011). Endogenous reactive oxygen species content and modulation of tyrosine phosphorylation during sperm capacitation. *Int. J. Androl.* 34, 411–419. doi: 10.1111/j.1365-2605.2010.01097.x

Dona, G., Tibaldi, E., Andrisani, A., Ambrosini, G., Sabbadin, C., Pagano, M. A., et al. (2020). Human sperm capacitation involves the regulation of the Tyr-phosphorylation level of the anion exchanger 1 (AE1). *Int. J. Mol. Sci.* 21:4063. doi: 10.3390/ijms21114063

Lerche, C., Bruhova, I., Lerche, H., Steinmeyer, K., Wei, A. D., Strutz-Seebohm, N., et al. (2007). Chromanol 293B binding in KCNQ1 (Kv7.1) channels involves electrostatic interactions with a potassium ion in the selectivity filter. *Mol. Pharmacol.* 71, 1503–1511. doi: 10.1124/mol.106.031682

Li, K., Sun, P., Wang, Y., Gao, T., Zheng, D., Liu, A., et al. (2021). Hsp90 interacts with Cdc37, is phosphorylated by PKA/PKC, and regulates Src phosphorylation in human sperm capacitation. *Andrology* 9, 185–195. doi: 10.1111/andr.12862

Li, K., Xue, Y., Chen, A., Jiang, Y., Xie, H., Shi, Q., et al. (2014). Heat shock protein 90 has roles in intracellular calcium homeostasis, protein tyrosine phosphorylation regulation, and progesterone-responsive sperm function in human sperm. *PLoS One* 9:e115841. doi: 10.1371/journal.pone.0115841

Lishko, P. V., Kirichok, Y., Ren, D., Navarro, B., Chung, J. J., and Clapham, D. E. (2012). The control of male fertility by spermatozoan ion channels. *Annu. Rev. Physiol.* 74, 453–475. doi: 10.1146/annurev-physiol-020911-153258

Lopez-Gonzalez, I., Torres-Rodriguez, P., Sanchez-Carranza, O., Solis-Lopez, A., Santi, C. M., Darszon, A., et al. (2014). Membrane hyperpolarization during human sperm capacitation. *Mol. Hum. Reprod.* 20, 619–629. doi: 10.1093/molehr/gau029

Lopez-Torres, A. S., and Chirinos, M. (2017). Modulation of human sperm capacitation by progesterone, estradiol, and luteinizing hormone. *Reprod. Sci.* 24, 193–201. doi: 10.1177/1933719116641766

Mannowetz, N., Naidoo, N. M., Choo, S. A., Smith, J. F., and Lishko, P. V. (2013). Slo1 is the principal potassium channel of human spermatozoa. *elife* 2:e01009. doi: 10.7554/eLife.01009

Mansell, S. A., Publicover, S. J., Barratt, C. L. R., and Wilson, S. M. (2014). Patch clamp studies of human sperm under physiological ionic conditions reveal three functionally and pharmacologically distinct cation channels. *Mol. Hum. Reprod.* 20, 392–408. doi: 10.1093/molehr/gau003

Martinez-Lopez, P., Santi, C. M., Trevino, C. L., Ocampo-Gutierrez, A. Y., Acevedo, J. J., Alisio, A., et al. (2009). Mouse sperm K+ currents stimulated by pH and cAMP possibly coded by Slo3 channels. *Biochem. Biophys. Res. Commun.* 381, 204–209. doi: 10.1016/j.bbrc.2009.02.008

Matamoros-Volante, A., and Treviño, C. L. (2020). Capacitation-associated alkalization in human sperm is differentially controlled at the subcellular level. *J. Cell Sci.* 133:23886. doi: 10.1242/jcs.238816

Nakajo, K., and Kubo, Y. (2015). KCNQ1 channel modulation by KCNE proteins *via* the voltage-sensing domain. *J. Physiol.* 593, 2617–2625. doi: 10.1113/jphysiol.2014.287672

Nowicka-Bauer, K., and Szymczak-Cendlak, M. (2021). Structure and function of ion channels regulating sperm motility-An overview. *Int. J. Mol. Sci.* 22:3259. doi: 10.3390/ijms22063259

Preston, P., Wartosch, L., Gunzel, D., Fromm, M., Kongsuphol, P., Ousingsawat, J., et al. (2010). Disruption of the K+ channel beta-subunit KCNE3 reveals an important role in intestinal and tracheal cl- transport. *J. Biol. Chem.* 285, 7165–7175. doi: 10.1074/jbc.M109.047829

Puga Molina, L. C., Luque, G. M., Balestrini, P. A., Marin-Briggiler, C. I., Romarowski, A., and Buffone, M. G. (2018). Molecular basis of human sperm capacitation. *Front. Cell Dev. Biol.* 6:72. doi: 10.3389/fcell.2018.00072

Roepke, T. K., Anantharam, A., Kirchhoff, P., Busque, S. M., Young, J. B., Geibel, J. P., et al. (2006). The KCNE2 potassium channel ancillary subunit is essential for gastric acid secretion. *J. Biol. Chem.* 281, 23740–23747. doi: 10.1074/jbc.M604155200

Santi, C. M., Martinez-Lopez, P., de la Vega-Beltran, J. L., Butler, A., Alisio, A., Darszon, A., et al. (2010). The SLO3 sperm-specific potassium channel plays a vital role in male fertility. *FEBS Lett.* 584, 1041–1046. doi: 10.1016/j.febslet.2010.02.005

Shimizu, T., Fujii, T., Takahashi, Y., Takahashi, Y., Suzuki, T., Ukai, M., et al. (2014). Up-regulation of Kv7.1 channels in thromboxane A2-induced colonic cancer cell proliferation. *Pflugers Arch.* 466, 541–548. doi: 10.1007/s00424-013-1341-x

Sun, J., and MacKinnon, R. (2017). Cryo-EM structure of a KCNQ1/CaM complex reveals insights into congenital long QT syndrome. *Cell* 169:e1049. doi: 10.1016/j.cell.2017.05.019

Sun, J., and MacKinnon, R. (2020). Structural basis of human KCNQ1 modulation and gating. *Cell* 180:e349. doi: 10.1016/j.cell.2019.12.003

Sun, P., Wang, Y., Gao, T., Li, K., Zheng, D., Liu, A., et al. (2021). Hsp90 modulates human sperm capacitation *via* the Erk1/2 and p38 MAPK signaling pathways. *Reprod. Biol. Endocrinol.* 19:39. doi: 10.1186/s12958-021-00723-2

Sun, X. H., Zhu, Y. Y., Wang, L., Liu, H. L., Ling, Y., Li, Z. L., et al. (2017). The Catsper channel and its roles in male fertility: a systematic review. *Reprod. Biol. Endocrinol.* 15:65. doi: 10.1186/s12958-017-0281-2

Tian, C., Vanoye, C. G., Kang, C., Welch, R. C., Kim, H. J., George, A. L. Jr., et al. (2007). Preparation, functional characterization, and NMR studies of human KCNE1, a voltage-gated potassium channel accessory subunit associated with deafness and long QT syndrome. *Biochemistry* 46, 11459–11472. doi: 10.1021/bi700705j

Tsevi, I., Vicente, R., Grande, M., Lopez-Iglesias, C., Figueras, A., Capella, G., et al. (2005). KCNQ1/KCNE1 channels during germ-cell differentiation in the rat: expression associated with testis pathologies. *J. Cell. Physiol.* 202, 400–410. doi: 10.1002/jcp.20132

Varano, G., Lombardi, A., Cantini, G., Forti, G., Baldi, E., and Luconi, M. (2008). Src activation triggers capacitation and acrosome reaction but not motility in human spermatozoa. *Hum. Reprod.* 23, 2652–2662. doi: 10.1093/humrep/den314

Visconti, P. E., Krapf, D., de la Vega-Beltran, J. L., Acevedo, J. J., and Darszon, A. (2011). Ion channels, phosphorylation and mammalian sperm capacitation. *Asian J. Androl.* 13, 395–405. doi: 10.1038/aja.2010.69

Vyklicka, L., and Lishko, P. V. (2020). Dissecting the signaling pathways involved in the function of sperm flagellum. *Curr. Opin. Cell Biol.* 63, 154–161. doi: 10.1016/j.ceb.2020.01.015

Wang, H., McGoldrick, L. L., and Chung, J.-J. (2020). Sperm ion channels and transporters in male fertility and infertility. *Nat. Rev. Urology* 18, 46–66. doi: 10.1038/s41585-020-00390-9

Wu, X., and Larsson, H. P. (2020). Insights into cardiac IKs (KCNQ1/KCNE1) channels regulation. *Int. J. Mol. Sci.* 21:9440. doi: 10.3390/ijms21249440

Xu, W. M., Shi, Q. X., Chen, W. Y., Zhou, C. X., Ni, Y., Rowlands, D. K., et al. (2007). Cystic fibrosis transmembrane conductance regulator is vital to sperm fertilizing capacity and male fertility. *Proc. Natl. Acad. Sci. U. S. A.* 104, 9816–9821. doi: 10.1073/pnas.0609253104

Yang, W. P., Levesque, P. C., Little, W. A., Conder, M. L., Shalaby, F. Y., and Blanar, M. A. (1997). KvLQT1, a voltage-gated potassium channel responsible for human cardiac arrhythmias. *Proc. Natl. Acad. Sci. U. S. A.* 94, 4017–4021. doi: 10.1073/pnas.94.8.4017

Yeung, C. H., and Cooper, T. G. (2008). Potassium channels involved in human sperm volume regulation--quantitative studies at the protein and mRNA levels. *Mol. Reprod. Dev.* 75, 659–668. doi: 10.1002/mrd.20812

Zeng, X. H., Yang, C., Kim, S. T., Lingle, C. J., and Xia, X. M. (2011). Deletion of the Slo3 gene abolishes alkalization-activated K+ current in mouse spermatozoa. *Proc. Natl. Acad. Sci. U. S. A.* 108, 5879–5884. doi: 10.1073/pnas.1100240108

Conflict of Interest: The authors declare that the research was conducted in the absence of any commercial or financial relationships that could be construed as a potential conflict of interest.

Publisher's Note: All claims expressed in this article are solely those of the authors and do not necessarily represent those of their affiliated organizations, or those of the publisher, the editors and the reviewers. Any product that may be evaluated in this article, or claim that may be made by its manufacturer, is not guaranteed or endorsed by the publisher.

Copyright © 2021 Gao, Li, Liang, Yu, Liu, Ni and Sun. This is an open-access article distributed under the terms of the Creative Commons Attribution License (CC BY). The use, distribution or reproduction in other forums is permitted, provided the original author(s) and the copyright owner(s) are credited and that the original publication in this journal is cited, in accordance with accepted academic practice. No use, distribution or reproduction is permitted which does not comply with these terms.

frontiers in Endocrinology

ORIGINAL RESEARCH
published: 10 November 2021
doi: 10.3389/fendo.2021.779183

Check for updates

OPEN ACCESS

Edited by:
Rick Francis Thorne,
The University of Newcastle, Australia

Reviewed by:
Wei Wu,
Nanjing Medical University, China
Fang Fang,
University of Science and Technology of China, China
Shuo Zhang,
Fudan University, China

***Correspondence:**
Ya-Jing Liu
yjl@ustc.edu.cn
Jin-Ping Qiao
jpqiao@ahmu.edu.cn
Xin Du
duxinbio@gmail.com
Yun-Xia Cao
caoyunxia6@126.com

†*These authors have contributed equally to this work*

Specialty section:
This article was submitted to Reproduction, a section of the journal Frontiers in Endocrinology

Received: *18 September 2021*
Accepted: *18 October 2021*
Published: *10 November 2021*

Citation:
Liu Y-J, Xing F, Zong K, Wang M-Y, Ji D-M, Zhao Y-H, Xia Y-H, Wang A, Shi L-G, Ding S-M, Wei Z-L, Qiao J-P, Du X and Cao Y-X (2021) Increased ApoE Expression in Follicular Fluid and the ApoE Genotype Are Associated With Endometriosis in Chinese Women. Front. Endocrinol. 12:779183. doi: 10.3389/fendo.2021.779183

Increased ApoE Expression in Follicular Fluid and the ApoE Genotype Are Associated With Endometriosis in Chinese Women

Ya-Jing Liu[1,2,3,4,5†], Fen Xing[1,2,3,4,5†], Kai Zong[6†], Meng-Yao Wang[1,2,3,4,5], Dong-Mei Ji[1,2,3,4,5], Yu-Hang Zhao[7], Yun-He Xia[7], An Wang[7], Ling-Ge Shi[1,2,3,4,5], Si-Min Ding[1,2,3,4,5], Zhao-Lian Wei[1,2,3,4,5], Jin-Ping Qiao[8*], Xin Du[9*] and Yun-Xia Cao[1,2,3,4,5*]*

[1] Reproductive Medicine Center, Department of Obstetrics and Gynecology, The First Affiliated Hospital of Anhui Medical University, Hefei, China, [2] National Health Commission (NHC) Key Laboratory of Study on Abnormal Gametes and Reproductive Tract, Anhui Medical University, Hefei, China, [3] Key Laboratory of Population Health Across Life Cycle (Anhui Medical University), Ministry of Education of the People's Republic of China, Hefei, China, [4] Anhui Province Key Laboratory of Reproductive Health and Genetics, Anhui Medical University, Hefei, China, [5] Biopreservation and Artificial Organs, Anhui Provincial Engineering Research Center, Anhui Medical University, Hefei, China, [6] Technical Center of Hefei Customs District, Hefei, China, [7] First Clinical Medical College, Anhui Medical University, Hefei, China, [8] Department of Clinical Laboratory, The First Affiliated Hospital of Anhui Medical University, Hefei, China, [9] 901st Hospital of People's Liberation Army (PLA) Joint Logistic Support Force, Hefei, China

More than 10% of women suffer from endometriosis (EMT) during their reproductive years. EMT can cause pain and infertility and requires further study from multiple perspectives. Previous reports have indicated that an increase inapolipoprotein E (ApoE) may be associated with a lower number of retrieved mature oocytes in older women, and an association between ApoE and spontaneous pregnancy loss may exist in patients with EMT. The purpose of this study was to investigate the existence of an increase in ApoE in follicular fluid (FF) and the possible relationship between ApoE and EMT in Chinese women. In the current study, 217 Chinese women (111 control subjects and 106 EMT patients) were included. The ApoE genotypes were identified by Sanger sequencing. We found that ApoE expression in FF was higher in patients with EMT than in the control group. In addition, a significant difference in ApoE4 carriers ($\epsilon3/\epsilon4$, $\epsilon4/\epsilon4$) was found between the control subjects and the patients with EMT. Furthermore, a nonparametric test revealed significant differences in the numbers of blastocysts and high-quality blastocysts, but not the hormone levels of FSH, LH, and E2, between the two groups. We also established a multifactor (BMI, high-quality blastocysts, and $\epsilon4$) prediction model with good sensitivity for identifying patients who may suffer from EMT. Our results

demonstrate that ApoE expression in FF is increased in EMT, the ApoE-ϵ4 allele is significantly linked to EMT, and a combined analysis of three factors (BMI, high-quality blastocysts, and ϵ4) could be used as a predictor of EMT.

Keywords: apolipoprotein E, endometriosis, follicular fluid, genotype, multifactor prediction model

INTRODUCTION

Endometriosis (EMT), which is a common disease in women of reproductive age (1), is characterized by a chronic inflammatory process (2, 3) in which endometrial tissue grows outside the uterine body. EMT affects more than 10% of women of reproductive age in the world, and approximately 30%–50% of these women experience chronic pain and infertility (4). The specific etiology of EMT has not yet been clarified, and its incidence may be associated with a countercurrent flow of menstrual blood, sex hormone disorders, immune factors, and genetic factors (5). Thus, an investigation of the factors contributing to EMT might be crucial to elucidating its etiology.

An increasing number of studies indicate that apolipoprotein E (ApoE) is linked to inflammation and disease risk, and a higher proinflammatory state is associated with the ϵ4 allele (6). ApoE, which is a multifunctional protein that is widely found in mammals, consists of 299 amino acids and has a molecular mass of 34 kDa (7). ApoE is a component of very low-density lipoprotein, which transports peripheral cholesterol to the liver for metabolism. Thus, the important role of ApoE in lipid transport has been widely studied (8, 9). The ApoE genotype also affects the cholesterol and lipid levels in plasma and brain (10). The human ApoE gene is encoded by the long arm of chromosome 19. ApoE is primarily synthesized in liver and brain tissues and is also expressed in the adrenal gland, ovary, kidney, and skeletal muscle (11). In addition, both rat and human ovarian granulosa cells produce ApoE *in vitro*. Polymorphisms in ApoE were first proposed by Utermann (12). The three most common isoforms of ApoE are ApoE2, ApoE3, and ApoE4, and these combine to form six genotypes: ϵ2/ϵ2, ϵ3/ϵ3, ϵ4/ϵ4, ϵ2/ϵ3, ϵ2/ϵ4, and ϵ3/ϵ4. The differences between these genotypes are mainly due to differences in the amino acids at positions 112 and 158 in the amino acid chain of the protein. ApoE3 contains a cysteine residue at position 112 and an arginine residue at position 158 (E3=Cys112/Arg158), whereas ApoE2 has cysteine residues at both positions (E2=Cys112/Cys158), and ApoE4 contains arginine residues at both sites (E4=Arg112/Arg158) (13). ApoE-ϵ4 is a risk factor for a variety of diseases, such as Alzheimer's disease (AD) (14), cardiovascular disease (15), and hyperlipidemia (16). ApoE is a major source of cholesterol precursors for the synthesis of ovarian estrogen and progesterone (13), and a relationship between the serum estrogen level and ApoE exists in human ovarian follicular fluid (FF) (17), which suggests that ApoE might play an important role in the ovary. Furthermore, a previous study indicated that an increase in the ApoE levels might be linked to a lower number of retrieved mature oocytes in older women (18), and an association between ApoE and spontaneous pregnancy loss may exist in patients with EMT (19). This study aimed to investigate whether ApoE expression is increased in FF and explore the possible association between APOE genotypes and EMT in Chinese women.

MATERIALS AND METHODS

Subjects

The control group consisted of subjects undergoing *in vitro* fertilization and embryo transfer (IVF-ET) for tubal factors and/or male factor infertility in the Reproductive Medicine Center, the First Affiliated Hospital of Anhui Medical University. The experimental group consisted of patients diagnosed with EMT at the First Affiliated Hospital of Anhui Medical University. A total of 111 controls and 106 patients with EMT were enrolled in this study. The majority of the patients with EMT included in the study were diagnosed with ovarian chocolate cysts, and the rest of the patients with EMT were diagnosed laparoscopically. The inclusion criteria were as follows: (1) patients who met the clinical diagnostic criteria for EMT (20); (2) patients aged 21–36 years; and (3) patients who voluntarily participated in the study and signed informed consent forms. The exclusion criteria were as follows: (1) patients with malignant tumors; (2) patients with metabolic diseases; and (3) patients with serious endocrine diseases. This study was approved by the Medical Ethics Committee of the First Affiliated Hospital of Anhui Medical University. Each subject provided written informed consent prior to entering the study.

Determination of the ApoE Genotype

DNA was extracted from peripheral blood samples. Primers were designed, and PCR amplification was performed. Sanger sequencing was used to determine the APOE genotype.

Follicular Fluid Collection

Follicular fluid (FF) was collected from women undergoing *in vitro* fertilization and embryo transfer (IVF-ET) after obtaining informed patient consent and approval from the ethical committees at the First Affiliated Hospital of Anhui Medical University. Briefly, after retrieval of the cumulus-oocyte complex, the discarded FF was centrifuged for 10 min at 12,000 rpm and 4°C. The supernatant was collected and maintained at −80°C until assayed.

Western Blot

Protein was extracted from FF according to a previously reported procedure. The denatured protein was separated by 12% SDS-PAGE and transferred to a PVDF membrane. Then, the membranes were blocked with 5% nonfat dry milk diluted

with Tris-buffered saline with Tween 20 (TBST) for 2 h and incubated with antihuman ApoE antibody (1:5,000) and tubulin (Sigma) (1:10,000) overnight at 4°C. The next day, the membranes were washed three times in TBST and incubated with horseradish peroxidase (HRP)-conjugated rabbit antigoat or goat antirabbit secondary antibodies for 1.5 h at room temperature. The protein bands were detected using an enhanced chemiluminescence detection system (Bio-Rad, Hercules, CA, USA).

Data Analysis

The average values ± standard deviations were used to describe the general characteristics of the control group and patients with EMT, and the APOE alleles (ϵ2, ϵ3, and ϵ4) were examined against Hardy-Weinberg equilibrium by χ^2 test. The counting data were tested by *t*-test, nonparametric test, or χ^2 test, and all the data were analyzed using SPSS 23 software. $p < 0.05$ was considered to indicate statistical significance. Univariate analysis was performed to identify the variables with significant differences between the two groups. Multivariate logistic regression analysis was conducted to construct a histogram model for predicting endometriosis using R4.0.3.

RESULTS

ApoE Levels in the FF of the Control Group and Patients With EMT

The follicular microenvironment in patients with EMT is closely related to infertility; thus, ApoE expression was detected in the FF of patients with EMT. As shown in **Figures 1A, B**, ApoE expression was higher in the FF of patients in the EMT group than in that of the control subjects ($p < 0.05$). ApoE genotypes were confirmed by Sanger sequencing (**Figures 1C–G**).

Descriptive Characteristics of the Control and EMT Groups

The general characteristics of the control group and the patients with EMT are shown in **Table 1**. The control group included 111 subjects between 23 and 34 years of age, and the EMT group included 106 patients between 21 and 36 years of age. No significant differences in age ($p = 0.055$), infertility time ($p = 0.065$), or egg number retrieved ($p = 0.091$) were detected between the groups, but significant differences in the BMI ($p = 0.024$), number of blastocysts ($p = 0.018$), and number of high-quality blastocysts ($p = 0.004$) were found.

The frequencies of APOE genotypes in the control and EMT groups were as follows: control group, 0 for ϵ2/ϵ2, 1.8% for ϵ2/ϵ3, 0 for ϵ2/ϵ4, 92.8% for ϵ3/ϵ3, 4.5% for ϵ3/ϵ4, and 0.9% for ϵ4/ϵ4; patients with EMT, 0 for ϵ2/ϵ2, 13.2% for ϵ2/ϵ3, 1.9% for ϵ2/ϵ4, 68% for ϵ3/ϵ3, 13.2% for ϵ3/ϵ4, and 3.7% for ϵ4/ϵ4 (**Table 2**). The distribution of ApoE genotypes in both the control and EMT groups followed Hardy-Weinberg equilibrium (**Table 2**).

Association of the ApoE Genotype With EMT

In this study, we analyzed associations among the ApoE genotypes in the control and EMT groups. Interestingly, a

TABLE 1 | General characteristics of control subjects and patients with EMT.

Parameters	Control (*n* = 111)	EMT (*n* = 106)	*t*/*z*	*p*-value
Age	28.369 ± 2.347	29.094 ± 3.109	−1.932	0.055
BMI (kg/m^2)	22.661 ± 3.968	21.626 ± 2.636	2.275	0.024*
Infertility time	3 (2, 4)	2 (1, 4)	−1.846	0.065
Numbers of eggs	12 (9, 20)	11 (7, 17)	−1.688	0.091
Numbers of blastocysts	5 (3, 8)	3.5 (2, 6)	−2.369	0.018*
High-quality blastocysts	5 (2, 7)	3 (1, 5)	−2.888	0.004**

*The values show the means ± SD or medians. Student's t-test and χ^2 were performed. BMI, body mass index. Six individuals were included in the statistical analysis. *p < 0.05; **p < 0.01.*

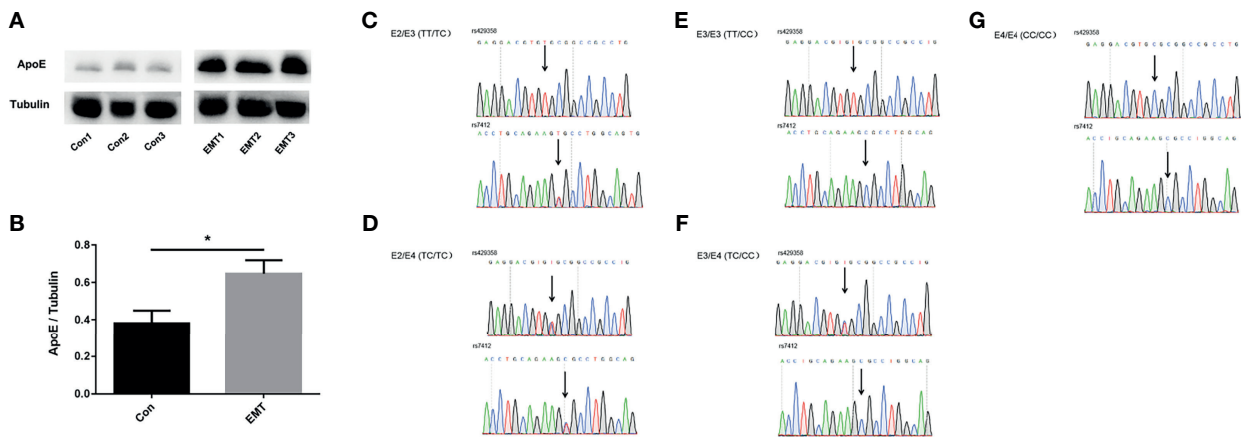

FIGURE 1 | ApoE levels in the follicular fluid (FF) of the control group and patients with EMT. **(A, B)** Representative Western blotting results showing ApoE expression in the FF of the control subjects and the patients with EMT. Tubulin was used as an internal control. The data are expressed as the means ± SEMs; *$p < 0.05$. **(C–G)** Representative Sanger sequencing for E2/E3,E2/E4,E3/E3, E3/E4,E4/E4 genotype; The arrows indicate the positionof the single nucleotide polymorphism.

TABLE 2 | Frequencies of the ApoE genotype and frequencies in the control group and patients with EMT.

	Control (%)	EMT (%)	*p*-value
Genotype			
ϵ2/ϵ2	0 (0)	0 (0)	
ϵ2/ϵ3	2 (1.8)	14 (13.2)	
ϵ2/ϵ4	0 (0)	2 (1.9)	
ϵ3/ϵ3	103 (92.8)	72 (68.0)	
ϵ3/ϵ4	5 (4.5)	14 (13.2)	
ϵ4/ϵ4	1 (0.9)	4 (3.7)	
Allele frequency			
ϵ2	2 (0.9)	16 (7.5)	
ϵ3	213 (95.9)	172 (81.1)	
ϵ4	7 (3)	24 (11.3)	
H-W-E *p*-value	0.104	0.114	
ApoE-ϵ4			
ϵ3/ϵ4, ϵ4/ϵ4	6 (5.4)	18 (16.9)	0.006**

*χ^2 test was performed. **p < 0.01.*

higher number of E4 carriers (ϵ3/ϵ4, ϵ4/ϵ4) was found in the EMT group than in the control group (**Table 2**, $p < 0.01$).

Hormone Levels in the Control and EMT Groups

The differences in hormone levels between the control group and the patients with EMT are shown in **Table 3**. No statistically significant differences in the levels of FSH ($p = 0.798$), LH ($p = 0.930$), or E2 ($p = 0.172$) were detected.

Prediction Model for Patients With EMT

As shown in **Figure 2A**, the results of the multivariate analysis showed that the BMI, high-quality blastocysts, and ApoE-ϵ4 were influencing factors for EMT. We then established a prediction model for patients suffering from EMT (**Figure 2B**). Receiver operating characteristic (ROC) analysis is usually used as a performance indicator to evaluate the quality of a prediction model. The area under the ROC curve (AUC) can be employed to assess the accuracy of the predictions made by the prediction model. To test the predictive ability of the established model for patients with EMT, the multifactor sensitivity (**Figure 3A**, AUC = 0.693) and each of the three factors sensitivity (**Figure 3B**, BMI, AUC = 0.554; high-quality blastocysts, AUC = 0.613; ApoE-ϵ4, AUC = 0.558) of the model for predicting EMT were investigated. We found that the multifactor prediction model exhibited better sensitivity than the single-factor prediction model. Subsequently, a correction curve was generated using the prediction model for patients suffering from EMT (**Figure 3C**).

DISCUSSION

In the present study, we investigated whether ApoE plays a vital role in the pathogenesis of EMT and found that ApoE expression was increased in the FF of patients with EMT compared with that of the control subjects. In addition, we analyzed the differences in the ApoE genotypes between the control and EMT groups. We found a higher number of E4 carriers (ϵ3/ϵ4, ϵ4/ϵ4) in the EMT group than in the control group ($p < 0.01$), which suggests an important role of ApoE-ϵ4 in the pathogenesis of EMT.

TABLE 3 | FSH/LH/E2 levels in the control group and patients with EMT.

Parameters	Control (*n* = 111)	EMT (*n* = 106)	*t/z*	*p*-value
FSH	7.30 (6.27,8.55)	7.30 (5.74,8.88)	−0.256	0.798
LH	4.42 (3.27, 6.07)	4.75 (3.36, 5.83)	−0.088	0.930
E2	128 (59.5, 227.75)	156.5 (72.25, 238.30)	−1.365	0.172

Nonparametric test analysis was performed.

Previous studies have shown that ϵ3 is the most abundant ApoE genotype in the human population, with a frequency of 49%–90%, followed by ϵ4 with a frequency of 5%–37%, and ϵ2 was the least abundant genotype, with a frequency of 0%–14% (14). These findings are consistent with our analytical results that showed the proportion of ϵ3 was highest in both the control and EMT groups and that the proportion of ϵ2 in the control group was as low as 1.8%. Most studies on ApoE have focused on cardiovascular disease and Alzheimer's disease risks due to its role related to lipids (21). However, the effects of ApoE go far beyond these diseases because this protein can affect a number of diseases, such as fertility, diabetes, and obesity (22–24).

ApoE is expressed in the endometrium and granulosa cells of the ovary to varying degrees (13). The involvement of lipoproteins and sterols in the regulation of ovarian function is complex due to the multitude of cell types and compartments in ovarian follicles. It has been reported that the growth of follicles is affected by the synthesis of hormones and growth factors (25), including ApoE, and the increase in ApoE observed in older women might be associated with the lower number of retrieved mature oocytes (18). Furthermore, an association between ApoE and spontaneous pregnancy loss might exist in patients with EMT (19), which suggests that ApoE plays a vital role in the pathogenesis of EMT. These findings are consistent with our results that the level of ApoE in the FF of patients with EMT was significantly higher than that in the FF of control subjects ($p < 0.05$).

This study revealed a difference in the BMI between the two groups ($p = 0.024$), which is consistent with the previous finding that patients with EMT have a lower BMI than control subjects (20). Although no significant difference in the number of eggs was found between the two groups ($p = 0.091$), we found that the numbers of blastocysts and high-quality blastocysts in the control group was significantly higher than that in patients with EMT. Blastocysts, particularly high-quality blastocysts, from patients with EMT were damaged to varying degrees. Furthermore, we also analyzed the hormone levels of the two groups and found no significant difference in the FSH, E2, and LH levels between the two groups, which is consistent with the results from previous studies (26). In addition, a multifactor prediction model for patients suffering from EMT was successfully established. This model exhibited good predictive significance, with an AUG value greater than 0.693. The established model also provides evidence that can be used to predict the occurrence and development of EMT.

This study has some limitations. First, previous studies have shown that inflammation is the central process in EMT, which can lead to pain, fibrosis, adhesion formation, and infertility (2, 27).

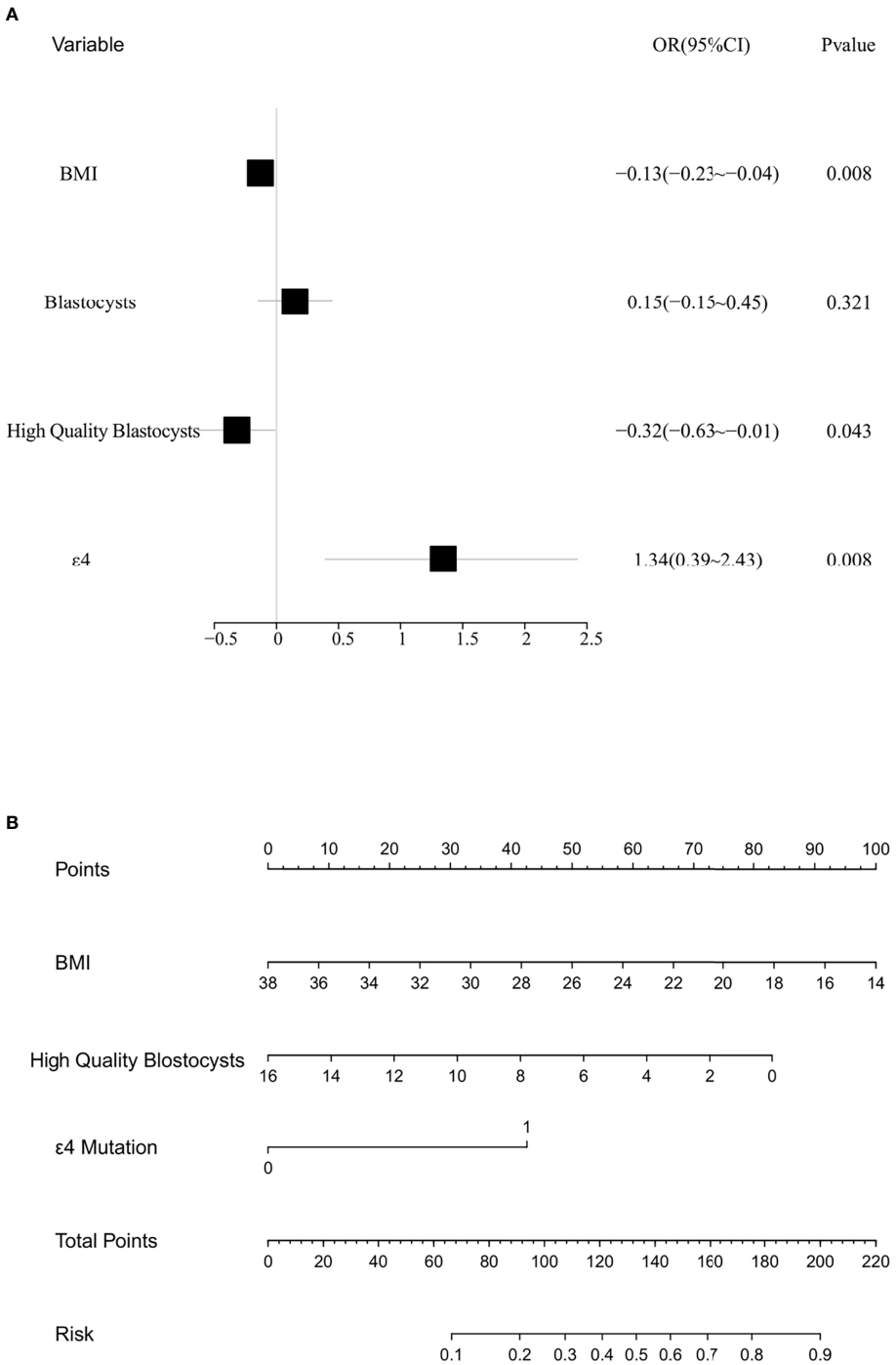

FIGURE 2 | Multivariate analysis and risk assessment of the control subjects and patients with EMT. **(A)** Forest map from the multivariate analysis of the control subjects and patients with EMT; BMI, $p = 0.008$; high-quality blastocysts, $p = 0.043$; ApoE-ϵ4, $p = 0.008$. **(B)** Nomograph for predicting patients with EMT.

Inflammation plays an important role in the etiology and pathophysiology of EMT (28, 29). Furthermore, ApoE-ϵ4 is reportedly associated with higher levels of inflammation (18). The cytokines in the human FF and the relationship between ApoE expression and the cytokines in the human FF of patients with EMT will be investigated in our future studies. In addition, an increasing number of studies have focused on the role of autophagy in EMT and have shown that autophagy plays a vital role in EMT (30). However, ApoE is reportedly associated with autophagy (31). As a result, ApoE might contribute to the development of EMT in part by

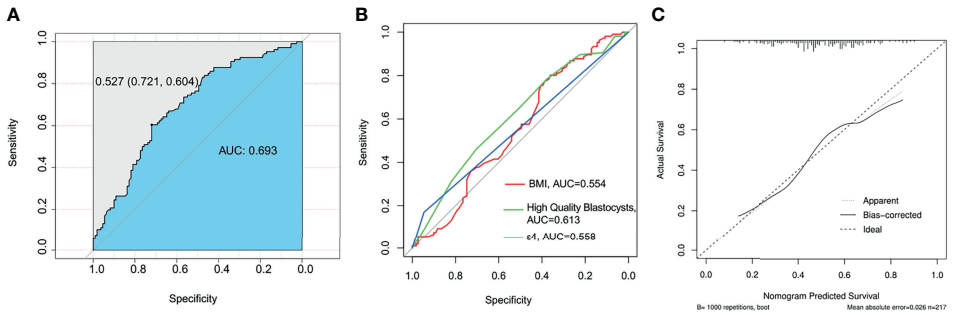

FIGURE 3 | ROC curve of the prediction model and nomogram for patients suffering from EMT. The AUC value should be in the range of 0.5 to 1.0. An AUC of 0.5 corresponds to a random prediction, and the criterion 0.5 < AUC < 1 indicates that the model has predictive significance. **(A)** Multifactor sensitivity for predictingpatients with EMT; AUC=0.693. **(B)** Sensitivity to each of the following three factors for predicting patients with EMT: BMI, AUC=0.554; high-quality blastocysts, AUC=0.613; and ApoE-ε4, AUC=0.558. **(C)** A nomogram was drawn to assess the agreement between the predicted results and the observed actual results. The dashed lines represent the predicted results, and the solid lines represent the actual results. The close fit between the predicted results and the actual results indicates that the prediction effect could be considered good; mean absolute error = 0.026; n = 217.

regulating autophagy, which is a topic that we will investigate in the future. In addition, it has been reported that growth factors, such as BMP15 and GDF9, are local paracrine and autocrine factors that play an important role in regulating follicular development and ovarian function (32) and a significant role in the pathophysiology of EMT. The potential existence of an association between ApoE and BMP15 or GDF9 in the FF of patients with EMT is also a research topic that we will investigate in our future studies. Furthermore, the sample size should be increased in future studies.

In conclusion, this study provides further evidence showing that ApoE expression was increased in the FF and that ApoE4 is associated with EMT in Chinese women. In addition, we established a multifactor prediction model with good sensitivity for identifying patients who may suffer from EMT, and a combined analysis of three factors (BMI, high-quality blastocysts, and ϵ4) could be used to predict EMT. The effects of ApoE on the occurrence and development of EMT require further research.

DATA AVAILABILITY STATEMENT

The original contributions presented in the study are included in the article/supplementary material. Further inquiries can be directed to the corresponding authors.

ETHICS STATEMENT

The studies involving human participants were reviewed and approved by the ethics committee of clinical medical research, First Affiliated Hospital of Anhui Medical University. The patients/participants provided their written informed consent to participate in this study.

AUTHOR CONTRIBUTIONS

Y-JL, FX, and KZ contributed equally to this work. Y-JL, Y-XC, XD, and J-PQ were responsible for the conceptualization and supervision of the study. FX and KZ performed the experiments, analyzed the data, and constructed the tables and figures. Y-JL, XD, and J-PQ designed the experiments and interpreted the data. M-YW, D-MJ, Y-HZ, Y-HX, AW, L-GS, S-MD, and Z-LW were responsible for technical and material support. FX wrote the original manuscript, which was edited by Y-JL, Y-XC, XD, and J-PQ. All authors read and approved the final version of the manuscript.

FUNDING

The present work was supported by the National Natural Science Foundation of China (81771653), the Key Research and Development Program of Anhui Province (202004j07020043), the Nonprofit Central Research Institute Fund of the Chinese Academy of Medical Sciences (2019PT310002), the Key Science Research Project in Universities of Anhui Province (KJ2017A194), the Overseas Study and Research Program for Excellent Young Talents in Universities of Anhui Province (gxgwfx2021017), Research Fund of Anhui Institute of translational medicine (ZHYX2020A001), and the Key Project of Medical and Health Program of PLA (15DX009).

REFERENCES

1. Petraglia F, Arcuri F, de Ziegler D, Chapron C. Inflammation: A Link Between Endometriosis and Preterm Birth. *Fertil Steril* (2012) 98(1):36–40. doi: 10.1016/j.fertnstert.2012.04.051
2. Bulun SE, Yilmaz BD, Sison C, Miyazaki K, Bernardi L, Liu S, et al. Endometriosis. *Endocr Rev* (2019) 40(4):1048–79. doi: 10.1210/er.2018-00242
3. Kobayashi H, Higashiura Y, Shigetomi H, Kajihara H. Pathogenesis of Endometriosis: The Role of Initial Infection and Subsequent Sterile Inflammation (Review). *Mol Med Rep* (2014) 9(1):9–15. doi: 10.3892/mmr.2013.1755

4. Sarria-Santamera A, Orazumbekova B, Terzic M, Issanov A, Chaowen C, et al. Systematic Review and Meta-Analysis of Incidence and Prevalence of Endometriosis. *Healthcare (Basel)* (2020) 9(1):29–44. doi: 10.3390/healthcare9010029
5. Czyzyk A, Podfigurna A, Szeliga A, Meczekalski B. Update on Endometriosis Pathogenesis. *Minerva Ginecol* (2017) 69(5):447–61. doi: 10.23736/S0026-4784.17.04048-5
6. Jofre-Monseny L, Minihane AM, Rimbach G. Impact of apoE Genotype on Oxidative Stress, Inflammation and Disease Risk. *Mol Nutr Food Res* (2008) 52(1):131–45. doi: 10.1002/mnfr.200700322
7. Mahley RW, Apolipoprotein E. From Cardiovascular Disease to Neurodegenerative Disorders. *J Mol Med (Berl)* (2016) 94(7):739–46. doi: 10.1007/s00109-016-1427-y
8. Butterfield DA, Mattson MP. Apolipoprotein E and Oxidative Stress in Brain With Relevance to Alzheimer's Disease. *Neurobiol Dis* (2020) 138:104795. doi: 10.1016/j.nbd.2020.104795
9. Marais AD. Apolipoprotein E in Lipoprotein Metabolism, Health and Cardiovascular Disease. *Pathology* (2019) 51(2):165–76. doi: 10.1016/j.pathol.2018.11.002
10. Chernick D, Ortiz-Valle S, Jeong A, Qu W, Li L. Peripheral *Versus* Central Nervous System APOE in Alzheimer's Disease: Interplay Across the Blood-Brain Barrier. *Neurosci Lett* (2019) 708:134306. doi: 10.1016/j.neulet.2019.134306
11. Martinez-Martinez AB, Torres-Perez E, Devanney N, Del Moral R, Johnson LA, Arbones-Mainar JM. Beyond the CNS: The Many Peripheral Roles of APOE. *Neurobiol Dis* (2020) 138:104809. doi: 10.1016/j.nbd.2020.104809
12. Utermann G, Hees M, Steinmetz A. Polymorphism of Apolipoprotein E and Occurrence of Dysbetalipoproteinaemia in Man. *Nature* (1977) 269 (5629):604–7. doi: 10.1038/269604a0
13. Oria RB, de Almeida JZ, Moreira CN, Guerrant RL, Figueiredo JR. Apolipoprotein E Effects on Mammalian Ovarian Steroidogenesis and Human Fertility. *Trends Endocrinol Metab* (2020) 31(11):872–83. doi: 10.1016/j.tem.2020.06.003
14. Van Giau V, Bagyinszky E, An SSA, Kim SY. Role of Apolipoprotein E in Neurodegenerative Diseases. *Neuropsychiatr Dis Treat* (2015) 11:1723–37. doi: 10.2147/NDT.S84266
15. Dankner R, Avraham SB, Harats D, Chetrit A. ApoE Genotype, Lipid Profile, Exercise, and the Associations With Cardiovascular Morbidity and 18-Year Mortality. *J Gerontol A Biol Sci Med Sci* (2020) 75(10):1887–93. doi: 10.1093/gerona/glz232
16. Li W, Liu F, Liu R, Zhou X, Li G, Xiao S. APOE E4 Is Associated With Hyperlipidemia and Obesity in Elderly Schizophrenic Patients. *Sci Rep* (2021) 11(1):14818. doi: 10.1038/s41598-021-94381-4
17. Kacperczyk M, Kmieciak A, Kratz EM. The Role of ApoE Expression and Variability of Its Glycosylation in Human Reproductive Health in the Light of Current Information. *Int J Mol Sci* (2021) 22(13):7197–211. doi: 10.3390/ijms22137197
18. Von Wald T, Monisova Y, Hacker MR, Yoo SW, Penzias AS, Reindollar RR, et al. Age-Related Variations in Follicular Apolipoproteins may Influence Human Oocyte Maturation and Fertility Potential. *Fertil Steril* (2010) 93 (7):2354–61. doi: 10.1016/j.fertnstert.2008.12.129
19. Collazo MS, Porrata-Doria T, Flores I, Acevedo SF. Apolipoprotein E Polymorphisms and Spontaneous Pregnancy Loss in Patients With Endometriosis. *Mol Hum Reprod* (2012) 18(7):372–7. doi: 10.1093/molehr/gas004
20. Parasar P, Ozcan P, Terry KL. Endometriosis: Epidemiology, Diagnosis and Clinical Management. *Curr Obstet Gynecol Rep* (2017) 6(1):34–41. doi: 10.1007/s13669-017-0187-1
21. Abondio P, Sazzini M, Garagnani P, Boattini A, Monti D, Franceschi C, et al. The Genetic Variability of APOE in Different Human Populations and Its Implications for Longevity. *Genes (Basel)* (2019) 10(3):222–49. doi: 10.3390/genes10030222
22. van Exel E, Koopman JJE, van Bodegom D, Meij JJ, de Knijff P, Ziem JB, et al. Effect of APOE Epsilon4 Allele on Survival and Fertility in an Adverse Environment. *PLoS One* (2017) 12(7):e0179497. doi: 10.1371/journal.pone.0179497
23. Shinohara M, Suzuki K, Bu G, Sato N. Interaction Between APOE Genotype and Diabetes in Longevity. *J Alzheimers Dis* (2021) 82(2):719–26. doi: 10.3233/JAD-210125
24. Farup PG, Rootwelt H, Hestad K. APOE - A Genetic Marker of Comorbidity in Subjects With Morbid Obesity. *BMC Med Genet* (2020) 21(1):146. doi: 10.1186/s12881-020-01082-2
25. Demeestere I, Centner J, Gervy C, Englert Y, Delbaere A. Impact of Various Endocrine and Paracrine Factors on *In Vitro* Culture of Preantral Follicles in Rodents. *Reproduction* (2005) 130(2):147–56. doi: 10.1530/rep.1.00648
26. Tanase A, Nemescu D, Popescu R, Toma BF, Matasariu RD, Onofriescu M. Fsh Receptor and Fsh Beta Chain Polymorphism Involvement in Infertility and Endometriosis Disease. *Acta Endocrinol (Buchar)* (2020) 16(2):142–7. doi: 10.4183/aeb.2020.142
27. Halis G, Arici A. Endometriosis and Inflammation in Infertility. *Ann N Y Acad Sci* (2004) 1034:300–15. doi: 10.1196/annals.1335.032
28. Giacomini E, Minetto S, Piani L, Pagliardini L, Somigliana E, Viganò P. Genetics and Inflammation in Endometriosis: Improving Knowledge for Development of New Pharmacological Strategies. *Int J Mol Sci* (2021) 22 (16):9033–48. doi: 10.3390/ijms22169033
29. Samimi M, Pourhanifeh MH, Mehdizadehkashi A, Eftekhar T, Asemi Z. The Role of Inflammation, Oxidative Stress, Angiogenesis, and Apoptosis in the Pathophysiology of Endometriosis: Basic Science and New Insights Based on Gene Expression. *J Cell Physiol* (2019) 234(11):19384–92. doi: 10.1002/jcp.28666
30. Yang HL, Mei J, Chang K-K, Zhou W-J, Huang L-Q, Li MQ. Autophagy in Endometriosis. *Am J Transl Res* (2017) 9(11):4707–25.
31. Okutsu M, Yamada M, Tokizawa K, Marui S, Suzuki K, Lira VA, et al. Regular Exercise Stimulates Endothelium Autophagy *via* IL-1 Signaling in ApoE Deficient Mice. *FASEB J* (2021) 35(7):e21698. doi: 10.1096/fj.202002790RR
32. Hendarto H, Yohanes Ardianta Widyanugraha M, Widjiati W. Curcumin Improves Growth Factors Expression of Bovine Cumulus-Oocyte Complexes Cultured in Peritoneal Fluid of Women With Endometriosis. *Int J Reprod BioMed* (2018) 16(12):775–82. doi: 10.18502/ijrm.v16i12.3683

Conflict of Interest: The authors declare that the research was conducted in the absence of any commercial or financial relationships that could be construed as a potential conflict of interest.

Publisher's Note: All claims expressed in this article are solely those of the authors and do not necessarily represent those of their affiliated organizations, or those of the publisher, the editors and the reviewers. Any product that may be evaluated in this article, or claim that may be made by its manufacturer, is not guaranteed or endorsed by the publisher.

Copyright © 2021 Liu, Xing, Zong, Wang, Ji, Zhao, Xia, Wang, Shi, Ding, Wei, Qiao, Du and Cao. This is an open-access article distributed under the terms of the Creative Commons Attribution License (CC BY). The use, distribution or reproduction in other forums is permitted, provided the original author(s) and the copyright owner(s) are credited and that the original publication in this journal is cited, in accordance with accepted academic practice. No use, distribution or reproduction is permitted which does not comply with these terms.

frontiers in Endocrinology

ORIGINAL RESEARCH
published: 11 November 2021
doi: 10.3389/fendo.2021.774997

Integrated Analysis of Hub Genes and MicroRNAs in Human Placental Tissues from *In Vitro* Fertilization-Embryo Transfer

Shuheng Yang[1], Wei Zheng[1], Chen Yang[1], Ruowen Zu[1], Shiyu Ran[1], Huan Wu[1], Mingkun Mu[1], Simin Sun[1], Nana Zhang[1], Rick F. Thorne[2,3] and Yichun Guan[1]**

[1] Center for Reproductive Medicine, The Third Affiliated Hospital of Zhengzhou University, Zhengzhou, China, [2] Translational Research Institute, Henan Provincial People's Hospital, Zhengzhou, China, [3] Academy of Medical Sciences, Zhengzhou University, Zhengzhou, China

OPEN ACCESS

Edited by:
Claus Yding Andersen,
University of Copenhagen, Denmark

Reviewed by:
Liu Wang,
Mayo Clinic Arizona, United States
Yuhua Shi,
Shandong University, China

***Correspondence:**
Rick F. Thorne
rick.thorne@newcastle.edu.au
Yichun Guan
lisamayguan@163.com

Specialty section:
This article was submitted to Reproduction, a section of the journal Frontiers in Endocrinology

Received: 13 September 2021
Accepted: 22 October 2021
Published: 11 November 2021

Citation:
Yang S, Zheng W, Yang C, Zu R, Ran S, Wu H, Mu M, Sun S, Zhang N, Thorne RF and Guan Y (2021) Integrated Analysis of Hub Genes and MicroRNAs in Human Placental Tissues from In Vitro Fertilization-Embryo Transfer. Front. Endocrinol. 12:774997. doi: 10.3389/fendo.2021.774997

Objective: Supraphysiological hormone exposure, *in vitro* culture and embryo transfer throughout the *in vitro* fertilization-embryo transfer (IVF-ET) procedures may affect placental development. The present study aimed to identify differences in genomic expression profiles between IVF-ET and naturally conceived placentals and to use this as a basis for understanding the underlying effects of IVF-ET on placental function.

Methods: Full-term human placental tissues were subjected to next-generation sequencing to determine differentially expressed miRNAs (DEmiRs) and genes (DEGs) between uncomplicated IVF-ET assisted and naturally conceived pregnancies. Gene ontology (GO) enrichment analysis and transcription factor enrichment analysis were used for DEmiRs. MiRNA-mRNA interaction and protein-protein interaction (PPI) networks were constructed. In addition, hub genes were obtained by using the STRING database and Cytoscape. DEGs were analyzed using GO and Kyoto Encyclopedia of Genes and Genomes (KEGG) pathway analysis. Differentially expressed miRNAs were validated through qRT-PCR.

Results: Compared against natural pregnancies, 12 DEmiRs and 258 DEGs were identified in IVF-ET placental tissues. In a validation cohort, it was confirmed that hsa-miR-204-5p, hsa-miR-1269a, and hsa-miR-941 were downregulation, while hsa-miR-4286, hsa-miR-31-5p and hsa-miR-125b-5p were upregulation in IVF-ET placentas. Functional analysis suggested that these differentially expressed genes were significantly enriched in angiogenesis, pregnancy, PI3K-Akt and Ras signaling pathways. The miRNA-mRNA regulatory network revealed the contribution of 10 miRNAs and 109 mRNAs while EGFR was the most highly connected gene among ten hub genes in the PPI network.

Conclusion: Even in uncomplicated IVF-ET pregnancies, differences exist in the placental transcriptome relative to natural pregnancies. Many of the differentially expressed genes in IVF-ET are involved in essential placental functions, and moreover, they provide a ready resource of molecular markers to assess the association between placental function and safety in IVF-ET offspring.

Keywords: *in vitro* fertilization-embryo transfer, placenta, differentially expressed genes, MiRNA-mRNA, next-generation sequencing

INTRODUCTION

In vitro fertilization-embryo transfer (IVF-ET) is the main method of assisted reproductive technology (ART), and can improve the success rates of infertility treatment (1, 2). The use of this procedure has been steadily increasing worldwide and for example, in China, the average number of ART treatments performed now exceeds 700,000 annually (3). The vast majority of children successfully delivered through ART are healthy (4). Nonetheless, there are increased risks of several pregnancy-related complications, including gestational diabetes (5), pre-eclampsia (6), placenta previa (7), abnormal placental growth, preterm delivery (8), and low birth weight (9). Some reports have suggested that the adverse perinatal outcomes occur due to IVF-ET procedures such as supraphysiological estrogen level during stimulation, *in vitro* culture, and microscopic manipulation (10, 11). However, the underlying causes of IVF-ET-associated complications are largely unknown, although many conceptually appear related to placental vascular complications and the resulting effects on fetal development.

MicroRNAs (miRNAs) represent a major class of non-coding RNAs consisting of single-stranded RNAs of approximately 18-25 nucleotides in length (12). They function as negative gene regulators by binding to the 3' UTR of messenger RNAs (mRNAs), to either prevent protein translation or to direct the mRNA towards degradation (13). The placenta expresses many ubiquitous as well as specific miRNAs and a growing body of evidence proposes that miRNAs function as important regulators of placental development (14). Here, various miRNAs have been shown to control the differentiation, replication, apoptosis, invasion/migration and angiogenesis of trophoblasts, indicating the widespread contribution of miRNAs to the placental growth (15, 16). For example, miR-346 and miR-582-3p down-regulate the expression of endocrine gland-derived vascular endothelial growth factor (*EG-VEGF*) and inhibit trophoblast cell invasion and migration (17). miR-191 inhibits angiogenesis by activating the nuclear factor-κB (NF-κB) signaling pathway (18). It was also found that miR-29b inhibited trophoblast invasion and angiogenesis by suppressing vascular endothelial growth factor (*VEGF*) expression (19). In addition, animal experiments in mice revealed that miR-450a-3p played a role in inhibiting cell proliferation, promoting apoptosis and interfering with embryonic development through regulating the target gene *Bub1* (20). However, the impact of specific microRNAs in IVF-ET placental tissue, and their potential impact on related gene regulatory networks has to date been poorly investigated.

This study aimed to understand the differences in placental genomic expression profiles comparing IVF-ET and natural pregnancy-derived placentas, and the link between IVF-ET manipulation and placental structure and function. We used next-generation sequencing techniques to analyze of miRNA and mRNA expression profiles in IVF-ET and natural gestational placental tissue. Based on co-expression analysis and online prediction. we established a miRNA-mRNA regulatory network comprising 10 miRNAs and 109 mRNAs together with a PPI network comprised of ten hub genes. Furthermore, we verified that miR-204-5p, miR-1269a and miR-941 were downregulated in IVF-ET placentals thereby proposing these as key regulators involved in the effects of IVF-ET on placental development and function. Moreover, our study constitutes a verified resource for enabling further investigation into the transcriptomic and mechanistic differences between IVF-ET and naturally conceived pregnancies with the goal of providing new targets to assess the safety of IVF-ET in the clinic.

MATERIALS AND METHODS

Tissue Collection and Ethics

Placental tissue samples were collected from women who underwent caesarean deliveries after IVF-ET assisted (n=3) or natural conceived (n=3) pregnancies. Inclusion criteria included full-term singleton delivery after IVF-ET, with age between 20 and 35 years, 37-42 gestational weeks, infant birth weight between 2500 g and 4000 g, and uncomplicated pregnancies. Three strictly matched natural pregnancies were selected as controls with matching parameters: delivery, maternal age, parity, and gestational duration (**Table 1**). A validation cohort of 8 uncomplicated IVF-ET and 8 normal conception patients were similarly collected (**Table 2**). We used an equal number of male and female placentals for both discovery and validation cohorts and selected tissue from the middle placenta throughout to minimize sampling bias. All placental tissues were rinsed extensively with ice cold PBS and stored at -80°C until later RNA extraction. Tissue collection was approved by the Ethics Committee of the Third Affiliated Hospital of Zhengzhou University with written informed consent provided by all patients prior to sample collection.

RNA Extraction and Sequencing

Total RNA was isolated from placental tissue using the mirVana RNA Isolation Kit (Cat #. AM1561, Austin TX, US) according to

TABLE 1 | Clinical characteristics of IVF-ET and controls for high-throughput sequencing.

Cases	Age (years)	Gravidity	Parity	Gestational week at delivery	Mode of delivery	Sex of the baby	Birth weight(g)	Weight of placenta(g)	Baby/placenta weight
Control 1	27	1	0	39	Cesarean	Female	3150	500	6.30
Control 2	28	1	0	40.29	Cesarean	Male	3850	630	6.11
Control 3	21	1	0	39.71	Cesarean	Male	3500	510	6.86
IVF-ET 1	31	2	0	38.14	Cesarean	Male	3000	540	5.56
IVF-ET 2	33	1	0	38.57	Cesarean	Female	2800	480	5.83
IVF-ET 3	29	1	0	38.14	Cesarean	Male	3100	540	5.74

the manufacturer's instructions. RNA concentration and integrity were then verified using an Agilent Bioanalyzer 2100 (Agilent technologies Santa Clara, US) before subjecting the samples to library preparation and sequencing. The concentration and size of the constructed libraries were measured using a Qubit® 2.0 Fluorometer (Life Technologies, USA) and Agilent 2100 Bioanalyzer, respectively. The samples were prepared according to the HiSeq 2500 User Guide, and the flow cell with the cluster was loaded on the Illumina HiSeq 2500 (50-bp single-end FASTQ reads). The number of sequencing reads per sample was at least 10M and the proportion of bases with mass greater than 20 was greater than 95%, and the quality control meets the requirements of data analysis.

Differential Expression Analysis

The DESeq2 package of R version 3.5.2 (http://www.r-project.org) was used to define differentially expressed miRNAs (DEmiRs) and genes (DEGs) with the Bayesian method used to correct batch effects. MiRNAs and mRNAs with statistical significance between the IVF-ET and control groups were selected according to the threshold criterion of fold change (FC) >1.5 and $P < 0.05$. Volcano maps were created in the R studio using the plot packages to illustrate the differential expression of DEmiRs and DEGs.

GO Enrichment Analysis for the Targets of Transcription Factors

DEmiRs were uploaded to FunRich software to screen for upstream transcription factors, which is primarily used for functional enrichment and interaction network analysis of genes and proteins, as well as enrichment targets for transcription factor pathways (21). For interaction network analysis between miRNAs, gene/mRNA, and transcription factors, gene ontogeny (GO) enrichment analysis was also used (22, 23).

Construction of the miRNA-mRNA Regulatory Networks

The miRWalk V2.0, StarBase and TargetScan databases were used to predict the target mRNAs of the miRNAs identified as DEmiRs. Subsequently, the predicted DEGs were matched with the experimentally determined DEGs to develop miRNA-mRNA regulatory networks with visualization using Cytoscape software (http://www.cytoscape.org/) (24). All node degrees, proximity and presence of the regulatory network were simultaneously computed.

GO and KEGG Enrichment Analyses

For gene ontology (GO) and Kyoto Encyclopedia of Genes and Genomes (KEGG) pathway analysis of DEGs, we used the Database for Annotation, Visualization and Integrated Discovery (DAVID) and used ggplot2 packages in the R studio to identify significantly altered biological processes (BPs), cellular components (CCs), molecular functions (MFs) and pathways associated with DEGs ($P < 0.05$).

Protein-Protein Interaction (PPI) Network Analysis and Hub Gene Identification

Differentially expressed gene data was uploaded to the STRING database (http://www.string-db.org/) (25). Interactions with a composite score of >0.4 were considered significant. The target genes in the PPI network act as nodes and the line from two nodes indicates relevant interactions. Cytoscape software was used to visualize the PPI network. We screened the top 10 genes with the highest degree of correlation to the others as hub genes with the CytoHubba plugin of Cytoscape (26).

TABLE 2 | Clinical characteristics of IVF-ET and controls.

Clinical features	IVF-ET (n = 8)	Control (n = 8)	*P* value
Maternal age (years)	31.13 ± 2.58	28.63 ± 2.67	0.078
Gestational week at delivery	39.41 ± 0.69	39.43 ± 0.86	0.967
Mode of delivery	Cesarean	Cesarean	
Birth weight(g)	3512.50 ± 410.64	3686.25 ± 302.04	0.351
Infant sex			
Female	4	4	
Male	4	4	
Baby/placenta weight	5.94 ± 0.46	5.69 ± 0.70	0.387

Data are presented as mean ± SD. t-test. IVF-ET, in vitro fertilization-embryo transfer.

Quantitative Real-Time Polymerase Chain Reaction (qRT-PCR)

One μg total RNA was reverse transcribed into cDNA using the ReverTra Ace qPCR RT Kit (Toyobo, Japan) according to the manufacturers' instructions. Specific primers were used to synthesize the cDNA of miRNAs. qRT-PCR reactions were performed with the indicated primers (**Table 3**) in triplicate 20 μL reactions using the SYBR Green Realtime PCR Master Mix (Toyobo, Japan) on a StepOnePlus™ Real-Time PCR System. Cycling conditions were as follows: 95°C for 60 seconds, 40 cycles of 95°C for 15 seconds, 60°C for 15 seconds, and 72°C for 45 seconds. The results were normalized to U6 and the relative changes calculated using the $2^{-\Delta\Delta Ct}$ method (27).

Statistical Analysis

Data were presented as means ± standard deviations (SD) for quantitative variables and the Student's *t*-test used to assess differences between groups. Otherwise, for discrete variables the Mann-Whitney *U*-test was used. A value of $P < 0.05$ was regarded as statistically significant. SPSS 21.0 and GraphPad Prism 6.0 were used for analysis.

RESULTS

Identification of Differentially Regulated Genes in IVF-ET Placentals

The schema of the overall study and analysis approach is presented in **Figure 1**. High throughput sequencing analysis was performed to analyze the expression profiles of miRNAs and mRNAs in placentals from uncomplicated full-term IVF-ET and natural conception pregnancies. From these data we identified a total of 12 differentially expressed miRNAs (DEmiRs; **Figure 2A**) including 4 downregulated miRNAs: hsa-miR-1269a, hsa-miR-204-5p, hsa-miR-224-5p and hsa-miR-941, and 8 upregulated miRNAs: hsa-miR-1269b, hsa-miR-125b-5p, hsa-miR-193b-3p, hsa-miR-193b-5p, hsa-miR-31-5p, hsa-miR-371a-5p, hsa-miR-4286 and hsa-miR-9-5p (**Table 4**). We also identified 258 differentially expressed mRNAs consisting of 52 downregulated and 206 upregulated DEGs (**Figure 2B** and **Supplementary Table SI**).

Verification of the DEmiRs by qRT-PCR in Placental Tissues

To ensure the veracity of the high throughput sequencing analysis, it was necessary to validate our findings using alternative methodology and samples. On the basis of subsequent bioinformatics (see below), we selected 6 of the 12 DEmiRs (3 downregulated and 3 upregulated, respectively) and analyzed their expression using qRT-PCR in a validation cohort of 8 IVF-ET and 8 normal conception placentas. Instructively, we found that the relative expression levels of hsa-miR-204-5p, hsa-miR-1269a, and hsa-miR-941 were significantly downregulated whereas hsa-miR-4286, hsa-miR-31-5p and hsa-miR-125b-5p were all upregulated, respectively, in IVF-ET compared to the control placentas (**Figures 3A–F**). These results suggest that the dysregulation of these miRNAs commonly occurs in IVF-ET pregnancies but further verification will be required to support the general veracity of the global sequencing data and analysis of the study.

Transcription Factor Enrichment and GO Enrichment Analysis

Transcription factors often represent the critical final step in signal transduction pathways. To investigate the enrichment of transcription factor targets likely associated with the genetic landscape of the IVF-ET placenta, we filtered out the top 10 transcription factors most closely linked to the DEmiRs. In deceasing probability order, this analysis identified SP1, EGR1, SP4, KLF7, ONECUT1, MYF5, TCF3, NFIC, SRF, and HOXB4 (**Figure 4A**). It indicates a regulatory interaction between these transcription factors and DEmiRs. Intriguingly, SP1 was apparently able to regulate majority of the DEmiRs.

In concert with these findings, GO enrichment analysis indicated that the top 5 biological progress (BP) terms with the most enriched targets of the DEmiRs involved signal transduction; regulation of nucleobase, nucleoside, nucleotide and nucleic acid metabolism, transport, apoptosis, and regulation of immune response (**Figure 4B**). GO enrichment

TABLE 3 | Oligonucleotides used in this study.

Primer sets name	Reverse transcriptase primer (5′ to 3′)	Real-time quantitative PCR primer (5′ to 3′)
U6	AACGCTTCACGAATTTGCGT	F:CTCGCTTCGGCAGCACA R: AACGCTTCACGAATTTGCGT
has-miR-204-5p	GTCGTATCCAGTGCAGGGTCCGAGGTAT TCGCACTGGATACGACAGGCAT	F: CGCGTTCCCTTTGTCATCCT R:AGTGCAGGGTCCGAGGTATT
has-miR-1269a	GTCGTATCCAGTGCAGGGTCCGAGGTAT TCGCACTGGATACGACCCAGTA	F: CGCTGGACTGAGCCGTG R: AGTGCAGGGTCCGAGGTATT
has-miR-941	GTCGTATCCAGTGCAGGGTCCGAGGTAT TCGCACTGGATACGACGCACAT	F: CACCCGGCTGTGTGCAC R: AGTGCAGGGTCCGAGGTATT
has-miR-4286	GTCGTATCCAGTGCAGGGTCCGAGGTAT TCGCACTGGATACGACGGTACC	F: GCGCGACCCCACTCCT R: AGTGCAGGGTCCGAGGTATT
has-miR-31-5p	GTCGTATCCAGTGCAGGGTCCGAGGTAT TCGCACTGGATACGACAGCTAT	F: GCGAGGCAAGATGCTGGC R: AGTGCAGGGTCCGAGGTATT
has-miR-125b-5p	GTCGTATCCAGTGCAGGGTCCGAGGTAT TCGCACTGGATACGACTCACAA	F: CGCGTCCCTGAGACCCTAAC R: AGTGCAGGGTCCGAGGTATT

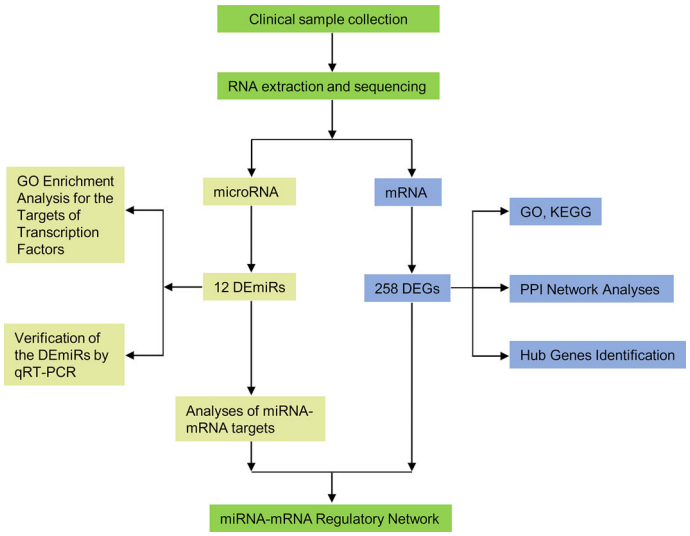

FIGURE 1 | Flow diagram of the study design. DEmiRs, differentially expressed miRNAs; DEGs, differentially expressed genes; GO, Gene Ontology; KEGG, Kyoto Encyclopedia of Genes and Genomes; PPI, protein-protein interaction.

terms associated with molecular function (MF) indicated most of the genes were involved in transcription factor activity, transporter activity, RNA binding, Receptor signaling complex scaffold activity, and GTPase activity (**Figure 4C**). The top 5 enriched cellular component (CC) terms were nucleus, cytoplasm, Golgi apparatus, lysosome and membrane raft (**Figure 4D**).

Construction of miRNA-mRNA Regulatory Networks

Reliable identification of miRNA targets is still an imprecise process, but it is widely appreciated that predictions can be improved using the outputs of multiple algorithms (28). Consequently, we employed three databases (miRWalk V2.0, StarBase and TargetScan) to analyze the potential impact of the DEmiRs on the placental transcriptome. Screening miRNA targets based on the overlapping results of the three databases and the intersection with DEGs. This analysis yielded paired interactions between 109 DEGs with 10 of the 12 identified DEmiRs. The network of miRNA-mRNA interactions was visualized in Cytoscape (**Figure 5**) and the target genes of the DEmiRs are listed in **Table 5**. Notably, among these, the four downregulated DEmiRs, particularly hsa-miR-204-5p, hsa-miR-1269a and hsa-miR-941, formed the most extensive interactive network with multiple gene targets while the upregulated DEmiRs aligned with a more discrete set of target genes.

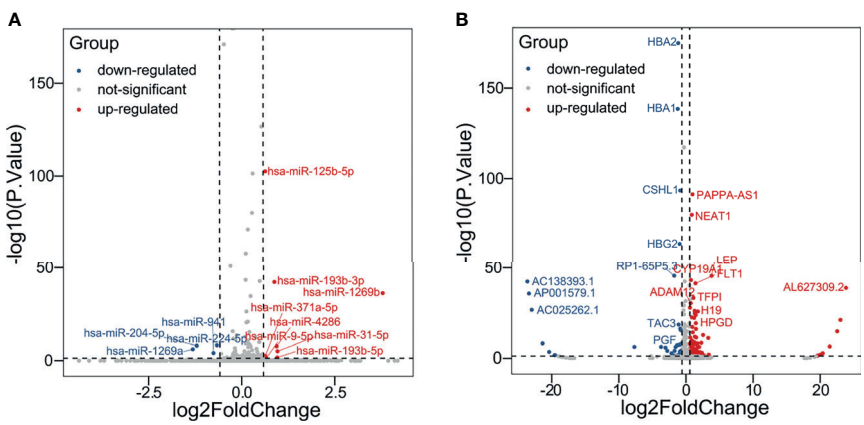

FIGURE 2 | Identification of DEmiRs and DEGs. Volcano plots illustrating **(A)** DEmiRs and **(B)** DEGs in placental tissues determined by comparing IVF-ET (n = 3) with normal conception (n = 3) pregnancies. Differential expression thresholds employed for deriving DEmiRs and DEGs involved fold change (FC) >1.5 and $P < 0.05$. Red and blue points represent significantly upregulated or downregulated miRNAs/mRNAs, respectively.

TABLE 4 | The 12 differentially expressed miRNAs (DEmiRs) in IVF-ET.

Symbol	*P* Value	logFC	Up/Down
hsa-miR-941	<0.001	-0.758138251	Down
hsa-miR-9-5p	0.047	0.659018502	Up
hsa-miR-4286	<0.001	0.938226403	Up
hsa-miR-371a-5p	0.003	0.633507315	Up
hsa-miR-31-5p	<0.001	0.962107998	Up
hsa-miR-224-5p	<0.001	-0.664686886	Down
hsa-miR-204-5p	<0.001	-1.207550612	Down
hsa-miR-193b-5p	0.020	0.954586891	Up
hsa-miR-193b-3p	<0.001	0.878208945	Up
hsa-miR-1269b	<0.001	3.787867629	Up
hsa-miR-1269a	<0.001	-1.314083333	Down
hsa-miR-125b-5p	<0.001	0.639432322	Up

IVF-ET, in vitro fertilization-embryo transfer; FC, fold change.

Functional Enrichment Analysis of the DEGs

Independent of the preceding analysis, we utilized ggplot2 and enrichment analysis to profile GO annotations and KEGG pathways associated with the differentially expressed genes. These predictions would allow an improved understanding of the functional impact of the genes dysregulated in IVF-ET. As illustrated, the top 10 enriched GO and KEGG terms are presented in categories of biological processes (BPs), cellular components (CCs), molecular functions (MFs) and defined KEGG pathway identifiers (**Figure 6**).

Notably, this analysis revealed significant enrichment for BP entries aligned with angiogenesis, pregnancy, cell adhesion, positive regulation of transcription from the RNA polymerase II promoter and positive regulation of angiogenesis (**Figure 6A**). Furthermore, the protein binding, poly (A) RNA binding and transcriptional activator activity accounted for the majority of MF terms (**Figure 6B**) while the most enriched CCs were extracellular exosome, membrane, and extracellular region (**Figure 6C**). The top 10 most highly enriched KEGG classifications included the PI3K-Akt and Ras signaling pathways along with focal adhesion (**Figure 6D**).

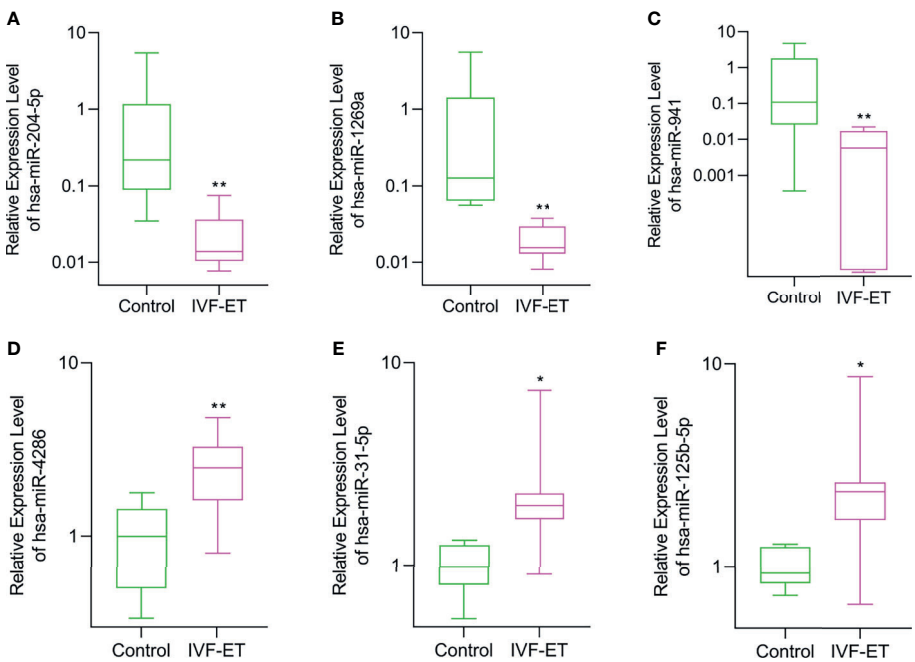

FIGURE 3 | Validation of differential expression of randomly selected DEmiRs in IVF-ET *versus* control placental tissues. The relative expression levels of **(A)** hsa-miR-204-5p, **(B)** hsa-miR-1269a, **(C)** hsa-miR-941, **(D)** hsa-miR-4286, **(E)** hsa-miR-31-5p and **(F)** hsa-miR-125b-5p were measured in an independent cohort of placental tissues from uncomplicated IVF-ET (n = 8) and natural conceived pregnancies (n = 8). Box and whisker plot with relative expression plotted in log scale showing the range (whiskers), first and third quartiles (boxes) and median values. $^{*}P < 0.05$, $^{**}P < 0.01$.

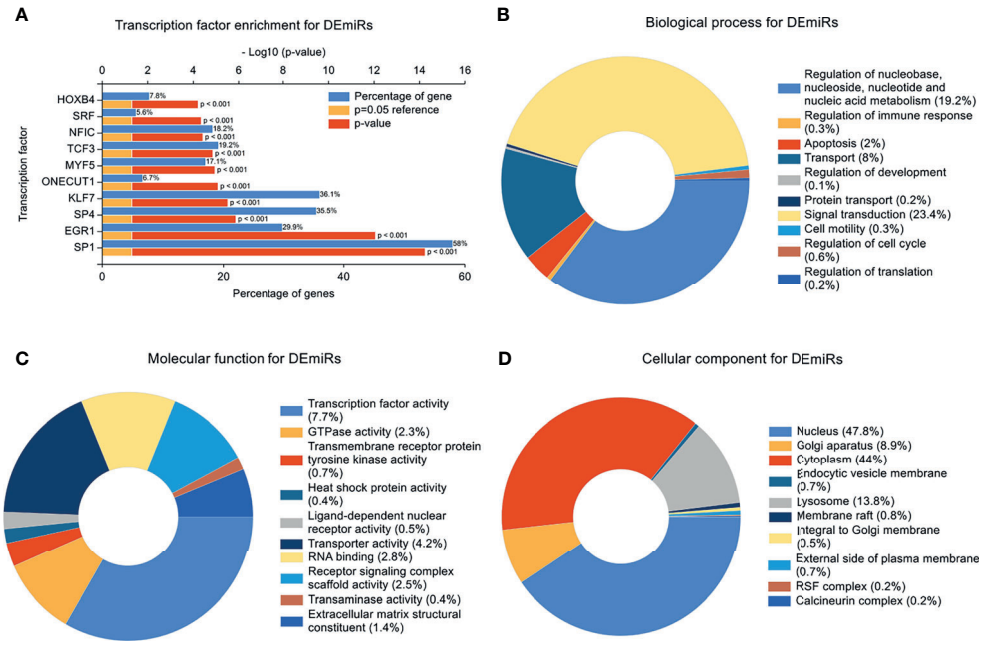

FIGURE 4 | Transcription Factor Enrichment and GO Enrichment Analysis. **(A)** Transcription factors (TF) of the differentially expressed miRNAs (DEmiRs) from FunRich. Blue bars, orange bars, and red bars represent percentage of predicted genes, reference of P=0.05, and *p* value, respectively. **(B)** mRNAs involved in biological process terms for DEmiRs. **(C)** mRNAs involved in molecular function terms for DEmiRs. **(D)** mRNAs involved in cellular component terms for DEmiRs.

Construction of Protein-Protein Interaction (PPI) Networks

Using the DEGs we next built a PPI network using the online STRING database and tools in Cytoscape. The network was mapped to a limit of 148 DEGs (**Figure 7**). Node size is proportional to the degree of the node itself. Edge width is proportional to the combined degree between genes. We assessed their degree of connectivity and identified 10 hub genes, and the genes are listed in **Table 6**.

Biological Analysis of the Hub Genes

Highly-connected genes with a network are considered master regulatory elements otherwise known as hub genes (29). We used the cytoHubba plugin of Cytoscape to reveal the ten most strongly related interactions amongst the DEGs in IVF-ET. This approach generated 10 nodes with 37 edges with the most likely hub genes consisting of *EGFR*, *FOS*, *SERPINE1*, *LEP*, *HGF*, *EGR1*, *SPP1*, *HNRNPA2B1*, *IGF2* and *ENG* (**Figure 8A**). In addition, KEGG analysis of the top 10 enrichment pathways were identified (**Figures 8B, C**).

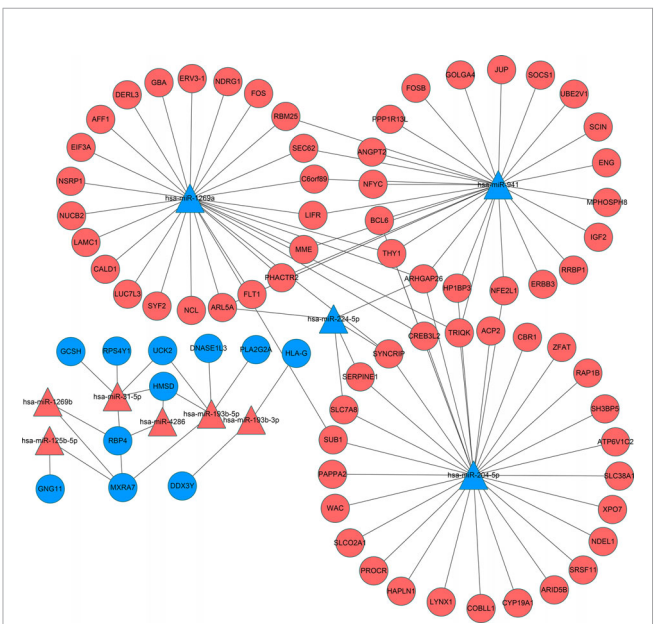

FIGURE 5 | Interaction networks of miRNA and target DEGs in IVF-ET placenta tissues. microRNAs are represented by triangles and mRNAs are represented by circles. Red indicates genes with up-regulated expression and blue indicates genes with down-regulated expression. miRNA, microRNA; mRNA, messenger RNA; IVF-ET, *in vitro* fertilization-embryo transfer.

DISCUSSION

As one of the main tools of ART, IVF-ET can improve the success rate of infertility treatments for many affected couples.

TABLE 5 | The miRNA-mRNA network.

Symbol	Up/ Down	Count	Target mRNA
hsa-miR-941	Down	28	RBM25, MPHOSPH8, SOCS1, SEC62, HP1BP3, JUP, NFE2L1, THY1, FLT1, GOLGA4, TRIQK, C6orf89, NFYC, PPP1R13L, ARHGAP26, IGF2, BCL6, LIFR, ANGPT2, FOSB, SCIN, PHACTR2, RRBP1, ARL5A, MME, ERBB3, UBE2V1, ENG
hsa-miR-4286	Up	2	RBP4, HMSD
hsa-miR-31-5p	Up	5	GCSH, UCK2, HMSD, MXRA7, RPS4Y1
hsa-miR-224-5p	Down	5	SYNCRIP, ARHGAP26, ARL5A, SERPINE1, SLC7A8
hsa-miR-204-5p	Down	30	PAPPA2, WAC, SUB1, PROCR, SLCO2A1, HAPLN1, HP1BP3, LYNX1, NFE2L1, THY1, ACP2, CBR1, COBLL1, SLC7A8, CREB3L2, ARID5B, SRSF11, TRIQK, SYNCRIP, ARHGAP26, BCL6, XPO7, SLC38A1, ATP6V1C2, ZFAT, NDEL1, SH3BP5, RAP1B, SERPINE1, CYP19A1
hsa-miR-193b-5p	Up	5	UCK2, DNASE1L3, HMSD, MXRA7, PLA2G2A
hsa-miR-193b-3p	Up	2	HLA-G, DDX3Y
hsa-miR-1269b	Up	2	RBP4, MXRA7
hsa-miR-1269a	Down	28	RBM25, SYF2, SUB1, NCL, FOS, CALD1, THY1, SEC62, LAMC1, AFF1, LUC7L3, NUCB2, EIF3A, C6orf89, NSRP1, CREB3L2, TRIQK, FLT1, SYNCRIP, ARHGAP26, NDRG1, LIFR, PHACTR2, ARL5A, ERV3-1, DERL3, MME, GBA
hsa-miR-125b-5p	Up	2	GNG11, MXRA7

Nonetheless, despite its use for several decades and widespread acceptance, there are still uncertainties associated with IVF-ET in terms of perinatal risks and offspring health. On this basis we hypothesized that complications associated with IVF-ET may be associated with the altered expression of genes that regulate placental development and function. Consequently, we performed genome-wide miRNA and mRNA analyses comparing placentas from IVF-ET assisted and naturally conceived pregnancies. The choice of samples from uncomplicated births was deliberate, as large gene differences from pathological births would be expected while more fundamental changes could be revealed by the experimental design used.

Foremost we considered the epigenetic regulatory mechanisms involving miRNAs as these are recognized effectors of placental-mediated complications during pregnancy (15). Indeed, there has been strong interest in miRNAs as predictive biomarkers for the detection of pathologies in pregnancy with the villous trophoblast being a major source of miRNAs found in maternal circulation (30). Such changes in circulating miRNAs would naturally reflect the changes occurring within the placenta. Our analysis produced a

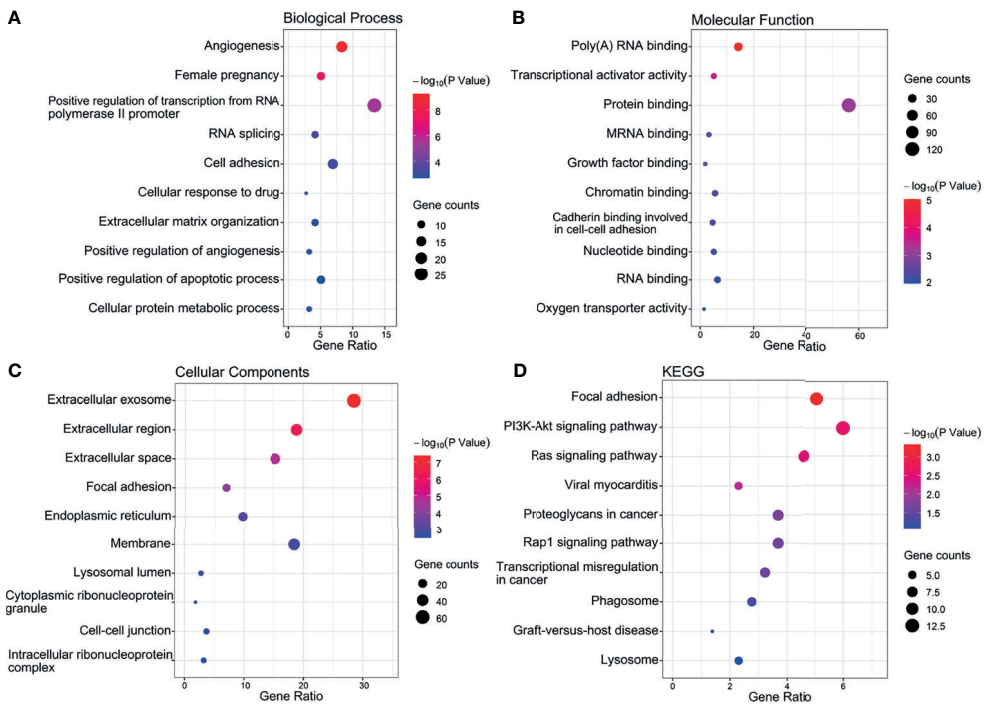

FIGURE 6 | Top 10 significant enrichment GO and KEGG terms of DEGs. **(A)** BP, biological process. **(B)** MF, molecular function. **(C)** CC, cellular component. **(D)** KEGG, Kyoto Encyclopedia of Genes and Genomes.

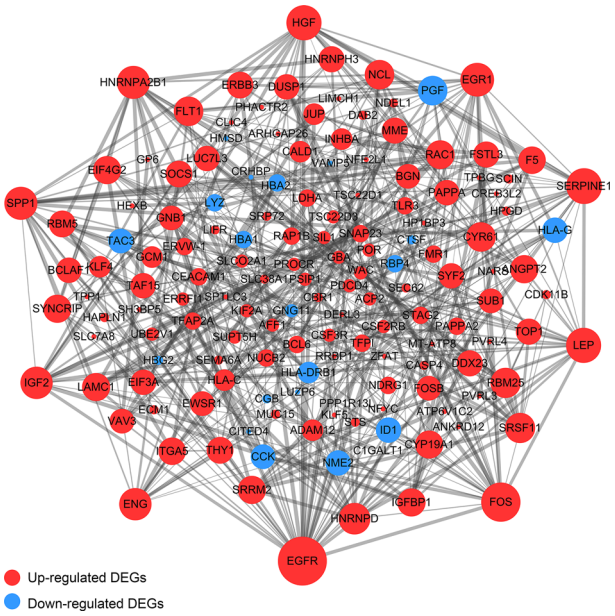

FIGURE 7 | The PPI Network of DEGs. The upregulated genes were exhibited by the red color, while the blue color exhibited the downregulated genes. Node size is proportional to the degree of the node itself. Edge width is proportional to the combined degree between genes.

shortlist of 12 miRNAs that were differentially expressed in IVF-ET compared to placental tissue from natural pregnancies.

Three of the 12 differentially expressed miRNAs were confirmed in an independent cohort to be specifically downregulated in IVF-ET placentas, i.e., hsa-miR-204-5p, hsa-miR-1269a and hsa-miR-941. Notably, all three microRNAs have been previously implicated in placental dysfunction and potential fetal growth complications although the underlying mechanisms generally remain unclear. The downregulation of miR-204-5p is associated with fetal growth abnormalities and is enriched in related biological pathways and has also been found to be regulated in the presence of adverse pregnancy-related outcomes (31). For instance, miR-204-5p can inhibit angiogenesis by regulating pro-angiogenic genes such as *ANGPT1* and members of the *VEGF* family (32). miR-1269a was found to be a risk factor for ectopic pregnancy, and currently known risk factors include assisted reproductive technologies such as *in vitro* artificial insemination and hormonal stimulation (33). It has also been suggested that miR-941 is expressed in trophoblast cells and involved in insulin-related intracellular signaling pathways such as Wnt signaling, phosphoinositide-3-kinase, TGF-β signaling, and PPAR-gamma (34). In addition, miR-941 has been shown to target Keap1 to activate the Nrf2 signaling pathway, which in turn protects human endometrial cells from oxygen and glucose deprivation-re-oxygenation induced oxidative stress and programmed necrosis (35). These correlates provide a compelling rationale for the functional significance of these miRNAs in IVF-ET fetal growth.

TABLE 6 | The top 10 genes in the network are ranked in order of degree.

Rank	Symbol	Score
1	EGFR	40
2	FOS	27
3	SERPINE1	21
3	LEP	21
5	HGF	19
5	EGR1	19
7	SPP1	18
8	HNRNPA2B1	17
9	IGF2	16
9	ENG	16

Given the central importance of miRNA expression in the execution of the transcriptional programs, we predicted transcription factors that might regulate these DEmiRs. The top ranked transcription factor was specificity protein 1 (SP1), a zinc finger transcription factor that binds to a variety of GC-rich motifs and regulates the expression and function of miRNAs as well as the expression of genes associated with embryonic development and differentiation (36, 37). SP1 has been shown to regulate the placental glucocorticoid barrier by repressing the expression of 11β-hydroxysteroid dehydrogenase type 2, leading to fetal growth restriction (FGR) (38). One study identified the interaction of miR-331-3p with SP1 and the interaction of miR-331-3p and miR-1908-5p with glycosyltransferases as a novel mechanism for ABO blood group regulation (39). The second ranked hit in the TF analysis was EGR1 which has been previously implicated in follicular development, ovulation, corpus luteum formation and placental angiogenesis (40), and plays a key role in placental implantation (41). Notably, EGR1 was also identified in the construction of the PPI network.

Here we screened key genes altered in IVF-ET placental tissue based on mRNA next-generation sequencing data and online tools to identify ten hub genes. Among these, EGFR signals through Src- and ERK-mediated pathways activated by VEGFR2. Placental trophoblast cells are enriched in *EGFR* (42) and activation of *EGFR* regulates the proliferation, migration and invasive capacity of extravillous trophoblast cells (43). *FOS* is another molecule involved in angiogenesis. *FOS* belongs to the transcription factor-activated protein 1 (AP-1) superfamily, which is responsible for a variety of cellular processes, including proliferation, differentiation, apoptosis, hypoxia, angiogenesis and steroidogenesis (44, 45), as demonstrated in trophoblast cells (46). *LEP*, an important metabolic hormone, is highly expressed in the placenta and regulates placental, fetal growth and angiogenesis (47). *SPP1*, also called osteopontin (*OPN*), is located in the cytoplasm of placental syncytiotrophoblast and capillary endothelial cells and is considered a marker of placental bed remodeling. Placental development occurs in a hypoxic environment and can stimulate angiogenesis through upregulation of the vascular endothelial growth factor inhibitor of fibrinolytic plasminogen activator 1 (*SERPINE1*) (48).

Considering the important role of these key genes in placental development and angiogenesis, it was instructive to consider how

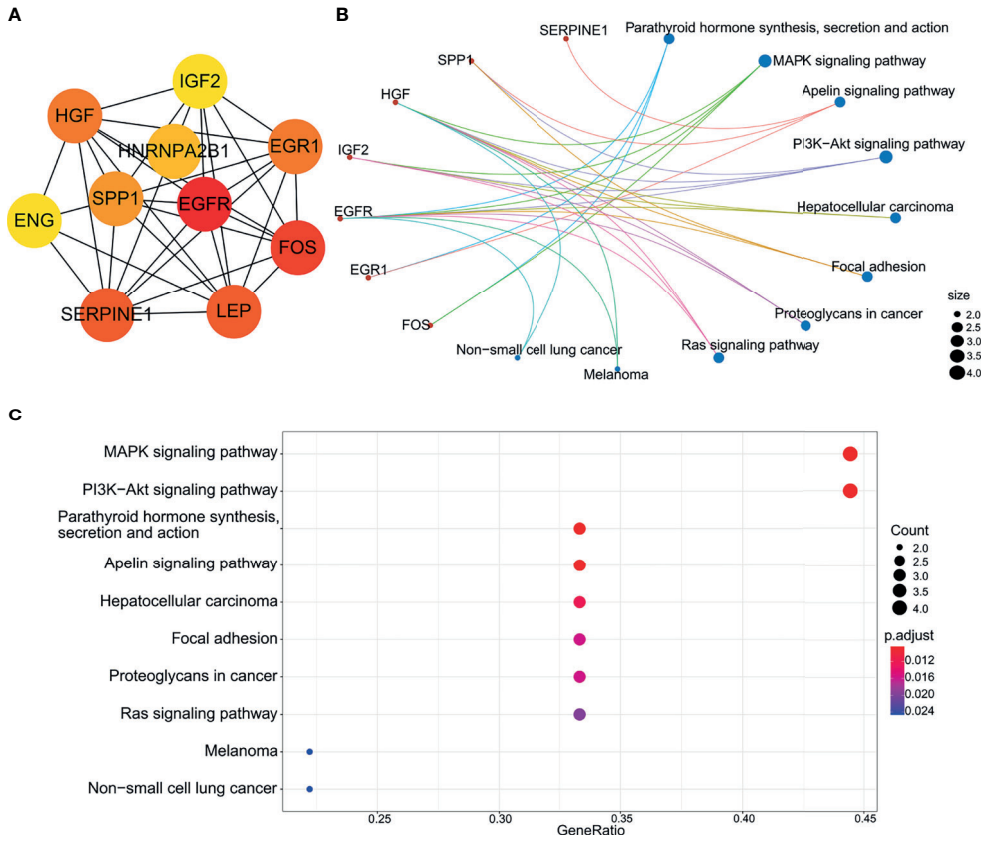

FIGURE 8 | Biological analysis of hub genes. **(A)** The interaction of 10 hub genes. **(B)** and **(C)** the top 10 KEGG enrichment analysis by R language.

these gene networks were impacted by altered miRNA expression. We used the intersection of miRNA and mRNA sequencing data to construct a microRNA-mRNA network. This analysis revealed more complexity in predicted interactions for the downregulated DeMiRs compared to their upregulated counterparts. Indeed, the downregulated DeMiRs display a far more extensive repertoire of target genes, particularly, hsa-miR-204-5p, hsa-miR-1269a and hsa-miR-941, for which, as discussed above, have tangible functional links to different aspects of placental regulation. Nonetheless, more work is needed to determine which gene targets are most functionally important but further understanding of the underlying mechanisms may help to reduce pregnancy complications and improve offspring safety.

Our current study has its limitations. The discovery cohort was small and we only validated selected miRNAs in the placentas of 8 IVF-ET assisted conception patients and 8 normal controls, which may reduce the reliability of our findings. Moreover, while we were diligent to sex match the placentals and minimize sampling bias by location, placental tissue is known to be divided into maternal, intermediate and fetal zones with different gene expression profiles (49) and inter-placental differences are inevitable. Moreover, the molecular interactions and proposed functional relationships proposed by the bioinformatic analyses need formal verification in both experimental and clinical settings. Thus, more work is needed to explore the specific functions of differentially expressed genes in IVF-ET placentas and their mechanisms.

CONCLUSIONS

In summary, we constructed a miRNA-mRNA regulatory network to regulate the expression of genes essential for IVF-ET placental development and function using bioinformatic analysis. Our data reveal both previously identified miRNAs and mRNAs associated with placental dysfunction and pregnancy complications along with novel candidates. As such these data represent a ready resource for subsequent investigations into the effects of IVF-ET on placental development and function and may provide a basis for future prevention and treatment of adverse perinatal outcomes.

DATA AVAILABILITY STATEMENT

The data presented in the study is deposited in the NCBI repository, accession number GSE186149.

ETHICS STATEMENT

Tissue collection was approved by the Ethics Committee of the Third Affiliated Hospital of Zhengzhou University. The patients/participants provided their written informed consent to participate in this study. Written informed consent was obtained from the individual(s) for the publication of any potentially identifiable images or data included in this article.

AUTHOR CONTRIBUTIONS

SY conducted the majority of the experiments and prepared the manuscript. WZ, MM, and SS were involved in the analysis and interpretation of the data. CY, RZ, NZ, SR, and HW collected samples of placenta and clinical data. RT contributed to the revision and critical discussion of the article. YG was engaged in research design, article drafting and critical discussion. All authors contributed to the article and approved the submitted version.

FUNDING

This work was supported by the Henan Province Science and Technology Tackling Plan awarded to YG (Grant no. 202102310061) with further funding support from the State Key Laboratory of Reproductive Medicine, Nanjing Medical University awarded to YG (Grant no. SKLRM-K201902 and SKLRM-K201903).

ACKNOWLEDGMENTS

The authors thank the participants who contributed to this study together with the clinical members involved in the care of our patients.

SUPPLEMENTARY MATERIAL

The Supplementary Material for this article can be found online at: https://www.frontiersin.org/articles/10.3389/fendo.2021.774997/full#supplementary-material

REFERENCES

1. Kushnir VA, Barad DH, Albertini DF, Darmon SK, Gleicher N. Systematic Review of Worldwide Trends in Assisted Reproductive Technology 2004-2013. *Reprod Biol Endocrinol* (2017) 15(1):6. doi: 10.1186/s12958-016-0225-2
2. Levine AD, Boulet SL, Kissin DM. Contribution of Assisted Reproductive Technologyto Overall Births by Maternal Age in the UnitedStates, 2012-2014. *JAMA* (2017) 317(12):1272–3. doi: 10.1001/jama.2016.21311
3. Lv H, Diao F, Du J, Chen T, Meng Q, Ling X, et al. Assisted Reproductive Technology and Birth Defects in a Chinese Birth Cohort Study. *Lancet Regional Health - Western Pacific* (2021) 7:100090. doi: 10.1016/j.lanwpc.2020.100090
4. Nejat EJ, Buyuk E. Reproductive Technologies and the Risk of Birth Defects. *N Engl J Med* (2012) 367(9):875; author reply 875–6. doi: 10.1056/NEJMc1206859
5. Wei SQ, Bilodeau-Bertrand M, Lo E, Auger N. Effect of Publicly Funded Assisted Reproductive Technology on Maternal and Infant Outcomes: A Pre- and Post-Comparison Study. *Hum Reprod* (2021) 36(1):219–28. doi: 10.1093/humrep/deaa270
6. Imudia AN, Awonuga AO, Doyle JO, Kaimal AJ, Wright DL, Toth TL, et al. Peak Serum Estradiol Level During Controlled Ovarian Hyperstimulation Is Associated With Increased Risk of Small for Gestational Age and Preeclampsia in Singleton Pregnancies After *In Vitro* Fertilization. *Fertil Steril* (2012) 97(6):1374–9. doi: 10.1016/j.fertnstert.2012.03.028
7. Romundstad LB, Romundstad PR, Sunde A, von During V, Skjaerven R, Vatten LJ. Increased Risk of Placenta Previa in Pregnancies Following IVF/ICSI; A Comparison of ART and Non-ART Pregnancies in the Same Mother. *Hum Reprod* (2006) 21(9):2353–8. doi: 10.1093/humrep/del153
8. Johnson KM, Hacker MR, Thornton K, Young BC, Modest AM. Association Between *In Vitro* Fertilization and Ischemic Placental Disease by Gestational Age. *Fertil Steril* (2020) 114(3):579–86. doi: 10.1016/j.fertnstert.2020.04.029
9. Heo JS, Lee HJ, Lee MH, Choi CW. Comparison of Neonatal Outcomes of Very Low Birth Weight Infants by Mode of Conception: *In Vitro* Fertilization Versus Natural Pregnancy. *Fertil Steril* (2019) 111(5):962–70. doi: 10.1016/j.fertnstert.2019.01.014
10. Yang X, Li Y, Li C, Zhang W. Current Overview of Pregnancy Complications and Live-Birth Outcome of Assisted Reproductive Technology in Mainland China. *Fertil Steril* (2014) 101(2):385–91. doi: 10.1016/j.fertnstert.2013.10.017
11. Hansen M, Kurinczuk JJ, Milne E, de Klerk N, Bower C. Assisted Reproductive Technology and Birth Defects: A Systematic Review and Meta-Analysis. *Hum Reprod Update* (2013) 19(4):330–53. doi: 10.1093/humupd/dmt006
12. Santamaria X, Taylor H. MicroRNA and Gynecological Reproductive Diseases. *Fertil Steril* (2014) 101(6):1545–51. doi: 10.1016/j.fertnstert.2014.04.044
13. Fasanaro P, Greco S, Ivan M, Capogrossi MC, Martelli F. microRNA: Emerging Therapeutic Targets in Acute Ischemic Diseases. *Pharmacol Ther* (2010) 125(1):92–104. doi: 10.1016/j.pharmthera.2009.10.003
14. Mayor-Lynn K, Toloubeydokhti T, Cruz AC, Chegini N. Expression Profile of microRNAs and mRNAs in Human Placentas From Pregnancies Complicated by Preeclampsia and Preterm Labor. *Reprod Sci* (2011) 18(1):46–56. doi: 10.1177/1933719110374115
15. Fu G, Brkic J, Hayder H, Peng C. MicroRNAs in Human Placental Development and Pregnancy Complications. *Int J Mol Sci* (2013) 14(3):5519–44. doi: 10.3390/ijms14035519
16. Vaiman D. Genes, Epigenetics and miRNA Regulation in the Placenta. *Placenta* (2017) 52:127–33. doi: 10.1016/j.placenta.2016.12.026
17. Su MT, Tsai PY, Tsai HL, Chen YC, Kuo PL. miR-346 and miR-582-3p-Regulated EG-VEGF Expression and Trophoblast Invasion *via* Matrix Metalloproteinases 2 and 9. *Biofactors* (2017) 43(2):210–9. doi: 10.1002/biof.1325
18. Gu Y, Ampofo E, Menger MD, Laschke MW. miR-191 Suppresses Angiogenesis by Activation of NF-KappaB Signaling. *FASEB J* (2017) 31(8):3321–33. doi: 10.1096/fj.201601263R
19. Li P, Guo W, Du L, Zhao J, Wang Y, Liu L, et al. microRNA-29b Contributes to Pre-Eclampsia Through Its Effects on Apoptosis, Invasion and Angiogenesis of Trophoblast Cells. *Clin Sci (Lond)* (2013) 124(1):27–40. doi: 10.1042/CS20120121
20. Luo M, Weng Y, Tang J, Hu M, Liu Q, Jiang F, et al. MicroRNA-450a-3p Represses Cell Proliferation and Regulates Embryo Development by Regulating Bub1 Expression in Mouse. *PLoS One* (2012) 7(10):e47914. doi: 10.1371/journal.pone.0047914
21. Pathan M, Keerthikumar S, Chisanga D, Alessandro R, Ang CS, Askenase P, et al. A Novel Community Driven Software for Functional Enrichment Analysis of Extracellular Vesicles Data. *J Extracell Vesicles* (2017) 6(1):1321455. doi: 10.1080/20013078.2017.1321455
22. Pathan M, Keerthikumar S, Ang CS, Gangoda L, Quek CY, Williamson NA, et al. FunRich: An Open Access Standalone Functional Enrichment and Interaction Network Analysis Tool. *Proteomics* (2015) 15(15):2597–601. doi: 10.1002/pmic.201400515

23. Zhou J, Hui X, Mao Y, Fan L. Identification of Novel Genes Associated With a Poor Prognosis in Pancreatic Ductal Adenocarcinoma *via* a Bioinformatics Analysis. *Biosci Rep* (2019) 39(8):BSR20190625. doi: 10.1042/BSR20190625
24. Smoot ME, Ono K, Ruscheinski J, Wang PL, Ideker T. Cytoscape 2.8: New Features for Data Integration and Network Visualization. *Bioinformatics* (2011) 27(3):431–2. doi: 10.1093/bioinformatics/btq675
25. Szklarczyk D, Franceschini A, Wyder S, Forslund K, Heller D, Huerta-Cepas J, et al. STRING V10: Protein-Protein Interaction Networks, Integrated Over the Tree of Life. *Nucleic Acids Res* (2015) 43(Database issue):D447–52. doi: 10.1093/nar/gku1003
26. Su G, Morris JH, Demchak B, Bader GD. Biological Network Exploration With Cytoscape 3. *Curr Protoc Bioinf* (2014) 47:8.13.1–8.13.24. doi: 10.1002/0471250953.bi0813s47
27. Chang S, Chen W, Yang J. Another Formula for Calculating the Gene Change Rate in Real-Time RT-PCR. *Mol Biol Rep* (2009) 36(8):2165–8. doi: 10.1007/s11033-008-9430-1
28. Oliveira AC, Bovolenta LA, Nachtigall PG, Herkenhoff ME, Lemke N, Pinhal D. Combining Results From Distinct MicroRNA Target Prediction Tools Enhances the Performance of Analyses. *Front Genet* (2017) 8:59. doi: 10.3389/fgene.2017.00059
29. Yu D, Lim J, Wang X, Liang F, Xiao G. Enhanced Construction of Gene Regulatory Networks Using Hub Gene Information. *BMC Bioinf* (2017) 18(1):186. doi: 10.1186/s12859-017-1576-1
30. Morales-Prieto DM, Ospina-Prieto S, Schmidt A, Chaiwangyen W, Markert UR. Elsevier Trophoblast Research Award Lecture: Origin, Evolution and Future of Placenta miRNAs. *Placenta* (2014) 35 Suppl:S39–45. doi: 10.1016/j.placenta.2013.11.017
31. Rodosthenous RS, Burris HH, Sanders AP, Just AC, Dereix AE, Svensson K, et al. Second Trimester Extracellular microRNAs in Maternal Blood and Fetal Growth: An Exploratory Study. *Epigenetics* (2017) 12(9):804–10. doi: 10.1080/15592294.2017.1358345
32. Chen X, Mangala LS, Mooberry L, Bayraktar E, Dasari SK, Ma S, et al. Identifying and Targeting Angiogenesis-Related microRNAs in Ovarian Cancer. *Oncogene* (2019) 38(33):6095–108. doi: 10.1038/s41388-019-0862-y
33. Zhang S, Sun Q, Jiang X, Gao F. Clinical Significance of Expression of Hsa-Mir-1247 and Hsa-Mir-1269a in Ectopic Pregnancy Due to Salpingitis. *Exp Ther Med* (2018) 15(6):4901–5. doi: 10.3892/etm.2018.5998
34. Hu HY, He L, Fominykh K, Yan Z, Guo S, Zhang X, et al. Evolution of the Human-Specific microRNA miR-941. *Nat Commun* (2012) 3(1):1145. doi: 10.1038/ncomms2146
35. Li SP, Cheng WN, Li Y, Xu HB, Han H, Li P, et al. Keap1-Targeting microRNA-941 Protects Endometrial Cells From Oxygen and Glucose Deprivation-Re-Oxygenation *via* Activation of Nrf2 Signaling. *Cell Commun Signal* (2020) 18(1):32. doi: 10.1186/s12964-020-0526-0
36. Marin M, Karis A, Visser P, Grosveld F, Philipsen S. Transcription Factor Sp1 Is Essential for Early Embryonic Development But Dispensable for Cell Growth and Differentiation. *Cell* (1997) 89(4):619–28. doi: 10.1016/s0092-8674(00)80243-3
37. Thomas K, Wu J, Sung DY, Thompson W, Powell M, McCarrey J, et al. SP1 Transcription Factors in Male Germ Cell Development and Differentiation. *Mol Cell Endocrinol* (2007) 270(1-2):1–7. doi: 10.1016/j.mce.2007.03.001
38. Fan F, Shen W, Wu S, Chen N, Tong X, Wang F, et al. Sp1 Participates in the Cadmium-Induced Imbalance of the Placental Glucocorticoid Barrier by Suppressing 11beta-HSD2 Expression. *Environ Pollut* (2020) 261:113976. doi: 10.1016/j.envpol.2020.113976
39. Kronstein-Wiedemann R, Nowakowska P, Milanov P, Gubbe K, Seifried E, Bugert P, et al. Regulation of ABO Blood Group Antigen Expression by miR-331-3p and miR-1908-5p During Hematopoietic Stem Cell Differentiation. *Stem Cells* (2020) 38(10):1348–62. doi: 10.1002/stem.3251
40. Guo B, Tian XC, Li DD, Yang ZQ, Cao H, Zhang QL, et al. Expression, Regulation and Function of Egr1 During Implantation and Decidualization in Mice. *Cell Cycle* (2014) 13(16):2626–40. doi: 10.4161/15384101.2014.943581
41. Yang W, Lu Z, Zhi Z, Liu L, Deng L, Jiang X, et al. Increased miRNA-518b Inhibits Trophoblast Migration and Angiogenesis by Targeting EGR1 in Early Embryonic Arrest. *Biol Reprod* (2019) 101(4):664–74. doi: 10.1093/biolre/ioz109/5530751
42. Clemente L, Boeldt DS, Grummer MA, Morita M, Morgan TK, Wiepz GJ, et al. Adenoviral Transduction of EGFR Into Pregnancy-Adapted Uterine Artery Endothelial Cells Remaps Growth Factor Induction of Endothelial Dysfunction. *Mol Cell Endocrinol* (2020) 499:110590. doi: 10.1016/j.mce.2019.110590
43. Denison FC, Battersby S, King AE, Szuber M, Jabbour HN. Prokineticin-1: A Novel Mediator of the Inflammatory Response in Third-Trimester Human Placenta. *Endocrinology* (2008) 149(7):3470–7. doi: 10.1210/en.2007-1695
44. Choi Y, Rosewell KL, Brannstrom M, Akin JW, Curry TEJr., Jo M. FOS, a Critical Downstream Mediator of PGR and EGF Signaling Necessary for Ovulatory Prostaglandins in the Human Ovary. *J Clin Endocrinol Metab* (2018) 103(11):4241–52. doi: 10.1210/jc.2017-02532
45. Preston GA, Lyon TT, Yin Y, Lang JE, Solomon G, Annab L, et al. Induction of Apoptosis by C-Fos Protein. *Mol Cell Biol* (1996) 16(1):211–8. doi: 10.1128/mcb.16.1.211
46. Renaud SJ, Kubota K, Rumi MA, Soares MJ. The FOS Transcription Factor Family Differentially Controls Trophoblast Migration and Invasion. *J Biol Chem* (2014) 289(8):5025–39. doi: 10.1074/jbc.M113.523746
47. Ashworth CJ, Hoggard N, Thomas L, Mercer JG, Wallace JM, Lea RG. Placental Leptin. *Rev Reprod* (2000) 5(1):18–24. doi: 10.1530/ror.0.0050018
48. Delforce SJ, Lumbers ER, Morosin SK, Wang Y, Pringle KG. The Angiotensin II Type 1 Receptor Mediates the Effects of Low Oxygen on Early Placental Angiogenesis. *Placenta* (2019) 75:54–61. doi: 10.1016/j.placenta.2018.12.001
49. Sood R, Zehnder JL, Druzin ML, Brown PO. Gene Expression Patterns in Human Placenta. *Proc Natl Acad Sci USA* (2006) 103(14):5478–83. doi: 10.1073/pnas.0508035103

Conflict of Interest: The authors declare that the research was conducted in the absence of any commercial or financial relationships that could be construed as a potential conflict of interest.

Publisher's Note: All claims expressed in this article are solely those of the authors and do not necessarily represent those of their affiliated organizations, or those of the publisher, the editors and the reviewers. Any product that may be evaluated in this article, or claim that may be made by its manufacturer, is not guaranteed or endorsed by the publisher.

Copyright © 2021 Yang, Zheng, Yang, Zu, Ran, Wu, Mu, Sun, Zhang, Thorne and Guan. This is an open-access article distributed under the terms of the Creative Commons Attribution License (CC BY). The use, distribution or reproduction in other forums is permitted, provided the original author(s) and the copyright owner(s) are credited and that the original publication in this journal is cited, in accordance with accepted academic practice. No use, distribution or reproduction is permitted which does not comply with these terms.

frontiers in Endocrinology

ORIGINAL RESEARCH
published: 17 November 2021
doi: 10.3389/fendo.2021.765639

Novel Loss-of-Function Mutations in *DNAH1* Displayed Different Phenotypic Spectrum in Humans and Mice

Ranjha Khan[1‡], Qumar Zaman[1‡], Jing Chen[1‡], Manan Khan[1†‡], Ao Ma[1], Jianteng Zhou[1], Beibei Zhang[1], Asim Ali[1], Muhammad Naeem[2], Muhammad Zubair[1], Daren Zhao[1], Wasim Shah[1], Mazhar Khan[1], Yuanwei Zhang[1], Bo Xu[3], Huan Zhang[1]* and Qinghua Shi[1]**

[1] First Affiliated Hospital of University of Science and Technology of China (USTC), Hefei National Laboratory for Physical Sciences at Microscale, School of Basic Medical Sciences, Division of Life Sciences and Medicine, Chinese Academy of Sciences (CAS) Center for Excellence in Molecular Cell Science, University of Science and Technology of China, Hefei, China, [2] Medical Genetics Research Laboratory, Department of Biotechnology, Quaid-i-Azam University, Islamabad, Pakistan, [3] Reproductive and Genetic Hospital, The First Affiliated Hospital of University of Science and Technology of China (USTC), Division of Life Sciences and Medicine, University of Science and Technology of China, Hefei, China

Male infertility is a prevalent disorder distressing an estimated 70 million people worldwide. Despite continued progress in understanding the causes of male infertility, idiopathic sperm abnormalities such as multiple morphological abnormalities of sperm flagella (MMAF) still account for about 30% of male infertility. Recurrent mutations in *DNAH1* have been reported to cause MMAF in various populations, but the underlying mechanism is still poorly explored. This study investigated the MMAF phenotype of two extended consanguineous Pakistani families without manifesting primary ciliary dyskinesia symptoms. The transmission electron microscopy analysis of cross-sections of microtubule doublets revealed a missing central singlet of microtubules and a disorganized fibrous sheath. SPAG6 staining, a marker generally used to check the integration of microtubules of central pair, further confirmed the disruption of central pair in the spermatozoa of patients. Thus, whole-exome sequencing (WES) was performed, and WES analysis identified two novel mutations in the *DNAH1* gene that were recessively co-segregating with MMAF phenotype in both families. To mechanistically study the impact of identified mutation, we generated *Dnah1* mice models to confirm the *in vivo* effects of identified mutations. Though *Dnah1*$^{\triangle iso1/\triangle iso1}$ mutant mice represented MMAF phenotype, no significant defects were observed in the ultrastructure of mutant mice spermatozoa. Interestingly, we found DNAH1 isoform2 in *Dnah1*$^{\triangle iso1/\triangle iso1}$ mutant mice that may be mediating the formation of normal ultrastructure in the absence of full-length protein. Altogether we are first reporting the possible explanation of inconsistency between mouse and human *DNAH1* mutant phenotypes, which will pave the way for further understanding of the underlying pathophysiological mechanism of MMAF.

Keywords: MMAF, male infertility, mutant mice, *DNAH1*, central singlet

OPEN ACCESS

Edited by:
Furhan Iqbal,
Bahauddin Zakariya University, Pakistan

Reviewed by:
Yanwei Sha,
Xiamen University, China
Faiz Rasul,
Peking University, China
Saima Malik,
University of Alabama at Birmingham, United States

****Correspondence:***
Bo Xu
bioxubo@mail.ustc.edu.cn
Huan Zhang
likemoonriver@126.com
Qinghua Shi
qshi@ustc.edu.cn

†Present address:
Manan Khan,
Department of Biotechnology and Genetic Engineering Hazara University, Mansehra, Pakistan

‡These authors have contributed equally to this work

Specialty section:
This article was submitted to Reproduction, a section of the journal Frontiers in Endocrinology

Received: *27 August 2021*
Accepted: *22 October 2021*
Published: *17 November 2021*

Citation:
Khan R, Zaman Q, Chen J, Khan M, Ma A, Zhou J, Zhang B, Ali A, Naeem M, Zubair M, Zhao D, Shah W, Khan M, Zhang Y, Xu B, Zhang H and Shi Q (2021) Novel Loss-of-Function Mutations in DNAH1 Displayed Different Phenotypic Spectrum in Humans and Mice. Front. Endocrinol. 12:765639. doi: 10.3389/fendo.2021.765639

INTRODUCTION

Male infertility is a global health concern with social and psychological impact on more than 70 million infertile men (1). Recent studies have demonstrated that sperm defects, such as reduced sperm count, decreased sperm motility, and abnormal morphology, are directly linked with male infertility (2). Sperm motility is required for normal fertilization, and around 80% of infertility is caused by compromised sperm motility (3). Subsequently, sperm morphology is also an important player necessary for sperm locomotion, and defects in sperm morphologies are associated with a major form of male infertility (4). Defects in sperm morphology are generally manifested with a wide range of phenotypic variations in the head, neck, mid-piece, and tail of spermatozoa. Among these, the most common type of abnormities is found in the form of multiple morphological abnormalities of sperm flagella (MMAF) in asthenospermia patients. The most common defects of sperm flagella observed in MMAF phenotype include coiled, bent, irregular, short, absent, or irregular-width flagella (5). Normal sperm flagella contain a typical axonemal arrangement of nine peripheral microtubules and two central microtubules (CP), which are further surrounded by dense outer fiber and fibrous sheath (6). This basic structure of flagella remains conserved through the process of evolution. Any structural aberrations in these components of sperm flagella are associated with a wide range of MMAF phenotypes which further caused a reduction of sperm motility or even sperm immobility and eventually male infertility.

DNAH1 (MIM 603332) is an essential gene that encodes inner dynein arm (IDA) heavy chain, which are believed to strengthen the link between radial spokes and outer doublet (7). IDA, an ATPase-based protein complex, is responsible for beat generation and regulation of flagellar movement (8, 9). Recurrent mutations in *DNAH1* are commonly associated with MMAF in various populations (7, 10, 11). Moreover, researchers are extensively investigating the molecular mechanism of MMAF by generating knockout (KO) mice models of various genes that have been associated with MMAF phenotype in humans (6). Until now, mutations in various genes, such as *CFAP43*, *CFAP44*, *CFAP47*, *CFAP58*, *CFAP65*, *CFAP69*, *CFAP70*, *CFAP74*, *CFAP91*, *CFAP206*, *CFAP251*, *DNAH1*, *DNAH2*, *DNAH6*, *DNAH8*, *DNAH10*, *DNAH17*, *WDR19*, *ARMC2*, *TTC21A*, *TTC29*, *FSIP2*, *AK7*, *CEP135*, *SPEF2*, *QRICH2*, *DZIP1*, *BRWD1*, *DRC1*, *STK33*, *etc.*, have been reported with MMAF phenotype (10, 12–25). However, a discrepancy exists in the *Dnah1* KO mouse model and human phenotype (26, 27). A previous study demonstrated that *Dnah1* KO mice are completely infertile due to defects in sperm motility, but the ultrastructure of flagella did not show any abnormalities in their components (26). On the other hand, *DNAH1* mutant human sperm ultrastructure was severely compromised because of lacking CP and other defects. Thus, uncovering the inconsistency between human and mouse phenotypes of the *DNAH1* gene required a deeper study to discover the unknown isoforms mediating the intact formation of normal ultrastructure of mouse sperm flagella in the absence of full-length DNAH1 protein.

In the present study, we recruited two extended consanguineous Pakistani families suffering from male infertility due to the MMAF phenotype. Subsequently, whole-exome sequencing (WES) identified two novel mutations in the *DNAH1* gene that were recessively co-segregating with infertility phenotype in both families. Furthermore, we generated *Dnah1* mice models to confirm the *in vivo* effects of identified mutations. Interestingly, we found *Dnah1* isoform2 in $Dnah1^{\triangle iso1/\triangle iso1}$ mutant mice that may be mediating the formation of normal ultrastructure in the absence of full-length protein. Altogether we are the first one to present the possible explanation of inconsistency between mouse and human *DNAH1* mutant phenotype, which will pave the way for further understanding of the underlying pathophysiological mechanism of MMAF.

MATERIALS AND METHODS

Recruitment of Families and Phenotype Confirmation

Two consanguineous families from Pakistan, comprising six male patients, were enrolled to investigate the underlying genetic cause of male infertility. Detailed pedigrees were constructed according to the provided information by the parents of the patients. An initial physical and andrological examination displayed that all patients have normal body mass index and no primary ciliary dyskinesia (PCD) symptoms. Other associated diseases, such as hypogonadotropic hypogonadism, cryptorchidism, varicocele, seminal ductal obstruction, testicular trauma, and andrological tumor, were also not observed. Two repeated semen analyses were performed according to the WHO manual of 2010, and all the parameters were recorded (**Table 1**). We also recruited the fertile siblings of patients and their parents to serve as a positive control for genetic analysis. The study was approved by a bioethical committee of Pakistan and the ethical review board of the University of Science and Technology of China. Informed consent was obtained from all participants of both families.

WES and Linkage Analysis

Genomic DNA was extracted from all available members of both families by using QIAamp Blood DNA Mini Kit (QIAGEN) as per the protocol of the manufacturer. WES was conducted on III:2, IV:1, III:3, V:1, V:2, V:3, and V:5 from family members of PK-INF-15 and PK-INF-319, respectively, previously reported in (28). Briefly, WES data from the selected members were enriched by the Agilent SureSelect XT Human All Exon Kit. The Illumina HiSeq XTEN platform accompanied next-generation sequencing. The obtained raw reads were aligned to the human genome reference assembly (GRCh37/hg19) using the Burrows-Wheeler Aligner (29). Next, the Picard software was engaged to remove polymerase chain reaction (PCR) duplicates and evaluate the quality of variants. DNA sequence variants were analyzed by the best practice genome analysis kit (30). VCF files were used for

TABLE 1 | Clinical characteristics of patients.

	Reference values	PK-INF-15	PK-INF-319		
		IV:1	V:1	V:2	V:3
Gene	–	*DNAH1*	*DNAH1*	*DNAH1*	*DNAH1*
cDNA mutation	–	c.7646_7647InsC	c.6212T>G	c.6212T>G	c.6212T>G
Protein alteration	–	p.N2549Qfs*61	p.C1789Y	p.C1789Y	p.C1789Y
Fertility	–	Infertile	Infertile	Infertile	Infertile
Age (years old)[a]	–	1978	1980	1984	1986
Years of marriage	–	2003	2005	2007	2010
Height/weight (cm/kg)	–	183.0/70.0	183.0/99.0	180.0/86.0	180.0/86.0
Semen parameters[b]					
Semen volume (ml)	>1.5	1.5	2.4 ± 0.4	2.5 ± 0.5	3.8 ± 0.8
Semen pH	Alkaline	Alkaline	Alkaline	Alkaline	Alkaline
Sperm concentration (10^6/ml)	>15	6.0	3.0 ± 0.5	7.0 ± 4.0	20.0 ± 5.0
Normal sperm morphology (%)	>4	0	2.6	0.6	–
Motile sperm (%)	>40	0	0	0.5 ± 0.5	0
Progressively motile sperm (%)	>32	0	0	0	0
Sperm flagella					
Morphologically normal (%)	–	0	2.6	0.6	–
Absent (%)	–	11.0	24.7	26.8	–
Short (%)	–	22.0	24.3	26.2	–
Coiled (%)	–	19.0	30.5	29.2	–
Bent (%)	–	5.0	4.8	8.0	–
Irregular caliber (%)	–	43.0	13.1	9.2	–

[a]*Ages at the manuscript submission.* [b]*Reference values were published by WHO in 2010.*

parametric linkage analysis, as described previously (31), and four linkage regions were identified with a logarithm of odds (LOD) score of more than 0.5. Further screening was opted for the variants that were located on linkage regions and following Mendelian inheritance pattern.

Filtering and Selection of Candidate Variants

Only variants that have depth >×20, genotype quality >90, and 0.5-cM intervals between each other were designated as markers. MERLIN software was employed on genotyped single-nucleotide polymorphism for linkage analysis with these parameters: due to consanguinity in the families, recessive mode of inheritance was adopted, with a disease allele frequency of 0.001 and 100% penetrance. A number of five peaks with a LOD score of more than 0.5 were considered as linkage regions. The variants that resided in the linkage regions were further annotated by ANNOVAR using the NCBI RefSeq gene annotation. We adopted the following filtration strategy to select potential candidate disease-causing variants in patients: (i) variants that were heterozygous in the father and control brothers and homozygous in patients were retained; (ii) variants with minor allele frequency of more than 0.01 in public databases such as 1000 Genome project (32), ESP6500 (33), or ExAC database (34), and variants homozygous in our in-house WES variants call set generated from 578 fertile male samples (41 Pakistanis, 254 Chinese, and 283 Europeans) were excluded; (iii) variants that affect protein sequence and predicted to be deleterious by around 10 of 13 *in silico* employed tools were kept; and (iv) variants which have a predominant expression in the testes and their inactivation affects male fertility were retained based on spermatogenesis online database (35) and were checked by Sanger sequencing to verify Mendel inheritance pattern. All these strategies are more clearly explained in a flow chart diagram in **Supplementary Figure S2**. Finally, only *DNAH1* variants followed the inheritance pattern and thus were considered the potential candidates causing MMAF phenotype in subjects under investigation. The list of primers used for Sanger sequencing is shown in **Supplementary Table S1**.

Immunofluorescence Staining

Immunofluorescence on the spermatozoa of patients was performed, as we have previously reported (36). Briefly, sperm from patients were smeared on the clean slide and fixed with 4% paraformaldehyde followed by three times of washing in phosphate-buffered saline (PBS). The slides were permeabilized with 0.5% Triton X-100 for 30 min and blocked with 1% BSA. Next, the slides were incubated with primary antibodies, including α-tubulin (Sigma, F2168), DNAH1 (Abcam, ab122367), and SPAG6 (Proteintech, 12462-1-AP), overnight at 4°C. On the next day, the slides were washed with PBST (PBS containing Triton X-100) and incubated with secondary antibodies DAR555 (Molecular Probes, A31572) and GAM488 (Molecular Probes, A21121) for 1 h at 37°C. Finally, the slides were washed again and sealed with Hoechst and Vectashield. Images were captured by using a laser scanning confocal microscope (Olympus).

Electron Microscopy Analysis

Sperm samples from patients were processed in 0.1 M phosphate buffer (pH 7.4) containing 4% paraformaldehyde, 8% glutaraldehyde, and 0.2% picric acid at 4°C. Scanning and transmission electron microscopy (SEM and TEM) were performed as previously described, with minor modifications (36). Briefly, spermatozoa were washed in 0.1 M PBS four times, followed by fixation in 1% OsO_4 and dehydration. Then, samples

were infiltrated for acetone and epon resin mixture and embedded in sputter-coated (SCD 500, Bal-Tel). Thinly sectioned (70 mm) samples were stained with uranyl acetate and lead citrate. The morphology of spermatozoa was examined by Hitachi S-4800 field emission scanning electron microscope under an accelerating voltage of 15 kV. The ultrastructure of the samples was analyzed and captured by Tecnai 10 or 12Microscope (Philips) at 100 or 120 kV or by H-7650 microscope (Hitachi) at 100 kV.

Generation of Mutant Mice Models

Dnah1$^{-/-}$ and *Dnah1*$^{\triangle iso1/\triangle iso1}$ mice were generated by using CRISPR/Cas9 genome editing technology as previously reported (37). Briefly, single guide RNAs (sgRNAs) designed to target exon 2 and 49 of *Dnah1* to generate KO and mutant mice, respectively, were transcribed *in vitro* (Addgene, 5132). Single-strand oligodeoxynucleotides (ssODNs), with a mutation similar to family A2 patients and a synonymous mutation at the protospacer adjacent motif, were created by the Sangon Biotech system. The designed sgRNAs and ssODNs were microinjected with Cas9 mRNAs into the zygotes of B6D2F1 (C57BL/6×DBA/2J) mice, following a previously published methodology (38). The genotyping of newborn pups was determined by Sanger sequencing, and heterozygous Dnah1+/- and Dnah1+/△iso1 mice were bred to obtain the desired homozygous results of *Dnah1*$^{-/-}$ and *Dnah1*$^{\triangle iso1/\triangle iso1}$ mice for future experiments. The sequence of guide RNAs and all the primers used for genotyping is shown in **Supplementary Table S1**.

Western Blotting

Testes from 8-week-old *Dnah1*$^{-/-}$ and *Dnah1*$^{\triangle iso1/\triangle iso1}$ mice were detached and processed in radio-immunoprecipitation assay buffer (25 mM Tris-HCl, pH 7.6, 150 mM NaCl, 1% NP-40, 1% sodium deoxycholate, and 0.1% sodium dodecyl sulfate) complemented with protease inhibitors cocktail using a Tissuelyzer and then cleared by centrifugation. Western blotting was performed as previously reported (39). Nitrocellulose membranes were incubated with primary antibodies against DNAH1 (this study) and GAPDH overnight at 4°C. On the next day, membranes were washed in PBST and incubated with secondary antibodies for 1 h at room temperature. The blots were developed with chemiluminescence (Image Quant LAS 4000, GE Healthcare).

RNA Extraction and Reverse Transcriptase-PCR

According to the protocol of the manufacturer, total RNA from mice and control human testes was extracted by using Trizol (Invitrogen) kit. RT-PCR was conducted as we have previously described (40). The primer used for RT-PCR is listed in **Supplementary Table S1**.

Phenotypic Investigation of Mutant Mice

The fertility status of *Dnah1*$^{\triangle iso1/\triangle iso1}$ mice was assessed by caging each mutant mouse with two wild-type females (C57/BL) for 3 months. A total of five *Dnah1*$^{\triangle iso1/\triangle iso1}$ mice were tested, and none of them produce a single pup (**Table 2**). Testes morphology, sperm count, H&E, sperm morphology, and sperm motility were performed as previously described (36, 39).

RESULTS

Recruitment of Infertile Patients Manifesting MMAF Phenotype

In the present study, we recruited two infertile consanguineous Pakistani families (PK-INF-15 and PK-INF-319) consisting of six patients that were suffering from primary infertility (**Figure 1A**). The semen analysis of four patients showed a sufficient sperm concentration, while all sperms were immotile (**Table 1**). SEM and light microscopy investigation revealed abnormalities in sperm tail, displaying different defects of sperm flagella, including absent, short, coiled, bent, and irregular caliber, suggesting MMAF (**Supplementary Figures S1A, B**). Similarly, the SEM of sperm from patients also confirmed the MMAF phenotype (**Figure 1B**). Altogether these results indicated that MMAF accompanies the underlying cause of infertility in these families.

TABLE 2 | Characteristics of *Dnah1*$^{+/\triangle iso1}$, *Dnah1*$^{\triangle iso1/\triangle iso1}$, *Dnah1*$^{+/-}$, and *Dnah1*$^{-/-}$ male mice.

	Dnah1$^{+/\triangle iso1}$	*Dnah1*$^{\triangle iso1/\triangle iso1}$	*Dnah1*$^{+/-}$	*Dnah1*$^{-/-}$
Body weight (g)	24.87 ± 2.91	23.11 ± 2.63	19.28 ± 1.92	19.68 ± 4.32
Testis weight (mg)	188.1 ± 26.70	171.0 ± 17.70	128.5 ± 14.10	137.9 ± 36.8
Testis/body weight ratio (10^{-3})	7.56 ± 0.64	7.48 ± 1.27	6.77 ± 1.18	7.03 ± 0.95
Semen parameters				
Sperm count (10^7)	1.17 ± 0.15	0.45 ± 0.08	1.05 ± 0.12	0.51 ± 0.03
Motile sperm (%)	71.10 ± 7.08	26.53 ± 7.03	70.74	39.56
Progressively motile sperm (%)	43.12 ± 1.13	3.97 ± 2.11	54.59	10.67
Sperm flagella				
Normal (%)	81.84 ± 1.33	33.95 ± 7.58	84.01 ± 1.35	45.46 ± 5.91
Absent (%)	16.13 ± 0.73	53.11 ± 9.63	12.20 ± 2.67	48.56 ± 7.18
Short (%)	0.56 ± 0.19	3.68 ± 1.12	0.72 ± 0.32	1.12 ± 0.37
Coiled (%)	0.31 ± 0.28	2.37 ± 0.67	0.13 ± 0.13	1.19 ± 0.01
Bent (%)	0.98 ± 0.56	1.45 ± 0.69	2.50 ± 1.16	1.87 ± 1.14
Irregular (%)	0.19 ± 0.19	5.44 ± 1.30	0.43 ± 0.26	1.79 ± 0.66

For semen analysis, three 8-week-old mice were examined for each genotype. Data are presented as mean ± SEM.

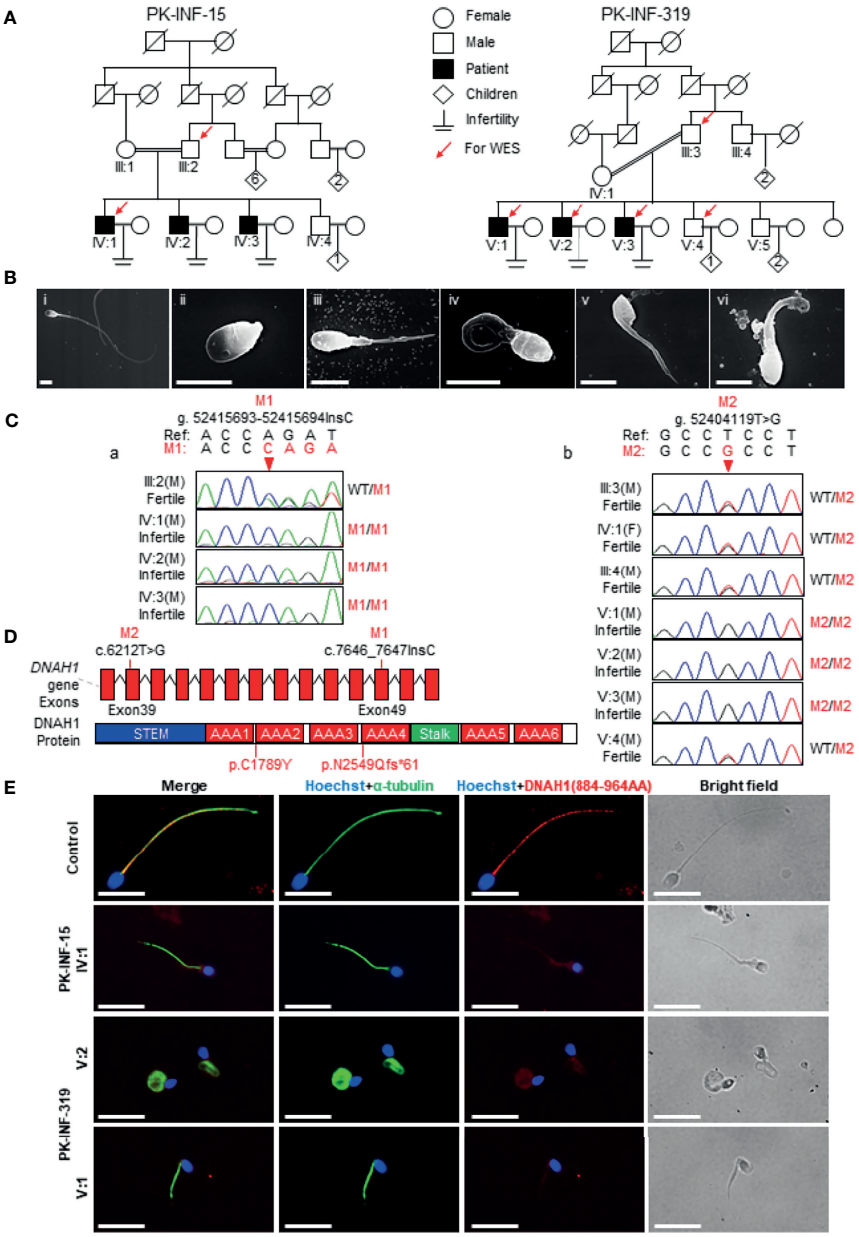

FIGURE 1 | Recruitment of infertile families displaying multiple morphological abnormalities of sperm flagella phenotype. **(A)** Two consanguineous Pakistani infertile families (PK-INF-15 and PK-INF-319), comprising six male patients, were recruited. Male individuals are represented by squares, while female individuals were indicated with a circle. Diamonds indicate offspring, and the numerals inside designate the number of offspring. Solid squares are used to indicate patients, slashes represent deceased family members, and parallel slash lines specify consanguineous marriages. The red arrows indicate the members selected for whole-exome sequencing. **(B)** Scanning electron microscopy of sperm control (i) and from patients [PK-INF-319], V:1 (ii, ii, and iv) and V:2 (v and vi)] displayed various defects of flagella, including absent, short, coiled, and irregular calibers. Scale bar, 10 um. **(C)** Chromatograms representing the segregation of *DNAH1* mutations in available members from families (a) PK-INF-15 and (b) PK-INF-319. The red arrows show the genomic position of *DNAH1* mutations. **(D)** An illustrative representation of DNAH1 gene and subsequent protein structure showing the identified mutation positions. **(E)** No DNAH1 signals were found on paraformaldehyde-fixed sperm from a patient stained against DNAH1 and α-tubulin, while intact DNAH1 signals were observed on sperm obtained from a healthy control. Scale bar, 10 um.

Whole-Exome-Identified Novel Loss-of-Function Mutations in *DNAH1*

In order to explore the underlying genetic cause of infertility, WES was performed on four patients, the control brother and their parents (III:2, IV:1, III:3, V:1, V:2, V:3, and V:4). Considering the consanguinity within the families, we screened the WES data and only retained the variants that displayed recessive inherence patterns. Furthermore, we filter the variants based on minor allele frequency,

testis-specific expression, and review of literature about the genes that have an association with the MMAF phenotype. In short, we identified two novel mutations in *DNAH1*: one was the insertion of C (c.7646_7647InsC, p.N2549Qfs*61), causing a truncation of protein in the family A1, and the other was a missense mutation (c.6212T>G, p.C1789Y) in family A2 (**Figure 1D**). Sanger sequencing on DNA from all available members of both families indicated that the mutations are recessively segregating in all patients with infertility phenotype (**Figures 1Ca, b**). To check the effect of these mutations on protein function, we performed immunofluorescence (IF) of DNAH1 and alpha-tubulin on sperm smear slides from patients IV:1, V:1, and V:2. The IF result showed the absence of DNAH1 signals on the sperm tail of patients, while positive signals of DNAH1 were observed on the control sample (**Figure 1E**). Thus, these results indicated that the identified mutations are loss-of-function mutations and caused transcript decay by non-sense mRNA-mediated decay.

Ultrastructural Analysis of Spermatozoa Displayed Numerous Defects in the Axonemal Structures

In order to investigate the axonemal structures, we performed TEM on patient (IV:1) spermatozoa. We statistically analyzed good-quality cross-sections of microtubule doublets from the patient and control spermatozoa samples and found that the central singlet of microtubules was missing in 66% of these sections (**Figures 2A, B**). Furthermore, the fibrous sheath was disorganized in 10% of the sections, and missing microtubule doublets were observed in 6% of analyzed sections. To further confirm the disruption of the central pair, we stained the sperm smear slides of the patients with SPAG6 antibody, which is a well-known marker generally used to check the integration of microtubules of the central pair. No signals of SPAG6 were observed on the sperm flagella of the patients, while sperm from the control individual displayed well-decorated signals on the entire tail of the flagella (**Figure 2C**). Overall, these results intimidated that the identified mutations have a deleterious effect on the axonemal structures of sperm flagella.

Generation of Mutant Mice Model

In order to study the *in vivo* effects of mutations, we generated $Dnah1^{-/-}$ mice by deletion of the *Dnah1* transcript and $Dnah1^{\triangle iso/\triangle iso1}$ mutant mice similar to a mutation in family A2 (c.7646_7647InsC) by using CRISPR/Cas9 genome editing technology (**Figure 3A**). Sanger sequencing of the PCR products confirmed the genotype of $Dnah1^{-/-}$and $Dnah1^{\triangle iso/\triangle iso1}$ mice (**Supplementary Figure S3A**). Furthermore, western blotting confirmed the absence of full-length DNAH1 protein in both mice models, while intact full-length DNAH1 (herein referred to as DNAH1 isoform1) protein was observed in $DNAH1^{+/\triangle iso1}$ and $DNAH1^{+/-}$ mice testes (**Figure 3B**). Interestingly, we observed the presence of a short isoform of DNAH1 (referred to as isoform2) in the testes of $Dnah1^{\triangle iso1/\triangle iso1}$ mice, while no such isoform was found in $Dnah1^{-/-}$ mice (**Figure 3C**). Thus, it can be deduced that the $Dnah1^{\triangle iso1/\triangle iso1}$ mice still harbor the short-length DNAH1 protein. Similarly, reverse transcriptase PCR with a specific primer corresponding to isoform2 of DNAH1 also verified the presence of a small-length transcript in $Dnah1^{\triangle iso1/\triangle iso1}$ and wild-type (WT) mice (**Supplementary Figures S2A, B**). Moreover, we performed RT-PCR on control human spermatozoa to check the presence of isoform2. However, no isoform2 was detected in control spermatozoa, while a clear band corresponding to isoform1 was observed (**Supplementary Figure S2C**).

Mutant Mice With Mild Ultrastructural Defects of Sperm Flagella

After confirming the deficiency of full-length DNAH1 protein in $Dnah1^{\triangle iso1/\triangle iso1}$ mice, we first scrutinized the fertility of mutant mice by caging one mutant mouse with two WT females for 3 months. During this duration, the female mice display vaginal plugs, demonstrating normal mating efficiency. However, no pregnancy was conceived, indicating that the $Dnah1^{\triangle iso1/\triangle iso1}$ mice were completely infertile (**Table 2**). Subsequently, testes morphology (**Supplementary Figure S3A**) and testes-to-body-weight ratio were comparable in mutant and WT mice (**Table 2**). On the other hand, reduced sperm count was evident in $Dnah1^{-/-}$ and $Dnah1^{\triangle iso1/\triangle iso1}$ mice (**Table 2**). Further examination of testis and epididymis section from $Dnah1^{\triangle iso1/\triangle iso1}$ mouse displayed an intact seminiferous tubule structure and the presence of all types of germ cells ranging from spermatogonia to spermatozoa (**Supplementary Figure S2C**). Similarly, an ample number of mature spermatozoa were present in the lumen of cauda in $Dnah1^{\triangle iso1/\triangle iso1}$ mouse, indicating that sperm production is not severely affected on the grass root level (**Supplementary Figure S3D**). Next, we analyzed sperm motility by CASA system and observed that progressive motility is severely compromised in $Dnah1^{\triangle iso1/\triangle iso1}$ mouse, while no progressive motile sperm was observed in $Dnah1^{-/-}$ mouse (**Table 2**). To explore the reason of reduced motility, we performed a comprehensive inspection of sperm morphology of $Dnah1^{\triangle iso1/\triangle iso1}$ mouse and $Dnah1^{-/-}$ mouse. Interestingly, we found that most of the spermatozoa (53/49%) lack full-length flagella structure, only possessing an intact head structure (**Figure 3D**), while few other abnormalities were observed (**Table 2**). Interestingly, there are still some (34/45%) sperm with normal flagella in $Dnah1^{\triangle iso1/\triangle iso,}$ and $Dnah1^{-/-}$ mouse, and the flagella without sperm head also have a normal morphology. On the other hand, ultrastructural investigation of sperm flagella from $Dnah1^{\triangle iso1/\triangle iso1}$ and $Dnah1^{-/-}$ mice displayed no significant variation in the architecture of axoneme (**Figures 3E, F**). However, statistical analysis indicated more abnormal sections in $Dnah1^{-/-}$ mouse than $Dnah1^{\triangle iso1/\triangle iso1}$ mouse, indicating that isoform2 may have a role in mediating the assembly and stabilization of axonemal structures. Altogether our study provided clues about the phenotype differences in *Dnah1* KO and *DNAH1* mutant human spermatozoa ultrastructure for the first time.

DISCUSSION

Sperm flagellum is a highly complex structure constituted by a series of proteins that mediate its assembly, composition, and function (41). Defects in sperm flagellum can occur by exogenous and endogenous factors, including genetic mutations that can also reduce sperm motility (42). Studies on mouse models have identified that several genes are required to properly develop the

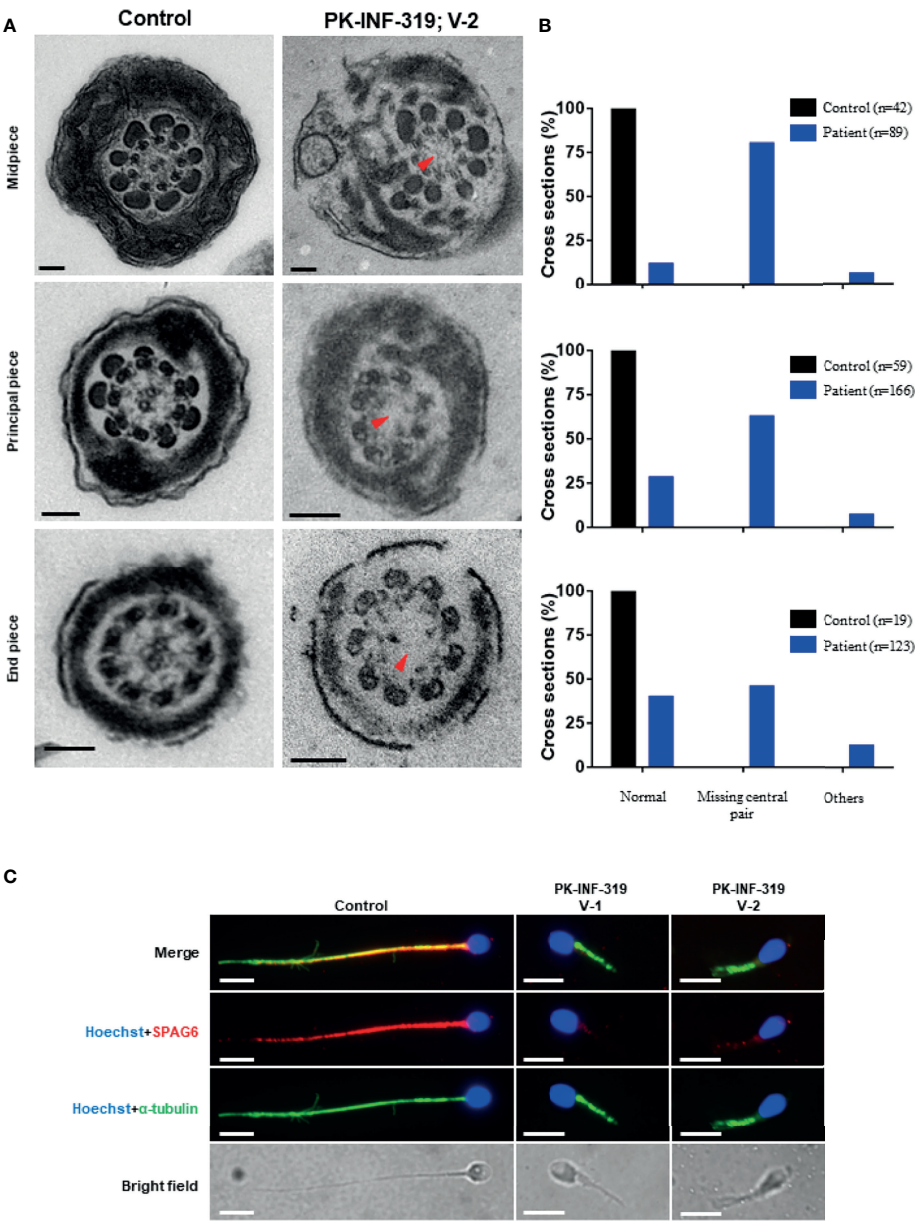

FIGURE 2 | Transmission electron microscopic investigation of spermatozoa from patients and healthy control. **(A)** The cross-section of a healthy control spermatozoa represented an intact axoneme structure comprised of doublets of microtubules, circularly arranged around a central pair complex of microtubules (nine + two organization), surrounded by outer dense fibers and fibrous sheath. The cross-section of a patient spermatozoa displayed a missing central singlet of microtubules and disorganized fibrous sheath. Scale bars, 500 um. **(B)** Graphs representing the cross-sections of microtubule doublets corresponding to midpiece, principal piece, and end piece were statistically analyzed in control and patient. **(C)** The patient spermatozoa were devoid of SPAG6 signals (marker to check the integration of microtubules of the central pair), indicating disruption of inner dynein arm, while well-decorated SPAG6 signals were observed on the tail of spermatozoa obtained from a healthy control. Scale bars, 10 um.

sperm flagellum. However, mutations in these genes are rarely reported in humans suffering from impaired motility due to the morphological defects of flagella. To date, variants in *AKAP4*, *CCDC39*, *DNAH1*, *CFAP43*, *CFAP44*, and *CFAP69* have been associated with MMAF phenotype in humans and mice (16, 27, 43–45). *DNAH1* is one of the most important members of the inner dynein arm and is considered an essential candidate gene for male infertility. The first mutation in *DNAH1* causing male infertility was reported in 2001 (26). Since then, various pathogenic mutations in *DNAH1* have been reported in various populations, causing male infertility (10, 11, 46, 47). However, most of the cases of altered sperm motility leading to human male infertility remain idiopathic. Thus, it is still difficult to identify the association between genetic mutations and impaired sperm motility.

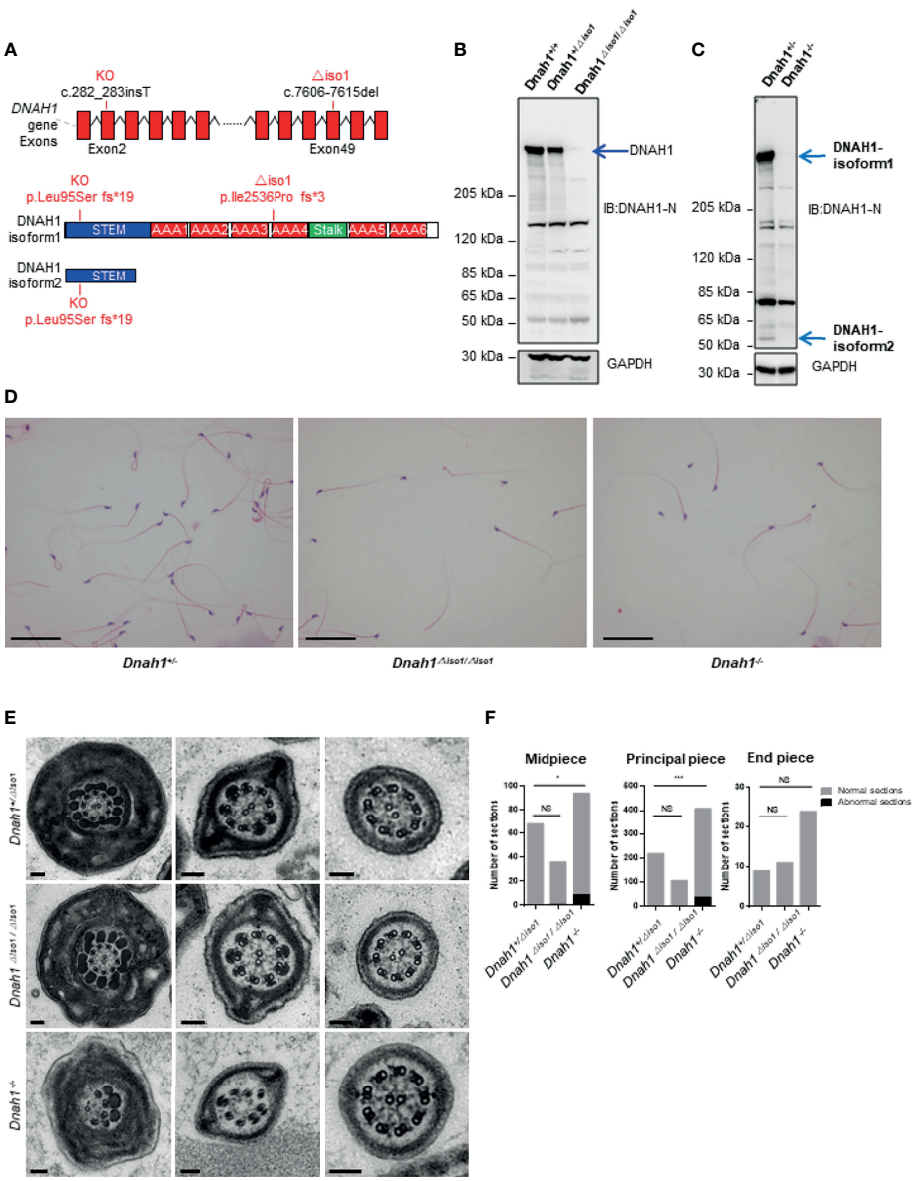

FIGURE 3 | Generation of *Dnah1*$^{-/-}$ and *Dnah1*$^{\triangle iso1/\triangle iso1}$ mice. **(A)** Representative *Dnah1* structure and strategy used to generate *Dnah1*$^{-/-}$ *and Dnah1*$^{\triangle iso1/\triangle iso1}$ mice through CRISPR/Cas9 genome editing technology by targeting exon 2 and exon 49, respectively. **(B, C)** Western blotting analysis confirmed the deletion of full-length DNAH1 protein in *Dnah1*$^{-/-}$ and *Dnah1*$^{\triangle iso1/\triangle iso1}$ mice testes, while isoform2 (50 kDa) still existed in *Dnah1*$^{\triangle iso1/\triangle iso1}$ mice testes. GAPDH was used as an internal control. **(D)** The sperm morphology analysis of *Dnah1*$^{\triangle iso1/\triangle iso1}$ mice displayed spermatozoa without a sperm tail. Scale bars, 10 um **(E)** Transmission electron microscopy investigation of *Dnah1*$^{\triangle iso1/\triangle iso1}$ mice spermatozoa showing an intact ultrastructure with the presence of a central pair and outer dense fibers, while abnormal sections were observed in *Dnah1*$^{-/-}$ mice spermatozoa. Scale bars, 10 um. **(F)** Quantification of normal and abnormal sections observed in the spermatozoa of *Dnah1*$^{-/-}$ and *Dnah1*$^{\triangle iso1/\triangle iso1}$ mice. *p < 0.05, ***p < 0.001 and NS, no significant difference.

In the current study, we recruited two extended consanguineous Pakistani families suffering from male infertility due to MMAF without having any symptoms of PCD. Next-generation sequencing identified two novel loss-of-function mutations in *DNAH1* (c.6212T>G, p.C1789Y, and c.7646_7647InsC, p.N2549Qfs*61) in family A1 and A2, respectively. These two variants were pathogenic in nature as no DNAH1 signals were observed on the sperm smear slides of the families of both patients, indicating that identified mutations caused the decay of mRNA transcript and the subsequent disruption of DNAH1 protein. Ultrastructural examination of patient spermatozoa revealed the absence of central singlet of microtubules, suggesting that mutations have adversely affected the axonemal structure. SPAG6 is an important marker that is widely used to check the integration microtubules of the central pair. No SPAG6 signals were observed on the patient spermatozoa, suggesting the disruption of the central pair.

Subsequently, we generated mutant mice by targeting exon 49 of *Dnah1*, and western blotting confirmed the absence of a full-length DNAH1 protein. However, a short protein, possibly encoded by N-terminal (isoform2), was observed in the mutant and WT mice.

Interestingly, we observed mild defects in the ultrastructure of spermatozoa from mutant mice. We thought that maybe the isoform2 is mediating the assembly of microtubules in the absence of full-length DNAH1 protein in mice. Previous studies suggested that the N-terminal of the heavy chain of DNAH1 forms a stem structure and is required for the assembly dynein complex and cargo attachment (26, 48). In order to eliminate the effect of N-terminal-mediated isoform2, we generated *Dnah1*$^{-/-}$ mice by targeting exon 2 that completely disrupted the N-terminal, and western blotting confirmed the absence of full-length as well as isoform2 DNAH1 protein. Surprisingly, the TEM analysis of the ultrastructure of spermatozoa from *Dnah1*$^{\triangle iso1/\triangle iso1}$ and *Dnah1*$^{-/-}$ mice still showed no significant phenotype. Though more abnormal sections were observed in *Dnah1*$^{-/-}$ mouse as compared to *Dnah1*$^{\triangle iso1/\triangle iso1}$ mouse, *Dnah1*$^{-/-}$ mice spermatozoa still displayed intact central singlet of microtubules, suggesting that KO animals have some hidden factors that could ensure correct axonemal biogenesis and organization or that complete disruption of the heavy chain did not influence the assembly of the other components of an axonemal structure in mice. Alternatively, it can be hypothesized that the role of *DNAH1* in axonemal structure is not as central in mice as it is in humans.

Surprisingly, most of the spermatozoa from *Dnah1*$^{\triangle iso1/\triangle iso1}$ mouse and *Dnah1*$^{-/-}$ mice displayed an absence of the entire flagellum tail, a different phenotype from patients. The inner dynein arms are arranged in seven molecular complexes, viewed as globular heads arranged in three-two-two groups and corresponding to three different types of inner arms (IDA1 to IDA3). We assumed that one of the IDA has been disorganized in *Dnah1* mutant mouse spermatozoa, leading to loss of connection between external doublets of the microtubules and the two central microtubules and ultimately affected the cargo system required for cytoskeleton organization. Another possibility is that *Dnah1*$^{\triangle iso1/\triangle iso1}$ and *Dnah1*$^{-/-}$ spermatozoa are defective in organizing the α- and β-tubulins required for spermiogenesis (49). Thus, it can be inferred that *DNAH1* also regulates the α- and β-tubulin complexes, which play crucial roles in sperm tail elongation during spermiogenesis.

It is reasonable to hypothesize that the position of mutations in *DNAH1* may have a different effect on the sperm flagellum structure, which can completely reduce the immobility of spermatozoa. Furthermore, the mutations in the N-terminal and C-terminal of DNAH1 can display different effects on the axonemal structure of human spermatozoa. Altogether our study described that the role of DNAH1 is more central in regulating the axonemal assembly and dimerization in humans than in mice. The finding of this study will pave the way for finding out other intrinsic factors responsible for different phenotypes of DNAH1 mutations in humans and mice. Finally, it is suggested that screening the deleterious mutations of *DNAH1*could be important for the clinical molecular diagnosis of male infertility.

DATA AVAILABILITY STATEMENT

The original contributions presented in the study are included in the article/**Supplementary Material**. Further inquiries can be directed to the corresponding authors.

ETHICS STATEMENT

The studies involving human participants were reviewed and approved by the Bioethical Committee of Pakistan and the ethical review board of the University of Science and Technology of China (USTC). The patients/participants provided their written informed consent to participate in this study. The animal study was reviewed and approved by the ethical review board of the USTC.

AUTHOR CONTRIBUTIONS

RK, JC, AM, and BZ performed the experiments. QZ, ManK, AA, MZ, WS, and MazK recruited the patients, performed semen analysis, and collected patient samples. MN gave insightful discussion and constructive comments on the manuscript. DZ and JZ performed the whole-exome sequencing (WES) and WES data analysis. QS, HZ, BX, YZ, and RK conceived and supervised the study, designed and analyzed the experiments, and wrote the manuscript. All authors contributed to the article and approved the submitted version.

FUNDING

This work was supported by the National Natural Science Foundation of China (32070850) and National Key Research and Developmental Program of China (2018YFC1004700).

SUPPLEMENTARY MATERIAL

The Supplementary Material for this article can be found online at: https://www.frontiersin.org/articles/10.3389/fendo.2021.765639/full#supplementary-material

Supplementary Figure S1 | Sperm morphology analysis. **(A)** Typical flagellar appearance in control subject. **(B)** Various defects of sperm flagella, such as absent, short, coiled, and bent, were common in the spermatozoa of patients.

Supplementary Figure S2 | Presence of *DNAH1* isoform 2 in mutant and wild-type (WT) mice. **(A)** Gel electrophoresis of cDNA products (one, three, and five WT mice cDNA product; two, four, and six *Dnah1*$^{\triangle iso1/\triangle iso1}$ cDNA mice products) confirmed the presence of isoform 2 mRNA. **(B)** Corresponding Sanger sequencing of WT and *Dnah1*$^{\triangle iso1/\triangle iso1}$ mice cDNA further verified the presence of isoform 2 in *Dnah1*$^{\triangle iso1/\triangle iso1}$ mice. **(C)** Gel electrophoresis of cDNA product from control human spermatozoa confirmed the absence of isoform2 in humans.

Supplementary Figure S3 | Genotyping and spermatogenesis in *Dnah1*$^{-/-}$ and *Dnah1*$^{\triangle iso1/\triangle iso1}$ mice. **(A)** Representative chromatograms from *Dnah1*$^{+/-}$, *Dnah1*$^{+/\triangle iso1}$, *Dnah1*$^{-/-}$, and *Dnah1*$^{\triangle iso1/\triangle iso1}$ mice confirming their genotype. The red letters indicate the changes in the DNA sequences. **(B)** Representative image of testes from adult rom *Dnah1*$^{+/-}$, *Dnah1*$^{+/\triangle iso1}$, *Dnah1*$^{-/-}$, and *Dnah1*$^{\triangle iso1/\triangle iso1}$ mice. Scale bars, 1 cm. **(C)** H&E staining of testes and caudal epididymis from adult *Dnah1*$^{+/\triangle iso1}$ and *Dnah1*$^{\triangle iso1/\triangle iso1}$ mice. Scale bars, 50 μm.

REFERENCES

1. Krausz C, Riera-Escamilla A. Genetics of Male Infertility. *Nat Rev Urol* (2018) 15(6):369–84. doi: 10.1038/s41585-018-0003-3
2. Coutton C, Escoffier J, Martinez G, Arnoult C, Ray PF. Teratozoospermia: Spotlight on the Main Genetic Actors in the Human. *Hum Reprod Update* (2015) 21(4):455–85. doi: 10.1093/humupd/dmv020
3. Curi SM, Ariagno JI, Chenlo PH, Mendeluk GR, Pugliese MN, Sardi Segovia LM, et al. Asthenozoospermia: Analysis of a Large Population. *Arch Androl* (2003) 49(5):343–9. doi: 10.1080/01485010390219656
4. Beurois J, Cazin C, Kherraf ZE, Martinez G, Celse T, Touré A, et al. Genetics of Teratozoospermia: Back to the Head. *Best Pract Res Clin Endocrinol Metab* (2020) 2(101473):101473. doi: 10.1016/j.beem.2020.101473
5. Yang SM, Li HB, Wang JX, Shi YC, Cheng HB, Wang W, et al. Morphological Characteristics and Initial Genetic Study of Multiple Morphological Anomalies of the Flagella in China. *Asian J Androl* (2015) 17(3):513–5. doi: 10.4103/1008-682X.146100
6. Lehti MS, Sironen A. Formation and Function of Sperm Tail Structures in Association With Sperm Motility Defects. *Biol Reprod* (2017) 97(4):522–36. doi: 10.1093/biolre/iox096
7. Yang X, Zhu D, Zhang H, Jiang Y, Hu X, Geng D, et al. Associations Between DNAH1 Gene Polymorphisms and Male Infertility: A Retrospective Study. *Med (Baltimore)* (2018) 97(49):e13493. doi: 10.1097/MD.0000000000013493
8. Wilson KS, Gonzalez O, Dutcher SK, Bayly PV. Dynein-Deficient Flagella Respond to Increased Viscosity With Contrasting Changes in Power and Recovery Strokes. *Cytoskeleton (Hoboken)* (2015) 72(9):477–90. doi: 10.1002/cm.21252
9. Burgess SA, Walker ML, Sakakibara H, Knight PJ, Oiwa K, et al. Dynein Structure and Power Stroke. *Nature* (2003) 421(6924):715–8. doi: 10.1038/nature01377
10. Sha Y, Yang X, Mei L, Ji Z, Wang X, Ding L, et al. DNAH1 Gene Mutations and Their Potential Association With Dysplasia of the Sperm Fibrous Sheath and Infertility in the Han Chinese Population. *Fertil Steril* (2017) 107 (6):1312–8.e2. doi: 10.1016/j.fertnstert.2017.04.007
11. Amiri-Yekta A, Coutton C, Kherraf ZE, Karaouzène T, Le Tanno P, Sanati MH, et al. Whole-Exome Sequencing of Familial Cases of Multiple Morphological Abnormalities of the Sperm Flagella (MMAF) Reveals New DNAH1 Mutations. *Hum Reprod* (2016) 31(12):2872–80. doi: 10.1093/humrep/dew262
12. Tang S, Wang X, Li W, Yang X, Li Z, Liu W, et al. Biallelic Mutations in CFAP43 and CFAP44 Cause Male Infertility With Multiple Morphological Abnormalities of the Sperm Flagella. *Am J Hum Genet* (2017) 100(6):854–64. doi: 10.1016/j.ajhg.2017.04.012
13. Liu C, Tu C, Wang L, Wu H, Houston BJ, Mastrorosa FK, et al. Deleterious Variants in X-Linked CFAP47 Induce Asthenoteratozoospermia and Primary Male Infertility. *Am J Hum Genet* (2021) 108(2):309–23. doi: 10.1016/j.ajhg.2021.01.002
14. He X, Liu C, Yang X, Lv M, Ni X, Li Q, et al. Bi-Allelic Loss-Of-Function Variants in CFAP58 Cause Flagellar Axoneme and Mitochondrial Sheath Defects and Asthenoteratozoospermia in Humans and Mice. *Am J Hum Genet* (2020) 107(3):514–26. doi: 10.1016/j.ajhg.2020.07.010
15. Li W, Wu H, Li F, Tian S, Kherraf ZE, Zhang J, et al. Biallelic Mutations in CFAP65 Cause Male Infertility With Multiple Morphological Abnormalities of the Sperm Flagella in Humans and Mice. *J Med Genet* (2020) 57(2):89–95. doi: 10.1136/jmedgenet-2019-106344
16. Dong FN, Amiri-Yekta A, Martinez G, Saut A, Tek J, Stouvenel L, et al. Absence of CFAP69 Causes Male Infertility Due to Multiple Morphological Abnormalities of the Flagella in Human and Mouse. *Am J Hum Genet* (2018) 102(4):636–48. doi: 10.1016/j.ajhg.2018.03.007
17. Beurois J, Martinez G, Cazin C, Kherraf ZE, Amiri-Yekta A, Thierry-Mieg N, et al. CFAP70 Mutations Lead to Male Infertility Due to Severe Astheno-Teratozoospermia. A Case Report. *Hum Reprod* (2019) 34(10):2071–9. doi: 10.1093/humrep/dez166
18. Sha Y, Wei X, Ding L, Ji Z, Mei L, Huang X, et al. Biallelic Mutations of CFAP74 may Cause Human Primary Ciliary Dyskinesia and MMAF Phenotype. *J Hum Genet* (2020) 65(11):961–9. doi: 10.1038/s10038-020-0790-2
19. Martinez G, Beurois J, Dacheux D, Cazin C, Bidart M, Kherraf ZE, et al. Biallelic Variants in MAATS1 Encoding CFAP91, A Calmodulin-Associated and Spoke-Associated Complex Protein, Cause Severe Astheno-Teratozoospermia and Male Infertility. *J Med Genet* (2020) 57(10):708–16. doi: 10.1136/jmedgenet-2019-106775
20. Shen Q, Martinez G, Liu H, Beurois J, Wu H, Amiri-Yekta A, et al. Bi-Allelic Truncating Variants in CFAP206 Cause Male Infertility in Human and Mouse. *Hum Genet* (2021) 140(9):1367–77. doi: 10.1007/s00439-021-02313-z
21. Li W, He X, Yang S, Liu C, Wu H, Liu W, et al. Biallelic Mutations of CFAP251 Cause Sperm Flagellar Defects and Human Male Infertility. *J Hum Genet* (2019) 64(1):49–54. doi: 10.1038/s10038-018-0520-1
22. Touré A, Martinez G, Kherraf ZE, Cazin C, Beurois J, Arnoult C, et al. The Genetic Architecture of Morphological Abnormalities of the Sperm Tail. *Hum Genet* (2021) 140(1):21–42. doi: 10.1007/s00439-020-02113-x
23. Lv M, Liu W, Chi W, Ni X, Wang J, Cheng H, et al. Homozygous Mutations in DZIP1 can Induce Asthenoteratospermia With Severe MMAF. *J Med Genet* (2020) 57(7):445–53. doi: 10.1136/jmedgenet-2019-106479
24. Zhang J, He X, Wu H, Zhang X, Yang S, Liu C, et al. Loss of DRC1 Function Leads to Multiple Morphological Abnormalities of the Sperm Flagella and Male Infertility in Human and Mouse. *Hum Mol Genet* (2021) 30(21):1996–2011. doi: 10.1093/hmg/ddab171
25. Ma H, Zhang B, Khan A, Zhao D, Ma A, Jianteng Z, et al. Novel Frameshift Mutation in STK33 Is Associated With Asthenozoospermia and Multiple Morphological Abnormality of the Flagella. *Hum Mol Genet* (2021) 30 (21):1977–84. doi: 10.1093/hmg/ddab165
26. Neesen J, Kirschner R, Ochs M, Schmiedl A, Habermann B, Mueller C, et al. Disruption of an Inner Arm Dynein Heavy Chain Gene Results in Asthenozoospermia and Reduced Ciliary Beat Frequency. *Hum Mol Genet* (2001) 10(11):1117–28. doi: 10.1093/hmg/10.11.1117
27. Ben Khelifa M, Coutton C, Zouari R, Karaouzène T, Rendu J, Bidart M, et al. Mutations in DNAH1, Which Encodes an Inner Arm Heavy Chain Dynein, Lead to Male Infertility From Multiple Morphological Abnormalities of the Sperm Flagella. *Am J Hum Genet* (2014) 94(1):95–104. doi: 10.1016/j.ajhg.2013.11.017
28. Yin H, Ma H, Hussain S, Zhang H, Xie X, Jiang L, et al. A Homozygous FANCM Frameshift Pathogenic Variant Causes Male Infertility. *Genet Med* (2019) 21(1):62–70. doi: 10.1038/s41436-018-0015-7
29. Li H, Durbin R. Fast and Accurate Short Read Alignment With Burrows-Wheeler Transform. *Bioinformatics* (2009) 25(14):1754–60. doi: 10.1093/bioinformatics/btp324
30. McKenna A, Hanna M, Banks E, Sivachenko A, Cibulskis K, Kernytsky A, et al. The Genome Analysis Toolkit: A MapReduce Framework for Analyzing Next-Generation DNA Sequencing Data. *Genome Res* (2010) 20(9):1297–303. doi: 10.1101/gr.107524.110
31. Smith KR, Bromhead CJ, Hildebrand MS, Shearer AE, Lockhart PJ, Najmabadi H, et al. Reducing the Exome Search Space for Mendelian Diseases Using Genetic Linkage Analysis of Exome Genotypes. *Genome Biol* (2011) 12(9):2011–12. doi: 10.1186/gb-2011-12-9-r85
32. Auton A, Brooks LD, Durbin RM, Garrison EP, Kang HM, Korbel JO, et al. A Global Reference for Human Genetic Variation. *Nature* (2015) 526(7571):68–74. doi: 10.1038/nature15393
33. Fu W, O'Connor TD, Jun G, Kang HM, Abecasis G, Leal SM, et al. Analysis of 6,515 Exomes Reveals the Recent Origin of Most Human Protein-Coding Variants. *Nature* (2013) 493(7431):216–20. doi: 10.1038/nature11690
34. Lek M, Karczewski KJ, Minikel EV, Samocha KE, Banks E, Fennell T, et al. Analysis of Protein-Coding Genetic Variation in 60,706 Humans. *Nature* (2016) 536(7616):285–91. doi: 10.1038/nature19057
35. Zhang Y, Zhong L, Xu B, Yang Y, Ban R, Zhu J, et al. SpermatogenesisOnline 1.0: A Resource for Spermatogenesis Based on Manual Literature Curation and Genome-Wide Data Mining. *Nucleic Acids Res* (2013) 41(Database issue): D1055–62. doi: 10.1093/nar/gks1186
36. Zhang B, Ma S, Khan T, Ma A, Li T, Zhang H, et al. A DNAH17 Missense Variant Causes Flagella Destabilization and Asthenozoospermia. *J Exp Med* (2020) 217(2):20182365. doi: 10.1084/jem.20182365
37. Yang H, Wang H, Shivalila CS, Cheng AW, Shi L, Jaenisch R. One-step Generation of Mice Carrying Reporter and Conditional Alleles by CRISPR/Cas-mediated Genome Engineering. *Cell* (2013) 154:1370–9. doi: 10.1016/j.cell.2013.08.022

38. Shen B, Zhang W, Zhang J, Zhou J, Wang J, Chen L, et al. Efficient Genome Modification by CRISPR-Cas9 Nickase With Minimal Off-Target Effects. *Nat Methods* (2014) 11(4):399–402. doi: 10.1038/nmeth.2857
39. Gao Q, Khan R, Yu C, Alsheimer M, Jiang X, Ma H, et al. The Testis-Specific LINC Component SUN3 Is Essential for Sperm Head Shaping During Mouse Spermiogenesis. *J Biol Chem* (2020) 295(19):6289–98. doi: 10.1074/jbc.RA119.012375
40. Khan R, Ye J, Yousaf A, Shah W, Aftab A, Shah B, et al. Evolutionarily Conserved and Testis-Specific Gene, 4930524B15Rik, Is Not Essential for Mouse Spermatogenesis and Fertility. *Mol Biol Rep* (2020) 47(7):5207–13. doi: 10.1007/s11033-020-05595-0
41. Vyklicka L, Lishko PV. Dissecting the Signaling Pathways Involved in the Function of Sperm Flagellum. *Curr Opin Cell Biol* (2020) 63:154–61. doi: 10.1016/j.ceb.2020.01.015
42. Inaba K. Molecular Architecture of the Sperm Flagella: Molecules for Motility and Signaling. *Zoolog Sci* (2003) 20(9):1043–56. doi: 10.2108/zsj.20.1043
43. Turner RM, Musse MP, Mandal A, Klotz K, Jayes FC, Herr JC, et al. Molecular Genetic Analysis of Two Human Sperm Fibrous Sheath Proteins, AKAP4 and AKAP3, in Men With Dysplasia of the Fibrous Sheath. *J Androl* (2001) 22 (2):302–15. doi: 10.1002/j.1939-4640.2001.tb02184.x
44. Merveille AC, Davis EE, Becker-Heck A, Legendre M, Amirav I, Bataill G, et al. CCDC39 Is Required for Assembly of Inner Dynein Arms and the Dynein Regulatory Complex and for Normal Ciliary Motility in Humans and Dogs. *Nat Genet* (2011) 43(1):72–8. doi: 10.1038/ng.726
45. Coutton C, Vargas AS, Amiri-Yekta A, Kherraf ZE, Ben Mustapha SF, Le Tanno P, et al. Mutations in CFAP43 and CFAP44 Cause Male Infertility and Flagellum Defects in Trypanosoma and Human. *Nat Commun* (2018) 9 (1):017–02792. doi: 10.1038/s41467-017-02792-7
46. Wambergue C, Zouari R, Fourati Ben Mustapha S, Martinez G, Devillard F, Hennebicq S, et al. Patients With Multiple Morphological Abnormalities of the Sperm Flagella Due to DNAH1 Mutations Have a Good Prognosis Following Intracytoplasmic Sperm Injection. *Hum Reprod* (2016) 31 (6):1164–72. doi: 10.1093/humrep/dew083
47. Wang X, Jin H, Han F, Cui Y, Chen J, Yang C, et al. Homozygous DNAH1 Frameshift Mutation Causes Multiple Morphological Anomalies of the Sperm Flagella in Chinese. *Clin Genet* (2017) 91(2):313–21. doi: 10.1111/cge.12857
48. Myster SH, Knott JA, Wysocki KM, O'Toole E, Porter ME. Domains in the 1alpha Dynein Heavy Chain Required for Inner Arm Assembly and Flagellar Motility in Chlamydomonas. *J Cell Biol* (1999) 146(4):801–18. doi: 10.1083/jcb.146.4.801
49. Kierszenbaum AL. Intramanchette Transport (IMT): Managing the Making of the Spermatid Head, Centrosome, and Tail. *Mol Reprod Dev* (2002) 63(1):1–4. doi: 10.1002/mrd.10179

Conflict of Interest: The authors declare that the research was conducted in the absence of any commercial or financial relationships that could be construed as a potential conflict of interest.

Publisher's Note: All claims expressed in this article are solely those of the authors and do not necessarily represent those of their affiliated organizations, or those of the publisher, the editors and the reviewers. Any product that may be evaluated in this article, or claim that may be made by its manufacturer, is not guaranteed or endorsed by the publisher.

Copyright © 2021 Khan, Zaman, Chen, Khan, Ma, Zhou, Zhang, Ali, Naeem, Zubair, Zhao, Shah, Khan, Zhang, Xu, Zhang and Shi. This is an open-access article distributed under the terms of the Creative Commons Attribution License (CC BY). The use, distribution or reproduction in other forums is permitted, provided the original author(s) and the copyright owner(s) are credited and that the original publication in this journal is cited, in accordance with accepted academic practice. No use, distribution or reproduction is permitted which does not comply with these terms.

frontiers in Endocrinology

REVIEW
published: 24 February 2022
doi: 10.3389/fendo.2022.838858

What Does Androgen Receptor Signaling Pathway in Sertoli Cells During Normal Spermatogenesis Tell Us?

Jia-Ming Wang[†], *Zhen-Fang Li*[†] *and Wan-Xi Yang*[*]

The Sperm Laboratory, College of Life Sciences, Zhejiang University, Hangzhou, China

OPEN ACCESS

Edited by:
Artur Mayerhofer, Ludwig Maximilian University of Munich, Germany

Reviewed by:
Subeer Majumdar, National Institute of Animal Biotechnology (NIAB), India
Silvana A. Andric, University of Novi Sad, Serbia

***Correspondence:**
Wan-Xi Yang
wxyang@zju.edu.cn

[†]*These authors have contributed equally to this work*

Specialty section:
This article was submitted to Reproduction, a section of the journal Frontiers in Endocrinology

Received: *18 December 2021*
Accepted: *01 February 2022*
Published: *24 February 2022*

Citation:
Wang J-M, Li Z-F and Yang W-X (2022) What Does Androgen Receptor Signaling Pathway in Sertoli Cells During Normal Spermatogenesis Tell Us? Front. Endocrinol. 13:838858. doi: 10.3389/fendo.2022.838858

Androgen receptor signaling pathway is necessary to complete spermatogenesis in testes. Difference between androgen binding location in Sertoli cell classifies androgen receptor signaling pathway into classical signaling pathway and non-classical signaling pathway. As the only somatic cell type in seminiferous tubule, Sertoli cells are under androgen receptor signaling pathway regulation *via* androgen receptor located in cytoplasm and plasma membrane. Androgen receptor signaling pathway is able to regulate biological processes in Sertoli cells as well as germ cells surrounded between Sertoli cells. Our review will summarize the major discoveries of androgen receptor signaling pathway in Sertoli cells and the paracrine action on germ cells. Androgen receptor signaling pathway regulates Sertoli cell proliferation and maturation, as well as maintain the integrity of blood-testis barrier formed between Sertoli cells. Also, Spermatogonia stem cells achieve a balance between self-renewal and differentiation under androgen receptor signaling regulation. Meiotic and post-meiotic processes including Sertoli cell - Spermatid attachment and Spermatid development are guaranteed by androgen receptor signaling until the final sperm release. This review also includes one disease related to androgen receptor signaling dysfunction named as androgen insensitivity syndrome. As a step further ahead, this review may be conducive to develop therapies which can cure impaired androgen receptor signaling in Sertoli cells.

Keywords: androgen receptor, Sertoli cell, signaling pathway, spermatogenesis, androgen insensitivity syndrome

1 INTRODUCTION

Male infertility is currently a major problem worldwide and causes substantial psychological and social distress (1). It not only puts a huge economic burden on patients, but also poses a great challenge to the health-care system. Male infertility is due to abnormal sperm parameters in the male partner and contributes to 50% of all cases of infertility, highlighting the importance of normal spermatogenesis (2, 3).

Spermatogenesis is a complex process that is under precise regulation. Starting from spermatogonia stem cell (SSC) producing differentiated spermatogonia, spermatogonia transform into spermatocytes which then undergo meiotic divisions to produce round spermatids (4). Round spermatids undergo cytodifferentiation to form spermatozoa, which are ultimately released to the lumen (5).

As the only somatic cell type in seminiferous tubules (6), Sertoli cells (SCs) make normal spermatogenesis possible by providing the nutrition necessary for the development of germ cells (7), forming blood-testis barrier (BTB) between SCs in mammalian testes (8, 9), attaching to germ cells (GCs) through adherens junctions (10) and phagocytosing apoptotic GCs for recycling (11). SCs function like a nurse to take good care of spermatogenesis (12). These functions of SCs are regulated by both extrinsic and intrinsic factors. The former factors include hormone and paracrine molecules and the latter include genomic regulators. Here, we review androgen receptor (AR) signaling pathway in SCs, a pathway that provides an excellent example of a combination of extrinsic and intrinsic regulation. AR begins its expression 3-5 days after birth in rodent testis while AR expression begins about 5 months after birth in men (13, 14). In men, its expression in SCs peaks during stage III of the six stages (15). AR signaling pathway can be classified into classical signaling pathway and non-classical signaling pathway with different functions and different efficiencies. It has been shown that abnormal AR signaling can impair spermatogenesis (16). Although decades of studies have brought us a better understanding of AR signaling in spermatogenesis using altered testosterone signaling model, Sertoli cell androgen receptor knockout model, specificity-affecting androgen receptor knock in model as well as Ribo-Tag mouse model, not enough information has been gained to lift the veil of its beauty. As a result, it is necessary to review current work about androgen receptor signaling pathway in SCs and put forward suggestions for future studies. Ultimately, all of our hard work aims to achieve "bench to bedside" translation that can be used to develop therapies for illnesses related to hormone dysfunction.

We surveyed articles in the PubMed database using the following search terms: androgen receptor*, Sertoli cell*, spermatogonia*, maturation and differentiation*, spermatogenesis*, meiosis*, spermatid* and androgen-insensitive syndrome*. We will present this review at the cellular/molecular level in six parts: SC proliferation and maturation, SSC self-renewal and differentiation, spermatocyte meiosis, BTB integrity maintenance, Sertoli cell - Spermatid adhesion, and sperm release (**Figure 1**). The experimental models involved in this review include mice, rats, boars, lambs, zebrafish and humans. We include some contradictory results in this review and present our opinions. We also discuss androgen insensitive syndrome (AIS), briefly reviewing its pathogenesis, diagnosis and offering suggestions for better diagnosis and treatment.

2 STRUCTURE OF ANDROGEN RECEPTOR

The gene encoding AR is located on the X chromosome, belonging to nuclear receptor subfamily 3, group C, member 4. It consists of 8 exons that encode 4 domains: an N-terminal domain (exon 1), a DNA-binding domain (exon 2 and exon 3), a hinge region that contains the nuclear localization signal (exon 3 and exon 4) and a ligand-binding domain (exons 4-8) (17, 18).

The N-terminal domain contains activation function domain-1 which is constitutively active (15). The DNA-binding domain contains two zinc fingers to complex with its hormone response element, where each of them is coordinated by four cysteines. One zinc finger is involved in direct DNA binding mediated by the P(proximal) box, which recognizes the specific hormone response element half-site 5′-AGAACA-3′. The other zinc finger is involved in a "head-to-head" receptor dimerization through the D(istal) box (19–22). The hinge region contains the nuclear localization signal which is essential for nuclear import. Residues from the major nuclear localization signal site 629-RKLKKL-634 contribute to importinα binding (23–25). Then the ligand-binding domain consists of 11 α-helices and two small, two-stranded β-sheets arranged in a typical three-layer antiparallel helical sandwich fold (26, 27). Binding of androgen to ligand-binding domain can activate the receptor. Both of these structures are important for androgen receptor function, though the structure of full-length androgen receptor has not been solved yet.

3 OVERVIEW OF ANDROGEN RECEPTOR SIGNALING PATHWAY IN SERTOLI CELLS

In adult rodent testes, the AR expression level in SCs is low except during stage VI-VIII of the seminiferous epithelium (28). In men, its expression in SCs peaks during stage III of the six stages (29). This stage-specific peak of AR expression in SCs is coordinated with initiation of testosterone-dependent processes that is essential for spermatogenesis such as appearance of preleptotene spermatocytes and the initiation of meiosis during stages VII–VIII, as confirmed by Sertoli cell androgen receptor knock out model and androgen receptor knock out model (5). It is reasonable that AR signaling in SCs mediates paracrine action on germ cells and autocrine action on themselves to form a microenvironment for meiosis completion.

Stimulated by luteinizing hormone in the pituitary gland which is part of the hypothalamus-pituitary-gonadal axis, Leydig cells produce androgen. When androgen saturates the AR of SCs and binds to AR, the AR signaling pathway is activated (30). Testosterone is the most abundant androgen produced in the testis. Another important androgen is dihydrotestosterone (DHT), which is produced by peripheral tissues where 5α-reductases reduce testosterone to DHT (31, 32). When hormone levels in the targeted tissue are low, DHT is more potent than testosterone due to its higher binding affinity for AR. When the testosterone level in the testis is high, there are no differences between testosterone and DHT (33). Testosterone concentrations in the testes of men (340–2000 nM) are 25 to 125-fold greater than those in serum (8.75–35 mM), similar to the situation in rodent testes (5). The testosterone level needed to maintain spermatogenesis is approximately 10-25% of the intratesticular testosterone level (34). AR signaling pathway in

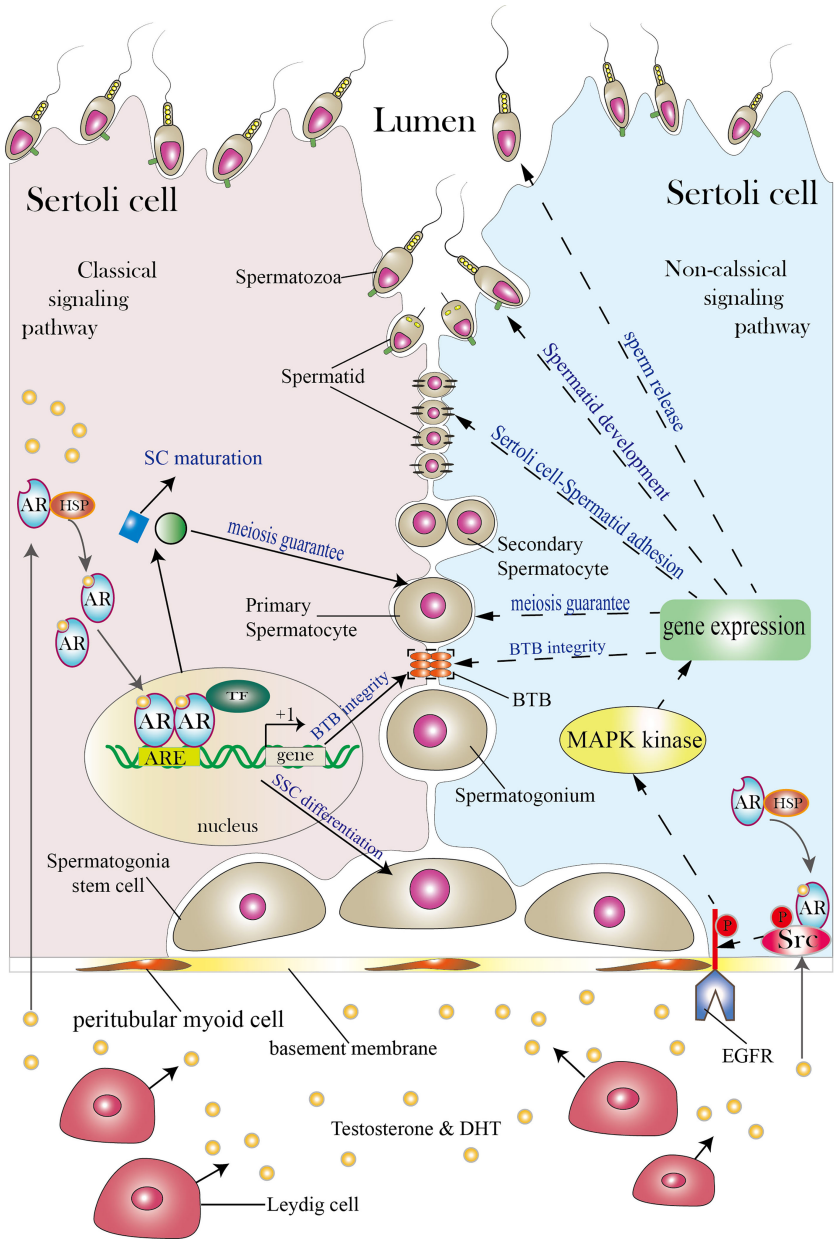

FIGURE 1 | Classical and non-classical AR signaling pathways in SCs. The SC shown on the left illustrates the classical signaling pathway, while the SC shown on the right illustrates the non-classical signaling pathway (both classical and non-classical signaling pathways can exist in a single SC; the two pathways are presented in separate cells for simplicity). Between the two neighboring SCs are germ cells (spermatogonia stem cells, spermatogonia, primary spermatocytes, secondary spermatocytes, spermatids and spermatozoa). SCs function as a nurse to take good care of normal spermatogenesis as spermatogonia stem cells develop into spermatozoa in the lumen. Androgen secreted by Leydig cells diffuses through the plasma membrane and binds to the AR complex in the cytoplasm to activate the classical signaling pathway. The AR then detaches from the HSP complex and enters the nucleus to form AR dimers. Dimerized ARs bind to the AREs of their target genes and thereby regulate their transcription. The classical signaling pathway can promote SC maturation, induce SSC differentiation, guarantee spermatocyte meiosis, and ensure BTB integrity. The non-classical signaling pathway begins with translocation of the AR from the cytoplasm to the plasma membrane. There, the AR interacts with Src and causes it to phosphorylate EGFR, and this in turn activates MAPK kinases to regulate targeted gene transcription. The non-classical signaling pathway can regulate processes including BTB integrity, spermatocyte meiosis, Sertoli cell-Spermatid adhesion, spermatid development and sperm release. The three orange ovals in the figure represent the BTB, and the two black lines represent cell–cell adhesion. TF is short for transcription factor. Areas for which controversy exists are not included in the figure but are discussed in the article.

SCs can be divided into classical signaling pathway and non-classical signaling pathway. The main differences between them lie in androgen binding location and response speed. Androgen binds to cytoplasmic AR in classical signaling pathway while in non-classical signaling pathway androgen binds to AR on plasma membrane. Compared with non-classical pathway, classical pathway requires more time to show transcriptional activity change after androgen binding to androgen receptor (35).

3.1 Classical Signaling Pathway

Before binding to androgen, AR in the cytoplasm binds to chaperones and cochaperones, such as heat shock proteins (HSP) HSP23, HSP40, HSP56, HSP70, HSP90 *via* its ligand-binding domain (17). When androgen in the cytoplasm binds to AR, AR detaches from chaperone and cochaperone protein complexes and exposes its ligand-binding domain (23, 24, 36). With the help of importins, the AR monomer transits into the nucleus, where 2 AR monomers dimerize to create AR homodimers. AR homodimers then bind to androgen response elements (AREs) in the promoter regions of targeted genes to regulate their transcription (37, 38). In addition, activation function domain-1 presenting in AR dimer N-terminal domain and activation function domain-2 presenting in its ligand-binding domain can recruit coactivators and corepressors that activate or repress targeted gene transcription activity (17). However, the binding sites for AR homodimers are not restricted to AREs; AR homodimers can also bind to some response elements for other transcription factor (39, 40). Notably, the classical AR signaling is relatively slow, usually 30-45 minutes is needed to induce activation or suppression of transcription, not considering the time required for protein synthesis and secretion (35).

3.2 Non-Classical Signaling Pathway

To date, three types of non-classical signaling pathway have been identified in the testis. Here is the first type, as well as the main type. When the intratesticular testosterone level is relatively low (10-250 nM), testosterone binds to the AR located in the cell membrane and activates the non-classical AR signaling pathway within 1 minute (41). In the TM4 Sertoli cell line, the transport of cytoplasmic ARs to the membrane is facilitated by caveolin-1 (42). Testosterone binds to membrane AR which then interacts with the SH3 domain of SRC proto-oncogene (Src). Src then phosphorylates the epidermal growth factor receptor (EGFR) which activates Ras kinase. This activates MAPK cascades (Ras-Raf-MEK-ERK). Phosphorylated ERK can phosphorylate ribosomal protein S6 kinase A1($p90^{Rsk}$). Activated $p90^{Rsk}$ translocate into nucleus, where it activates transcription factors such as cAMP-response element-binding protein (CREB), which binds to the cAMP-response element (CRE) of the targeted gene to regulate transcription (41, 43).

An *in vitro* study in which the TM4 cell line was exposed to testosterone levels of 10-100 nM demonstrated that testosterone can also activate a second non-classical signaling pathway, the phosphatidylinositol 3 kinase (PI3K)/Akt pathway, directly by activating the PI3K subunit p85α. Phosphorylated Akt can activate Src and this facilitates the translocation of cytoplasmic AR to the plasma membrane (44). In addition to these *in vitro* studies, some *in vivo* studies also showed that testosterone can activate the non-classical signaling pathway in SCs (35, 45).

Another type of non-classical signaling pathway has only been found in immature Sertoli cells. Testosterone causes depolarization of Sertoli cells within thirty seconds due to closed K^+_{ATP} channel. This close is caused by G protein-mediated activation of phospholipase C. This action results in a rapid influx of Ca^{2+} and the activation of signaling molecules (46–48).

Recently, Zrt- and Irt-like protein 9 (ZIP9), a novel membrane-bound androgen receptor unrelated to classic AR, was found in the 93RS2 Sertoli cell line which has no cytoplasmic AR. ZIP9 participates in the phosphorylation of CREB and ATF1 *via* ERK1/2 to induce the expression of claudin proteins that are components of BTB. The relationship between AR signaling and ZIP9 signaling remains to be researched in the future (49).

4 ANDROGEN RECEPTOR SIGNALING PATHWAY IN SERTOLI CELLS CAN REGULATE SPERMATOGENESIS

4.1 Role of AR Mediated Signaling in Sertoli Cell Proliferation and Maturation

SC proliferation occurs during fetal and early neonatal life in rodents, and in the fetal and peripubertal periods in higher primates when SCs undergo mitosis to increase their number (50). During the end of neonatal period or prepubertal period, SC proliferation stops. Then SCs maturation begins during puberty period, switching from an immature, proliferate state to a mature, non-proliferate state during which SCs establish BTB and acquire the ability to sustain spermatogenesis (51) AR signaling can participate in SC maturation process. Although it remains to be investigated if AR signaling in SCs influences SC proliferation, we still review studies in this field (**Figure 2**).

4.1.1 Sertoli Cell Proliferation

According to our knowledge, final testis size, number of germ cells and sperm output are closely connected to the number of SCs. This emphasizes the significance of SC proliferation. When porcine testis was treated with AR antagonists during postnatal proliferation, an increased number of SCs per testis was detected (52). However, SC numbers were increased in young ram lambs following prenatal exposure to testosterone (53). This is not contradictory, because administration of exogenous testosterone increases negative hypothalamic feedback and may reduce intratesticular testosterone levels, leading to decreased androgen signaling. However, when comparing the number of SCs per testis in Sertoli cell androgen receptor knockout (SCARKO) mice and androgen receptor knockout (ARKO) mice with the control group, researchers found that the SCARKO mice did not show significant differences compared to the controls, whereas the ARKO mice showed a significant decrease in SC number, indicating that in mice AR in SCs has little impact on SCs proliferation (54, 55). A similar

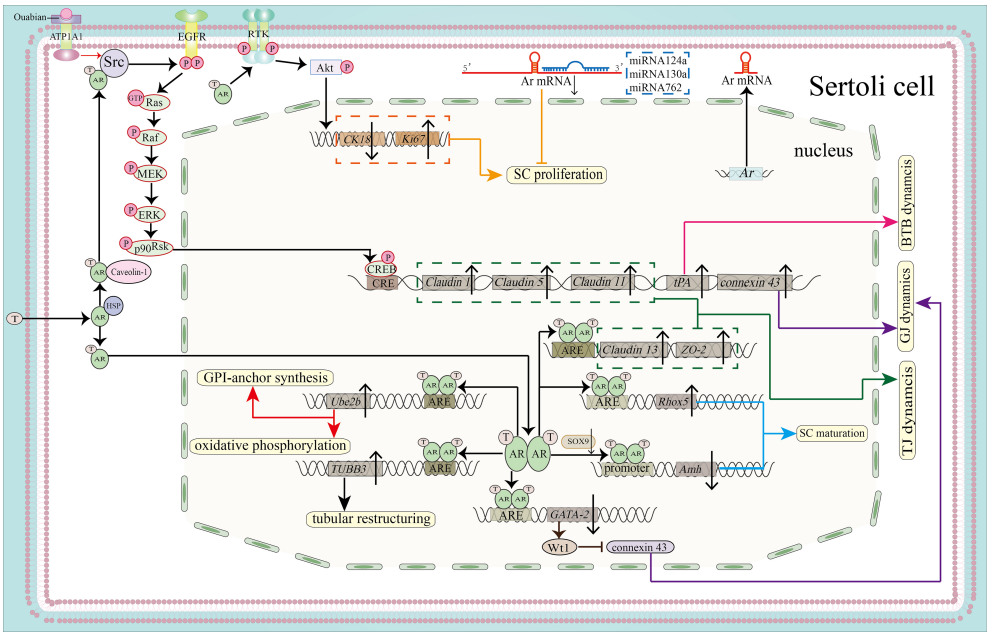

FIGURE 2 | Function of the AR signaling pathway in SC proliferation, maturation and BTB integrity. By activating the PI3K/Akt pathway, the AR can promote SC proliferation by downregulating *CK18* and upregulating *Ki67* (shown in orange). MicroRNAs, including miR124a, miRNA130a and miRNA762, can inhibit SC proliferation by binding to the 3'-UTR of *Ar* mRNA (also shown in orange). AR dimers can bind to the AREs of *Rhox5* and *Amh* to promote the expression of *Rhox5* and inhibit the expression of *Amh*, leading to SC maturation (blue). Binding to the ARE of *TUBB3* induces tubular restructuring and achieve proper SC nuclei location, another process that is important in SC maturation. *Ube2b*, activated by the classical signaling pathway, is able to induce GPI-anchor synthesis and oxidative phosphorylation (shown in red). Both the classical and the non-classical signaling pathways are necessary for BTB integrity. The expression of *Claudin13* and *tight junction protein 2 isoform 3 (ZO-2)*is upregulated by classical AR signaling, together with upregulated expression of *Claudin1*, *Claudin5*, *Claudin11* and *tPA* by non-classical signaling. These molecules regulate BTB dynamics (shown in pink) and TJ dynamics (shown in green). In addition, AR dimerization binds to the promoter of *GATA-2* to inhibit its expression. GATA-2 can induce *Wt1* expression, while Wt1 inhibits the protein expression level of connexin 43 to regulate GJ dynamics. Ouabain increases the expression of *connexin 43 via* the ATP1A1/Src/EGFR/ERK/CREB signaling pathway (shown in purple).

phenomenon was found when researchers used a testicular feminization mouse (*Tfm*) model that lacks functional AR in all cells (56). It is difficult to reconcile these results. We think that the expression of AR in SCs is undetectable or very weak during most of the periods in which these cells proliferate. While AR on other cell types such as peritubular myoid cells, which express AR at relatively high level, may contribute to SC proliferation. Hu et al. recently found that AR could interact directly with PI3K regulatory subunit p85α to activate kinase Akt and that this represses the expression of Cytokeratin 18 (CK18) (a marker of immature and dysfunctional SCs) and induces the expression of Ki67 (a marker of SC proliferation), thereby preserving SC proliferation in mice (57). Since the experiments were conducted on mature mice, additional experiments on prepubertal mice are needed to test this result, although it is true that some immature SCs are present in mature mice. Considering these results as a whole, it seems that role of AR signaling in SC proliferation is species-specific and phase-specific. We suggest that future studies test different species with the aims of understanding and combining their AR expression patterns in SCs, their intratesticular androgen levels and their SC proliferation patterns to provide a better understanding of the role of AR in SC proliferation.

4.1.2 Sertoli Cell Maturation

Followed by cessation of SC proliferation comes to SC maturation. Around SC maturation, AR expression level is progressively upregulated until all SCs express AR (58). AR in SCs is key mediator for SC molecular and cytoskeleton maturation (59–61).

In molecular level, several molecules important for maturation are under AR signaling regulation (51) and the level of heterochromatin (62). Among them, Anti Mullerian hormone (AMH) has been widely researched. AMH is crucial for fetal sex differentiation by regressing the Müllerian ducts in male (13, 63). Secreted by immature SCs, AMH has become a biomarker for testicular function in males during the prepubertal period which is tightly regulated by AR (64). During the postnatal period, AMH level can be maintained by androgen epi-testosterone through non-classical AR signaling pathway when intracellular AR level is very low (65). Other transcription factors, such as sex determining region Y-box 9 (SOX9), steroidogenic factor 1 (SF1) can bind to their own response elements to promote *Amh* transcription (66). Around the onset of puberty, upregulation of AR expression downregulates AMH expression by blocking SF1 binding to its response elements or interacting with SF1 response elements to

prevent SF1from exerting a stimulatory effect on *Amh* transcription (67). An *in vitro* study using TM4 Sertoli cells and C3H10T1/2 cell line demonstrated that AR could downregulate AMH expression by repressing SOX9, consistent with the findings in the azoospermia patients and mice *in vivo* (68).

Besides molecular level, AR signaling is necessary for SC cytoskeleton maturation. In SCARKO mice, relatively normal SCs nuclei were displaced from the basal basement and dispersed throughout the seminiferous tubules, probably resulting from the disrupted position of vimentin and the presence of thicker basal lamina, both of which participate in the linkage between nuclei and the cell membrane (69). Another group observed that SC nuclei formed one or two layered rings located in the center of tubule in mice in which AR function had been ablated (70). Suppressed expression of connexin 43(Cx43) in mice resulted in an intermediate state of SCs between proliferation and maturation, along with weaker AR immunostaining (71). The impaired SCs maturation observed in this model probably resulted from disrupted AR function. AR can also regulate microtubular composition and structure in SC so as to yield proper SC shape *via* Class III β tubulin (TUBB3) in mice and rats through classical signaling pathway (72).

Premature expression of ARs in postnatal mouse SCs resulted in fewer SCs, although GCs development accelerated in a gain-of-function mouse model (73). When the AR transgene was injected into a prenatal mouse model, precocious maturation of SCs occurred and limited the window for SC proliferation. The production of fewer SCs can lead to lower-than-normal sperm output (74).

4.1.3 Factors Regulating Androgen Receptor Mediated Sertoli Cell Proliferation and Maturation

Precise regulation of Smad2/Smad3 is important both for SC proliferation and SC maturation (72). Type II A activin promotes immature testis growth along with timely appropriate AR expression *via* Smad3. The expression of Smad3 is then downregulated, and this is associated with cessation of SC proliferation and progression of the cells to terminal differentiation. AR activation can induce *Smad2* transcription, which will further promote SC maturation through shifting from using Smad3 only to using both Smad2 and Smad3 under activin A activation. In $Smad3^{-/-}$ mice, delayed maturation of SCs was accompanied by reduced levels of AR and Smad2 (75).

In recent years, microRNAs (miRNAs) have been found to regulate SC proliferation and maturation. miR-124a binds to the 3'-UTR of *Ar* mRNA and downregulate AR expression, thereby inhibiting the proliferation of immature porcine SCs, while the coactivator really interesting new gene (RING) finger protein 4 (RNF4) binds to AR and promotes porcine SCs proliferation by elevating Proliferation cell nuclear antigen (a marker of cell proliferation) mRNA transcript levels (76). miR-762 promotes porcine SC maturation by inhibiting binding of RNF4 to AR (77). Moreover, miR-130a has been shown to inhibit AR expression, although its impact on SC proliferation and maturation remains to be elucidated (78). Additionally, the relationship of miR-133b (79) and miR-638 (80), which regulate SC proliferation and maturation, to AR remains to be investigated (**Figure 2**).

Importantly, the relationship between SC maturation and spermatogenesis is not well understood. We hypothesize that AR-regulated lipid metabolism in mature SCs can provide energy for spermatogenesis (81); for example, AR signaling in SCs induces the expression of ubiquitin-conjugating enzyme E2B (*Ube2b*) which regulates the expression of genes related to glycosylphosphatidylinositol (GPI)-anchor biosynthesis and oxidative phosphorylation (82). So does AR-regulated glucose uptake. The non-classical pathway participates in the regulation of glucose uptake *via* the cytochrome C oxidase (83). Also, BTB formed between SCs can facilitate normal spermatogenesis, as we will discuss later.

4.2 Role of AR Mediated Signaling in Spermatogonia Stem Cells Self-Renewal and Differentiation

Following the migration of gonocytes to the basement membrane and their differentiation into spermatogonia stem cells (5), SSCs are influenced by a network of signaling that can trigger SSC self-renewal and differentiation. AR signaling in SCs has been found to participate in these two processes, probably promoting SSC differentiation and repressing SSC self-renewal, although it is not clear whether both of classical and non-classical signaling in SCs contribute to these processes in all species (**Figure 3**).

4.2.1 Wnt5a

Wnt5a, which refers to Wingless-type MMTV Integration Site Family Member 5A, is secreted by SCs in mice. Several studies found that *Wnt5a* expression is regulated by androgen and that it promotes SSCs self-renewal. Both *in vitro* and *in vivo* studies confirmed that Wnt5a can increase SSC self-renewal division after androgen blockage in mice SCs (84). In addition, Crespo et al. found that in zebrafish one androgen, 11-ketotestosterone (11-KT), indirectly inhibits SSC self-renewal by inhibiting prostaglandin E2 (PGE2) in SCs. Otherwise, PGE2 promotes SSC self-renewal by upregulating *Wnt5a* expression (85). However, more investigations should focus on the existence of AREs within the promoter of *Wnt5a* to confirm the exact signaling pathway in SCs through which androgen exerts its effects.

4.2.2 Plzf

Promyelocytic leukemia zinc finger (*Plzf*), a key transcription suppressor gene, has been characterized as a marker for undifferentiated SSCs in rodents (86) and primates (87). *Plzf* is important for SSC maintenance (45). Recently, *in vivo* and *in vitro* studies found that after activation of AR signaling in SCs, AR homodimer binds to the ARE region of GATA binding protein 2 (*GATA-2*) to inhibit its expression; this can further decrease WT1 transcription factor (*Wt1*) expression since Wt1 expression requires binding of GATA-2to its promoter. Wt1 binds to β1-integrin and increases its expression in SCs; β1-integrin will interact with unknown molecules on the surface of

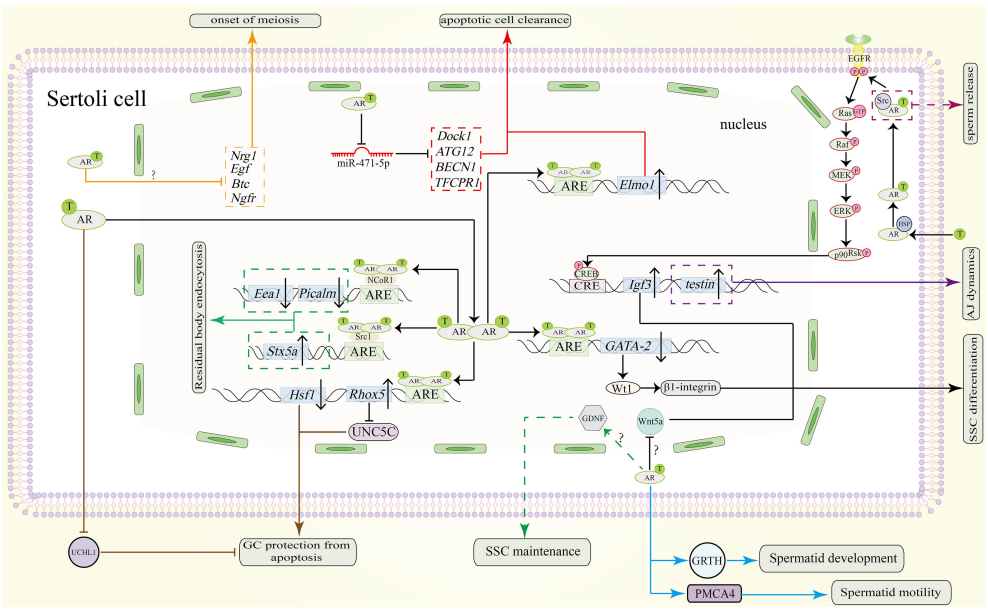

FIGURE 3 | Function of the AR signaling pathway in SCs in spermatogenesis. AR dimers in the nucleus can bind to the ARE of *GATA-2* to inhibit its expression. Downregulated protein levels of GATA-2 downregulate Wt1 and β1-integrin to promote SSC differentiation. The AR also promotes SSC differentiation by repressing Wnt5a. However, the precise pathway between AR and Wnt5a remains unknown. Through unknown pathway, AR allows SCs to secret GDNF for SSC maintenance (shown in green dotted line). Testosterone can also induce the expression of *Igf3* through a non-classical signaling pathway to promote SSC differentiation. Through an unknown pathway, the AR represses the expression of *Nrg1*, *Egf*, *Btc* and *Ngfr* to induce the onset of meiosis (shown in orange). To protect GCs from apoptosis during meiosis, AR dimers bind to the AREs in the promoters of *Rhox5* and *Hsf1*. Upregulated protein levels of Rhox5 repress Unc5c expression (shown in brown). Downregulation of *Hsf1* can also protect GCs from apoptosis (shown in brown). Also, AR signaling in SCs can inhibit UCHL1 expression in spermatocytes to prevent them from apoptosis (shown in brown). In addition, the clearance of apoptotic cells is also important. Testosterone inhibits miR-471-5p and thereby upregulates the expression of *Dock1*, *ATG12*, *BECN1* and *TFCPR1*, resulting in clearance by SCs (shown in red). Elmo1 upregulation by AR dimerization can also promote this process (shown in red). During spermiogenesis and spermiation, non-classical signaling induces the expression of *testin*, which is needed for proper adherence junctions (AJ) dynamics (purple solid line). The residual body from the maturing sperm will be absorbed by the concerted action of Stx5a, Picalm and Eea1 (shown in green). AR dimers also bind to the coactivator Src1 to induce the expression of *Stx5a* and to the corepressor NCoR1 to repress the expression of *Picalm* and *Eea1*. Spermatid development is also regulated by AR signaling. AR signaling in SCs induce GRTH and PMCA4 transcription and expression in spermatids which will promote their development and motility respectively (shown in blue line). Sperm release is facilitated by Src-mediated molecular processes (indicated by the purple dotted line). '?' indicates an unknown pathway.

SSCs, to induce *Plzf* expression. As a result, activation of classical AR signaling pathway can promote SSC differentiation by downregulating *Plzf* expression. We propose that the exact molecules that interact with β1-integrin on SSC surface should be identified to determine a more concise relationship between SCs and SSCs (88).

4.2.3 Other Factors

In zebrafish, Insulin like growth factor 3 (*Igf3*) mRNA transcript level was found to be upregulated by androgen; this can promote SSC differentiation through non-classical signaling pathway (89). Reproductive homeobox 5 gene (*Rhox5*), which is directly regulated by classical AR pathway, also contributes to spermatogonia differentiation (90). Besides, *in vitro* study found that testosterone can increase Glial-derived neurotrophic factor (GDNF) secretion by Sertoli cell (91). Glial-derived neurotrophic factor secreted will promote Gdnf family receptor α1 and proto-oncogene Rearranged expression during Transfection expression for SSC self-renewal and maintenance (92).

4.3 Role of AR Mediated Signaling in Spermatocytes Meiosis

In diploid organisms, the sexual differentiation requires the production of haploid gametes *via* meiosis, a process in which two consecutive cell divisions occur after a round of DNA replication (93). During prophase I of meiosis, leptotene and zygotene stages produce the DNA double strand breaks (DSBs) needed for DNA recombination, along with the chiasmata required for homologous chromosome separation. Following the zygotene stage is pachytene stage, in which the synapsis is completed, and DNA combination is finished as well as DSBs repair. In SCs, the AR signaling pathway is believed to be important in these stages (94) (**Figure 3**).

Loss of spermatocytes and spermatids in rodents occurred as a result of decreased intratesticular testosterone level in hypophysectomy, gonadotropin-releasing hormone antagonist treatments and hypogonadal (*hpg*) models (95). Above results indicate that testosterone mediated AR signaling is necessary for normal meiosis. Furthermore, inhibition of AR-Src interaction

resulted in inactivation of non-classical signaling pathway in mice. Arrested meiosis was observed at the first spermatogenic wave (45). Moreover, in SCARKO mice where classical signaling pathway is blocked, De et al. observed loss of primary spermatocytes during stages VI-VII, a time when AR shows high protein expression level (96). These results suggest that both classical and non-classical AR signaling in SCs are indispensable for normal meiosis (**Figure 3**). In their attempt to determine the precise process that is regulated by AR signaling, Su et al. found that in SCARKO mice, meiosis arrest occurred in prophase I; cells failed to divide, and spermatocytes failed to acquire competence for the meiotic division phase (97). Although meiosis appeared to progress to a mid-pachytene-like cytological state, most germ cells stalled at an early-pachytene transcriptome stage (98). Precisely, meiosis arrest occurred between leptotene/zygotene to early–mid pachytene transition.

We conclude that there are two causes of meiotic arrest: chromosomal dysfunction and germ cell apoptosis.

4.3.1 Chromosomal Dysfunction

The fact that AR expression peaks at stages VI-VIII of meiosis, coinciding with the preleptotene and leptotene stages, suggests that the AR might mediate the preparation of SCs for chromosomal synapsis and recombination. Male germ cells can enter prophase I of meiosis normally and undergo normal DSBs formation in the absence of AR signaling (5). However, the problems happened on DSBs repair and chromosome synapsis. In SCARKO mice, chromosome synapsis was incomplete, as shown by the fact that Chen et al. detected a significantly larger number of univalent chromosomes in spermatocytes than in the control group. Additionally, RAD51 and DMC1 which are required for resolution of DSBs and homologous recombination, along with TEX15, BRCA1, BRCA2 and PALB2 which load RAD51 and DMC1 onto DSBs sites, showed decreased protein expression in SCARKO mice. Furthermore, activation of AR can negatively regulate Epidermal growth factors (EGFs), including *Egf*, betacellulin (*Btc*) and neuregulin 1 (*Nrg1*). These EGFs bind to their corresponding receptors (EGFR, ERBB4) on the surface of spermatocytes and stimulate the accumulation of above homologous recombination factors for appropriate prophase preparation (94). At the synaptonemal complex, nuclear autoantigenic sperm protein (NASP) inhibits formation of CDC2/cyclinB1 complex *via* HSP70-2 which are important for G2/M transition. NASP showed elevated expression after androgen manipulation. Other genes that show changes in transcript after androgen manipulation, such as *Mapre1*, *Ruvbl1*, *Tuba1c*, *Tuba3a* and *Tubb2c*, are related to spindle dynamics and the formation of dynactin complexes (99). Although fewer spermatocytes may gain competence to enter metaphase I, they cannot complete meiosis due to the lack of normal spindle dynamics, and this may account for the disruption in post-meiotic differentiation. More proteins account for chromosome synapsis and dynamics that is under AR regulation deserve to be confirmed to establish the AR downstream signaling network by taking advantage of the development of proteomics.

4.3.2 Germ Cell Apoptosis

GC apoptosis, especially apoptosis of spermatocytes, is another cause of meiotic arrest. This is not difficult to understand, since spermatocytes are cells that undergo meiosis. Through single cell transcript analysis technology, genes related to apoptosis have been identified. *Aldh1a1*, *Igfbps*, and mitochondrial membrane and oxidative phosphorylation transcripts were upregulated in SCARKO mice (98). Another group found that androgen deprivation led to a decreased expression of *Aldh2*, *Prdx6* and *Gstm5*, which encode protectors of oxidative stress (99). Other genes related to androgen-dependent apoptosis, such as *Diablo*, *Cbl*, *Hsf1* showed increased expression in mice after androgen deprivation or knocking out AR in SCs (97, 100). Hu et al. showed that Rhox5 can repress expression of Unc-5 Netrin Receptor C(UNC5C) which can promote spermatocyte apoptosis *in vitro* (101). Since Rhox5 is regulated by classical signaling pathway (90, 102, 103), it needs to be determined whether AR signaling represses UNC5C expression and thereby protects spermatocytes from apoptosis. Recently, Marina et al. found that ubiquitin carboxyl-terminal hydrolase L1(UCHL1) is negatively regulated by androgen. Decreased level of androgen leads to increased level of UCHL1 in spermatocytes, which will lead to deubiquitination of the pro-apoptotic factor p53. Deubiquitination of p53 triggers germ cell death (104). In addition, phagocytic clearance of apoptotic germ cells by SCs is vital for meiosis because phagocytosis of dying GCs provides lipid sources for SCs which will provide ATP for GCs development. Lower androgen increases the expression of miR-471-5p, resulting in inhibition of *Dock1, Tecpr1, Atg12* and *Becn1*. This leads to impaired LC3-associated phagocytosis. Besides, inhibition of *Dock1, Rac1-GTPase* in this model leads to disrupted engulfment of SCs (11). Both of these inhibitions impair clearance of apoptotic GCs by SCs. Another protein Elmo1, which is upregulated by classical AR signaling *in vivo*, participates in apoptotic germ cells clearance by SCs and functions downstream of Dock1 and Rac1-GTPase (73, 105).

Many of the transcription factors and regulators related to AR signaling that have been found are not mentioned here. These factors can participate in the regulation of meiosis. For additional information on these factors, please see **Table 1**. For additional genes that show changes in expression after androgen manipulation, please see the supplied references (98, 99, 123).

Based on the evidences presented above, we propose the reasons for meiotic arrest when AR signaling in SC is impaired. Chromosomal dysfunction or breakage can induce oxidative stress that cannot be repressed because of the decreased level of oxidative stress protectors. This leads to apoptosis of some spermatocytes. The presence of increased number of apoptotic cells, the failure to clear apoptotic cells combined with DNA damage trigger the inner meiotic checkpoint and cause meiosis to halt in prophase I. Future studies might focus on the roles of genes related to AR signaling that have been mined through mRNA transcript analysis in meiosis and attempt to determine whether they play permissive roles or instructive roles for meiosis.

TABLE 1 | Transcription regulators, upstream regulators and downstream regulators of Androgen receptor signaling during spermatogenesis.

Regulators		species	function	reference
Coactivator				
	ARID4B/4A	mice	BTB integrity Timely SC maturation Normal meiosis Normal Rhox5 function Post-meiotic differentiation	(106, 107)
	ARIP4	rats	Normal Rhox5 function Germ cells proliferation	(108)
	SRC-2	human	Sustainable production of spermatozoa	(109)
	TRAM-1	human	Regulation of transcription	(110)
	PSPC1	mice	Promote AR transactivation	(111)
	NONO	mice	Promote AR transactivation	(111)
	SFPQ	mice	Promote AR transactivation	(111)
	SRC-1	rats	Promote residual body absorption	(112)
Corepressor				
	DjA1	mice	Inhibit spermatocyte death Promote round spermatid differentiation Maintain adhesion junctions	(113)
	HBO-1	human	Participate DNA replication Initiate and maintain spermatogenesis	(109)
	NCOR1	rats	Promote residual body absorption	(112)
Upstream regulators				
	P110βPI3-kinase	mice	Spermatocyte differentiation	(114)
	Tzfp	mice	Normal cross-over through pachynema Germ cell formation Repress AR signaling	(115)
	NF-κB	rats	Activate transcription of AR	(116)
	LncNONO-AS	goats	Activate AR expression *via* NONO	(117)
Downstream regulators				
	Rhox5	mice	Enter prophase during prepuberty Facilitate the first step of meiosis during puberty Sperm release BTB remodeling	(101, 102)
	FGF2	mice	Trigger spermatogonia proliferation and differentiation Meiosis initiation	(118)
	Aard	mice	Normal spermatogenesis Regulate transcription activity	(119)
	Cbl	rats	Activate androgen-dependent	(120)
	PMCA4	mice	Movement and motility of sperm	(121)
	Hsf1	mice	Protect immature gem cells	(100)
	Ube2b	mice	glycosylphosphatidylinositol (GPI)-anchor biosynthesis and oxidative phosphorylation	(82)
	Elmo1	mice	Sertoli cell mediated phagocytic clearance of apoptotic germ cells	(105)
	Spinlw1	rats	Sperm motility	(122)
	testin	mice	Adhesion junction dynamics	(113)

4.4 Role of AR Mediated Signaling in Maintenance of Blood-Testis Barrier

SCs in mammalian testis can divide the seminiferous epithelium into basal and adluminal compartments through the construction of BTB. During stages VII-VIII of seminiferous epithelium cycle when the AR expression level peaks in rodents, BTB undergoes restructuring to facilitate the translocation of preleptotene spermatocytes from the basal area to the apical area where they will complete the entire processes of meiosis and post-meiotic processes. This transition, facilitated by testosterone, requires breakage of the 'old' BTB before preleptotene spermatocytes and formation of 'new' BTB after preleptotene spermatocytes entering into adluminal compartment (97, 124). Moreover, BTB shields haploid germ cells from recognition by the innate immune system; and this is why we also call it 'immune barrier' (125). BTB includes many types of junctions: tight junctions (TJs), gap junctions (GJs), desmosomes, basal ectoplasmic specialization (ES). These junctions undergo dynamic changes to fulfill their roles. Exposure of SC cultures to adenovirus constructs expressing inhibitors of either classical or non-classical AR signaling pathway led to increased permeability of BTB, suggesting that both classical and non-classical signaling pathway are important for BTB integrity, probably through regulating junction proteins (45, 126). (**Figure 2**).

4.4.1 Tight Junction

Classical signaling pathway regulates proper tight junction dynamic. In mouse models with mutations in exon1 of AR, increased permeability of BTB was observed (124, 127).

Although the BTB appears to be present in this model under microscopic examination, it is incomplete as we found biotin enter into adluminal area with the help of biotin tracer (127). Reversibly, BTB were strengthened after testosterone treatment of an SC culture system with disrupted AR function (128). To further investigate the molecular basis of these effects, microarray analysis was used to identify the genes that may be involved. The mRNA transcript level of tight junction protein including Claudin 3, Claudin 11, Claudin 13 were all downregulated while Occludin and Claudin 26 showed elevated transcript levels after ablation of exon1 of AR in mice (129). Among them, Claudin 3 which is not essential for fertility, is expressed in the newly formed BTB after preleptotene spermatocytes migrate past the old BTB (127). Claudin 13 shows a similar expression pattern to Claudin 3. CHIP-seq assays found putative AREs in the promoter regions of *Claudin 13* and *tight junction protein 2 isoform 3*, indicating a potential classical signaling regulation pattern. In contrast to Claudin 3, Claudin 11 preserves its expression throughout the seminiferous cycle. Besides, membrane-associated GUK family of proteins including *tight junction protein 1*, *tight junction protein 2 isoform 1*, *tight junction protein 2 isoform 2*, and *tight junction protein 2 isoform 3*, can function as a bridge that links tight junction proteins to the cytoskeleton like actin filaments. Their mRNA transcripts were found to be downregulated in mouse SCs after ablation of AR (129–131). What's more, it was found that tight junction proteins can enter the nuclei of SCs and regulate their own transcription (132), indicating possible tight junction proteins compensatory effects in $Cldn3^{-/-}$ mutant mice.

Apart from its directly regulation of TJ proteins, non-classical signaling can regulate TJ proteins *via* tissue type plasminogen activator (tPA) during stages VII-VIII of spermatogenesis when BTB undergoes restructuring (133). We also know that tPA is involved in BTB degradation (134), indicating a potential role of tPA in BTB dynamics. Moreover, Dietze et al. and Bulldan et al. found that Claudin 1, Claudin 5 and Claudin 11 protein levels were upregulated by CREB protein (49, 135, 136). These results further support the idea that non-classical androgen signaling can maintain BTB integrity by regulating tight junction dynamics.

Besides, in heat-treated monkey testes, AR regulates reversible changes in BTB integrity *via* Par complex (Par6-Par3, Par6-aPKC, and Par6-Cdc42) targeting TJ proteins (ZO-1 and occludin) and basal ES proteins (N-cadherin, E-cadherin, α-catenin, β-catenin, and γ-catenin) (137).

Based on the results described above, we hypothesize that although the transition of preleptotene spermatocytes into adluminal compartment is not blocked when AR signaling in SC is prevented, the amount of claudin available for remodeling BTB (Claudin 3, Claudin 11, Claudin 13) is insufficient under these conditions. Besides, the downregulated tight junction proteins are not sufficient to enter the nucleus and increase their own transcription, let alone to recruit more claudins to the BTB. While Occludin and Claudin26 show relatively upregulated mRNA transcript levels, this is not enough to compensate for the loss of other tight junction proteins. Thus, humoral immunity against self-antigens is mounted, resulting in disruption of normal spermatogenesis.

4.4.2 Gap Junction

Connexin 43 (Cx43), one gap junction protein, also under AR regulation as shown by its reduced mRNA transcript levels and protein expression levels in adult pig testes treated with flutamide, an anti-androgen (138). Interestingly, we also found weak AR immunostaining and partial disruption of AR signaling in SCs in Sertoli cell specific knock-out of connexin 43 mice (71). Xia et al. found that androgen can regulate the expression of Wt1 indirectly by inhibiting GATA-2expression. Androgen inhibits GATA-2 expression through the classical pathway. Wt1 can bind to the promoter of Cx43 and inhibit its expression, indicating that androgen can promote Cx43 expression by downregulating GATA-2 and Wt1 (139). What's more, ouabain binding to its receptor ATP1A1can upregulate Cx43 expression *via* non-classical signaling pathway *in vivo* (140). The relationship between Cx43 and AR deserves further investigation. It remains to be determined whether reversing one of them (Cx43 or AR) can restore the other to normal level in human and correct impaired spermatogenesis, though it is possible that treating hpg mice with DHT can restore the expression and localization of Cx43 to the BTB (141).

4.4.3 Blood-Testis Barrier Renewal

The endocytosis of old BTB proteins for renewal is also important for BTB integrity (142). Testosterone can promote the endocytosed occludin to the BTB location through recycling pathway (124). Other cells such as Madin-Darby canine kidney cells and epithelial cells can internalize occluding and claudin *via* clathrin- and caveolin-mediated pathways (143, 144). Coincidentally, Su et al. found that testosterone increases levels of clathrin and caveolin-1 in SCs (145), this suggests that AR signaling may participate in tight junction protein endocytosis for renewal *via* the clathrin and caveolin-1 pathways. This possibility needs further investigation.

Since AR signaling is important for BTB integrity, what will happen if AR is overexpressed under normal conditions? The influence of a tighter BTB on spermatogenesis remains unknown. We suggest an *in vitro* AR overexpression experiment to answer this question. Recently, in muscle cells, it was found that AR can participate in IGF-1/IGF-1R-PI3K/Akt-mTOR pathway (146). We also know that mTOR signaling can regulate BTB dynamic by balancing the levels of F-actin binding proteins epidermal growth factor receptor pathway substrate 8 and actin related protein 3 (147). Therefore, we suggest investigation into crosstalk between AR and mTOR pathway and its downstream molecules related to actin-binding proteins in germ cell lines.

4.5 Role of AR Mediated Signaling in Sertoli Cell - Spermatid Adhesion and Sperm Release

Before spermiogenesis occurs, round spermatids are linked to SCs by desmosomes. When the cycle of seminiferous epithelium

enters into stage VII, the round spermatids begin to elongate accompanied by the replacement of desmosome anchors with new specialized adhering proteins. We call the structure formed in this way as apical ectoplasmic specialization (ES). The proteins that form ES disassemble before sperm release during stage VIII. The complexes connecting SC and elongated spermatids are tubulobulbar complex and the focal adhesion-related disengagement complex. AR signaling pathway is important in two processes during spermiogenesis and final spermiation: Sertoli cell – Spermatid adhesion and sperm release (**Figures 2**, **3**).

The importance of AR signaling in Sertoli cell - Spermatid adhesion and sperm release is elucidated by two *in vivo* model. First, in rats that received subdermal testosterone and oestradiol (TE) implants to lower the intratesticular testosterone level, researchers found loss of stage VIII and late spermatids (148, 149). Additionally, hypomorphic SCARKO mice displayed premature release of round spermatids as well as blockage of terminal differentiation and release of elongated spermatids. The unreleased mature spermatids were degenerated or phagocytized by SCs (149, 150).

4.5.1 Sertoli Cell - Spermatid Adhesion

The molecular mechanism through which Sertoli cell - Spermatid adhesion occurs has been elucidated. Based on experiments in which adenovirus constructs were used to express different AR mutants that impair the classical or nonclassical pathways and on other experiments in which inhibitors of ERK kinase and Src kinase were added to an SC-GC coculture system, it is proposed by study that non-classical AR signaling pathway contributes dominantly to Sertoli cell-Spermatid adhesion, while activation of the classical AR signaling pathway is not sufficient to permit Spermatids binding to SCs (151). Testosterone can promote the attachment of spermatids to SCs in Sertoli cell -Spermatid co-culture system by activation ERK and Src, which belong to the non-classical signaling pathway (152). Terada et al. found that testin, which can be induced by non-classical signaling pathway, is important for Sertoli cell - Spermatid adhesion. Overexpression of testin can block spermatid differentiation, probably due to excessive adhesion to SCs (113). However, an *in vivo* study adopting TE implants brought about not only the loss of spermatids but also the activation of ERK before sperm release, along with breakage association of N-cadherin and β-catenin indicating disruption of ES (153). This result seems contradictory to *in vitro* study. One possible reason maybe that the formation of ES requires ERK activation only at the beginning of formation rather than during the entire process.

4.5.2 Sperm Release

Round spermatids develop into elongated sperm before final releasing.

Gonadotropin Regulated Testicular Helicase (GRTH/DDX25) is significant in this process, mainly by participating on the nuclear export and transport of specific mRNAs as well as the structural integrity of Chromatoid Bodies of round spermatids (154). As an RNA helicase and only DEAD-box family member regulated by androgen in spermatids, GRTH/DDX25 transcription in spermatid is regulated by AR signaling pathway in Sertoli cells through a paracrine fashion. Germ cell nuclear factor (GCNF) in spermatids can promote GRTH/DDX25 transcription and expression in response to androgen regulation (155–158). However, the signal relayed to spermatids remains to be further elucidated.

Before releasing sperm, SCs endocytose the residual body from maturing sperm. Kumar et al. found that AR dimerization can recruit corepressor nuclear receptor corepressor 1 (NCoR1) to the ARE of phosphatidylinositol binding clathrin assembly protein (*Picalm)* and early endosome antigen 1 (*Eea1)* and thereby inhibit their expression. Coactivator steroid receptor coactivator-1 (Src1) can be recruited to ARE of syntaxin 5 (*Stx5a)* and induce its expression (112, 159, 160). Since the products of these 3 genes are located around tubule bulbar complexes and participate in endocytosis and intracellular transport, it is possible that they are involved in residual body absorption.

Activation of Src is important for sperm release (161, 162). The injection of Src inhibitor into rat testis can block the release of elongating spermatids, while injection of an ERK inhibitor has little effect on sperm release (152, 163). Additionally, O'Donnell et al. pointed out that the disengagement complex, including α6β1 integrin which associates with Src, and tyrosine-phosphorylated focal adhesion kinase (FAK), remains associated with sperm that fail to be released. Both Src and FAK can be phosphorylated on activation of non-classical androgen signaling (149). Further study confirmed that activated non-classical signaling target Src is near the head of sperm to be released (164).

Also, sperm motility is significant during sperm release. Located in elongated spermatids, ATPase Ca^{++} transporting plasma membrane 4 (PMCA4) is critical for sperm motility (165). Recently, it was found that PMCA4 is positively regulated by AR signaling in SCs both *in vitro* and *in vivo* (121).

In a summary, non-classical AR signaling promotes Sertoli cell – Spermatid adhesion by activating both ERK and Src while promoting sperm release by activating Src. Considering the above study, future studies might focus on achieving a deeper understanding of the different effects of Src to immature spermatid and mature spermatid as well as the impact of both ERK and Src to other kinds of proteins in apical ES.

5 DISCUSSION ON ANDROGEN INSENSITIVITY SYNDROME: PRESENT ADVANCES AND FUTURE THERAPIES

Infertility is an emerging worldwide public health issue. Approximately 20-70% of cases are due to male infertility (166). For most men suffering from infertility, the primary cause is low quality and low quantity of sperm (167). Hormones, including androgens, are necessary for spermatogenesis. We have reviewed AR signaling in SCs above. Clinical mutations in androgen receptor can cause reproductive diseases such as Androgen insensitivity syndrome, Sertoli cell-only syndrome and

Obstructive azoospermia. Here we will focus on androgen insensitivity syndrome, which is closely related to AR mutations in SCs.

Androgen insensitivity syndrome (AIS) is an X-linked recessive disorder of sex development in patients with the 46, XY karyotype (168). According to the National Institutes of health, approximately 2-5 in 100000 people may have AIS. The biochemical mechanism behind AIS is the inability of cells expressing AR to respond to androgen, leading to incomplete or absent genital virilization of the 46, XY embryo (169). Specifically, the mutations in AR result in disrupted capacity of binding to testosterone or DHT, leading to impaired differentiation of the Wolffian ducts and impaired virilization of the external male genitalia respectively (170). At present, AIS is classified into two categories, AIS type I and AIS type II. In AIS type I, mutations exist in AR itself; this type of AIS can be further classified into complete AIS (CAIS), partial AIS (PAIS) and mild AIS (MAIS) according to the AR mutation level, while mutations in AIS type II occur in molecules downstream of AR rather than in AR itself (171). The clinical phenotype of CAIS is characterized by an external female phenotype with undescended testes (172), PAIS leads to different ranges of hypospadias and ambiguous genitalia (173) and individuals with MAIS display a male phenotype, sometimes with gynecomastia, and insufficient sperm production (174). Recent years, studies and many case reports have revealed different AR mutations in patients with AIS. Mutations found up to now include gene deletion, mutations in transactivation domain, mutations in the DNA binding domain, mutations in the ligand binding domain. (For additional information, please see review (175)) In addition, even individuals without a mutation in the AR gene can show an AIS-like syndrome, indicating that mutations may have occurred somewhere else (176).

Currently, researches on AIS focus mainly on recording patient phenotypes and detecting AR mutations through sequencing of AR gene. Various AR mutations have been found to date (177). Inadequate research on associated gene expression patterns presents much difficulties for the development of therapies, especially for type II AIS. In addition, few studies have used testicular histology to examine the effects of AR mutations on testis. Recently, one CAIS patient showed unusually high level of AMH and SOX9, accompanied by immature SCs, a phenomenon that has been linked in a mouse model to the AR/SOX9/AMH pathway discussed above (178). AMH, along with Inhibin B, which may have positive or inverse correlation with AMH, is thought to be appealing subject for study by endocrinologists because patients with androgen insensitivity or defects in androgen synthesis have normal or high levels of AMH (179).

Notably, a high level of estrogen was found in patients with CAIS, and this may explain the development of breast cancer in some of these patients. Supporting this idea, it is known that testosterone can be converted into estrogen *via* aromatase and luteinizing hormone can stimulate testicular estrogen synthesis. Researchers have found high levels of luteinizing hormone and testosterone in AIS patients (168, 175, 180). Interestingly, apolipoprotein D (APOD), which is induced by DHT, is a potential candidate marker for the detection of AIS, especially for type II AIS. Treating type II AIS patients with DHT can induce endogenous APOD expression but the level of APOD is below the calculated cut-off (181). Other molecular pathways downstream of AR in AIS patients are remaining to be elucidated. One question arises for our molecular research. Although mice and rats have high homology with humans, some phenotypes in AIS patients cannot be reproduced in mouse or rat models. Although this is a significant barrier in our research, we should not be pessimistic. In a comparison of control males and CAIS females, significant differences in the transcription levels of 612 genes were found at the cellular level, suggesting that androgens may play a role in transcriptome regulation in humans (182). We are pleased to see that AR can regulate the transcriptome level in mouse models (98); this observation can guide us to investigate genes with known function in mouse models in our clinical diagnosis and to research genes that show no overlap between two species in mice to determine their function.

In summary, our opinions are that the diagnosis for AIS should combine power from different fields of study. For geneticists, family history is recommended to record for prenatal diagnosis, along with determining the patient's karyotype after birth (183). Some important biomarkers, such as AMH, estrogen, luteinizing hormone and testosterone should be measured at birth or at puberty to distinguish AIS from androgen synthesis deficiency by endocrinologists. Cytologists and histologists use fine needle aspiration cytology (184) and histopathology to examine the state of SCs and the testicular lumen, and the results obtained may be compared with results obtained from patients with other syndromes like, such as Sertoli cell-only syndrome or nonobstructive azoospermia, possibly benefiting from therapies for those diseases. Finding associated genes and impaired signaling pathway are tasks for molecular biologists. Combined efforts are powerful.

At present, the most common treatment for CAIS is gonadectomy in early adulthood. There are two reasons for this: 1) an undescended testis has an increased risk of malignant transformation after puberty; and 2) testosterone produced by the testis can be converted to estrogen, so puberty will occur naturally (185, 186). Besides, treatment for PAIS vary between different patients. Treatments currently include androgen supplementation at puberty, surgeries to repair hypospadias and bring undescended testes into the scrotum. Personal treatment should combine diagnosis, sex assignment and biochemical examination (187). Previous study using AR transgene model restored the impaired spermatogenesis in SC AR mutant mice (188). Whether transfection of AR constructs into human SCs can benefit AIS patients remains to be elucidated.

Moreover, the job of a doctor is not only to treat patients physically, but also to treat them psychologically. Helping AIS patients overcome their psychological disorders and live a normal life without discrimination is a responsible behavior for doctors and for society as a whole.

6 CONCLUSION AND PERSPECTIVE

Both classical and non-classical androgen receptor signaling pathway are essential for spermatogenesis. These two pathways

not only regulate genomic action in Sertoli cells but also influence germ cells between Sertoli cells through paracrine action. Sertoli cells are expected to be a new therapeutic target. However, rare studies focus on the relationship between androgen receptor signaling pathway, Sertoli cell and clinical diseases. The transgenic model developed recently which is able to activate only classical or non-classical signaling pathway, allows us to screen more genes related to androgen receptor signaling pathway. These genes are helpful for us to develop therapies for treating infertility. Moreover, spermatogonia transplantation is a method to inject spermatogonia into seminiferous tubule lumen and promote spermatogonia to form colonization at basement area, which may cure fertility fundamentally. The problem about making spermatogonia migrating from adluminal area to basement area may be solved by androgen therapies because lowering testicular testosterone level can open BTB reversibly.

AUTHOR CONTRIBUTIONS

J-MW, Z-FL, and W-XY conceived of and authored the paper. All authors contributed to the article and approved the submitted version.

FUNDING

This work was supported in part by National Natural Science Foundation of China (No 32072954).

ACKNOWLEDGMENTS

The authors want to show their appreciation to all members of the Sperm Laboratory in Zhejiang University for their support, encouragement, and assistance.

REFERENCES

1. Agarwal A, Baskaran S, Parekh N, Cho C-L, Henkel R, Vij S, et al. Male Infertility. *Lancet* (2021) 397(10271):319–33. doi: 10.1016/s0140-6736(20)32667-2
2. Sharlip ID, Jarow JP, Belker AM, Lipshultz LI, Sigman M, Thomas AJ, et al. Best Practice Policies for Male Infertility. *Fertil Steril* (2002) 77(5):873–82. doi: 10.1016/s0015-0282(02)03105-9
3. Practice Committee of the American Society for Reproductive Medicine. Diagnostic Evaluation of the Infertile Male: A Committee Opinion. *Fertil Steril* (2015) 103(3):e18–25. doi: 10.1016/j.fertnstert.2014.12.103
4. de Kretser DM, Loveland KL, Meinhardt A, Simorangkir D, Wreford N. Spermatogenesis. *Hum Reprod (Oxf Eng)* (1998) 13 Suppl 1:1–8. doi: 10.1093/humrep/13.suppl_1.1
5. Walker WH. Androgen Actions in the Testis and the Regulation of Spermatogenesis. *Adv Exp Med Biol* (2021) 1288:175–203. doi: 10.1007/978-3-030-77779-1_9
6. Iliadou PK, Tsametis C, Kaprara A, Papadimas I, Goulis DG. The Sertoli Cell: Novel Clinical Potentiality. *Hormones (Athens Greece)* (2015) 14(4):504–14. doi: 10.14310/horm.2002.1648
7. Crisóstomo L, Alves MG, Gorga A, Sousa M, Riera MF, Galardo MN, et al. Molecular Mechanisms and Signaling Pathways Involved in the Nutritional Support of Spermatogenesis by Sertoli Cells. *Methods Mol Biol (Clifton NJ)* (2018) 1748:129–55. doi: 10.1007/978-1-4939-7698-0_11
8. Ma W, Li S, Ma S, Jia L, Zhang F, Zhang Y, et al. Zika Virus Causes Testis Damage and Leads to Male Infertility in Mice. *Cell* (2016) 167(6):1511–24.e10. doi: 10.1016/j.cell.2016.11.016
9. Kaur G, Thompson LA, Dufour JM. Sertoli Cells–Immunological Sentinels of Spermatogenesis. *Semin Cell Dev Biol* (2014) 30:36–44. doi: 10.1016/j.semcdb.2014.02.011
10. Wong CH, Xia W, Lee NP, Mruk DD, Lee WM, Cheng CY. Regulation of Ectoplasmic Specialization Dynamics in the Seminiferous Epithelium by Focal Adhesion-Associated Proteins in Testosterone-Suppressed Rat Testes. *Endocrinology* (2005) 146(3):1192–204. doi: 10.1210/en.2004-1275
11. Panneerdoss S, Viswanadhapalli S, Abdelfattah N, Onyeagucha BC, Timilsina S, Mohammad TA, et al. Cross-Talk Between miR-471-5p and Autophagy Component Proteins Regulates LC3-Associated Phagocytosis (LAP) of Apoptotic Germ Cells. *Nat Commun* (2017) 8(1):598. doi: 10.1038/s41467-017-00590-9
12. Petersen C, Soder O. The Sertoli Cell–a Hormonal Target and 'Super' Nurse for Germ Cells That Determines Testicular Size. *Horm Res* (2006) 66(4):153–61. doi: 10.1159/000094142
13. Boukari K, Meduri G, Brailly-Tabard S, Guibourdenche J, Ciampi ML, Massin N, et al. Lack of Androgen Receptor Expression in Sertoli Cells Accounts for the Absence of Anti-Mullerian Hormone Repression During Early Human Testis Development. *J Clin Endocrinol Metab* (2009) 94(5):1818–25. doi: 10.1210/jc.2008-1909
14. Buzek SW, Sanborn BM. Increase in Testicular Androgen Receptor During Sexual Maturation in the Rat. *Biol Reprod* (1988) 39(1):39–49. doi: 10.1095/biolreprod39.1.39
15. Callewaert L, Van Tilborgh N, Claessens F. Interplay Between Two Hormone-Independent Activation Domains in the Androgen Receptor. *Cancer Res* (2006) 66(1):543–53. doi: 10.1158/0008-5472.Can-05-2389
16. Soffientini U, Rebourcet D, Abel MH, Lee S, Hamilton G, Fowler PA, et al. Identification of Sertoli Cell-Specific Transcripts in the Mouse Testis and the Role of FSH and Androgen in the Control of Sertoli Cell Activity. *BMC Genomics* (2017) 18(1):972. doi: 10.1186/s12864-017-4357-3
17. Chaturvedi AP, Dehm SM. Androgen Receptor Dependence. *Adv Exp Med Biol* (2019) 1210:333–50. doi: 10.1007/978-3-030-32656-2_15
18. Rey RA. The Role of Androgen Signaling in Male Sexual Development at Puberty. *Endocrinology* (2021) 162(2):1–16. doi: 10.1210/endocr/bqaa215
19. Shaffer PL, Jivan A, Dollins DE, Claessens F, Gewirth DT. Structural Basis of Androgen Receptor Binding to Selective Androgen Response Elements. *Proc Natl Acad Sci USA* (2004) 101(14):4758–63. doi: 10.1073/pnas.0401123101
20. Claessens F, Alen P, Devos A, Peeters B, Verhoeven G, Rombauts W. The Androgen-Specific Probasin Response Element 2 Interacts Differentially With Androgen and Glucocorticoid Receptors. *J Biol Chem* (1996) 271(32):19013–6. doi: 10.1074/jbc.271.32.19013
21. Verrijdt G, Schoenmakers E, Haelens A, Peeters B, Verhoeven G, Rombauts W, et al. Change of Specificity Mutations in Androgen-Selective Enhancers. Evidence for a Role of Differential DNA Binding by the Androgen Receptor. *J Biol Chem* (2000) 275(16):12298–305. doi: 10.1074/jbc.275.16.12298
22. Schoenmakers E, Verrijdt G, Peeters B, Verhoeven G, Rombauts W, Claessens F. Differences in DNA Binding Characteristics of the Androgen and Glucocorticoid Receptors can Determine Hormone-Specific Responses. *J Biol Chem* (2000) 275(16):12290–7. doi: 10.1074/jbc.275.16.12290
23. Ni L, Llewellyn R, Kesler CT, Kelley JB, Spencer A, Snow CJ, et al. Androgen Induces a Switch From Cytoplasmic Retention to Nuclear Import of the Androgen Receptor. *Mol Cell Biol* (2013) 33(24):4766–78. doi: 10.1128/MCB.00647-13
24. Haelens A, Tanner T, Denayer S, Callewaert L, Claessens F. The Hinge Region Regulates DNA Binding, Nuclear Translocation, and Transactivation of the Androgen Receptor. *Cancer Res* (2007) 67(9):4514–23. doi: 10.1158/0008-5472.CAN-06-1701
25. Clinckemalie L, Vanderschueren D, Boonen S, Claessens F. The Hinge Region in Androgen Receptor Control. *Mol Cell Endocrinol* (2012) 358(1):1–8. doi: 10.1016/j.mce.2012.02.019
26. Matias PM, Donner P, Coelho R, Thomaz M, Peixoto C, Macedo S, et al. Structural Evidence for Ligand Specificity in the Binding Domain of the Human Androgen Receptor. Implications for Pathogenic Gene Mutations. *J Biol Chem* (2000) 275(34):26164–71. doi: 10.1074/jbc.M004571200

27. Tan MH, Li J, Xu HE, Melcher K, Yong EL. Androgen Receptor: Structure, Role in Prostate Cancer and Drug Discovery. *Acta Pharmacol Sin* (2015) 36 (1):3–23. doi: 10.1038/aps.2014.18
28. Bremner WJ, Millar MR, Sharpe RM, Saunders PT. Immunohistochemical Localization of Androgen Receptors in the Rat Testis: Evidence for Stage-Dependent Expression and Regulation by Androgens. *Endocrinology* (1994) 135(3):1227–34. doi: 10.1210/endo.135.3.8070367
29. Suárez-Quian CA, Martínez-García F, Nistal M, Regadera J. Androgen Receptor Distribution in Adult Human Testis. *J Clin Endocrinol Metab* (1999) 84(1):350–8. doi: 10.1210/jcem.84.1.5410
30. Smith LB, Walker WH. The Regulation of Spermatogenesis by Androgens. *Semin Cell Dev Biol* (2014) 30:2–13. doi: 10.1016/j.semcdb.2014.02.012
31. Swerdloff RS, Dudley RE, Page ST, Wang C, Salameh WA. Dihydrotestosterone: Biochemistry, Physiology, and Clinical Implications of Elevated Blood Levels. *Endocr Rev* (2017) 38(3):220–54. doi: 10.1210/er.2016-1067
32. Fluck CE, Meyer-Boni M, Pandey AV, Kempna P, Miller WL, Schoenle EJ, et al. Why Boys Will be Boys: Two Pathways of Fetal Testicular Androgen Biosynthesis are Needed for Male Sexual Differentiation. *Am J Hum Genet* (2011) 89(2):201–18. doi: 10.1016/j.ajhg.2011.06.009
33. Grino PB, Griffin JE, Wilson JD. Testosterone at High Concentrations Interacts With the Human Androgen Receptor Similarly to Dihydrotestosterone. *Endocrinology* (1990) 126(2):1165–72. doi: 10.1210/endo-126-2-1165
34. Ramaswamy S, Weinbauer GF. Endocrine Control of Spermatogenesis: Role of FSH and LH/ Testosterone. *Spermatogenesis* (2014) 4(2):e996025. doi: 10.1080/21565562.2014.996025
35. Shang Y, Myers M, Brown M. Formation of the Androgen Receptor Transcription Complex. *Mol Cell* (2002) 9(3):601–10. doi: 10.1016/s1097-2765(02)00471-9
36. Saporita AJ, Zhang Q, Navai N, Dincer Z, Hahn J, Cai X, et al. Identification and Characterization of a Ligand-Regulated Nuclear Export Signal in Androgen Receptor. *J Biol Chem* (2003) 278(43):41998–2005. doi: 10.1074/jbc.M302460200
37. Denayer S, Helsen C, Thorrez L, Haelens A, Claessens F. The Rules of DNA Recognition by the Androgen Receptor. *Mol Endocrinol* (2010) 24(5):898–913. doi: 10.1210/me.2009-0310
38. Sahu B, Pihlajamaa P, Dubois V, Kerkhofs S, Claessens F, Janne OA. Androgen Receptor Uses Relaxed Response Element Stringency for Selective Chromatin Binding and Transcriptional Regulation. *vivo Nucleic Acids Res* (2014) 42(7):4230–40. doi: 10.1093/nar/gkt1401
39. Kallio PJ, Poukka H, Moilanen A, Jänne OA, Palvimo JJ. Androgen Receptor-Mediated Transcriptional Regulation in the Absence of Direct Interaction With a Specific DNA Element. *Mol Endocrinol* (1995) 9 (8):1017–28. doi: 10.1210/mend.9.8.7476976
40. Heckert LL, Wilson EM, Nilson JH. Transcriptional Repression of the Alpha-Subunit Gene by Androgen Receptor Occurs Independently of DNA Binding But Requires the DNA-Binding and Ligand-Binding Domains of the Receptor. *Mol Endocrinol* (1997) 11(10):1497–506. doi: 10.1210/mend.11.10.9996
41. Fix C, Jordan C, Cano P, Walker WH. Testosterone Activates Mitogen-Activated Protein Kinase and the cAMP Response Element Binding Protein Transcription Factor in Sertoli Cells. *Proc Natl Acad Sci USA* (2004) 101 (30):10919–24. doi: 10.1073/pnas.0404278101
42. Deng Q, Wu Y, Zhang Z, Wang Y, Li M, Liang H, et al. Androgen Receptor Localizes to Plasma Membrane by Binding to Caveolin-1 in Mouse Sertoli Cells. *Int J Endocrinol* (2017) 2017:3985916. doi: 10.1155/2017/3985916
43. Cheng J, Watkins SC, Walker WH. Testosterone Activates Mitogen-Activated Protein Kinase *via* Src Kinase and the Epidermal Growth Factor Receptor in Sertoli Cells. *Endocrinology* (2007) 148(5):2066–74. doi: 10.1210/en.2006-1465
44. Deng Q, Zhang Z, Wu Y, Yu W-y, Zhang J, Jiang Z-M, et al. Non-Genomic Action of Androgens is Mediated by Rapid Phosphorylation and Regulation of Androgen Receptor Trafficking. *Cell Physiol Biochem* (2017) 43(1):223–36. doi: 10.1159/000480343
45. Toocheck C, Clister T, Shupe J, Crum C, Ravindranathan P, Lee TK, et al. Mouse Spermatogenesis Requires Classical and Nonclassical Testosterone Signaling. *Biol Reprod* (2016) 94(1):11. doi: 10.1095/biolreprod.115.132068
46. Lieberherr M, Grosse B. Androgens Increase Intracellular Calcium Concentration and Inositol 1,4,5-Trisphosphate and Diacylglycerol Formation *via* a Pertussis Toxin-Sensitive G-Protein. *J Biol Chem* (1994) 269(10):7217–23. doi: 10.1016/S0021-9258(17)37270-8
47. Von Ledebur EI, Almeida JP, Loss ES, Wassermann GF. Rapid Effect of Testosterone on Rat Sertoli Cell Membrane Potential. Relationship With K+ATP Channels. *Horm Metab Res = Hormon- und Stoffwechselforschung = Horm Metabol* (2002) 34(10):550–5. doi: 10.1055/s-2002-35426
48. Loss ES, Jacobsen M, Costa ZS, Jacobus AP, Borelli F, Wassermann GF. Testosterone Modulates K(+)ATP Channels in Sertoli Cell Membrane *via* the PLC-PIP2 Pathway. *Horm Metab Res = Hormon- und Stoffwechselforschung = Horm Metabol* (2004) 36(8):519–25. doi: 10.1055/s-2004-825753
49. Bulldan A, Dietze R, Shihan M, Scheiner-Bobis G. Non-Classical Testosterone Signaling Mediated Through ZIP9 Stimulates Claudin Expression and Tight Junction Formation in Sertoli Cells. *Cell Signal* (2016) 28(8):1075–85. doi: 10.1016/j.cellsig.2016.04.015
50. Lucas TF, Nascimento AR, Pisolato R, Pimenta MT, Lazari MF, Porto CS. Receptors and Signaling Pathways Involved in Proliferation and Differentiation of Sertoli Cells. *Spermatogenesis* (2014) 4:e28138. doi: 10.4161/spmg.28138
51. Sharpe RM, McKinnell C, Kivlin C, Fisher JS. Proliferation and Functional Maturation of Sertoli Cells, and Their Relevance to Disorders of Testis Function in Adulthood. *Reproduction* (2003) 125(6):769–84. doi: 10.1530/rep.0.1250769
52. Legacki E, Conley AJ, Nitta-Oda BJ, Berger T. Porcine Sertoli Cell Proliferation After Androgen Receptor Inactivation. *Biol Reprod* (2015) 92 (4):93. doi: 10.1095/biolreprod.114.125716
53. Rojas-Garcia PP, Recabarren MP, Sir-Petermann T, Rey R, Palma S, Carrasco A, et al. Altered Testicular Development as a Consequence of Increase Number of Sertoli Cell in Male Lambs Exposed Prenatally to Excess Testosterone. *Endocrine* (2013) 43(3):705–13. doi: 10.1007/s12020-012-9818-5
54. O'Shaughnessy PJ, Monteiro A, Abel M. Testicular Development in Mice Lacking Receptors for Follicle Stimulating Hormone and Androgen. *PloS One* (2012) 7(4):e35136. doi: 10.1371/journal.pone.0035136
55. Tan KA, Turner KJ, Saunders PT, Verhoeven G, De Gendt K, Atanassova N, et al. Androgen Regulation of Stage-Dependent Cyclin D2 Expression in Sertoli Cells Suggests a Role in Modulating Androgen Action on Spermatogenesis. *Biol Reprod* (2005) 72(5):1151–60. doi: 10.1095/biolreprod.104.037689
56. Johnston H, Baker PJ, Abel M, Charlton HM, Jackson G, Fleming L, et al. Regulation of Sertoli Cell Number and Activity by Follicle-Stimulating Hormone and Androgen During Postnatal Development in the Mouse. *Endocrinology* (2004) 145(1):318–29. doi: 10.1210/en.2003-1055
57. Hu S, Liu D, Liu S, Li C, Guo J. Lycium Barbarum Polysaccharide Ameliorates Heat-Stress-Induced Impairment of Primary Sertoli Cells and the Blood-Testis Barrier in Rat *via* Androgen Receptor and Akt Phosphorylation. *Evid Based Complement Alternat Med* (2021) 2021:5574202. doi: 10.1155/2021/5574202
58. Edelsztein NY, Rey RA. Importance of the Androgen Receptor Signaling in Gene Transactivation and Transrepression for Pubertal Maturation of the Testis. *Cells* (2019) 8(8):861. doi: 10.3390/cells8080861
59. Shah W, Khan R, Shah B, Khan A, Dil S, Liu W, et al. The Molecular Mechanism of Sex Hormones on Sertoli Cell Development and Proliferation. *Front Endocrinol (Lausanne)* (2021) 12:648141. doi: 10.3389/fendo.2021.648141
60. Martins AD, Alves MG, Simões VL, Dias TR, Rato L, Moreira PI, et al. Control of Sertoli Cell Metabolism by Sex Steroid Hormones Is Mediated Through Modulation in Glycolysis-Related Transporters and Enzymes. *Cell Tissue Res* (2013) 354(3):861–8. doi: 10.1007/s00441-013-1722-7
61. Berger T. Testicular Estradiol and the Pattern of Sertoli Cell Proliferation in Prepuberal Bulls. *Theriogenology* (2019) 136:60–5. doi: 10.1016/j.theriogenology.2019.06.031
62. Krzanowska H, Bilińska B. Number of Chromocentres in the Nuclei of Mouse Sertoli Cells in Relation to the Strain and Age of Males From Puberty to Senescence. *J Reprod Fertil* (2000) 118(2):343–50. doi: 10.1530/jrf.0.1180343

63. Shan LX, Bardin CW, Hardy MP. Immunohistochemical Analysis of Androgen Effects on Androgen Receptor Expression in Developing Leydig and Sertoli Cells. *Endocrinology* (1997) 138(3):1259–66. doi: 10.1210/endo.138.3.4973
64. Josso N, Rey RA. What Does AMH Tell Us in Pediatric Disorders of Sex Development? *Front Endocrinol (Lausanne)* (2020) 11:619. doi: 10.3389/fendo.2020.00619
65. da Rosa LA, Escott GM, Simonetti RB, da Silva JCD, Werlang ICR, Goldani MZ, et al. Role of Non-Classical Effects of Testosterone and Epitestosterone on AMH Balance and Testicular Development Parameters. *Mol Cell Endocrinol* (2020) 511:110850. doi: 10.1016/j.mce.2020.110850
66. Lasala C, Schteingart HF, Arouche N, Bedecarrás P, Grinspon RP, Picard JY, et al. SOX9 and SF1 are Involved in Cyclic AMP-Mediated Upregulation of Anti-Mullerian Gene Expression in the Testicular Prepubertal Sertoli Cell Line SMAT1. *Am J Physiol Endocrinol Metab* (2011) 301(3):E539–47. doi: 10.1152/ajpendo.00187.2011
67. Edelsztein NY, Racine C, di Clemente N, Schteingart HF, Rey RA. Androgens Downregulate Anti-Mullerian Hormone Promoter Activity in the Sertoli Cell Through the Androgen Receptor and Intact Steroidogenic Factor 1 Sites. *Biol Reprod* (2018) 99(6):1303–12. doi: 10.1093/biolre/ioy152
68. Lan KC, Chen YT, Chang C, Chang YC, Lin HJ, Huang KE, et al. Up-Regulation of SOX9 in Sertoli Cells From Testiculopathic Patients Accounts for Increasing Anti-Mullerian Hormone Expression *Via Impaired Androgen Receptor Signaling*. *PloS One* (2013) 8(10):e76303. doi: 10.1371/journal.pone.0076303
69. Wang G, Weng CC, Shao SH, Zhou W, de Gendt K, Braun RE, et al. Androgen Receptor in Sertoli Cells Is Not Required for Testosterone-Induced Suppression of Spermatogenesis, But Contributes to Sertoli Cell Organization in Utp14b Jsd Mice. *J Androl* (2009) 30(3):338–48. doi: 10.2164/jandrol.108.006890
70. Willems A, Batlouni SR, Esnal A, Swinnen JV, Saunders PT, Sharpe RM, et al. Selective Ablation of the Androgen Receptor in Mouse Sertoli Cells Affects Sertoli Cell Maturation, Barrier Formation and Cytoskeletal Development. *PloS One* (2010) 5(11):e14168. doi: 10.1371/journal.pone.0014168
71. Chojnacka K, Brehm R, Weider K, Hejmej A, Lydka M, Kopera-Sobota I, et al. Expression of the Androgen Receptor in the Testis of Mice With a Sertoli Cell Specific Knock-Out of the Connexin 43 Gene (SCCx43KO(-/-)). *Reprod Biol* (2012) 12(4):341–6. doi: 10.1016/j.repbio.2012.10.007
72. De Gendt K, Denolet E, Willems A, Daniels VW, Clinckemalie L, Denayer S, et al. Expression of Tubb3, a Beta-Tubulin Isotype, Is Regulated by Androgens in Mouse and Rat Sertoli Cells. *Biol Reprod* (2011) 85(5):934–45. doi: 10.1095/biolreprod.110.090704
73. Hazra R, Corcoran L, Robson M, McTavish KJ, Upton D, Handelsman DJ, et al. Temporal Role of Sertoli Cell Androgen Receptor Expression in Spermatogenic Development. *Mol Endocrinol* (2013) 27(1):12–24. doi: 10.1210/me.2012-1219
74. Hazra R, Upton D, Desai R, Noori O, Jimenez M, Handelsman DJ, et al. Elevated Expression of the Sertoli Cell Androgen Receptor Disrupts Male Fertility. *Am J Physiol Endocrinol Metab* (2016) 311(2):E396–404. doi: 10.1152/ajpendo.00159.2016
75. Itman C, Wong C, Hunyadi B, Ernst M, Jans DA, Loveland KL. Smad3 Dosage Determines Androgen Responsiveness and Sets the Pace of Postnatal Testis Development. *Endocrinology* (2011) 152(5):2076–89. doi: 10.1210/en.2010-1453
76. Yang X, Feng Y, Li Y, Chen D, Xia X, Li J, et al. AR Regulates Porcine Immature Sertoli Cell Growth *via* Binding to RNF4 and miR-124a. *Reprod Domest Anim* (2021) 56(3):416–26. doi: 10.1111/rda.13877
77. Ma C, Song H, Yu L, Guan K, Hu P, Li Y, et al. miR-762 Promotes Porcine Immature Sertoli Cell Growth *via* the Ring Finger Protein 4 (RNF4) Gene. *Sci Rep* (2016) 6:32783. doi: 10.1038/srep32783
78. Li C, Yang B, Pan P, Ma Q, Wu Y, Zhang Z, et al. MicroRNA-130a Inhibits Spermatogenesis by Directly Targeting Androgen Receptor in Mouse Sertoli Cells. *Mol Reprod Dev* (2018) 85(10):768–77. doi: 10.1002/mrd.23058
79. Yao C, Sun M, Yuan Q, Niu M, Chen Z, Hou J, et al. MiRNA-133b Promotes the Proliferation of Human Sertoli Cells Through Targeting GLI3. *Oncotarget* (2016) 7(3):2201–19. doi: 10.18632/oncotarget.6876
80. Hu P, Guan K, Feng Y, Ma C, Song H, Li Y, et al. miR-638 Inhibits Immature Sertoli Cell Growth by Indirectly Inactivating PI3K/AKT Pathway *via* SPAG1 Gene. *Cell Cycle* (2017) 16(23):2290–300. doi: 10.1080/15384101.2017.1380130
81. Raut S, Kumar AV, Deshpande S, Khambata K, Balasinor NH. Sex Hormones Regulate Lipid Metabolism in Adult Sertoli Cells: A Genome-Wide Study of Estrogen and Androgen Receptor Binding Sites. *J Steroid Biochem Mol Biol* (2021) 211:105898. doi: 10.1016/j.jsbmb.2021.105898
82. Mou L, Zhang Q, Wang Y, Zhang Q, Sun L, Li C, et al. Identification of Ube2b as a Novel Target of Androgen Receptor in Mouse Sertoli Cells. *Biol Reprod* (2013) 89(2):32. doi: 10.1095/biolreprod.112.103648
83. Matzkin ME, Pellizzari EH, Rossi SP, Calandra RS, Cigorraga SB, Frungieri MB. Exploring the Cyclooxygenase 2 (COX2)/15d-Δ(12,14)PGJ(2) System in Hamster Sertoli Cells: Regulation by FSH/testosterone and Relevance to Glucose Uptake. *Gen Comp Endocrinol* (2012) 179(2):254–64. doi: 10.1016/j.ygcen.2012.08.020
84. Tanaka T, Kanatsu-Shinohara M, Lei Z, Rao CV, Shinohara T. The Luteinizing Hormone-Testosterone Pathway Regulates Mouse Spermatogonial Stem Cell Self-Renewal by Suppressing WNT5A Expression in Sertoli Cells. *Stem Cell Rep* (2016) 7(2):279–91. doi: 10.1016/j.stemcr.2016.07.005
85. Crespo D, Lemos MS, Zhang YT, Safian D, Norberg B, Bogerd J, et al. PGE2 Inhibits Spermatogonia Differentiation in Zebrafish: Interaction With Fsh and an Androgen. *J Endocrinol* (2020) 244(1):163–75. doi: 10.1530/JOE-19-0309
86. Costoya JA, Hobbs RM, Barna M, Cattoretti G, Manova K, Sukhwani M, et al. Essential Role of Plzf in Maintenance of Spermatogonial Stem Cells. *Nat Genet* (2004) 36(6):653–9. doi: 10.1038/ng1367
87. Hermann BP, Sukhwani M, Lin CC, Sheng Y, Tomko J, Rodriguez M, et al. Characterization, Cryopreservation, and Ablation of Spermatogonial Stem Cells in Adult Rhesus Macaques. *Stem Cells* (2007) 25(9):2330–8. doi: 10.1634/stemcells.2007-0143
88. Wang J, Li J, Xu W, Xia Q, Gu Y, Song W, et al. Androgen Promotes Differentiation of PLZF(+) Spermatogonia Pool *via* Indirect Regulatory Pattern. *Cell Commun Signal* (2019) 17(1):57. doi: 10.1186/s12964-019-0369-8
89. Nobrega RH, Morais RD, Crespo D, de Waal PP, de Franca LR, Schulz RW, et al. Fsh Stimulates Spermatogonial Proliferation and Differentiation in Zebrafish *via* Igf3. *Endocrinology* (2015) 156(10):3804–17. doi: 10.1210/en.2015-1157
90. Maiti S, Meistrich ML, Wilson G, Shetty G, Marcelli M, McPhaul MJ, et al. Irradiation Selectively Inhibits Expression From the Androgen-Dependent Pem Homeobox Gene Promoter in Sertoli Cells. *Endocrinology* (2001) 142(4):1567–77. doi: 10.1210/endo.142.4.8076
91. Mayerhofer A. Peritubular Cells of the Human Testis: Prostaglandin E(2) and More. *Andrology* (2020) 8(4):898–902. doi: 10.1111/andr.12669
92. Zaker H, Razi M, Mahmoudian A, Soltanalinejad F. Boosting Effect of Testosterone on GDNF Expression in Sertoli Cell Line (TM4); Comparison Between TM3 Cells-Produced and Exogenous Testosterone. *Gene* (2022) 812:146112. doi: 10.1016/j.gene.2021.146112
93. Ma H, Cooke HJ, Shi Q. Meiosis: Recent Progress and New Opportunities. *J Genet Genom* (2014) 41(3):83–5. doi: 10.1016/j.jgg.2014.01.004
94. Chen SR, Hao XX, Zhang Y, Deng SL, Wang ZP, Wang YQ, et al. Androgen Receptor in Sertoli Cells Regulates DNA Double-Strand Break Repair and Chromosomal Synapsis of Spermatocytes Partially Through Intercellular EGF-EGFR Signaling. *Oncotarget* (2016) 7(14):18722–35. doi: 10.18632/oncotarget.7916
95. O'Shaughnessy PJ. Hormonal Control of Germ Cell Development and Spermatogenesis. *Semin Cell Dev Biol* (2014) 29:55–65. doi: 10.1016/j.semcdb.2014.02.010
96. De Gendt K, Swinnen JV, Saunders PT, Schoonjans L, Dewerchin M, Devos A, et al. A Sertoli Cell-Selective Knockout of the Androgen Receptor Causes Spermatogenic Arrest in Meiosis. *Proc Natl Acad Sci USA* (2004) 101(5):1327–32. doi: 10.1073/pnas.0308114100
97. Su L, Mruk DD, Lee WM, Cheng CY. Differential Effects of Testosterone and TGF-Beta3 on Endocytic Vesicle-Mediated Protein Trafficking Events at the Blood-Testis Barrier. *Exp Cell Res* (2010) 316(17):2945–60. doi: 10.1016/j.yexcr.2010.07.018
98. Larose H, Kent T, Ma Q, Shami AN, Harerimana N, Li JZ, et al. Regulation of Meiotic Progression by Sertoli-Cell Androgen Signaling. *Mol Biol Cell* (2020) 31(25):2841–62. doi: 10.1091/mbc.E20-05-0334

99. Stanton PG, Sluka P, Foo CF, Stephens AN, Smith AI, McLachlan RI, et al. Proteomic Changes in Rat Spermatogenesis in Response to *In Vivo* Androgen Manipulation; Impact on Meiotic Cells. *PloS One* (2012) 7(7): e41718. doi: 10.1371/journal.pone.0041718
100. Yang L, Wang Y, Zhang Q, Lai Y, Li C, Zhang Q, et al. Identification of Hsf1 as a Novel Androgen Receptor-Regulated Gene in Mouse Sertoli Cells. *Mol Reprod Dev* (2014) 81(6):514–23. doi: 10.1002/mrd.22318
101. Hu Z, Shanker S, MacLean JA2nd, Ackerman SL, Wilkinson MF. The RHOX5 Homeodomain Protein Mediates Transcriptional Repression of the Netrin-1 Receptor Gene Unc5c. *J Biol Chem* (2008) 283(7):3866–76. doi: 10.1074/jbc.M706717200
102. Lindsey JS, Wilkinson MF. Pem: A Testosterone- and LH-Regulated Homeobox Gene Expressed in Mouse Sertoli Cells and Epididymis. *Dev Biol* (1996) 179(2):471–84. doi: 10.1006/dbio.1996.0276
103. Bhardwaj A, Sohni A, Lou CH, De Gendt K, Zhang F, Kim E, et al. Concordant Androgen-Regulated Expression of Divergent Rhox5 Promoters in Sertoli Cells. *Endocrinology* (2022) 163(1):1–17. doi: 10.1210/endocr/bqab237
104. Câmara ML, Almeida TB, de Santi F, Rodrigues BM, Cerri PS, Beltrame FL, et al. Fluoxetine-Induced Androgenic Failure Impairs the Seminiferous Tubules Integrity and Increases Ubiquitin Carboxyl-Terminal Hydrolase L1 (UCHL1): Possible Androgenic Control of UCHL1 in Germ Cell Death? *Biomed Pharmacother = Biomed Pharmacother* (2019) 109:1126–39. doi: 10.1016/j.biopha.2018.10.034
105. Elliott MR, Zheng S, Park D, Woodson RI, Reardon MA, Juncadella IJ, et al. Unexpected Requirement for ELMO1 in Clearance of Apoptotic Germ Cells *In Vivo*. *Nature* (2010) 467(7313):333–7. doi: 10.1038/nature09356
106. Wu RC, Jiang M, Beaudet AL, Wu MY. ARID4A and ARID4B Regulate Male Fertility, a Functional Link to the AR and RB Pathways. *Proc Natl Acad Sci USA* (2013) 110(12):4616–21. doi: 10.1073/pnas.1218318110
107. Wu RC, Zeng Y, Pan IW, Wu MY. Androgen Receptor Coactivator ARID4B Is Required for the Function of Sertoli Cells in Spermatogenesis. *Mol Endocrinol* (2015) 29(9):1334–46. doi: 10.1210/me.2015-1089
108. Domanskyi A, Zhang FP, Nurmio M, Palvimo JJ, Toppari J, Janne OA. Expression and Localization of Androgen Receptor-Interacting Protein-4 in the Testis. *Am J Physiol Endocrinol Metab* (2007) 292(2):E513–22. doi: 10.1152/ajpendo.00287.2006
109. Vija L, Meduri G, Comperat E, Vasiliu V, Izard V, Ferlicot S, et al. Expression and Characterization of Androgen Receptor Coregulators, SRC-2 and HBO1, During Human Testis Ontogenesis and in Androgen Signaling Deficient Patients. *Mol Cell Endocrinol* (2013) 375(1-2):140–8. doi: 10.1016/j.mce.2013.05.004
110. Tan JA, Hall SH, Petrusz P, French FS. Thyroid Receptor Activator Molecule, TRAM-1, Is an Androgen Receptor Coactivator. *Endocrinology* (2000) 141 (9):3440–50. doi: 10.1210/endo.141.9.7680
111. Kuwahara S, Ikei A, Taguchi Y, Tabuchi Y, Fujimoto N, Obinata M, et al. PSPC1, NONO, and SFPQ Are Expressed in Mouse Sertoli Cells and may Function as Coregulators of Androgen Receptor-Mediated Transcription. *Biol Reprod* (2006) 75(3):352–9. doi: 10.1095/biolreprod.106.051136
112. Kumar A, Dumasia K, Deshpande S, Balasinor NH. Direct Regulation of Genes Involved in Sperm Release by Estrogen and Androgen Through Their Receptors and Coregulators. *J Steroid Biochem Mol Biol* (2017) 171:66–74. doi: 10.1016/j.jsbmb.2017.02.017
113. Terada K, Yomogida K, Imai T, Kiyonari H, Takeda N, Kadomatsu T, et al. A Type I DnaJ Homolog, DjA1, Regulates Androgen Receptor Signaling and Spermatogenesis. *EMBO J* (2005) 24(3):611–22. doi: 10.1038/sj.emboj.7600549
114. Guillermet-Guibert J, Smith LB, Halet G, Whitehead MA, Pearce W, Rebourcet D, et al. Novel Role for P110beta PI 3-Kinase in Male Fertility Through Regulation of Androgen Receptor Activity in Sertoli Cells. *PloS Genet* (2015) 11(7):e1005304. doi: 10.1371/journal.pgen.1005304
115. Furu K, Klungland A. Tzfp Represses the Androgen Receptor in Mouse Testis. *PloS One* (2013) 8(4):e62314. doi: 10.1371/journal.pone.0062314
116. Zhang L, Charron M, Wright WW, Chatterjee B, Song CS, Roy AK, et al. Nuclear factor-kappaB Activates Transcription of the Androgen Receptor Gene in Sertoli Cells Isolated From Testes of Adult Rats. *Endocrinology* (2004) 145(2):781–9. doi: 10.1210/en.2003-0987
117. Zhao Z, Qiao L, Dai Z, He Q, Lan X, Huang S, et al. LncNONO-AS Regulates AR Expression by Mediating NONO. *Theriogenology* (2020) 145:198–206. doi: 10.1016/j.theriogenology.2019.10.025
118. Gonzalez-Herrera IG, Prado-Lourenco L, Pileur F, Conte C, Morin A, Cabon F, et al. Testosterone Regulates FGF-2 Expression During Testis Maturation by an IRES-Dependent Translational Mechanism. *FASEB J* (2006) 20 (3):476–8. doi: 10.1096/fj.04-3314fje
119. Geng Q, Ni LW, Ouyang B, Hu YH, Zhao Y, Guo J. Alanine and Arginine Rich Domain Containing Protein, Aard, Is Directly Regulated by Androgen Receptor in Mouse Sertoli Cells. *Mol Med Rep* (2017) 15(1):352–8. doi: 10.3892/mmr.2016.6028
120. El Chami N, Ikhlef F, Kaszas K, Yakoub S, Tabone E, Siddeek B, et al. Androgen-Dependent Apoptosis in Male Germ Cells is Regulated Through the Proto-Oncoprotein Cbl. *J Cell Biol* (2005) 171(4):651–61. doi: 10.1083/jcb.200507076
121. Sun R, Liang H, Guo H, Wang Z, Deng Q. PMCA4 Gene Expression is Regulated by the Androgen Receptor in the Mouse Testis During Spermatogenesis. *Mol Med Rep* (2021) 23(2):152. doi: 10.3892/mmr.2020.11791
122. Silva EJ, Patrao MT, Tsuruta JK, O'Rand MG, Avellar MC. Epididymal Protease Inhibitor (EPPIN) is Differentially Expressed in the Male Rat Reproductive Tract and Immunolocalized in Maturing Spermatozoa. *Mol Reprod Dev* (2012) 79(12):832–42. doi: 10.1002/mrd.22119
123. Eacker SM, Shima JE, Connolly CM, Sharma M, Holdcraft RW, Griswold MD, et al. Transcriptional Profiling of Androgen Receptor (AR) Mutants Suggests Instructive and Permissive Roles of AR Signaling in Germ Cell Development. *Mol Endocrinol* (2007) 21(4):895–907. doi: 10.1210/me.2006-0113
124. Yan HH, Mruk DD, Lee WM, Cheng CY. Blood-Testis Barrier Dynamics are Regulated by Testosterone and Cytokines *via* Their Differential Effects on the Kinetics of Protein Endocytosis and Recycling in Sertoli Cells. *FASEB J* (2008) 22(6):1945–59. doi: 10.1096/fj.06-070342
125. Meng J, Greenlee AR, Taub CJ, Braun RE. Sertoli Cell-Specific Deletion of the Androgen Receptor Compromises Testicular Immune Privilege in Mice. *Biol Reprod* (2011) 85(2):254–60. doi: 10.1095/biolreprod.110.090621
126. Li MW, Xia W, Mruk DD, Wang CQ, Yan HH, Siu MK, et al. Tumor Necrosis Factor {Alpha} Reversibly Disrupts the Blood-Testis Barrier and Impairs Sertoli-Germ Cell Adhesion in the Seminiferous Epithelium of Adult Rat Testes. *J Endocrinol* (2006) 190(2):313–29. doi: 10.1677/joe.1.06781
127. Meng J, Holdcraft RW, Shima JE, Griswold MD, Braun RE. Androgens Regulate the Permeability of the Blood-Testis Barrier. *Proc Natl Acad Sci USA* (2005) 102(46):16696–700. doi: 10.1073/pnas.0506084102
128. Kaitu'u-Lino TJ, Sluka P, Foo CF, Stanton PG. Claudin-11 Expression and Localisation is Regulated by Androgens in Rat Sertoli Cells *In Vitro*. *Reproduction* (2007) 133(6):1169–79. doi: 10.1530/REP-06-0385
129. Chakraborty P, William Buaas F, Sharma M, Smith BE, Greenlee AR, Eacker SM, et al. Androgen-Dependent Sertoli Cell Tight Junction Remodeling is Mediated by Multiple Tight Junction Components. *Mol Endocrinol* (2014) 28 (7):1055–72. doi: 10.1210/me.2013-1134
130. Denolet E, De Gendt K, Allemeersch J, Engelen K, Marchal K, Van Hummelen P, et al. The Effect of a Sertoli Cell-Selective Knockout of the Androgen Receptor on Testicular Gene Expression in Prepubertal Mice. *Mol Endocrinol* (2006) 20(2):321–34. doi: 10.1210/me.2005-0113
131. Wang RS, Yeh S, Chen LM, Lin HY, Zhang C, Ni J, et al. Androgen Receptor in Sertoli Cell is Essential for Germ Cell Nursery and Junctional Complex Formation in Mouse Testes. *Endocrinology* (2006) 147(12):5624–33. doi: 10.1210/en.2006-0138
132. Traweger A, Fuchs R, Krizbai IA, Weiger TM, Bauer HC, Bauer H. The Tight Junction Protein ZO-2 Localizes to the Nucleus and Interacts With the Heterogeneous Nuclear Ribonucleoprotein Scaffold Attachment Factor-B. *J Biol Chem* (2003) 278(4):2692–700. doi: 10.1074/jbc.M206821200
133. Guo J, Shi YQ, Yang W, Li YC, Hu ZY, Liu YX. Testosterone Upregulation of Tissue Type Plasminogen Activator Expression in Sertoli Cells: tPA Expression in Sertoli Cells. *Endocrine* (2007) 32(1):83–9. doi: 10.1007/s12020-007-9014-1
134. Gunnarsson M, Lecander I, Abrahamsson PA. Factors of the Plasminogen Activator System in Human Testis, as Demonstrated by *in-Situ*

Hybridization and Immunohistochemistry. *Mol Hum Reprod* (1999) 5 (10):934–40. doi: 10.1093/molehr/5.10.934
135. Dietze R, Shihan M, Stammler A, Konrad L, Scheiner-Bobis G. Cardiotonic Steroid Ouabain Stimulates Expression of Blood-Testis Barrier Proteins Claudin-1 and -11 and Formation of Tight Junctions in Sertoli Cells. *Mol Cell Endocrinol* (2015) 405:1–13. doi: 10.1016/j.mce.2015.02.004
136. Papadopoulos D, Dietze R, Shihan M, Kirch U, Scheiner-Bobis G. Dehydroepiandrosterone Sulfate Stimulates Expression of Blood-Testis-Barrier Proteins Claudin-3 and -5 and Tight Junction Formation *via* a Gnalpha11-Coupled Receptor in Sertoli Cells. *PloS One* (2016) 11(3): e0150143. doi: 10.1371/journal.pone.0150143
137. Li XX, Chen SR, Shen B, Yang JL, Ji SY, Wen Q, et al. The Heat-Induced Reversible Change in the Blood-Testis Barrier (BTB) Is Regulated by the Androgen Receptor (AR) *via* the Partitioning-Defective Protein (Par) Polarity Complex in the Mouse. *Biol Reprod* (2013) 89(1):12. doi: 10.1095/biolreprod.113.109405
138. Kopera I, Durlej M, Hejmej A, Knapczyk-Stwora K, Duda M, Slomczynska M, et al. Differential Expression of Connexin 43 in Adult Pig Testes During Normal Spermatogenic Cycle and After Flutamide Treatment. *Reprod Domest Anim* (2011) 46(6):1050–60. doi: 10.1111/j.1439-0531.2011.01783.x
139. Xia Q, Zhang D, Wang J, Zhang X, Song W, Chen R, et al. Androgen Indirectly Regulates Gap Junction Component Connexin 43 Through Wilms Tumor-1 in Sertoli Cells. *Stem Cells Dev* (2020) 29(3):169–76. doi: 10.1089/scd.2019.0166
140. Rajamanickam GD, Kastelic JP, Thundathil JC. The Ubiquitous Isoform of Na/K-ATPase (ATP1A1) Regulates Junctional Proteins, Connexin 43 and Claudin 11 *via* Src-EGFR-ERK1/2-CREB Pathway in Rat Sertoli Cells. *Biol Reprod* (2017) 96(2):456–68. doi: 10.1095/biolreprod.116.141267
141. McCabe MJ, Allan CM, Foo CF, Nicholls PK, McTavish KJ, Stanton PG. Androgen Initiates Sertoli Cell Tight Junction Formation in the Hypogonadal (Hpg) Mouse. *Biol Reprod* (2012) 87(2):38. doi: 10.1095/biolreprod.111.094318
142. Mruk DD, Cheng CY. The Mammalian Blood-Testis Barrier: Its Biology and Regulation. *Endocr Rev* (2015) 36(5):564–91. doi: 10.1210/er.2014-1101
143. Bruewer M, Utech M, Ivanov AI, Hopkins AM, Parkos CA, Nusrat A. Interferon-Gamma Induces Internalization of Epithelial Tight Junction Proteins *via* a Macropinocytosis-Like Process. *FASEB J* (2005) 19(8):923–33. doi: 10.1096/fj.04-3260com
144. Shen L, Turner JR. Actin Depolymerization Disrupts Tight Junctions *via* Caveolae-Mediated Endocytosis. *Mol Biol Cell* (2005) 16(9):3919–36. doi: 10.1091/mbc.e04-12-1089
145. Su L, Mruk DD, Lee WM, Cheng CY. Differential Effects of Testosterone and TGF-β3 on Endocytic Vesicle-Mediated Protein Trafficking Events at the Blood-Testis Barrier. *Exp Cell Res* (2010) 316(17):2945–60. doi: 10.1016/j.yexcr.2010.07.018
146. Yin L, Lu L, Lin X, Wang X. Crucial Role of Androgen Receptor in Resistance and Endurance Trainings-Induced Muscle Hypertrophy Through IGF-1/IGF-1r- PI3K/Akt- mTOR Pathway. *Nutr Metab (Lond)* (2020) 17:26. doi: 10.1186/s12986-020-00446-y
147. Wei Y, Zhou Y, Long C, Wu H, Hong Y, Fu Y, et al. Polystyrene Microplastics Disrupt the Blood-Testis Barrier Integrity Through ROS-Mediated Imbalance of Mtorc1 and Mtorc2. *Environ Pollut* (2021) 289:117904. doi: 10.1016/j.envpol.2021.117904
148. McLachlan RI, Wreford NG, O'Donnell L, de Kretser DM, Robertson DM. The Endocrine Regulation of Spermatogenesis: Independent Roles for Testosterone and FSH. *J Endocrinol* (1996) 148(1):1–9. doi: 10.1677/joe.0.1480001
149. Beardsley A, O'Donnell L. Characterization of Normal Spermiation and Spermiation Failure Induced by Hormone Suppression in Adult Rats. *Biol Reprod* (2003) 68(4):1299–307. doi: 10.1095/biolreprod.102.009811
150. Holdcraft RW, Braun RE. Androgen Receptor Function is Required in Sertoli Cells for the Terminal Differentiation of Haploid Spermatids. *Development* (2004) 131(2):459–67. doi: 10.1242/dev.00957
151. Walker WH. Non-Classical Actions of Testosterone and Spermatogenesis. *Philos Trans R Soc Lond B Biol Sci* (2010) 365(1546):1557–69. doi: 10.1098/rstb.2009.0258
152. Shupe J, Cheng J, Puri P, Kostereva N, Walker WH. Regulation of Sertoli-Germ Cell Adhesion and Sperm Release by FSH and Nonclassical Testosterone Signaling. *Mol Endocrinol* (2011) 25(2):238–52. doi: 10.1210/me.2010-0030
153. Zhang J, Wong CH, Xia W, Mruk DD, Lee NP, Lee WM, et al. Regulation of Sertoli-Germ Cell Adherens Junction Dynamics *via* Changes in Protein-Protein Interactions of the N-Cadherin-Beta-Catenin Protein Complex Which are Possibly Mediated by C-Src and Myotubularin-Related Protein 2: An *In Vivo* Study Using an Androgen Suppression Model. *Endocrinology* (2005) 146(3):1268–84. doi: 10.1210/en.2004-1194
154. Dufau ML, Kavarthapu R. Gonadotropin Regulation Testicular RNA Helicase, Two Decades of Studies on Its Structure Function and Regulation From Its Discovery Opens a Window for Development of a Non-Hormonal Oral Male Contraceptive. *Front Endocrinol (Lausanne)* (2019) 10:576. doi: 10.3389/fendo.2019.00576
155. Tang PZ, Tsai-Morris CH, Dufau ML. A Novel Gonadotropin-Regulated Testicular RNA Helicase. A New Member of the Dead-Box Family. *J Biol Chem* (1999) 274(53):37932–40. doi: 10.1074/jbc.274.53.37932
156. Sheng Y, Tsai-Morris CH, Gutti R, Maeda Y, Dufau ML. Gonadotropin-Regulated Testicular RNA Helicase (GRTH/Ddx25) is a Transport Protein Involved in Gene-Specific mRNA Export and Protein Translation During Spermatogenesis. *J Biol Chem* (2006) 281(46):35048–56. doi: 10.1074/jbc.M605086200
157. Villar J, Tsai-Morris CH, Dai L, Dufau ML. Androgen-Induced Activation of Gonadotropin-Regulated Testicular RNA Helicase (GRTH/Ddx25) Transcription: Essential Role of a Nonclassical Androgen Response Element Half-Site. *Mol Cell Biol* (2012) 32(8):1566–80. doi: 10.1128/mcb.06002-11
158. Kavarthapu R, Dufau ML. Germ Cell Nuclear Factor (GCNF/RTR) Regulates Transcription of Gonadotropin-Regulated Testicular RNA Helicase (GRTH/DDX25) in Testicular Germ Cells–The Androgen Connection. *Mol Endocrinol* (2015) 29(12):1792–804. doi: 10.1210/me.2015-1198
159. Yang TA, Yang YH, Song XC, Liu LL, Yang YF, Xing XM, et al. Comparative Studies on Testis, Epididymis and Serum Hormone Concentrations in Foxes, and Hybrids During the Pre-Breeding Period. *Anim Reprod Sci* (2019) 203:61–7. doi: 10.1016/j.anireprosci.2019.02.008
160. Ando K, Tomimura K, Sazdovitch V, Suain V, Yilmaz Z, Authelet M, et al. Level of PICALM, a Key Component of Clathrin-Mediated Endocytosis, is Correlated With Levels of Phosphotau and Autophagy-Related Proteins and Is Associated With Tau Inclusions in AD, PSP and Pick Disease. *Neurobiol Dis* (2016) 94:32–43. doi: 10.1016/j.nbd.2016.05.017
161. Russell LD, Clermont Y. Degeneration of Germ Cells in Normal, Hypophysectomized and Hormone Treated Hypophysectomized Rats. *Anatomical Rec* (1977) 187(3):347–66. doi: 10.1002/ar.1091870307
162. O'Donnell L, McLachlan RI, Wreford NG, de Kretser DM, Robertson DM. Testosterone Withdrawal Promotes Stage-Specific Detachment of Round Spermatids From the Rat Seminiferous Epithelium. *Biol Reprod* (1996) 55 (4):895–901. doi: 10.1095/biolreprod55.4.895
163. Lee NP, Cheng CY. Protein Kinases and Adherens Junction Dynamics in the Seminiferous Epithelium of the Rat Testis. *J Cell Physiol* (2005) 202(2):344–60. doi: 10.1002/jcp.20119
164. Chapin RE, Wine RN, Harris MW, Borchers CH, Haseman JK. Structure and Control of a Cell-Cell Adhesion Complex Associated With Spermiation in Rat Seminiferous Epithelium. *J Androl* (2001) 22(6):1030–52. doi: 10.1002/j.1939-4640.2001.tb03444.x
165. Olli KE, Li K, Galileo DS, Martin-DeLeon PA. Plasma Membrane Calcium ATPase 4 (PMCA4) Co-Ordinates Calcium and Nitric Oxide Signaling in Regulating Murine Sperm Functional Activity. *J Cell Physiol* (2018) 233 (1):11–22. doi: 10.1002/jcp.25882
166. Agarwal A, Mulgund A, Hamada A, Chyatte MR. A Unique View on Male Infertility Around the Globe. *Reprod Biol Endocrinol* (2015) 13:37. doi: 10.1186/s12958-015-0032-1
167. Hajder M, Hajder E, Husic A. The Effects of Total Motile Sperm Count on Spontaneous Pregnancy Rate and Pregnancy After IUI Treatment in Couples With Male Factor and Unexplained Infertility. *Med Arch* (2016) 70(1):39–43. doi: 10.5455/medarh.2016.70.39-43
168. Hornig NC, Holterhus PM. Molecular Basis of Androgen Insensitivity Syndromes. *Mol Cell Endocrinol* (2021) 523:111146. doi: 10.1016/j.mce.2020.111146
169. Witchel SF. Disorders of Sex Development. *Best Pract Res Clin Obstet Gynaecol* (2018) 48:90–102. doi: 10.1016/j.bpobgyn.2017.11.005

170. Veyssiere G, Berger M, Jean-Faucher C, de Turckheim M, Jean C. Testosterone and Dihydrotestosterone in Sexual Ducts and Genital Tubercle of Rabbit Fetuses During Sexual Organogenesis: Effects of Fetal Decapitation. *J Steroid Biochem* (1982) 17(2):149–54. doi: 10.1016/0022-4731(82)90114-5
171. Adachi M, Takayanagi R, Tomura A, Imasaki K, Kato S, Goto K, et al. Androgen-Insensitivity Syndrome as a Possible Coactivator Disease. *N Engl J Med* (2000) 343(12):856–62. doi: 10.1056/nejm200009213431205
172. Oakes MB, Eyvazzadeh AD, Quint E, Smith YR. Complete Androgen Insensitivity Syndrome–a Review. *J Pediatr Adolesc Gynecol* (2008) 21 (6):305–10. doi: 10.1016/j.jpag.2007.09.006
173. Hellmann P, Christiansen P, Johannsen TH, Main KM, Duno M, Juul A. Male Patients With Partial Androgen Insensitivity Syndrome: A Longitudinal Follow-Up of Growth, Reproductive Hormones and the Development of Gynaecomastia. *Arch Dis Child* (2012) 97(5):403–9. doi: 10.1136/archdischild-2011-300584
174. Hage M, Drui D, Francou B, Mercier S, Guiochon-Mantel A, Belaisch-Allart J, et al. Structural Analysis of the Impact of a Novel Androgen Receptor Gene Mutation in Two Adult Patients With Mild Androgen Insensitivity Syndrome. *Andrologia* (2021) 53(1):e13865. doi: 10.1111/and.13865
175. Gulia C, Baldassarra S, Zangari A, Briganti V, Gigli S, Gaffi M, et al. Androgen Insensitivity Syndrome. *Eur Rev Med Pharmacol Sci* (2018) 22 (12):3873–87. doi: 10.26355/eurrev_201806_15272
176. Deeb A, Mason C, Lee YS, Hughes IA. Correlation Between Genotype, Phenotype and Sex of Rearing in 111 Patients With Partial Androgen Insensitivity Syndrome. *Clin Endocrinol* (2005) 63(1):56–62. doi: 10.1111/j.1365-2265.2005.02298.x
177. Gottlieb B, Lehvaslaiho H, Beitel LK, Lumbroso R, Pinsky L, Trifiro M. The Androgen Receptor Gene Mutations Database. *Nucleic Acids Res* (1998) 26 (1):234–8. doi: 10.1093/nar/26.1.234
178. Bukhari I, Li G, Wang L, Iqbal F, Zhang H, Zhu J, et al. Effects of Androgen Receptor Mutation on Testicular Histopathology of Patient Having Complete Androgen Insensitivity. *J Mol Histol* (2017) 48(3):159–67. doi: 10.1007/s10735-017-9714-7
179. Cortes D, Clasen-Linde E, Hutson JM, Li R, Thorup J. The Sertoli Cell Hormones Inhibin-B and Anti Mullerian Hormone Have Different Patterns of Secretion in Prepubertal Cryptorchid Boys. *J Pediatr Surg* (2016) 51 (3):475–80. doi: 10.1016/j.jpedsurg.2015.08.059
180. Schweikert HU, Milewich L, Wilson JD. Aromatization of Androstenedione by Cultured Human Fibroblasts. *J Clin Endocrinol Metab* (1976) 43(4):785–95. doi: 10.1210/jcem-43-4-785
181. Appari M, Werner R, Wunsch L, Cario G, Demeter J, Hiort O, et al. Apolipoprotein D (APOD) Is a Putative Biomarker of Androgen Receptor Function in Androgen Insensitivity Syndrome. *J Mol Med (Berl)* (2009) 87 (6):623–32. doi: 10.1007/s00109-009-0462-3
182. Holterhus PM, Deppe U, Werner R, Richter-Unruh A, Bebermeier JH, Wunsch L, et al. Intrinsic Androgen-Dependent Gene Expression Patterns Revealed by Comparison of Genital Fibroblasts From Normal Males and Individuals With Complete and Partial Androgen Insensitivity Syndrome. *BMC Genomics* (2007) 8:376. doi: 10.1186/1471-2164-8-376
183. Shah R, Woolley MM, Costin G. Testicular Feminization: The Androgen Insensitivity Syndrome. *J Pediatr Surg* (1992) 27(6):757–60. doi: 10.1016/s0022-3468(05)80110-1
184. Dahiya S, Singh M, Mandal S, Jain SL, Rathore A, Lal P. Androgen Insensitivity Syndrome: Can Cytology Help? *Cytopathology* (2021) 33 (2);249–52. doi: 10.1111/cyt.13064
185. Hannema SE, Scott IS, Rajpert-De Meyts E, Skakkebaek NE, Coleman N, Hughes IA. Testicular Development in the Complete Androgen Insensitivity Syndrome. *J Pathol* (2006) 208(4):518–27. doi: 10.1002/path.1890
186. Looijenga LH, Hersmus R, Oosterhuis JW, Cools M, Drop SL, Wolffenbuttel KP. Tumor Risk in Disorders of Sex Development (DSD). *Best Pract Res Clin Endocrinol Metab* (2007) 21(3):480–95. doi: 10.1016/j.beem.2007.05.001
187. Hughes IA, Davies JD, Bunch TI, Pasterski V, Mastroyannopoulou K, MacDougall J. Androgen Insensitivity Syndrome. *Lancet* (2012) 380 (9851):1419–28. doi: 10.1016/s0140-6736(12)60071-3
188. Walker WH, Easton E, Moreci RS, Toocheck C, Anamthathmakula P, Jeyasuria P. Restoration of Spermatogenesis and Male Fertility Using an Androgen Receptor Transgene. *PloS One* (2015) 10(3):e0120783. doi: 10.1371/journal.pone.0120783

Conflict of Interest: The authors declare that the research was conducted in the absence of any commercial or financial relationships that could be construed as a potential conflict of interest.

Publisher's Note: All claims expressed in this article are solely those of the authors and do not necessarily represent those of their affiliated organizations, or those of the publisher, the editors and the reviewers. Any product that may be evaluated in this article, or claim that may be made by its manufacturer, is not guaranteed or endorsed by the publisher.

Copyright © 2022 Wang, Li and Yang. This is an open-access article distributed under the terms of the Creative Commons Attribution License (CC BY). The use, distribution or reproduction in other forums is permitted, provided the original author(s) and the copyright owner(s) are credited and that the original publication in this journal is cited, in accordance with accepted academic practice. No use, distribution or reproduction is permitted which does not comply with these terms.

GLOSSARY

11-KT	11-ketotestosterone
Aard	alanine and arginine rich domain
AIS	Androgen insensitive syndrome
AMH	Anti Mullerian hormone
APOD	apolipoprotein D
ARE	Androgen response element
ARID4A/AB	AT-rich interaction domain 4A/4B
ARIP4	androgen receptor-interacting protein 4
AR	androgen receptor
ARKO	Androgen receptor knock out
BTB	Blood-testis barrier
Btc	betacellulin
CAIS	Complete androgen insensitive syndrome
Cbl	calcineurin B-like protein
CK18	Cytokeratin 18
CRE	cAMP-response element
CREB	cAMP-response element-binding protein
Cx43	connexin 43
DHT	Dihydrotestosterone
DjA1	type 1 DnaJ protein
DSBs	DNA double strand breaks
Eea1	early endosome antigen 1
EGFR	Epidermal growth factor receptor
Elmo1	engulfment and cell motility 1
ES	Ectoplasmic specialization
FAK	Focal adhesion kinase
FGF2	Fibroblast growth factor 2
GATA-2	GATA binding protein 2
GC	Germ cell
GCNF	Germ cell nuclear factor
GDNF	Glial-derived neurotrophic factor
GJ	gap junction
GPI	Glycosylphosphatidylinositol
GRTH/DDX25	Gonadotropin Regulated Testicular Helicase
hpg	hypogonadal
Igf3	Insulin like growth factor 3
Hsf1	Heat shock transcription factor1
lncNONO-AS	target NONO lncRNA
MAIS	Mild androgen insensitive syndrome
NASP	nuclear autoantigenic sperm protein
NCoR1	nuclear receptor corepressor 1
Nrg1	neuregulin 1
NONO	non-POU domain-containing octamer-binding protein
p^{90RSK}	ribosomal protein S6 kinase A1
PAIS	Partial androgen insensitive syndrome
PGE2	prostaglandin E2
PI3K	phosphatidylinositol 3 kinase
Picalm	phosphatidylinositol binding clathrin assembly protein
Plzf	Promyelocytic leukemia zinc finger
PMCA4	ATPase Ca^{++} transporting plasma membrane 4
PSPC-1	paraspeckle component 1
Rhox5	Reproductive homeobox 5 gene
RNF4	really interesting new gene (RING) finger protein 4
SC	Sertoli cell
SCARKO	Sertoli cell androgen receptor knock out
SF1	steroidogenic factor 1
SFPQ	splicing factor proline/glutamine rich
SOX9	sex determining region Y-box 9
Spinlw1	Epididymal protease inhibitor
Src	SRC proto-oncogene
Src1	steroid receptor coactivator-1
SSC	Spermatogonia stem cell
Stx5a	syntaxin 5
T	testosterone
TE	testosterone and oestradiol
Tfm	testicular feminized mouse
tPA	type plasminogen activator
TJ	tight junction
TRAM-1	thyroid hormone receptor activator molecule-1
TUBB3	Class III βtubulin
Tzfp	testis zinc finger protein
Ube2b	ubiquitin-conjugating enzyme E2B
UCHC1	ubiquitincarboxyl-terminal hydrolase L1
UNC5C	Unc-5 Netrin Receptor C(UNC5C)
Wnt5a	Wingless-type MMTV Integration Site Family Member 5A
Wt1	WT1 transcription factor
ZIP9	Zrt- and Irt-like protein 9.

frontiers in Endocrinology

REVIEW
published: 28 February 2022
doi: 10.3389/fendo.2022.827724

Estrogen Receptor Function: Impact on the Human Endometrium

Kun Yu[1‡], *Zheng-Yuan Huang*[2‡], *Xue-Ling Xu*[1‡], *Jun Li*[3*], *Xiang-Wei Fu*[1*†] *and Shou-Long Deng*[4*†]

[1] National Engineering Laboratory for Animal Breeding, Key Laboratory of Animal Genetics, Breeding and Reproduction, Beijing Key Laboratory for Animal Genetic Improvement, College of Animal Science and Technology, China Agricultural University, Beijing, China, [2] Chelsea and Westminster Hospital, Department of Metabolism, Digestion and Reproduction, Imperial College London, London, United Kingdom, [3] Department of Reproductive Medicine, The First Hospital of Hebei Medical University, Shijiazhuang, China, [4] National Health Commission of China (NHC) Key Laboratory of Human Disease Comparative Medicine, Institute of Laboratory Animal Sciences, Chinese Academy of Medical Sciences and Comparative Medicine Center, Peking Union Medical College, Beijing, China

The physiological role of estrogen in the female endometrium is well established. On the basis of responses to steroid hormones (progesterone, androgen, and estrogen), the endometrium is considered to have proliferative and secretory phases. Estrogen can act in the endometrium by interacting with estrogen receptors (ERs) to induce mucosal proliferation during the proliferative phase and progesterone receptor (PR) synthesis, which prepare the endometrium for the secretory phase. Mouse knockout studies have shown that ER expression, including ERα, ERβ, and G-protein-coupled estrogen receptor (GPER) in the endometrium is critical for normal menstrual cycles and subsequent pregnancy. Incorrect expression of ERs can produce many diseases that can cause endometriosis, endometrial hyperplasia (EH), and endometrial cancer (EC), which affect numerous women of reproductive age. ERα promotes uterine cell proliferation and is strongly associated with an increased risk of EC, while ERβ has the opposite effects on ERα function. GPER is highly expressed in abnormal EH, but its expression in EC patients is paradoxical. Effective treatments for endometrium-related diseases depend on understanding the physiological function of ERs; however, much less is known about the signaling pathways through which ERs functions in the normal endometrium or in endometrial diseases. Given the important roles of ERs in the endometrium, we reviewed the published literature to elaborate the regulatory role of estrogen and its nuclear and membrane-associated receptors in maintaining the function of endometrium and to provide references for protecting female reproduction. Additionally, the role of drugs such as tamoxifen, raloxifene, fulvestrant and G-15 in the endometrium are also described. Future studies should focus on evaluating new therapeutic strategies that precisely target specific ERs and their related growth factor signaling pathways.

Keywords: endometrium, estrogen receptor α, estrogen receptor β, G-protein-coupled estrogen receptor, human

OPEN ACCESS

Edited by:
Shi Qinghua,
University of Science and Technology of China, China

Reviewed by:
Xin Du,
The 901th Hospital of the Joint Logistics Support Force of PLA, China
Manan Khan,
Hazara University, Pakistan

***Correspondence:**
Xiang-Wei Fu
fuxiangwei@cau.edu.cn
Shou-Long Deng
dengshoulong@cnilas.org
Jun Li
lijun8203@163.com

†ORCID:
Xiang-Wei Fu
orcid.org/0000-0003-1638-6852
Shou-Long Deng
orcid.org/0000-0003-1187-3037

‡*These authors have contributed equally to this work*

Specialty section:
This article was submitted to Reproduction, a section of the journal Frontiers in Endocrinology

Received: *02 December 2021*
Accepted: *01 February 2022*
Published: *28 February 2022*

Citation:
Yu K, Huang Z-Y, Xu X-L, Li J, Fu X-W and Deng S-L (2022) Estrogen Receptor Function: Impact on the Human Endometrium. Front. Endocrinol. 13:827724. doi: 10.3389/fendo.2022.827724

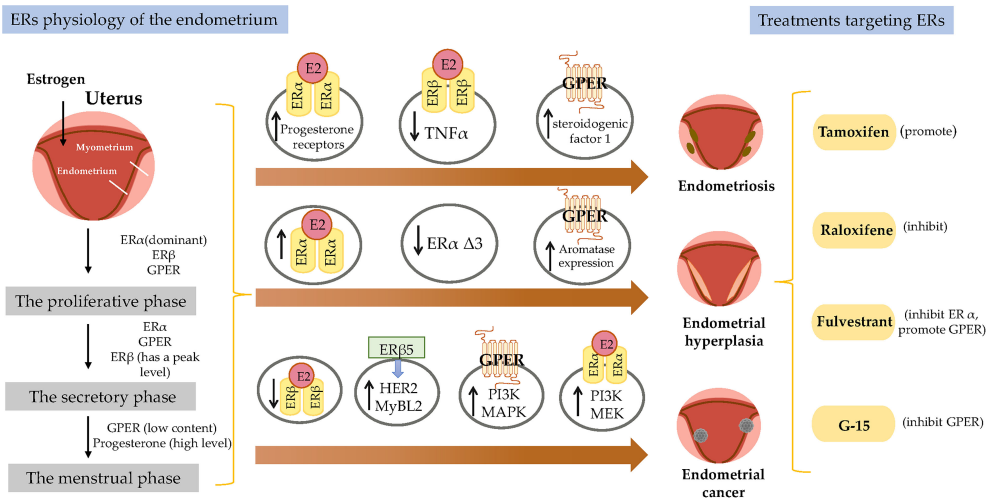

GRAPHICAL ABSTRACT |

INTRODUCTION

The endometrium is the primary target tissue for estrogen. The main function of the endometrium is to prepare for implantation and to maintain the pregnancy after embryo implantation. Estrogen exerts a critical influence on female reproduction *via* the two main classical estrogen receptors (ERs), ERα and ERβ, and perhaps through G-protein-coupled estrogen receptor (GPER; formerly GPR30) (1). Recent descriptions of the phenotypes of ER-knockout mice have also revealed key roles of estrogen signaling in the endometrium. Estrogen acts through ERs that are associated with the onset and maintenance of disease and tumor events, particularly in uterine tissue. This review focuses on recent advances in our knowledge of the role of ERs in the endometrium, animal models of ER deficiency in the uterus, and how ERs are involved in endometrial diseases and pharmacological treatments.

ER ACTIVATION

ERα and ERβ are members of the nuclear receptor (NR) superfamily and consist of five domains (A/B, DNA-binding; D, ligand-binding; and F) (**Figure 1**). The structurally distinct amino-terminal A/B domains share 17% amino-acid identity between the ERs, acting as ligand-independent activation function 1 (AF-1); AF-1 is involved in both inter-molecular and intra-molecular interactions as well as in activating gene transcription (2). The near-identical central C region (97% amino-acid identity) is the DNA-binding domain that allows ERs to dimerize. Acting as a flexible hinge, the D domain (36% amino-acid identity) contains a nuclear localization signal, is important for receptor dimerization and binding to chaperone heat-shock proteins and links the C domain to the multifunctional carboxyl-terminal (E) domain. The E domain, also known as the ligand-binding domain (LBD), shares 56% amino-acid identity between the ERs and is a globular region that comprises an 17β-estradiol (E2)-binding site, a dimerization interface (homo- and heterodimerization), and ligand-dependent coregulator interaction activity (activation function 2, AF-2); the LBD works synergistically with the amino-terminal domain to regulate gene transcription (3–6). The F domain shares 18% amino-acid identity between the ERs and is located at the extreme carboxyl-terminus of the receptors. In ERα, the F domain appears to modulate transcriptional activity, co-activator interactions, dimerization, and stability; however, its role in ERβ is unclear (7–9).

The uterus reacts to cyclical changes in estrogen and progesterone levels to prepare the embryo for implantation. Most known estrogen effects are mediated by ERα and ERβ, which regulate classical hormone signaling pathways (10). Both ERα and ERβ are expressed in the murine uterus (11). ER dimers bind to estrogen response elements (EREs) in the promoter regions of target genes, initiating the recruitment of co-activators, co-suppressors, and chromatin remodeling factors to activate or inhibit transcription of target genes. Despite the presence of similarities in initiation and termination, the ERE-dependent signaling pathway substantially differs between ERα and ERβ in terms of the mode and extent of transcription, presumably because their distinct amino-termini influence the magnitude of transcriptional responses (6, 12, 13). The amino-terminal A/B domains of ERα include the ligand-independent AF-1, while the LBD includes the ligand-dependent AF-2. Both AF-1 and AF-2 of ERα are necessary for uterine physiology because their functional integration is required to mediate transcription at full capacity in response to E2 in a tissue-specific manner (14, 15). In contrast, ERβ displays a lower affinity for ERE binding and considerably lower transcriptional activity in the E2-induced ERE-dependent genomic signaling pathway; moreover, it interacts with a different set of proteins,

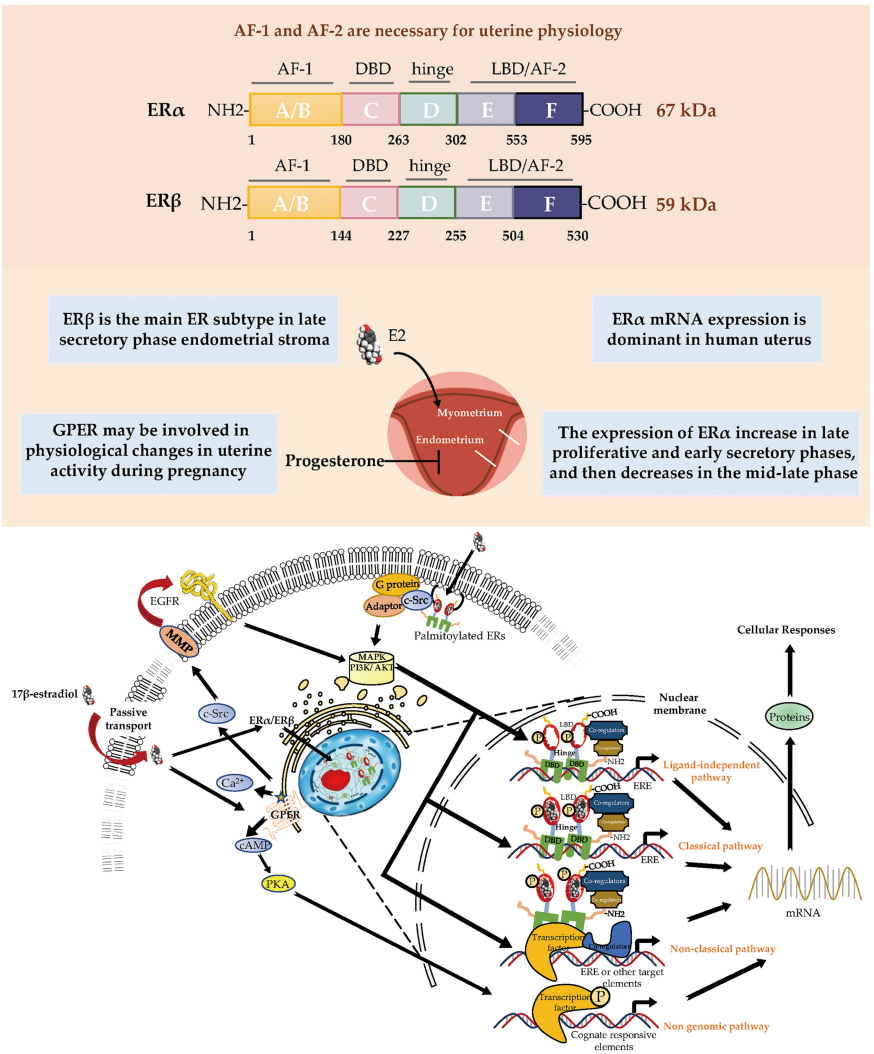

FIGURE 1 | Estrogen receptor-mediated signaling pathways in the endometrial. E2 promotes endometrial growth, while progesterone and other progesterone hormones block endometrial growth and promote differentiation. E2 mediates its biological response by binding to ERs *via* genomic and non-genomic pathways. There are 3 main mechanisms of genomic regulation. Firstly, in genomic regulation, E2 ligands passively enter the cells by diffusion. ERα and ERβ are located in the cytosol. The binding of E2 to the ER promotes the formation of dimers, enters the nucleus and is directly binding to EREs, or to transcription factors which regulate transcription of its target genes. Secondly, the nonclassical pathway involves binding the E2-bound ER to TFs that are already bound to the DNA. The third mechanism is hormone-independent. The ER can regulate E2 responses by activating the signaling of growth factors *via* the phosphorylation of different serine (118/167) residues on the receptor. In non-genomic regulation, binding of E2 to ERs and GPR30 at the plasma membrane leads to various nongenomic responses, such as calcium signaling, PKC, and cAMP/PKA pathways. E2, 17β-estradiol; ER, estrogen receptor; GPER, G-protein-coupled estrogen receptor; EGFR, epidermal growth factor receptor; PKA, protein kinase A; SF-1, steroidogenic factor 1; TNFα, tumor necrosis factor α; PR, progesterone receptor; MAPK, mitogen-activated protein kinases; PI3K, phosphoinositide-3-kinase. ERE, estrogen response element.

presumably because of the absence of AF-1 in its amino-terminus (6, 16). The N-terminal domain of ERβ is much shorter than the corresponding domain of ERα. Moreover, the amino-terminus of ERβ has been proven to impair receptor-ERE interactions and does not interact with the carboxyl-terminus (17, 18).

In the nonclassical pathway of estrogen action, ER can regulate genes that lack a canonical ERE. ER can activate or suppress gene expression by interacting with other transcription factors, such as activator protein-1 (AP-1), specificity protein-1 (SP-1), nuclear factor kappa-B (NF-κB) (19, 20). Jun and Fos are members of the AP-1 transcription factor family that can form Jun-Jun or Jun-Fos dimers; their basic regions can interact with a consensus sequence known as the TPA response element (21). Selective estrogen receptor modulators (SERMs) and selective estrogen receptor downregulators (SERDs) can activate the transcriptional responses mediated by ERα at TPA response element sites, while they cannot activate transcriptional responses mediated by ERβ (22–24). Another transcription factor, SP-1, binds to a consensus sequence known as the GC

box element. ERα has been shown to tether to GC box response element-bound SP-1, for which the amino-terminus of ERα is critical (25). In addition, in ligand-independent genomic events, ER activates growth factor signaling by phosphorylating different serine (118/167) residues on the receptor, thereby regulating the E2 response.

Beginning in the 1990s, there was increasing evidence that rapid modulation (within seconds or minutes) of estrogen-mediated signaling pathways occurs *via* a subpopulation of ERs located in or adjacent to the plasma membrane; these non-genomic effects induced by E2 were determined by the observation that exposure of uterine or ovarian cells to E2 could rapidly induce ion influx, cyclic adenosine monophosphate (cAMP) production, and phosphoinositide-3-kinase (PI3K) activation (26–30). In the 2000s, membrane ERs were characterized; these primarily consisted of GPR30/GPER, ER-X, and the Gq membrane ER (31–33).

Among all membrane ERs, GPER has been recognized as the major mediator of the rapid cellular effects of E2 because stimulating GPER activates metalloproteinases and induces the release of heparin-binding epidermal growth factor, which binds and activates epidermal growth factor receptor (EGFR); this interaction leads to the activation of downstream signaling molecules such as extracellular signal-regulated kinase 1/2 (ERK1/2), followed by the production of cyclic cAMP, intracellular calcium mobilization, and PI3K activation (34–37). Additionally, GPER indirectly regulates transcriptional activity through signaling mechanisms that involve cAMP, ERK, and PI3K (38) (**Figure 1**).

Regarding targeted therapies for GPER, the first GPER-selective agonist G-1 was identified in 2006. Subsequently, a GPER-selective antagonist G-15 was identified in 2009, followed in 2011 by G-36, a more selective GPER antagonist than G-15 (39, 40). Fulvestrant is a SERD that causes degradation or downregulation of ER, but acts as a GPER agonist (41).

TRANSCRIPTIONAL CONTROL BY ERS

E2 activity is mediated by the two classical nuclear hormone receptors, ERα and ERβ. Transcriptional regulation arises from the direct interaction of the ER with components of cellular transcriptional machinery. Cells can express a set of coregulators that can enhance or decrease the transcriptional activity of steroid hormone receptors, called ER coactivators and corepressors, respectively. Coregulators are crucial for ER transcriptional activity and have led us to recognize that there is a great deal of sophistication in transcriptional regulation. ER is able to bind to cofactors through the AF-1 and AF-2 domains, acting synergistically in the recruitment of coregulators. Coregulators are both targets and propagators of posttranslational modification codes and are involved in many steps of the gene expression process, including chromatin modification and remodeling, transcription initiation, elongation of RNA chains, mRNA splicing, mRNA translation, miRNA processing, and degradation of the activated NR coregulator complexes (42).

Approximately 200 coactivators play a central role in NR-mediated promotion of gene expression and are associated with cancer and other diseases. Many additional ERα coregulators have been found, although little is known about Erβ (43). Investigation of coregulators of ERs began in the 1990s and the first identified ERα coregulator was called steroid receptor co-activator (SRC-1). Co-expression of SRC-1 reverses the ability of ER to inhibit human progesterone receptor (PR) activation (44). Coregulators of ERα include the SRC/p160 group, histone acetyltransferase cAMP response element binding protein (CREB)/p300, ATP-dependent chromatin remodeling complexes such as SWI/SNF, E3 ubiquitin protein ligases, and steroid RNA activator (45). Then transcriptional corepressors have the NR corepressor and thyroid hormone receptors (46, 47). Therefore, nuclear ERs play a variety of roles and functions in different cells and tissues that are mediated by various intermediaries and differential utilization of coregulators (48).

From studies of cancer cells, we have learned that a large number of coregulators have specific structural motifs that affect their contact with the ER ligand binding domain. The ER crystal structure suggests that helix 12 lays across the ligand binding pocket when binding agonists, resulting in a surface suitable for the binding of LXXLL motifs found on coregulators. Conversely, we know that co-inhibitory factors block ER-mediated gene transcription by directly interacting with unbound ERs, using their corepressor NR box or by competing with coactivators (49). It has also been reported that some post-translational modifications, such as phosphorylation, methylation, ubiquitination, SUMOylation and acetylation, can affect the action of coregulatory factors that target gene expression (50, 51).

THE ROLE OF ERS IN ENDOMETRIAL PHYSIOLOGY

The dynamic expression pattern of steroid hormones and their receptors in the endometrium during the menstrual cycle has been established and drive cyclical growth, shedding, and regeneration of the endometrium. During the follicular phase of the menstrual cycle, estrogen, working through ERs, induces growth of the endometrium, producing a measurable thickening of the mucosa (52). After ovulation, the corpus luteum continues to produce a large amount of estrogen ligand in addition to progesterone. The presence of progesterone inhibits estrogen-induced endometrial growth and transforms the endometrium into a receptive state for blastocyst implantation (1). Physiologically, progesterone plays an important role in preventing endometrial hyperplasia (EH) (53). In animal models, high levels of estrogen without progesterone interference can lead to EH or cancer, suggesting that the balance between estrogens and progestogens is often dominated by estrogens during cancer formation (54, 55) (**Figure 1**).

During postnatal development, the uterus undergoes a unique pattern of changes in ER expression. ERα is weak and the proliferative activity is high from postnatal days 1 to 7 in the uterine stroma. In contrast, the cell proliferation rate is decreased

TABLE 1 | ER expression by uterine phase.

Tissue	Specific location	Period	Method	Results	References
ERα	The proliferative phase	The stroma and epithelial cells lining the glands	Real-time PCR; Immunocytochemistry	ERα mRNA was higher in the proliferative than in the secretory and menstrual phases	(59, 62, 63)
	The secretory phase	In the glands and stroma of the functionalis	Immunocytochemistry	ERα expression declined	(59)
	Days 7-27 of the normal cycle	Localized to perivascular smooth muscle Cells in nonpregnant endometrium	Monoclonal antibodies; immunocytochemistry	ERα was observed in muscle cells of uterine arteries	(59, 61)
ERβ	The proliferative phase	Predominantly in glandular epithelial cells	Using non-radioactive in-situ hybridization	ERβ mRNA concentrations were lower than ERα mRNA.	(64)
	The secretory phase	In nuclei of the glands and stroma	Real-time PCR; Immunocytochemistry	The mRNA expression of ERβ had a peak in the late secretory phase; ERβ declined much more in the glands than in the stroma	(59, 62)
	The proliferative and secretory phases of the menstrual cycle	In the endothelial cells	Immunohistochemistry	only ERβ was present in the endothelial cell population	(59)
GPER	The proliferative phase	In epithelium cells and stromal cells (epithelial cells are the main source of GPER mRNA)	Real-time PCR; Western blot; *In situ* hybridization;	High content (GPER predominantly localized in the mid- and late-proliferative phase)	(62)
	The secretory phase	In the stroma	Real-time PCR;	Low content (GPER dropped rapidly to low levels in the early secretory phase)	(62)
	The menstrual phase	In the stroma	Real-time PCR;	Low content	(62)
	In early pregnancy decidua phase	In glandular and luminal epithelium, and in the stroma	Real-time PCR; Western blot; Immunohistochemistry	Low content	(62)
	Myometrium	localized in the plasma membrane and in some areas colocalized with caveolae in myometrial smooth muscle cells	RT-PCR; Western blotting; Immunocytochemistry	concentrations of GPER mRNA and protein did not change across the not-in-labor to in-labor continuum	(65)

ER, estrogen receptor; GPER, G-protein-coupled estrogen receptor; RT-PCR, reverse transcription polymerase chain reaction.

from day 7 to puberty, but ERα expression in the epithelial and stroma cells is increased (56). The low rate of proliferation in the prepubertal period is due to estrogen levels being too low to activate ERα (57, 58). However, in the proliferative phase, ERα immunoreactivity is significantly stronger than ERβ immunoreactivity in the nuclei of epithelial, stromal, and muscle cells, suggesting ERα mRNA expression is dominant in the human uterus. Immunohistochemical localization revealed increased expression of ERα and ERβ in the late proliferative and early secretory phases, and then a decrease in the mid-late phase (59). ERβ is the main ER subtype expressed in the endometrial stroma in the late secretory phase (60). ERα and ERβ are differentially expressed in endometrial vascular endothelial cells and perivascular cells surrounding endometrial blood vessels. Monoclonal antibodies and immunocytochemistry have shown that ERα is localized to muscle cells of uterine arteries (61). Analysis of immunostaining confirmed that endometrial endothelial cells only express ERβ, which may be the target of selective agonists or antagonists for the ERβ subtype (59) (**Table 1**). It is notable that nonradioactive *in situ* hybridization confirmed that ERα and ERβ were localized in both epithelial and stromal cells of endometriotic tissues (66) (**Figure 1**).

The plasticity of the human endometrium is beyond other tissues, and it can still respond to steroid hormones and induce endometrial cycles after menopause. The post-menopausal endometrium has low circulating estrogen level and lacks progesterone, while androgen levels from adrenal glands are relatively unchanged. ERβ mRNA expression in the myometrium of postmenopausal women is significantly higher than in premenopausal women, while ERα expression is decreased (67). Thirty-one postmenopausal women underwent combined treatment with E2 and testosterone, which increased AR and ERβ expression in the endometrium (68). In contrast, levels of ERα and PRs in the endometrium were upregulated after estrogen-alone treatment (68). This study indicated that the antiproliferative effect of androgen treatment in the endometrium is associated with increased ERβ expression and that ERα may promote endometrial proliferation.

In humans, several studies have reported GPER mRNA and protein expression in the uterine epithelia (epithelial and stromal cells), endometrium, myometrium, and early pregnancy decidua (62, 65, 69). Real-time PCR and immunohistochemistry results showed that GPER mRNA was highly expressed in glandular epithelial cells in the mid- and late- proliferative phase, higher than during the secretory and menstrual phases. GPER expression levels were also found to decrease rapidly from the early secretory phase and remained low until the end of the cycle (62). In decidual tissue, GPER mRNA expression was localized in both the glandular and luminal epithelium and in the stroma (62). GPER activation enhanced contractile responses to oxytocin in the myometrium. These findings suggest that GPER may be involved in the physiological changes in human uterine activity during pregnancy (65). In general, several studies using cell and animal models have highlighted the importance of ER signaling in female reproduction. GPER is involved in cyclic alterations of endometrial estrogen action, and high GPER transcript levels were observed in the eutopic endometrium during the proliferative phase, whereas higher GPER mRNA expression has been shown during the secretory phase (70) (**Table 1**).

TABLE 2 | Summary of mouse models involving ERα and ERβ.

Organisms	Year	Type	Fertility	levels of E2	Notes	Reference
Mouse model	1995	ERαKO	NA	serum levels of E2 in the ERαKO female are more than 10-fold higher than those in the wild type	increased DNA synthesis, and transcription of the PR, lactoferrin, and glucose-6-phosphate dehydrogenase genes	(72)
	2000	$ERβ^{-/-}$ mice	poor reproductive capacity	NA	enlargement of the lumen; increase in volume and protein content of uterine secretion; induction of the luminal epithelial secretory protein	(74)
	2000	$ERβ^{-/-}$ mice	exhibit variable degrees of subfertility.	NA	reproductive tract normal	(75)
	2002; 2006	NERKI mice	the heterozygous NERKI females (AA/+) are described to be infertile;	steroid hormone levels are similar to wild-type females	have grossly enlarged uteri with cystic hyperplasia	(76, 77)
	2003	immature female mice were treated with ER subtype-selective agonist	NA	NA	inhibited PR and AR mRNA and protein expression	(78)
	2006	$ERβ^{-/-}$ mice	NA	NA	hyperproliferation and loss of differentiation in the uterine epithelium	(79)
	2009; 2014	EAAE mouse	infertility; females heterozygous for the EAAE ERα mutations are fertile	NA	the inability of E2 to induce uterine epithelial proliferation; has an ERα null–like phenotype; with impaired uterine growth and transcriptional activity; the hypoplastic uteri	(80, 81)
	2010	UtEpiαERKO	infertile	NA	the uterine epithelial E2-specific loss of response; increased uterine apoptosis	(82)
	2011	AF-2-mutated ERα knock-in (AF2ERKI)	infertile	high serum E2 levels	have hypoplastic uterine tissue and rudimentary mammary glands similar to ERαKO mice	(15)
	2013	mice lacking ERαAF-1 ($ERαAF\text{-}1^{0}$)	NA	NA	ERαAF-1 is required for E2-induced uterine epithelial cell proliferation	(83)

NA, not available or not assessed; ER, estrogen receptor; E2, estradiol; PR, progesterone receptor; AR, androgen receptor.

GPER is also found in the endometrium of women with endometriosis (71).

ROLES OF ERS IN THE ENDOMETRIUM

It is currently thought that E2-induced uterine epithelial cell proliferation is mediated by stromal ERα. ERα knockout mice showed no expression of estrogen responsive genes in the uterus, and the basic levels of PR mRNA in the αERKO uterus were equal to those in wild type mice (72). The levels of PR protein in the uterus of ERα knockout mice were at 60% of the level measured in a wild-type uterus, which is enough to induce the genomic responses mediated by progesterone but not enough to support embryo implantation (73). These observations suggest that ERα modulation of PR levels is not necessary for progesterone action in ERα knockout mouse uterus (**Table 2**).

ERs are dependent on AF-1 in the N-terminal domain and AF-2 in the C-terminal LBD to induce the specific conformational changes that are required for ER transcriptional activity (**Figure 1**). In the model of AF-2-mutated ERα knock-in (AF2ERKI), AF2ERKI homozygote female mice have hypoplastic uterine tissue and rudimentary mammary glands that are indistinguishable from ERα knockout mice (15). ERα AF-2 has been demonstrated to play a crucial role in the endometrial proliferative effect of E2. Furthermore, Abot et al. investigated the role of ERα AF-1 in the regulation of gene transcription and cell proliferation in the uterus. Targeted deletion of AF-1 in mice showed normal uterine development but delayed response to E2 (83). Nevertheless, in a study using the "EAAE" mouse, which has more severe DNA-binding domain mutations in ERα, uterine epithelial proliferation could not be induced through the estrogen signaling pathway, manifesting an ERα null-like phenotype with impaired uterine growth and transcriptional activity (80, 81) (**Table 2**). The ERα (EAAE/EAAE) mouse suggested that the DBD is necessary for estrogen action and the LBD is insufficient.

Nonclassical ERα knock-in (NERKI) mice with an ERα mutated at the DNA recognition helix that disrupts DNA binding but leaves nonclassical signaling intact have also been developed (**Table 2**). The uteri of NERKI mice are larger than those of ERα knockout mice but smaller than those of wild type mice. NERKI mice also have defective ovulation and underdeveloped mammary glands (76). The NERKI mice indicate that nonclassical ERα signaling plays a critical role in uterine growth and development, which is beneficial to restore the proliferation of luminal epithelial cells (77).

By establishing a uterine epithelial-specific ERα knockout (UtEpiαERKO) mouse line, it was found that while female UtEpiαERKO mice were infertile, they had regular estrous cycles and complete follicular development stages, indicating ovulation (82) (**Table 2**). Embryonic implantation was not observed in the uterus after natural mating or embryo transfer, suggesting that ERα in the uterine epithelium is necessary for embryo receptivity. E2 treatment to UtEpiαERKO mice

stimulated epithelial cell growth, but apoptosis in the epithelial cells significantly increased compared with wild type mice. These studies might help to determine how the proliferation of uterine epithelial is mediated by ERβ in the stroma, while uterine epithelial-derived ERα is required subsequent to proliferation to prevent epithelial apoptosis ensuring the full uterine epithelial response (82).

Despite ERα being the predominant ER in the adult rodent uterus, transcripts encoding ERβ have also been detected in wild type and ERα$^{-/-}$ murine uteri (11). The uteri of untreated ERβ$^{-/-}$ mice exhibit exaggerated responsiveness to E2, as indicated by enlargement of the lumen, increased volume and protein content of uterine secretions, and induction of the luminal epithelial secretory protein (74). The increased cell proliferation and exaggerated response to E2 in ERβ$^{-/-}$ mice suggest ERβ inhibits ERα function, resulting in an anti-proliferative function in the immature uterus. ERβ can act as a regulator of ERα-mediated gene transcription in the uterus, alternatively, it is responsible for downregulating PR in the luminal epithelium. Paradoxically, there is evidence that ERβ can partially compensate for loss of ERα in the reproductive tract, as the uterine phenotype of ERαβ double knockout mice is similar to the aggravated uterine phenotype of ERα knockout mice, whereas the reproductive tract of ERβ knockout mice appears normal (75) (**Table 2**). Meanwhile, the uterine epithelium of ERβ$^{-/-}$ mice showed hyperproliferation and loss of differentiation (79). This suggests that the absence of ERβ predisposes the uterus to abnormal endometrial proliferation. Fully mapping ERβ expression in the endometrium may be useful in identifying women at higher risk of EH.

A study examining the potential synergistic regulation of gene expression and uterine growth by the two receptors for estradiol, ERα and ERβ, using ER subtype-selective agonist ligands showed that the ERβ agonist diarylpropionitrile did not increase uterine weight or luminal epithelial cell proliferation, but inhibited PR and AR mRNA and protein expression (78) (**Table 2**). Additionally, ERβ can modulate ERα activity in a response-specific and dose-dependent manner (78).

The structure of GPER is dramatically different from that of ERα and ERβ. No obvious developmental or functional defects have been observed in the reproductive organs of GPER knockout mice (84–86). Treating wild-type mice with G-1 stimulates uterine epithelial proliferation despite a lower potency relative to that of E2; conversely, blocking GPER with G-15 reduces the E2-mediated proliferative response by approximately 50% (40). Stable knockdown of GPER substantially eliminated the tumor growth induced by autocrine motility factor (AMF) in EC, with significantly longer survival times in tumor-bearing mice (87). Conversely, Gao et al. demonstrated that in an ovariectomized mouse uterus, GPER activation by high-concentration G-1 altered the expression of E2-dependent uterine genes and mediated inhibition of ERK1/2 and phosphorylation of ERα (Ser118) in the stromal compartment; thus, they concluded that GPER is a negative regulator of ERα-dependent uterine growth in response to E2, suggesting an interaction between non-genomic and genomic ERs (69).

Estrogen plays a different role in embryo implantation and angiogenesis. This suggests that although studies in mouse models provide evidence for the role of ovarian steroid hormones in regulating uterine function, extrapolation of mouse endometrial estrogen findings to human conditions needs to be considered carefully. Despite their compelling results, many of the reviewed studies were limited by a lack of replication, small sample sizes, retrospective designs, publication bias, and/or the use of non-standardized tools to diagnose conditions.

THE ENDOMETRIUM AND ERS

Endometriosis

Endometriosis is the presence of endometrial cells outside the uterine cavity, which can invade local tissues and cause severe inflammation and adhesions. Approximately 15% of infertile women are reported to have endometriosis, although the true prevalence of endometriosis is unclear (88). Multiple cellular and molecular signaling pathways are likely to be involved in the pathogenesis of endometriosis.

Endometrial development and function are highly dependent on the cyclic secretion of sex steroid hormones and the expression of their cognate receptors (89). The endometrial cell types that are primarily targeted by steroid hormones include epithelial and stromal cells. Proliferation and differentiation of the endometrium are regulated by estrogens (90). Endometriosis typically involves higher levels of E2 than observed in a normal endometrium, which is due to higher gene expression levels of aromatase and 17β-hydroxysteroid dehydrogenase type 1 (91); the higher levels of E2 result in increased E2 binding and activation of ERs in endometriotic tissues, thereby stimulating estrogen-dependent growth. These higher levels of local E2 activity could contribute to the proliferation of endometriotic tissues (92). Estrogen-mediated changes in cell signaling presumably have important implications for the pathogenesis of endometriosis (93). For example, the invasion and migration of eutopic endometrial endometriosis stromal cells is regulated by the estrogen/H19/miR-216a-5p/ACTA2 axis (94). Alternatively, studies have implicated that tamoxifen and the phytoestrogen genistein can induce steroidogenic factor 1 (SF-1) target gene aromatase expression in a GPER-dependent manner to promote the proliferation of Ishikawa cells. Based on this finding, we hypothesized that GPRE/SF-1 may promote endometriosis by increasing local estrogen concentrations and mediating the proliferation of synthetic estrogens in combination with classical ER signaling (95) (**Figure 2**).

Estrogen activity is mediated *via* genomic pathways including nuclear ERα/β, as well as by more rapid, non-genomic pathways, such as ERα36 and GPER (96). Elevated estrogen promotes the expression of ERα and ERβ, which reach their highest levels in the late proliferation phase (97); however, aberrant levels of ERs are observed in women with endometriosis. Compared with endometrial tissue, ERβ mRNA and protein levels were more than 100-fold increased, while the levels of ERα were several times lower (98); inhibiting the enhanced ERβ activity *via* an

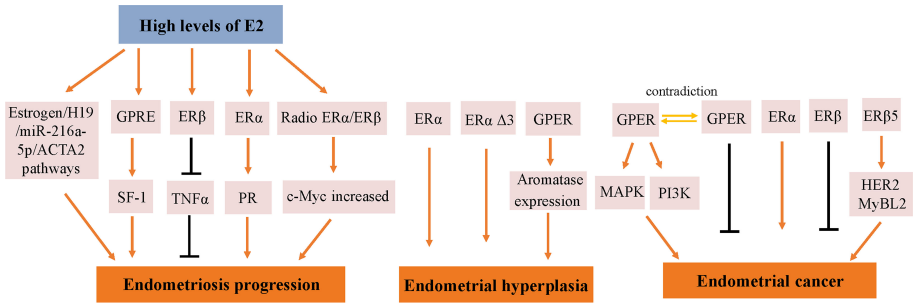

FIGURE 2 | Molecular pathways regulated by ER in endometrial diseases. E2, estradiol; ER, estrogen receptor; GPER, G-protein-coupled estrogen receptor; SF-1, steroidogenic factor 1; TNFα, tumor necrosis factor α; PR, progesterone receptor; MAPK, mitogen-activated protein kinases; PI3K, phosphoinositide-3-kinase.

ERβ-selective antagonist also suppressed the growth of ectopic lesions in mice (99). Notably, ERβ activity stimulates endometriotic progression: ERβ inhibits tumor necrosis factor α (TNFα)-induced apoptosis through interactions with apoptotic mechanisms to avoid endogenous immune surveillance of surviving cells (99). ERβ directly induces Ras-like estrogen-regulated growth inhibitor gene expression in an estrogen-dependent manner to enhance the proliferative activity of endometriotic tissues (100). The role of ERβ is presumably more complicated, because greatly elevated levels of ERβ are present in both the nucleus and cytoplasm of endometriotic tissues (101).

It remains controversial whether ERα exhibits an endometriotic tissue-specific pattern (102). Studies of ERα knockout mice with endometriosis have shown that ERα causes cell adhesion and proliferation and that it regulates inflammatory signaling in ectopic lesions (103). E2 increases the expression of PRs mainly through ERα activation, thereby mediating the effects of progesterone on the endometrium and triggering the secretory phase of endometrial circulation. Estrogen responsiveness is considerably complex, as indicated by the results obtained from experiments in mice and the findings in human tissues contain splice-form variants of ERα and ERβ. Moreover, the differential effects of estrogen on endometrial cells may depend on the total amount of cellular ERs and/or the ratio of ERα to ERβ (104).

EH

EH is a uterine pathology that involves a continuum of morphologic alterations that range from mild, reversible glandular hyperplasia to direct cancer precursors. Compared with the normal proliferative endometrium, the predominant characterization of EH is an increased endometrial gland-to-stroma ratio. During the reproductive period, the risk of EH is increased by conditions associated with intermittent or anovulation, such as Polycystic ovary syndrome. After menopause, when ovulation stops, EH is more common in women with increased circulating estrogen levels.

During the normal reproductive cycle, ERα expression in uterine epithelial cells is downregulated in the secretory phase. Hu et al. assessed the expression of ERα and ERβ in 114 patients using immunohistochemistry (105). The results indicated that from normal proliferation to simple and complex hyperplasia, the expression of ERα increased, while the expression of ERβ showed no significant change. Other studies have also revealed similar results. As early as 2003, Uchikawa et al. detected the expression levels of ERs in 20 normal endometrium samples, 36 hyperplastic endometrium samples, and 58 malignant endometrium samples, and found that ERα expression was increased in EHs compared with normal endometrium samples (106). In 2005, Bircan et al. described that ERα levels were significantly higher in EH than in the normal secretory endometrium (107).

However, different variants have different protein activities and different regulatory functions on ER signaling. ERα Δ3 lacks part of the DNA binding domain of exon 3 and inhibits estrogen-dependent transcription activation in a dominant negative way, which may potentially affect ERα signal transduction (108). The Δ3 variation is detected in prolactinoma, EH, and breast cancer, but not in the normal pituitary, normal endometrium, or endometrial cancer (EC) (109–111). For example, this variant was found in 19 of 21 EH cases, but not in any of 29 EC cases (110). Additionally, ERα Δ3 expression is reduced more than 30-fold in breast cancer compared with in the normal breast epithelium (112). It is speculated that the dominant negative activity of Δ3 may decrease normal estrogen signaling, and thus interfere with tumor progression and growth (**Figure 2**).

GPER is highly expressed in abnormal EH, and its expression trend follows that of ERα, which is gradually increased from the normal proliferative endometrium to simple EH, and then to a maximum in complex EH (**Figure 2**). This could imply that in normal and benign proliferation, GPER expression increases proportionally due to the induction of GPER by ERα (71, 113). Aromatase activity is not detected in the normal endometrium but is highly expressed in endometriosis and malignant endometrium cells (114, 115). Surprisingly, GPER activation increased aromatase expression in both endometriosis and malignant endometriosis cells (95). Thus, we speculate that the mechanism by which GPER regulates the growth of abnormal endometrial cells might be that it induces the expression of aromatase, increasing the synthesis of intracellular estrogen. In turn, estrogen activates intracellular

GPER by the intracellular pathway, further increasing the abnormal proliferation rate of cells.

EC

EC is an estrogen-dependent malignancy. The administration of estrogen alone for an extended period can increase the risk of EC in postmenopausal women. Some endometrial atypical hyperplasias can evolve into EC over a long period of time. EC is subdivided into two types on the basis of histopathology. Type I endometrial tumors, also known as low-grade endometrioid, which make up account for 75% of endometrial cases, are usually associated with high levels of ERα (116). Type II tumors include high-grade endometrioid tumors, serous tumors, clear cell tumors, carcinosarcomas, and mixed histology tumors. Carcinomas can typically be classified into two types according to their estrogenic state, type 1 (ER-positive EC) and type 2 (ER-negative EC).

In a previous study, the expression of GPER, estrogen, progesterone, EGFR, and Ki-67 in 47 EC patients treated between 1997 and 2001 based on early immunohistochemical methods showed that GPER was overexpressed in high-risk EC patients and was negatively correlated with PR expression (117). E2 and G-1 trigger the mitogen-activated protein kinase (MAPK) pathway in ER-negative KLE cells and ER-positive RL95-2 cells, which require GPER involvement (118). Li et al. investigated the relationship between AMF and GPER in EC (87). This mechanistic study demonstrated that the interaction between AMF and GPER activates PI3K signaling, which in turn accelerates the growth of EC cells (**Figure 2**). However, there have been inconsistent results regarding the expression of GPER in EC. In 2012, Krakstad et al. found decreased GPER mRNA and protein levels and increased ERα levels in high grade endometrial carcinoma, supporting the association between GPER loss and disease progression from primary to metastatic lesions (119). Furthermore, in another study, GPER expression in EC cells was found to be lower than in normal endometrial samples. Treating GPER-positive EC cells with the GPER agonist G-1 resulted in significant growth reduction, suggesting that GPER mRNA might be sufficient to mediate the antiproliferative effects of its ligand in EC (120) (**Figure 2**). Due to its high expression and mitogenic role in other tissues and cancers, among the three ERs encoded in the human genome, ERα and ERβ are considered to be the major mediators of pro-growth estrogen signaling in EC cells.

The results of studies investigating the expression and role of ERβ in EC are not yet fully known. ERβ may play a suppressive role in EC. Immunohistochemical results have shown decreased ERβ mRNA and protein levels in endometrioid EC compared with in normal proliferative endometrium or adjacent normal endometrium from post-menopausal control women (121, 122). In addition, Zhang et al. indicated that in ERβ knockout mice, there is an unusual proliferation of cells in the uterus (74). Nevertheless, ERβ also shows a potential tumorigenic effect. A C-terminally altered ERβ isoform, ERβ5, is upregulated in endometrial carcinoma and is associated with the expression of oncogenes such as HER2 and MyBL2 (123, 124) (**Figure 2**).

Analysis of The Cancer Genome Atlas data showed that the mean expression level of ERα in EC was 2.9-fold higher than that of ERβ (125). The reason for this may be that EC mainly affects postmenopausal women, and higher gonadotropin levels in postmenopausal women may downregulate ERβ (126). Because ERβ acts as a dominant negative regulator of ERα, the postmenopausal endometrium may promote uterine cell proliferation through unopposed ERα action (74). In terms of analyzing the relationship between ERα/ERβ and the clinical characteristics of EC patients, it was found that ERα expression is higher in the early stages of EC and decreased in advanced EC (127). Thus, ERα may promote the progression of EC by interacting with estrogen in endometrial atypical hyperplasia and the early stages of EC.

It is well known that obesity is one of the most common risk factors for EC because androgens are converted to estrogen in adipose tissue. In fact, ER mutations are present in 5.8% of primary ECs (128). In EC, ERα mutations are associated with worse outcomes and less obesity, so mutations in ERα might explain why women with normal body and without other risk factors also develop EC (129). Evaluation of an EC cell model that includes that D538G mutation revealed that mutant ER has estrogen-independent activity as well as an expanded set of genomic binding sites (130). Mutation confers estrogen-independent activity to ER, which causes gene expression changes. Understanding the molecular and pathological effects of ER mutations in EC will further our knowledge of ER mutant disease and may provide treatment options for patients with ER mutant tumors.

ER is used as a regulatory cofactor to regulate gene expression, and different transcription factors may be responsible for controlling the genomic interactions of ER in EC cells. Motif analysis of endometrial cancer-specific ER-bound sites, along with gene expression analysis, revealed that ETV4, a member of the ETS family, overlaps with 45% of ER binding sites in Ishikawa cells (131). In a recent study reported using CRISPR/Cas9 to knockout ETV4 in EC cells, genetic deletion of ETV4 resulted in a large reduction of ER binding signal at the majority of bound loci across the genome, leading to an expected decrease in the transcriptional response to E2 treatment and thus reduced cells growth (132). Qi et al. found that estrogen regulates the histone acetylation hMOF expression through activating the PI3K/Akt and Ras–Raf–MEK–ERK signaling pathway to promote cell cycle progression in EC cells (133). Unfortunately, although the role of ER in the development of EC has been demonstrated in numerous studies, there are still many gaps in our knowledge of ER in EC.

TREATMENTS TARGETING ERS

Hormone replacement therapy (HRT) has been used in menopausal women to relieve hot flashes, vaginal dryness, fluctuating emotions, irregular menses, chills, and sleeping problems. Pure antiestrogens represent an endocrine-targeted therapy for which the mechanism of action involves competition with ER ligands and ER downregulation. However, treating menopause symptoms with estrogen must be accompanied by a progestin component to avoid the effects of excess estrogen on the endometrium. Progesterone has been shown to downregulate ERs and stimulate direct PR-mediated effects that oppose estrogenic

actions. In a postmenopausal estrogen/progestin interventions trial, women assigned to estrogen alone were more likely to develop simple, complex, or atypical hyperplasia. Combining conjugated equine estrogens with cyclic or continuous progestin protected the endometrium from hyperplastic changes associated with estrogen-only therapy (134). A small but not significant reduction in the risk of EC was observed in a sequential combination regimen with estrogen and progesterone (135). In the early 2000s, the Women's Health Initiative raised numerous concerns regarding the use of hormone replacement therapy, as combined estrogen-progestin treatment was associated with a statistically significant increase in invasive breast cancer and in cardiovascular events after approximately five years of follow-up (136). Therefore, hormone replacement therapy use is now recommended to be relatively short-term (i.e., 3–5 years in post-menopausal women) and be administered at low doses; moreover, its use is very narrow and should be limited to women without a history of breast cancer and women who are not at increased risk of cardiovascular or thromboembolic disease (137). Consequently, novel ER modulators are necessary to maintain endocrine homeostasis.

Tamoxifen acts as an agonist in most estrogen target tissues, presumably in association with differences in the expression of co-activator and co-repressor proteins in different tissues, which result in the formation of distinct complexes with ERs (6, 138) (**Figure 3**). Tamoxifen stimulates ER dependent gene regulation in the uterus (139). In endometrial cells, tamoxifen-bound ERα is able to recruit coactivator proteins and to initiate gene transcription. This differential recruitment of coactivators contributes to the tissue specificity of tamoxifen ERα function (140). However, the estrogen agonist effects on the endometrium from partial agonists cannot be neglected and can manifest as increased endometrial thickness, endometrial polyps, leiomyomas, and EC (141–143). Tamoxifen may promote cancer development by upregulating ERα, PR, vascular endothelial growth factor, EGFR, mechanical target of rapamycin, IGF-1R, and C-MYC in EC cells (144, 145). In a randomized trial, Fornander et al. found that among 931 postmenopausal patients treated with tamoxifen, there was a 6.4-fold increase in the incidence of EC compared with controls (146). This could be related to the dose of tamoxifen used (40 mg per day), which is higher than what was used by other trials. Similarly, Fisher et al. demonstrated a significant increase in EC severity among women treated with tamoxifen, with a relative risk of 7.5 (147). It has been suggested that tamoxifen treatment has a cancer-promoting effect *via* GPER, which significantly stimulates the proliferation of endometrial cells (148). Because tamoxifen has a selective antiestrogenic effect in breast cancer but an agonistic estrogenic effect in the bones and the uterus/EC, it is not suitable for use in the general population due to the increased incidence of EC.

The mechanism of action of raloxifene occurs through binding to ERα and ERβ. This binding results in activation and blockade of estrogenic pathways in tissues that express ERs. The crystal structures of the LBD of ER in complex with the endogenous estrogen, E2, and the selective antagonist raloxifene, have shown that they are all bind in the same site within the core of the domain, but raloxifene induces a transcriptionally inactive LBD conformation (149). Raloxifene has estrogenic antagonistic effects in the uterus and breast. ERα blockade using raloxifene indicated that E2 alters endometrial cell proliferation *via* ERα. The antagonistic effect of raloxifene on estradiol-treated endometrial epithelial Ishikawa cells has been demonstrated by the altered expression of genes such as HOXA 10, leukemia inhibitory factor, PR, and EMX2 (150). Notably, raloxifene does not exhibit the endometrial side effects observed with tamoxifen (151, 152). In estrogen-stimulated ovariectomized rat surgical models of endometriosis, treatment with 10 mg/kg raloxifene for 7 to 14 days resulted in reduced uterine volumes (153). Adult female rhesus monkeys with spontaneous endometriosis treated with 10 mg/kg/d raloxifene for 90 days showed degeneration of endometrial tissue and attenuated uterine volume (154). Although raloxifene does not induce breast tenderness, EH, or EC, it may augment the risk of thromboembolic disease (1/1000 cases per year) as well as hot flashes (in 4%–6% of cases). Furthermore, raloxifene reduces proliferative markers in the epithelium of lesions in rodent models but not in the stroma, while the stromal component is the major contributor to

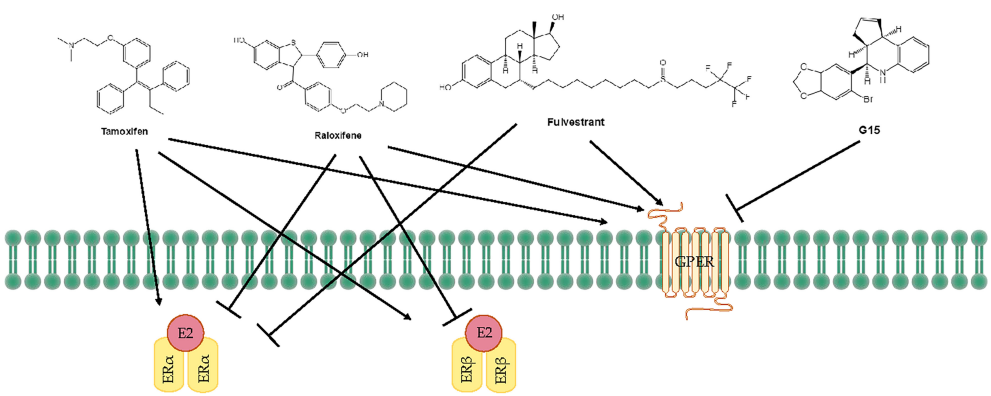

FIGURE 3 | Treatments for endometrial diseases. ER, estrogen receptor; GPER, G-protein-coupled estrogen receptor; EGFR, epidermal growth factor receptor; ERE, estrogen response element; MMP, matrix metallopeptidase; LBD, ligand-binding domain; P, phosphorylation.

endometriotic lesions (155). Petrie et al. have demonstrated that GPER plays an important role in the estrogen-mediated signaling of the ERα⁻/ERβ⁻ EC cell line Hec50 and the SERM raloxifene is an agonist for GPER (156). In contrast to tamoxifen or raloxifene, antagonists such as fulvestrant (also known as SERDs) show complete antagonism. It completely inhibits estrogen-mediated changes in gene transcription and therefore has no agonist activity. The large side chain that originates from the B ring prevents H12 of ERα from docking in the agonist conformation, thereby preventing co-activator binding and transcriptional activation (149, 157) (**Figure 3**). Other effects of fulvestrant include inhibition of receptor dimerization and nucleocytoplasmic shuttling of the ER (158). Tamoxifen, raloxifene, or fulvestrant have been shown to be agonists of GPER. However, pharmacological inhibition of GPER activity *in vivo* prevents estrogen-mediated tumor growth, and the selective GPER antagonist G-15 retarded the growth of endometrial carcinoma (40) (**Figure 3**).

CONCLUSION

This review provides a summary of the body of published systematic reviews and meta-analyses of the effects of different ERs on the endometrium. The endometrium is a dynamic tissue that undergoes proliferation, secretion, and menstrual during the menstrual cycle of the female reproductive age. The current findings show that unopposed endometrial exposure to estrogen increases the risk of EH and cancer and emphasize the importance of modulating ERs to control the development of endometrial diseases. Multiple variants of ER are involved in endometrial pathophysiology and signaling pathways. ERα promotes uterine cell proliferation and is strongly associated with an increased risk of EC, because it plays an important role in tumor development and metastasis by activating signaling pathways involved in promoting proliferation, resisting apoptosis, stimulating migration and invasion, and inducing angiogenesis. In contrast, the responses mediated by ERβ has a key opposite effect in the endometrium. GPER is normally expressed in the endometrial but is highly expressed in abnormal EH, whereas paradoxically expressed in patients with EC. More research is needed to elucidate the disease mechanisms that involve ERs.

It is well known that the identification of risk factors that are strongly associated with endometrial risk can help the identification of high-risk groups of women, which will benefit from targeted prevention strategies. The mechanisms of action of hormone therapy involves competition with the ER ligands and ER downregulation. Unfortunately, the role of HRT has been debated. Estrogen receptor modulators provide potential treatment for high-risk women. Among SERMs, tamoxifen therapy improves survival in Erα-positive primary and advanced breast cancer. However, in endometrial, many authors have confirmed that tamoxifen use may cause endometrial thickness and polyps (54, 159). Raloxifene, a second SERM, has a high affinity to ERα, with a relative binding affinity of 46% for human ERα compared with E2 (160). It has anti-estrogen effects on the uterus and protects the endometrium from hyperplasia and irregular bleeding caused by estrogen hyperstimulation. Fulvestrant is a non-agonistic ER antagonist that blocks the ER and inhibits the proliferative effects of estrogen on tumor cells. To better treat or cure endometrial disease, a deeper knowledge of the roles of ERα, ERβ or GPER and their interactions is required.

Although there are still many diseases for which estrogens have been implicated but the role of their receptors has not been elucidated. Endometrium-associated diseases may require simultaneous attacks on multiple targets or a systems approach for effective treatment. With the increased understanding of the molecular basis and the pathways related to specific disease progression, the era of molecularly targeted therapies has emerged as a most promising direction of research. To develop personalized therapies, the molecular regulation of endometriosis, EH and EC needs to be carefully studied. Because endometrial disease is essentially a hormone-dependent manifestation of high ER and PR expression, targeting ER may be a viable approach to develop novel treatment strategies for this disease. Screening of various compounds by molecular simulation can help to identify promising selective agonists or antagonists for the prevention and treatment of estrogen-affected endometrial diseases.

Further work is needed to develop new, more bioavailable SERMs/SERDs with better pharmacological properties, and therapies that inhibit all types of ERs. Furthermore, due to low bioavailability, it is expected to improve existing formulations to address the barriers to optimal SERM or SERD use and efficacy profiles.

AUTHOR CONTRIBUTIONS

KY, X-LX, and Z-YH reviewed the literature, wrote the manuscript, and designed the figures and tables. JL revised the draft. X-WF and S-LD made substantial contributions to the conception and design of the work and provided input into manuscript content and composition. All authors contributed to the article and approved the submitted version.

FUNDING

This work was supported by National Nature Science Foundation Project of China (No. 32072722,31101714, and 31372307).

ACKNOWLEDGMENTS

We thank Wei Yan, Ph.D. and Ryan Chastain-Gross, Ph.D. (from Liwen Bianji, Edanz Group China www.liwenbianji.cn/ac), for editing the English text of a draft of this manuscript. We thank James P. Mahaffey, PhD, from Liwen Bianji (Edanz) (www.liwenbianji.cn) for editing the English text of a draft of this manuscript.

REFERENCES

1. Critchley HOD, Saunders PTK. Hormone Receptor Dynamics in a Receptive Human Endometrium. *Reprod Sci* (2009) 16:191–9. doi: 10.1177/1933719108331121
2. Marino M, Galluzzo P, Ascenzi P. Estrogen Signaling Multiple Pathways to Impact Gene Transcription. *Curr Genomics* (2006) 7:497–508. doi: 10.2174/138920206779315737
3. Nilsson S, Makela S, Treuter E, Tujague M, Thomsen J, Andersson G, et al. Mechanisms of Estrogen Action. *Physiol Rev* (2001) 81:1535–65. doi: 10.1152/physrev.2001.81.4.1535
4. Mosselman S, Polman J, Dijkema R. ER Beta: Identification and Characterization of a Novel Human Estrogen Receptor. *FEBS Lett* (1996) 392:49–53. doi: 10.1016/0014-5793(96)00782-x
5. Kumar R, Johnson BH, Thompson EB. Overview of the Structural Basis for Transcription Regulation by Nuclear Hormone Receptors. *Essays Biochem* (2004) 40:27–39. doi: 10.1042/bse0400027
6. Yasar P, Ayaz G, User SD, Gupur G, Muyan M. Molecular Mechanism of Estrogen-Estrogen Receptor Signaling. *Reprod Med Biol* (2017) 16:4–20. doi: 10.1002/rmb2.12006
7. Arao Y, Hamilton KJ, Coons LA, Korach KS. Estrogen Receptor Alpha L543A,L544A Mutation Changes Antagonists to Agonists, Correlating With the Ligand Binding Domain Dimerization Associated With DNA Binding Activity. *J Biol Chem* (2013) 288:21105–16. doi: 10.1074/jbc.M113.463455
8. Koide A, Zhao C, Naganuma M, Abrams J, Deighton-Collins S, Skafar DF, et al. Identification of Regions Within the F Domain of the Human Estrogen Receptor Alpha That are Important for Modulating Transactivation and Protein-Protein Interactions. *Mol Endocrinol* (2007) 21:829–42. doi: 10.1210/me.2006-0203
9. Montano MM, Muller V, Trobaugh A, Katzenellenbogen BS. The Carboxy-Terminal F Domain of the Human Estrogen Receptor: Role in the Transcriptional Activity of the Receptor and the Effectiveness of Antiestrogens as Estrogen Antagonists. *Mol Endocrinol* (1995) 9:814–25. doi: 10.1210/mend.9.7.7476965
10. Paech K, Webb P, Kuiper GGJM, Nilsson S, Gustafsson JA, Kushner PJ, et al. Differential Ligand Activation of Estrogen Receptors ER Alpha and ER Beta at AP1 Sites. *Science* (1997) 277:1508–10. doi: 10.1126/science.277.5331.1508
11. Couse JF, Lindzey J, Grandien K, Gustafsson JA, Korach KS. Tissue Distribution and Quantitative Analysis of Estrogen Receptor-Alpha (ER Alpha) and Estrogen Receptor-Beta (ER Beta) Messenger Ribonucleic Acid in the Wild-Type and ER Alpha-Knockout Mouse. *Endocrinology* (1997) 138:4613–21. doi: 10.1210/en.138.11.4613
12. Li X, Huang J, Fluharty BR, Huang Y, Nott SL, Muyan M. What are Comparative Studies Telling Us About the Mechanism of ERbeta Action in the ERE-Dependent E2 Signaling Pathway? *J Steroid Biochem Mol Biol* (2008) 109:266–72. doi: 10.1016/j.jsbmb.2008.03.001
13. Huang J, Li X, Qiao T, Bambara RA, Hilf R, Muyan MA. Tale of Two Estrogen Receptors (ERs): How Differential ER-Estrogen Responsive Element Interactions Contribute to Subtype-Specific Transcriptional Responses. *Nucl Recept Signal* (2006) 4:e015. doi: 10.1621/nrs.04015
14. Billon-Gales A, Krust A, Fontaine C, Abot A, Flouriot G, Toutain C, et al. Activation Function 2 (AF2) of Estrogen Receptor-Alpha is Required for the Atheroprotective Action of Estradiol But Not to Accelerate Endothelial Healing. *Proc Natl Acad Sci U.S.A.* (2011) 108:13311–6. doi: 10.1073/pnas.1105632108
15. Arao Y, Hamilton KJ, Ray MK, Scott G, Mishina Y, Korach KS. Estrogen Receptor Alpha AF-2 Mutation Results in Antagonist Reversal and Reveals Tissue Selective Function of Estrogen Receptor Modulators. *Proc Natl Acad Sci U.S.A.* (2011) 108:14986–91. doi: 10.1073/pnas.1109180108
16. Li X, Huang J, Yi P, Bambara RA, Hilf R, Muyan M. Single-Chain Estrogen Receptors (ERs) Reveal That the ERalpha/beta Heterodimer Emulates Functions of the ERalpha Dimer in Genomic Estrogen Signaling Pathways. *Mol Cell Biol* (2004) 24:7681–94. doi: 10.1128/MCB.24.17.7681-7694.2004
17. Yi P, Bhagat S, Hilf R, Bambara RA, Muyan M. Differences in the Abilities of Estrogen Receptors to Integrate Activation Functions Are Critical for Subtype-Specific Transcriptional Responses. *Mol Endocrinol* (2002) 16:1810–27. doi: 10.1210/me.2001-0323
18. Huang J, Li X, Maguire CA, Hilf R, Bambara RA, Muyan M. Binding of Estrogen Receptor β to Estrogen Response Element in Situ Is Independent of Estradiol and Impaired by Its Amino Terminus. *Mol Endocrinol* (2005) 19:2696–712. doi: 10.1210/me.2005-0120
19. McDonnell DP, Norris JD. Connections and Regulation of the Human Estrogen Receptor. *Science* (2002) 296:1642–4. doi: 10.1126/science.1071884
20. Ray A, Prefontaine KE, Ray P. Down-Modulation of Interleukin-6 Gene-Expression by 17-Beta-Estradiol in the Absence of High-Affinity DNA-Binding by the Estrogen-Receptor. *J Biol Chem* (1994) 269:12940–6. doi: 10.1016/S0021-9258(18)99966-7
21. Karin M, Liu Z, Zandi E. AP-1 Function and Regulation. *Curr Opin Cell Biol* (1997) 9:240–6. doi: 10.1016/s0955-0674(97)80068-3
22. Webb P, Nguyen P, Valentine C, Lopez GN, Kwok GR, McInerney E, et al. The Estrogen Receptor Enhances AP-1 Activity by Two Distinct Mechanisms With Different Requirements for Receptor Transactivation Functions. *Mol Endocrinol* (1999) 13:1672–85. doi: 10.1210/mend.13.10.0357
23. Teyssier C, Belguise K, Galtier F, Chalbos D. Characterization of the Physical Interaction Between Estrogen Receptor α and JUN Proteins. *J Biol Chem* (2001) 276:36361–9. doi: 10.1074/jbc.M101806200
24. Cheung E, Acevedo ML, Cole PA, Kraus WL. Altered Pharmacology and Distinct Coactivator Usage for Estrogen Receptor-Dependent Transcription Through Activating Protein-1. *Proc Natl Acad Sci U.S.A.* (2005) 102:559–64. doi: 10.1073/pnas.0407113102
25. Saville B, Wormke M, Wang F, Nguyen T, Enmark E, Kuiper G, et al. Ligand-, Cell-, and Estrogen Receptor Subtype (α/β)-Dependent Activation at GC-Rich (Sp1) Promoter Elements. *J Biol Chem* (2000) 275:5379–87. doi: 10.1074/jbc.275.8.5379
26. Aronica SM, Kraus WL, Katzenellenbogen BS. Estrogen Action via the cAMP Signaling Pathway: Stimulation of Adenylate Cyclase and cAMP-Regulated Gene Transcription. *Proc Natl Acad Sci U.S.A.* (1994) 91:8517–21. doi: 10.1073/pnas.91.18.8517
27. Tesarik J, Mendoza C. Direct non-Genomic Effects of Follicular Steroids on Maturing Human Oocytes: Oestrogen Versus Androgen Antagonism. *Hum Reprod Update* (1997) 3:95–100. doi: 10.1093/humupd/3.2.95
28. Morley P, Whitfield JF, Vanderhyden BC, Tsang BK, Schwartz J.-L.J.E. A. New, Nongenomic Estrogen Action: The Rapid Release of Intracellular Calcium. *Endocrinology* (1992) 131:1305–12. doi: 10.1210/endo.131.3.1505465
29. Moriarty K, Kim K, Bender J. Estrogen Receptor-Mediated Rapid Signaling. *Endocrinology* (2006) 147:5557–63. doi: 10.1210/en.2006-0729
30. Micevych P, Kuo J, Christensen A. Physiology of Membrane Oestrogen Receptor Signalling in Reproduction. *J Neuroendocrinol* (2009) 21:249–56. doi: 10.1111/j.1365-2826.2009.01833.x
31. Revankar CM, Cimino DF, Sklar LA, Arterburn JB, Prossnitz ER. A Transmembrane Intracellular Estrogen Receptor Mediates Rapid Cell Signaling. *Science* (2005) 307:1625–30. doi: 10.1126/science.1106943
32. Rainville J, Pollard K, Vasudevan N. Membrane-Initiated non-Genomic Signaling by Estrogens in the Hypothalamus: Cross-Talk With Glucocorticoids With Implications for Behavior. *Front Endocrinol (Lausanne)* (2015) 6:18. doi: 10.3389/fendo.2015.00018
33. Smith A, Rønnekleiv O, Kelly MJS. Gq-mER Signaling has Opposite Effects on Hypothalamic Orexigenic and Anorexigenic Neurons. *Steroids* (2014) 81:31–5. doi: 10.1016/j.steroids.2013.11.007
34. Kelly MJ, Levin ER. Rapid Actions of Plasma Membrane Estrogen Receptors. *Trends Endocrinol Metab* (2001) 12:152–6. doi: 10.1016/s1043-2760(01)00377-0
35. Filardo EJ, Quinn JA, Frackelton ARJr., Bland KI. Estrogen Action *via* the G Protein-Coupled Receptor, GPR30: Stimulation of Adenylyl Cyclase and cAMP-Mediated Attenuation of the Epidermal Growth Factor Receptor-To-MAPK Signaling Axis. *Mol Endocrinol* (2002) 16:70–84. doi: 10.1210/mend.16.1.0758
36. Filardo EJ, Quinn JA, Bland KI, Frackelton ARJr. Estrogen-Induced Activation of Erk-1 and Erk-2 Requires the G Protein-Coupled Receptor Homolog, GPR30, and Occurs *via* trans-activation of the epidermal growth

factor receptor through release of HB-EGF. *Mol Endocrinol* (2000) 14:1649–60. doi: 10.1210/mend.14.10.0532
37. Prossnitz ER, Barton M. Estrogen Biology: New Insights Into GPER Function and Clinical Opportunities. *Mol Cell Endocrinol* (2014) 389:71–83. doi: 10.1016/j.mce.2014.02.002
38. Meyer MR, Haas E, Prossnitz ER, Barton M. Non-Genomic Regulation of Vascular Cell Function and Growth by Estrogen. *Mol Cell Endocrinol* (2009) 308:9–16. doi: 10.1016/j.mce.2009.03.009
39. Dennis MK, Field AS, Burai R, Ramesh C, Petrie WK, Bologa CG, et al. Identification of a GPER/GPR30 Antagonist With Improved Estrogen Receptor Counterselectivity. *J Steroid Biochem Mol Biol* (2011) 127:358–66. doi: 10.1016/j.jsbmb.2011.07.002
40. Dennis MK, Burai R, Ramesh C, Petrie WK, Alcon SN, Nayak TK, et al. *In Vivo* Effects of a GPR30 Antagonist. *Nat Chem Biol* (2009) 5:421–7. doi: 10.1038/nchembio.168
41. Jacenik D, Cygankiewicz AI, Krajewska WM. The G Protein-Coupled Estrogen Receptor as a Modulator of Neoplastic Transformation. *Mol Cell Endocrinol* (2016) 429:10–8. doi: 10.1016/j.mce.2016.04.011
42. Lonard DM, O'Malley B W. Nuclear Receptor Coregulators: Judges, Juries, and Executioners of Cellular Regulation. *Mol Cell* (2007) 27:691–700. doi: 10.1016/j.molcel.2007.08.012
43. Fuentes N, Silveyra P. Estrogen Receptor Signaling Mechanisms. *Adv Protein Chem Struct Biol* (2019) 116:135–70. doi: 10.1016/bs.apcsb.2019.01.001
44. Oñate SA, Tsai SY, Tsai MJ, O'Malley BW. Sequence and Characterization of a Coactivator for the Steroid Hormone Receptor Superfamily. *Science* (1995) 270:1354–7. doi: 10.1126/science.270.5240.1354
45. Lonard DM, O'Malley BW. The Expanding Cosmos of Nuclear Receptor Coactivators. *Cell* (2006) 125:411–4. doi: 10.1016/j.cell.2006.04.021
46. Chen JD, Evans RM. A Transcriptional Co-Repressor That Interacts With Nuclear Hormone Receptors. *Nature* (1995) 377:454–7. doi: 10.1038/377454a0
47. Wong MM, Guo C, Zhang J. Nuclear Receptor Corepressor Complexes in Cancer: Mechanism, Function and Regulation. *Am J Clin Exp Urol* (2014) 2:169–87.
48. Manavathi B, Samanthapudi VS, Gajulapalli VN. Estrogen Receptor Coregulators and Pioneer Factors: The Orchestrators of Mammary Gland Cell Fate and Development. *Front Cell Dev Biol* (2014) 2:34. doi: 10.3389/fcell.2014.00034
49. Hu X, Lazar MA. The CoRNR Motif Controls the Recruitment of Corepressors by Nuclear Hormone Receptors. *Nature* (1999) 402:93–6. doi: 10.1038/47069
50. Han SJ, Lonard DM, O'Malley BW. Multi-Modulation of Nuclear Receptor Coactivators Through Posttranslational Modifications. *Trends Endocrinol Metab* (2009) 20:8–15. doi: 10.1016/j.tem.2008.10.001
51. O'Malley BW, McKenna NJ. Coactivators and Corepressors: What's in a Name? *Mol Endocrinol* (2008) 22:2213–4. doi: 10.1210/me.2008-0201
52. Groothuis PG, Dassen HHNM, Romano A, Punyadeera C. Estrogen and the Endometrium: Lessons Learned From Gene Expression Profiling in Rodents and Human. *Hum Reprod Update* (2007) 13:405–17. doi: 10.1093/humupd/dmm009
53. Persson I. Cancer Risk in Women Receiving Estrogen-Progestin Replacement Therapy. *Maturitas* (1996) 23:S37–45. doi: 10.1016/0378-5122(96)01010-9
54. Vollmer G. Endometrial Cancer: Experimental Models Useful for Studies on Molecular Aspects of Endometrial Cancer and Carcinogenesis. *Endocr-Relat Cancer* (2003) 10:23–42. doi: 10.1677/erc.0.0100023
55. Newbold RR, Bullock BC, Mclachlan JA. Uterine Adenocarcinoma in Mice Following Developmental Treatment With Estrogens - A Model for Hormonal Carcinogenesis. *Cancer Res* (1990) 50:7677–81.
56. Li SF. Relationship Between Cellular DNA-Synthesis, Pcna Expression and Sex Steroid-Hormone Receptor Status in the Developing Mouse Ovary, Uterus and Oviduct. *Histochemistry* (1994) 102:405–13. doi: 10.1007/Bf00268912
57. Andrews WW, Mizejewski GJ, Ojeda SR. Development of Estradiol-Positive Feedback on Luteinizing-Hormone Release in the Female Rat - a Quantitative Study. *Endocrinology* (1981) 109:1404–13. doi: 10.1210/endo-109-5-1404
58. Meijsroelofs HMA, Uilenbroek JTJ, Degreef WJ, Dejong FH, Kramer P. Gonadotropin and Steroid Levels Around Time of 1st Ovulation in Rat. *J Endocrinol* (1975) 67:275–82. doi: 10.1677/joe.0.0670275
59. Critchley HOD, Brenner RM, Henderson TA, Williams K, Nayak NR, Slayden OD, et al. Estrogen Receptor Beta, But Not Estrogen Receptor Alpha, is Present in the Vascular Endothelium of the Human and Nonhuman Primate Endometrium. *J Clin Endocr Metab* (2001) 86:1370–8. doi: 10.1210/jc.86.3.1370
60. Lecce G, Meduri G, Ancelin M, Bergeron C, Perrot-Applanat M. Presence of Estrogen Receptor Beta in the Human Endometrium Through the Cycle: Expression in Glandular, Stromal, and Vascular Cells. *J Clin Endocr Metab* (2001) 86:1379–86. doi: 10.1210/jc.86.3.1379
61. Perrotapplanat M, Groyerpicard MT, Garcia E, Lorenzo F, Milgrom E. Immunocytochemical Demonstration of Estrogen and Progesterone Receptors in Muscle-Cells of Uterine Arteries in Rabbits and Humans. *Endocrinology* (1988) 123:1511–9. doi: 10.1210/endo-123-3-1511
62. Kolkova Z, Noskova V, Ehinger A, Hansson S, Casslen BG. Protein-Coupled Estrogen Receptor 1 (GPER, GPR 30) in Normal Human Endometrium and Early Pregnancy Decidua(Dagger). *Mol Hum Reprod* (2010) 16:743–51. doi: 10.1093/molehr/gaq043
63. Snijders MPML, Degoeij AFPM, Debetstebaerts MJC, Rousch MJM, Koudstaal J, Bosman FT. Immunocytochemical Analysis of Estrogen-Receptors and Progesterone Receptors in the Human Uterus Throughout the Menstrual-Cycle and After the Menopause. *J Reprod Fertil* (1992) 94:363–71. doi: 10.1530/jrf.0.0940363
64. Matsuzaki S, Fukaya T, Suzuki T, Murakami T, Sasano H, Yajima A. Oestrogen Receptor Alpha and Beta mRNA Expression in Human Endometrium Throughout the Menstrual Cycle. *Mol Hum Reprod* (1999) 5:559–64. doi: 10.1093/molehr/5.6.559
65. Maiti K, Paul JW, Read M, Chan EC, Riley SC, Nahar P. Smith, R. G-1-Activated Membrane Estrogen Receptors Mediate Increased Contractility of the Human Myometrium. *Endocrinology* (2011) 152:2448–55. doi: 10.1210/en.2010-0979
66. Matsuzaki S, Murakami T, Uehara S, Canis M, Sasano H, Okamura K. Expression of Estrogen Receptor Alpha and Beta in Peritoneal and Ovarian Endometriosis. *Fertil Steril* (2001) 75:1198–205. doi: 10.1016/S0015-0282(01)01783-6
67. Sakaguchi H, Fujimoto J, Aoki I, Tamaya T. Expression of Estrogen Receptor Alpha and Beta in Myometrium of Premenopausal and Postmenopausal Women. *Steroids* (2003) 68:11–9. doi: 10.1016/S0039-128x(02)00111-3
68. Zang H, Sahlin L, Masironi B, Hirschberg AL. Effects of Testosterone and Estrogen Treatment on the Distribution of Sex Hormone Receptors in the Endometrium of Postmenopausal Women. *Menopause* (2008) 15:233–9. doi: 10.1097/gme.0b013e318148bb99
69. Gao F, Ma XH, Ostmann AB, Das SK. GPR30 Activation Opposes Estrogen-Dependent Uterine Growth *via* Inhibition of Stromal ERK1/2 and Estrogen Receptor Alpha (ER Alpha) Phosphorylation Signals. *Endocrinology* (2011) 152:1434–47. doi: 10.1210/en.2010-1368
70. Yuguchi H, Tanabe A, Hayashi A, Tanaka Y, Okuda K, Yamashita Y, et al. The Expression Status of G Protein-Coupled Receptor GPR30 Is Associated With the Clinical Characteristics of Endometriosis. *Endocr Res* (2013) 38:223–31. doi: 10.3109/07435800.2013.774011
71. Plante BJ, Lessey BA, Taylor RN, Wang W, Bagchi MK, Yuan LW, et al. Protein-Coupled Estrogen Receptor (GPER) Expression in Normal and Abnormal Endometrium. *Reprod Sci* (2012) 19:684–93. doi: 10.1177/1933719111431000
72. Couse JF, Curtis SW, Washburn TF, Lindzey J, Lindzey J Fau - Golding TS, Golding Ts Fau - Lubahn DB, et al. Analysis of Transcription and Estrogen Insensitivity in the Female Mouse After Targeted Disruption of the Estrogen Receptor Gene. *Mol Endocrinol* (1995) 9:1441–54. doi: 10.1210/mend.9.11.8584021
73. Curtis SW, Clark J, Myers P, Korach KS. Disruption of Estrogen Signaling Does Not Prevent Progesterone Action in the Estrogen Receptor or Knockout Mouse Uterus. *P Natl Acad Sci USA* (1999) 96:3646–51. doi: 10.1073/pnas.96.7.3646
74. Zhang WH, Saji S, Makinen S, Cheng GJ, Jensen EV, Warner M, et al. Estrogen Receptor (ER) Beta, a Modulator of ER Alpha in the Uterus. *P Natl Acad Sci USA* (2000) 97:5936–41. doi: 10.1073/pnas.97.11.5936
75. Dupont S, Krust A, Gansmuller A, Dierich A, Chambon P, Mark M. Effect of Single and Compound Knockouts of Estrogen Receptors Alpha (ER Alpha) and Beta (ER Beta) on Mouse Reproductive Phenotypes. *Development* (2000) 127:4277–91. doi: 10.1242/dev.127.19.4277

76. Jakacka M, Ito M, Martinson F, Ishikawa T, Lee EJ, Jameson JL. An Estrogen Receptor (ER)alpha Deoxyribonucleic Acid-Binding Domain Knock-In Mutation Provides Evidence for Nonclassical ER Pathway Signaling *In Vivo*. *Mol Endocrinol* (2002) 16:2188–201. doi: 10.1210/me.2001-0174
77. O'Brien JE, Peterson TJ, Tong MH, Lee EJ, Pfaff LE, Hewitt SC, et al. Estrogen-Induced Proliferation of Uterine Epithelial Cells is Independent of Estrogen Receptor Alpha Binding to Classical Estrogen Response Elements. *J Biol Chem* (2006) 281:26683–92. doi: 10.1074/jbc.M601522200
78. Frasor J, Barnett DH, Danes JM, Hess R, Parlow AF, Katzenellenbogen BS. Response-Specific and Ligand Dose-Dependent Modulation of Estrogen Receptor (ER) Alpha Activity by ER Beta in the Uterus. *Endocrinology* (2003) 144:3159–66. doi: 10.1210/en.2002-0143
79. Wada-Hiraike O, Hiraike H, Okinaga H, Imamov O, Barros RPA, Morani A, et al. Role of Estrogen Receptor Beta in Uterine Stroma and Epithelium: Insights From Estrogen Receptor Beta(-/-) Mice. *P Natl Acad Sci USA* (2006) 103:18350–5. doi: 10.1073/pnas.0608861103
80. Hewitt SC, Li L, Grimm SA, Winuthayanon W, Hamilton KJ, Pockette B, et al. Novel DNA Motif Binding Activity Observed *In Vivo* With an Estrogen Receptor Alpha Mutant Mouse. *Mol Endocrinol* (2014) 28:899–911. doi: 10.1210/me.2014-1051
81. Ahlbory-Dieker DL, Stride BD, Leder G, Schkoldow J, Trolenberg S, Seidel H, et al. DNA Binding by Estrogen Receptor-Alpha Is Essential for the Transcriptional Response to Estrogen in the Liver and the Uterus. *Mol Endocrinol* (2009) 23:1544–55. doi: 10.1210/me.2009-0045
82. Winuthayanon W, Hewitt SC, Orvis GD, Behringer RR, Korach KS. Uterine Epithelial Estrogen Receptor Alpha is Dispensable for Proliferation But Essential for Complete Biological and Biochemical Responses. *P Natl Acad Sci USA* (2010) 107:19272–7. doi: 10.1073/pnas.1013226107
83. Abot A, Fontaine C, Raymond-Letron I, Flouriot G, Adlanmerini M, Buscato M, et al. The AF-1 Activation Function of Estrogen Receptor Alpha Is Necessary and Sufficient for Uterine Epithelial Cell Proliferation *In Vivo*. *Endocrinology* (2013) 154:2222–33. doi: 10.1210/en.2012-2059
84. Isensee J, Meoli L, Zazzu V, Nabzdyk C, Witt H, Soewarto D, et al. Expression Pattern of G Protein-Coupled Receptor 30 in LacZ Reporter Mice. *Endocrinology* (2009) 150:1722–30. doi: 10.1210/en.2008-1488
85. Hewitt SC, Harrell JC, Korach KS. Lessons in Estrogen Biology From Knockout and Transgenic Animals. *Annu Rev Physiol* (2005) 67:285–308. doi: 10.1146/annurev.physiol.67.040403.115914
86. Otto C, Fuchs I, Kauselmann G, Kern H, Zevnik B, Andreasen P, et al. GPR30 Does Not Mediate Estrogenic Responses in Reproductive Organs in Mice. *Biol Reprod* (2009) 80:34–41. doi: 10.1095/biolreprod.108.071175
87. Li YR, Jia YH, Bian YD, Tong H, Qu JJ, Wang K, et al. Autocrine Motility Factor Promotes Endometrial Cancer Progression by Targeting GPER-1. *Cell Commun Signal* (2019) 17:22. doi: 10.1186/s12964-019-0336-4
88. Bulletti C, Coccia ME, Battistoni S, Borini A. Endometriosis and Infertility. *J Assist Reprod Genet* (2010) 27:441–7. doi: 10.1007/s10815-010-9436-1
89. Giudice LC. Endometrium in PCOS: Implantation and Predisposition to Endocrine CA. *Best Pract Res Clin Endocrinol Metab* (2006) 20:235–44. doi: 10.1016/j.beem.2006.03.005
90. Shang K, Jia X, Qiao J, Kang J, Guan Y. Endometrial Abnormality in Women With Polycystic Ovary Syndrome. *Reprod Sci* (2012) 19:674–83. doi: 10.1177/1933719111430993
91. Delvoux B, Groothuis P, D'Hooghe T, Kyama C, Dunselman G, Romano A. Increased Production of 17β-Estradiol in Endometriosis Lesions is the Result of Impaired Metabolism. *J Clin Endocrinol Metab* (2009) 94:876–83. doi: 10.1210/jc.2008-2218
92. Zhang H, Zhao X, Liu S, Li J, Wen Z, Li M. 17βe2 Promotes Cell Proliferation in Endometriosis by Decreasing PTEN *via* Nfκb-Dependent Pathway. *Mol Cell Endocrinol* (2010) 317:31–43. doi: 10.1016/j.mce.2009.11.009
93. Tang ZR, Zhang R, Lian ZX, Deng SL, Yu K. Estrogen-Receptor Expression and Function in Female Reproductive Disease. *Cells* (2019) 8:1123. doi: 10.3390/cells8101123
94. Xu Z, Zhang L, Yu Q, Zhang Y, Yan L, Chen Z-J. The Estrogen-Regulated lncRNA H19/miR-216a-5p Axis Alters Stromal Cell Invasion and Migration *via* ACTA2 in Endometriosis. *Mol Hum Reprod* (2019) 25:550–61. doi: 10.1093/molehr/gaz040
95. Lin BC, Suzawa M, Blind RD, Tobias SC, Bulun SE, Scanlan TS, et al. Stimulating the GPR30 Estrogen Receptor With a Novel Tamoxifen Analogue Activates SF-1 and Promotes Endometrial Cell Proliferation. *Cancer Res* (2009) 69:5415–23. doi: 10.1158/0008-5472.Can-08-1622
96. Lin SL, Tu BB, Du XG, Yan LY, Qiao J. Lower Expression of ER-Alpha36 is Associated With the Development of Endometrial Hyperplasia in PCOS Patients. *Histol Histopathol* (2013) 28:1491–8. doi: 10.14670/HH-28.1491
97. Artimani T, Saidijam M, Aflatoonian R, Amiri I, Ashrafi M, Shabab N, et al. Estrogen and Progesterone Receptor Subtype Expression in Granulosa Cells From Women With Polycystic Ovary Syndrome. *Gynecol Endocrinol* (2015) 31:379–83. doi: 10.3109/09513590.2014.1001733
98. Bulun SE, Monsavais D, Pavone ME, Dyson M, Xue Q, Attar E, et al. Role of Estrogen Receptor-Beta in Endometriosis. *Semin Reprod Med* (2012) 30:39–45. doi: 10.1055/s-0031-1299596
99. Han SJ, Jung SY, Wu S-P, Hawkins SM, Park MJ, Kyo S, et al. Estrogen Receptor β Modulates Apoptosis Complexes and the Inflammasome to Drive the Pathogenesis of Endometriosis. *Cell* (2015) 163:960–74. doi: 10.1016/j.cell.2015.10.034
100. Monsivais D, Dyson MT, Yin P, Coon JS, Navarro A, Feng G, et al. ERbeta- and Prostaglandin E2-Regulated Pathways Integrate Cell Proliferation *via* Ras-Like and Estrogen-Regulated Growth Inhibitor in Endometriosis. *Mol Endocrinol* (2014) 28:1304–15. doi: 10.1210/me.2013-1421
101. Cheng CW, Licence D, Cook E, Luo F, Arends MJ, Smith SK, et al. Activation of Mutated K-Ras in Donor Endometrial Epithelium and Stroma Promotes Lesion Growth in an Intact Immunocompetent Murine Model of Endometriosis. *J Pathol* (2011) 224:261–9. doi: 10.1002/path.2852
102. Han SJ, O'Malley BW, DeMayo FJ. An Estrogen Receptor Alpha Activity Indicator Model in Mice. *Genesis* (2009) 47:815–24. doi: 10.1002/dvg.20572
103. Burns KA, Rodriguez KF, Hewitt SC, Janardhan KS, Young SL, Korach KS. Role of Estrogen Receptor Signaling Required for Endometriosis-Like Lesion Establishment in a Mouse Model. *Endocrinology* (2012) 153:3960–71. doi: 10.1210/en.2012-1294
104. Hapangama D, Kamal A, Bulmer J. Estrogen Receptor β: The Guardian of the Endometrium. *Hum Reprod Update* (2014) 21:174–93. doi: 10.1093/humupd/dmu053
105. Hu K, Zhong G, He F. Expression of Estrogen Receptors ER Alpha and ER Beta in Endometrial Hyperplasia and Adenocarcinoma. *Int J Gynecol Cancer* (2005) 15:537–41. doi: 10.1111/j.1525-1438.2005.15321.x
106. Uchikawa J, Shiozawa T, Shih HC, Miyamoto T, Feng YZ, Kashima H, et al. Expression of Steroid Receptor Coactivators and Corepressors in Human Endometrial Hyperplasia and Carcinoma With Relevance to Steroid Receptors and Ki-67 Expression. *Cancer* (2003) 98:2207–13. doi: 10.1002/cncr.11760
107. Bircan S, Ensari A, Ozturk S, Erdogan N, Dundar I, Ortac F. Immunohistochemical Analysis of C-Myc, C-Jun and Estrogen Receptor in Normal, Hyperplastic and Neoplastic Endometrium. *Pathol Oncol Res* (2005) 11:32–9. doi: 10.1007/Bf03032403
108. Wang YL, Miksicek RJ. Identification of a Dominant Negative Form of the Human Estrogen-Receptor. *Mol Endocrinol* (1991) 5:1707–15. doi: 10.1210/mend-5-11-1707
109. Zhang QX, Hilsenbeck SG, Fuqua SAW, Borg A. Multiple Splicing Variants of the Estrogen Receptor are Present in Individual Human Breast Turners. *J Steroid Biochem* (1996) 59:251–60. doi: 10.1016/S0960-0760(96)00120-3
110. Horvath G, Leser G, Hahlin M, Henriksson M. Exon Deletions and Variants of Human Estrogen Receptor mRNA in Endometrial Hyperplasia and Adenocarcinoma. *Int J Gynecol Cancer* (2000) 10:128–36. doi: 10.1046/j.1525-1438.2000.00009.x
111. Chaidarun SS, Klibanski A, Alexander JM. Tumor-Specific Expression of Alternatively Spliced Estrogen Receptor Messenger Ribonucleic Acid Variants in Human Pituitary Adenomas. *J Clin Endocr Metab* (1997) 82:1058–65. doi: 10.1210/jc.82.4.1058
112. Herynk MH, Fuqua SAW. Estrogen Receptor Mutations in Human Disease. *Endocr Rev* (2004) 25:869–98. doi: 10.1210/er.2003-0010
113. Levin ER. Plasma Membrane Estrogen Receptors. *Trends Endocrin Met* (2009) 20:477–82. doi: 10.1016/j.tem.2009.06.009
114. Brosens J, Verhoeven H, Campo R, Gianaroli L, Gordts S, Hazekamp J, et al. High Endometrial Aromatase P450 mRNA Expression is Associated With

Poor IVF Outcome. *Hum Reprod* (2004) 19:352–6. doi: 10.1093/humrep/deh075
115. Bulun SE, Fang ZJ, Imir G, Gurates B, Tamura M, Yilmaz B, et al. Aromatase and Endometriosis. *Semin Reprod Med* (2004) 22:45–50. doi: 10.1055/s-2004-823026
116. Sanderson PA, Critchley HOD, Williams ARW, Arends MJ, Saunders PTK. New Concepts for an Old Problem: The Diagnosis of Endometrial Hyperplasia. *Hum Reprod Update* (2017) 23:232–54. doi: 10.1093/humupd/dmw042
117. Smith HO, Leslie KK, Singh M, Qualls CR, Revankar CM, Joste NE, et al. GPR30: A Novel Indicator of Poor Survival for Endometrial Carcinoma. *Am J Obstet Gynecol* (2007) 196:386.e1–11. doi: 10.1016/j.ajog.2007.01.004
118. He YY, Cai B, Yang YX, Liu XL, Wan XP. Estrogenic G Protein-Coupled Receptor 30 Signaling is Involved in Regulation of Endometrial Carcinoma by Promoting Proliferation, Invasion Potential, and Interleukin-6 Secretion *via* the MEK/ERK Mitogen-Activated Protein Kinase Pathway. *Cancer Sci* (2009) 100:1051–61. doi: 10.1111/j.1349-7006.2009.01148.x
119. Krakstad C, Trovik J, Wik E, Engelsen IB, Werner HMJ, Birkeland E, et al. Loss of GPER Identifies New Targets for Therapy Among a Subgroup of ER Alpha-Positive Endometrial Cancer Patients With Poor Outcome. *Brit J Cancer* (2012) 106:1682–8. doi: 10.1038/bjc.2012.91
120. Skrzypczak M, Schuller S, Lattrich C, Ignatov A, Ortmann O, Treeck OG. Protein-Coupled Estrogen Receptor (GPER) Expression in Endometrial Adenocarcinoma and Effect of Agonist G-1 on Growth of Endometrial Adenocarcinoma Cell Lines. *Steroids* (2013) 78:1087–91. doi: 10.1016/j.steroids.2013.07.007
121. Paul M, Cholewa K, Mazurek U, Witek A, Wilczok T. Estrogen Receptor Beta Delta 6 (ER Beta Delta 6) Isoform in Human Endometrial Hyperplasia and Adenocarcinoma. *Cancer Invest* (2004) 22:211–8. doi: 10.1081/Cnv-120030209
122. Smuc T, Rizner TL. Aberrant Pre-Receptor Regulation of Estrogen and Progesterone Action in Endometrial Cancer. *Mol Cell Endocrinol* (2009) 301:74–82. doi: 10.1016/j.mce.2008.09.019
123. Skrzypczak M, Bieche I, Szymczak S, Tozlu S, Lewandowski S, Girault I, et al. Evaluation of mRNA Expression of Estrogen Receptor Beta and its Isoforms in Human Normal and Neoplastic Endometrium. *Int J Cancer* (2004) 110:783–7. doi: 10.1002/ijc.20224
124. Haring J, Skrzypczak M, Stegerer A, Lattrich C, Weber F, Gorse R, et al. Estrogen Receptor Beta Transcript Variants Associate With Oncogene Expression in Endometrial Cancer. *Int J Mol Med* (2012) 29:1127–36. doi: 10.3892/ijmm.2012.929
125. Rodriguez AC, Blanchard Z, Maurer KA, Gertz J. Estrogen Signaling in Endometrial Cancer: A Key Oncogenic Pathway With Several Open Questions. *Horm Cancer-Us* (2019) 10:51–63. doi: 10.1007/s12672-019-0358-9
126. Byers M, Kuiper GGJM, Gustafsson JA, ParkSarge OK. Estrogen Receptor-Beta mRNA Expression in Rat Ovary: Down-Regulation by Gonadotropins. *Mol Endocrinol* (1997) 11:172–82. doi: 10.1210/mend.11.2.9887
127. Hu GL, Zhang JB, Zhou XY, Liu JW, Wang Q, Zhang B. Roles of Estrogen Receptor Alpha and Beta in the Regulation of Proliferation in Endometrial Carcinoma. *Pathol Res Pract* (2020) 216:153149. doi: 10.1016/j.prp.2020.153149
128. Hoadley KA, Yau C, Hinoue T, Wolf DM, Lazar AJ, Drill E, et al. Cell-Of-Origin Patterns Dominate the Molecular Classification of 10,000 Tumors From 33 Types of Cancer. *Cell* (2018) 173:291–304. doi: 10.1016/j.cell.2018.03.022
129. Backes FJ, Walker CJ, Goodfellow PJ, Hade EM, Agarwal G, Mutch D, et al. Estrogen Receptor-Alpha as a Predictive Biomarker in Endometrioid Endometrial Cancer. *Gynecol Oncol* (2016) 141:312–7. doi: 10.1016/j.ygyno.2016.03.006
130. Blanchard Z, Vahrenkamp JM, Berrett KC, Arnesen S, Gertz J. Estrogen-Independent Molecular Actions of Mutant Estrogen Receptor 1 in Endometrial Cancer. *Genome Res* (2019) 29:1429–41. doi: 10.1101/gr.244780.118
131. Gertz J, Savic D, Varley KE, Partridge EC, Safi A, Jain P, et al. Distinct Properties of Cell-Type-Specific and Shared Transcription Factor Binding Sites. *Mol Cell* (2013) 52:25–36. doi: 10.1016/j.molcel.2013.08.037
132. Rodriguez AC, Vahrenkamp JM, Berrett KC, Clark KA, Guillen KP, Scherer SD, et al. ETV4 Is Necessary for Estrogen Signaling and Growth in Endometrial Cancer Cells. *Cancer Res* (2020) 80:1234–45. doi: 10.1158/0008-5472.can-19-1382
133. Qi Y, Tan M, Zheng M, Jin S, Wang H, Liu J, et al. Estrogen/estrogen Receptor Promotes the Proliferation of Endometrial Carcinoma Cells by Enhancing hMOF Expression. *Jpn J Clin Oncol* (2020) 50:241–53. doi: 10.1093/jjco/hyz174
134. Judd HL, Mebane-Sims I, Legault C, Wasilauskas C, Johnson S, Merino M. Effects of Hormone Replacement Therapy on Endometrial Histology in Postmenopausal Women. The Postmenopausal Estrogen/Progestin Interventions (PEPI) Trial. The Writing Group for the PEPI Trial. *Jama* (1996) 275:370–5. doi: 10.1001/jama.1996.03530290040035
135. D'Alonzo M, Bounous VE, Villa M, Biglia N. Current Evidence of the Oncological Benefit-Risk Profile of Hormone Replacement Therapy. *Med (Kaunas Lithuania)* (2019) 55:573. doi: 10.3390/medicina55090573
136. Utian WH, Speroff L, Ellman H, Dart C. Comparative Controlled Trial of a Novel Oral Estrogen Therapy, Estradiol Acetate, for Relief of Menopause Symptoms. *Menopause* (2005) 12:708–15. doi: 10.1097/01.gme.0000184220.63459.a8
137. Marjoribanks J, Farquhar C, Roberts H, Lethaby A, Lee J. Long-Term Hormone Therapy for Perimenopausal and Postmenopausal Women. *Cochrane Database Syst Rev* (2017) 1:CD004143. doi: 10.1002/14651858.CD004143.pub5
138. Vajdos FF, Hoth LR, Geoghegan KF, Simons SP, LeMotte PK, Danley DE, et al. The 2.0 A Crystal Structure of the ERalpha Ligand-Binding Domain Complexed With Lasofoxifene. *Protein Sci* (2007) 16:897–905. doi: 10.1110/ps.062729207
139. Shang Y. Molecular Mechanisms of Oestrogen and SERMs in Endometrial Carcinogenesis. *Nat Rev Cancer* (2006) 6:360–8. doi: 10.1038/nrc1879
140. Shang Y. Hormones and Cancer. *Cell Res* (2007) 17:277–9. doi: 10.1038/cr.2007.26
141. Deligdisch L. Hormonal Pathology of the Endometrium. *Mod Pathol* (2000) 13:285–94. doi: 10.1038/modpathol.3880050
142. Nijkang NP, Anderson L, Markham R, Manconi F. Endometrial Polyps: Pathogenesis, Sequelae and Treatment. *SAGE Open Med* (2019) 7:2050312119848247. doi: 10.1177/2050312119848247
143. Polin SA, Ascher SM. The Effect of Tamoxifen on the Genital Tract. *Cancer Imaging* (2008) 8:135. doi: 10.1102/1470-7330.2008.0020
144. Bai JX, Yan B, Zhao ZN, Xiao X, Qin WW, Zhang R, et al. Tamoxifen Represses miR-200 microRNAs and Promotes Epithelial-To-Mesenchymal Transition by Up-Regulating C-Myc in Endometrial Carcinoma Cell Lines. *Endocrinology* (2013) 154:635–45. doi: 10.1210/en.2012-1607
145. Tergas AI, Buell-Gutbrod R, Gwin K, Kocherginsky M, Temkin SM, Fefferman A, et al. Clinico-Pathologic Comparison of Type II Endometrial Cancers Based on Tamoxifen Exposure. *Gynecol Oncol* (2012) 127:316–20. doi: 10.1016/j.ygyno.2012.07.105
146. Fornander T, Cedermark B, Mattsson A, Skoog L, Theve T, Askergren J, et al. Adjuvant Tamoxifen in Early Breast-Cancer - Occurrence of New Primary Cancers. *Lancet* (1989) 1:117–20. doi: 10.1016/s0140-6736(89)91141-0
147. Fisher B, Costantino JP, Redmond CK, Fisher ER, Wickerham DL, Cronin WM, et al. Endometrial Cancer in Tamoxifen-Treated Breast-Cancer Patients - Findings From the National Surgical Adjuvant Breast and Bowel Project (Nsabp) B-14. *J Natl Cancer I* (1994) 86:527–37. doi: 10.1093/jnci/86.7.527
148. Ignatov T, Eggemann H, Semczuk A, Smith B, Bischoff J, Roessner A, et al. Role of GPR30 in Endometrial Pathology After Tamoxifen for Breast Cancer. *Am J Obstet Gynecol* (2010) 203:595.e9–16. doi: 10.1016/j.ajog.2010.07.034
149. Brzozowski AM, Pike AC, Dauter Z, Hubbard RE, Bonn T, Engstrom O, et al. Molecular Basis of Agonism and Antagonism in the Oestrogen Receptor. *Nature* (1997) 389:753–8. doi: 10.1038/39645
150. Kulak JJr., Ferriani RA, Komm BS, Taylor HS. Tissue Selective Estrogen Complexes (TSECs) Differentially Modulate Markers of Proliferation and Differentiation in Endometrial Cells. *Reprod Sci* (2013) 20:129–37. doi: 10.1177/1933719112463251
151. DeMichele A, Troxel AB, Berlin JA, Weber AL, Bunin GR, Turzo E, et al. Impact of Raloxifene or Tamoxifen Use on Endometrial Cancer Risk: A

Population-Based Case-Control Study. *J Clin Oncol* (2008) 26:4151–9. doi: 10.1200/JCO.2007.14.0921
152. Carneiro ALB, Spadella APC, Souza FA, Alves KBF, Araujo-Neto JT, Haidar MA, et al. Effects of Raloxifene Combined With Low-Dose Conjugated Estrogen on the Endometrium in Menopausal Women at High Risk for Breast Cancer. *Clinics (Sao Paulo Brazil)* (2021) 76:e2380. doi: 10.6061/clinics/2021/e2380
153. Swisher DK, Tague RM, Seyler DE. Effect of the Selective Estrogen-Receptor Modulator Raloxifene on Explanted Uterine Growth in Rats. *Drug Dev Res* (1995) 36:43–5. doi: 10.1002/ddr.430360107
154. Buelke-Sam J, Bryant HU, Francis PC. The Selective Estrogen Receptor Modulator, Raloxifene: An Overview of Nonclinical Pharmacology and Reproductive and Developmental Testing. *Reprod Toxicol* (1998) 12:217–21. doi: 10.1016/S0890-6238(98)00003-3
155. Altintas D, Kokcu A, Kandemir B, Tosun M, Cetinkaya MB. Comparison of the Effects of Raloxifene and Anastrozole on Experimental Endometriosis. *Eur J Obstet Gyn R B* (2010) 150:84–7. doi: 10.1016/j.ejogrb.2010.02.004
156. Petrie WK, Dennis MK, Hu C, Dai D, Arterburn JB, Smith HO, et al. Protein-Coupled Estrogen Receptor-Selective Ligands Modulate Endometrial Tumor Growth. *Obstet Gynecol Int* (2013) 2013:472720. doi: 10.1155/2013/472720
157. Shiau AK, Barstad D, Loria PM, Cheng L, Kushner PJ, Agard DA, et al. The Structural Basis of Estrogen Receptor/Coactivator Recognition and the Antagonism of This Interaction by Tamoxifen. *Cell* (1998) 95:927–37. doi: 10.1016/s0092-8674(00)81717-1
158. Dauvois S, White R, Parker MG. The Antiestrogen ICI 182780 Disrupts Estrogen Receptor Nucleocytoplasmic Shuttling. *J Cell Sci* (1993) 106(Pt 4):1377–88. doi: 10.1242/jcs.106.4.1377
159. Berlière M, Charles A, Galant C, Donnez J. Uterine Side Effects of Tamoxifen: A Need for Systematic Pretreatment Screening. *Obstet Gynecol* (1998) 91:40–4. doi: 10.1016/s0029-7844(97)00591-7
160. Komm BS, Mirkin S. An Overview of Current and Emerging SERMs. *J Steroid Biochem Mol Biol* (2014) 143:207–22. doi: 10.1016/j.jsbmb.2014.03.003

Conflict of Interest: The authors declare that the research was conducted in the absence of any commercial or financial relationships that could be construed as a potential conflict of interest.

Publisher's Note: All claims expressed in this article are solely those of the authors and do not necessarily represent those of their affiliated organizations, or those of the publisher, the editors and the reviewers. Any product that may be evaluated in this article, or claim that may be made by its manufacturer, is not guaranteed or endorsed by the publisher.

Copyright © 2022 Yu, Huang, Xu, Li, Fu and Deng. This is an open-access article distributed under the terms of the Creative Commons Attribution License (CC BY). The use, distribution or reproduction in other forums is permitted, provided the original author(s) and the copyright owner(s) are credited and that the original publication in this journal is cited, in accordance with accepted academic practice. No use, distribution or reproduction is permitted which does not comply with these terms.

frontiers | Frontiers in Endocrinology

ORIGINAL RESEARCH
published: 25 April 2022
doi: 10.3389/fendo.2022.852671

HOXA10 Regulates the Synthesis of Cholesterol in Endometrial Stromal Cells

Meixing Yu[1†], Jia Tang[2†], Yanqing Huang[1], Chenbing Guo[1], Peng Du[1], Ning Li[1] and Qingli Quan[2]*

[1] Guangzhou Women and Children's Medical Center, Guangzhou Medical University, Guangzhou, China, [2] NHC Key Laboratory of Male Reproduction and Genetics, Guangdong Provincial Reproductive Science Institute (Guangdong Provincial Fertility Hospital), Guangzhou, China

OPEN ACCESS

Edited by:
Rick Francis Thorne, The University of Newcastle, Australia

Reviewed by:
Hong Zhan, Zhejiang University, China
Vishakha Mahajan, The University of Auckland, New Zealand

***Correspondence:**
Qingli Quan
bioquanqingli@163.com

[†]These authors have contributed equally to this work

Specialty section:
This article was submitted to Reproduction, a section of the journal Frontiers in Endocrinology

Received: *11 January 2022*
Accepted: *17 March 2022*
Published: *25 April 2022*

Citation:
Yu M, Tang J, Huang Y, Guo C, Du P, Li N and Quan Q (2022) HOXA10 Regulates the Synthesis of Cholesterol in Endometrial Stromal Cells. Front. Endocrinol. 13:852671. doi: 10.3389/fendo.2022.852671

Background: The expression of homeobox A10 (HOXA10) in endometrial stromal cells is regulated by steroid hormones, especially by estrogen. As a precursor molecule of estrogen, abnormal cholesterol metabolism is significantly positively correlated with endometriosis. The purpose of this study was to explore the regulation of HOXA10 on cholesterol synthesis in endometrial stromal cells.

Method: mRNA expression data of eutopic endometrial stromal cell (ESC) and ovarian endometriotic cysts stromal cell (OESC) were download from the Gene Expression Omnibus (GEO) databases. Overexpression and silence of HOXA10 were conducted in cultured ESC and subjected to mRNA sequencing. The differentially expressed genes (DEGs) were selected by analyzing the sequencing data. Weighted gene co-expression network analysis (WGCNA) was applied to identify the key genes associated with HOXA10. The methylation rate of HOXA10 CpGs and the correlation between HOXA10 expression and the methylation in eutopic endometrial tissue (EU) and ovarian cyst (OC) were analyzed.

Results: HOXA10 in ESC was significantly higher expressed than that in OESC. Six key genes (HMGCR, MSMO1, ACAT2, HMGCS1, EBP, and SQLE), which were regulated by HOXA10, were identified from the salmon4 module by WGCNA. All these key genes were enriched in cholesterol synthesis. Moreover, the expression of HOXA10 was negatively related to its CpGs methylation rate.

Conclusion: In this study, six key genes that were regulated by HOXA10 were selected, and all of them were enriched in cholesterol synthesis. This finding provided a new insight into the metabolic mechanism of cholesterol in ESC. It also provided a potential treatment strategy for cholesterol metabolism maladjustment in patients with ovarian endometriosis.

Keywords: ovarian endometriosis, cholesterol synthesis, HOXA10 gene, endometrial stromal cell, estrogen

INTRODUCTION

Ovarian endometriosis (OEM) is a common gynecological disease and characterized by the presence of endometrial tissue outside the endometrial cavity, causing chronical pain and infertility (1–3). OEM is also an estrogen-dependent disease (4). Estrogen not only promotes the proliferation of normal endometrium and improves endometrial tissue implantation to the peritoneum but also stimulates local and systemic inflammation (5, 6).

One of the prerequisites for uterus normal function is the endometrium receptivity in which HOXA10, a transcription factor encoding gene, plays critical role (7, 8). In human endometrium, HOXA10 is expressed in both glandular and stromal cells and regulated by estrogens (9). HOXA10 is regulated by steroid hormones because there are functional estrogen response elements (EREs) in the 5′ transcription start site of HOXA10 (10). Additionally, HOXA10 also has a strong correlation with serum lipid in polycystic ovary syndrome (11).

It is reported that local steroid hormones (such as estrone, estradiol, and progesterone) of endometrial and endometriotic tissues are more determined by active local synthesis and metabolism instead of being determined by passive diffusion from circulating steroids (12, 13). In endometriotic lesions, estradiol biosynthesis is higher and estradiol inactivation is lower compared with the normal endometrium (12, 14). Hence, abnormal steroid hormone biosynthesis and metabolism is one of the factors contributing to endometriosis.

The parent molecule of steroid hormone is cholesterol (15). Abnormal cholesterol metabolism has been observed to be correlated with endometriosis (16). Melo et al. reported that the serum levels of low-density lipoprotein (LDL), non-high-density lipoprotein (non-HDL), triglyceride (TG), and total cholesterol (TC) are higher, and even the HDL : TC ratio is lower in patients with endometriosis compared with those without endometriosis (16). Additionally, Mu et al. found that patients with confirmed endometriosis had a significant greater risk of cardiovascular disease than patients without endometriosis (17). Furthermore, gonadotropin-releasing hormone (GnRH) antagonist, as a common medicine used in endometriosis treatment, can inhibit ovarian follicular growth and ovulation, leading to a decreased production of circulating estradiol and a reduced growth of ectopic endometrium. As a side effect of GnRH antagonist, the risk of cardiovascular disease caused by increased serum lipid (TG, LDL, HDL, and even the ratio of LDL cholesterol to HDL cholesterol) also increases at the prolonged low estrogen state (4, 18). These indicate the important role of regulation of cholesterol synthesis in EMs.

Considering the irreplaceable role of HOXA10 in endometrium function and its potential role in cholesterol synthesis, we first analyzed the expression of HOXA10 in both ESC and OESC and performed HOXA10 overexpression and RNA interference (RNAi) on the ESC. Then, the key genes that were associated with HOXA10 expression were screened. Furthermore, given that an abnormal hypermethylation of HOXA10 has been found in ectopic lesions (19), we also detected the methylation rate of the representative CpG sites of HOXA10 in eutopic and ectopic tissue. We want to figure out how HOXA10 acts in cholesterol synthesis in the endometrium. Our research partly illustrated the role of HOXA10 in cholesterol synthesis in endometriosis, which provides new insights for the development and treatment for OEMs.

METHODS AND MATERIALS

Patients Inclusion

Considering the potential regulatory effect of HOXA10 on the estrogen metabolism pathway, we first excluded patients who received hormone therapy. We enrolled 48 women with a history of OEMs or non-endometriosis-related disease (**Supplementary Table S1**). All study participants had a normal menstrual cycle and had not used oral contraception, hormonal therapy, or an intrauterine device for at least 3 months before the endometrial biopsy. Tissue samples were collected from patients by laparoscopic surgery or hysteroscopy during the proliferative phase of their menstrual cycle for the evaluation of pelvic pain, suspected ovarian cysts, or other unknown endometrial diseases. Then, all diagnoses were confirmed by tissue biopsy.

Data Collection and the HOXA10 mRNA Expression Level Analysis in ESC and OESC

The mRNA expression microarray dataset (GSE136412) was downloaded from the GEO database (https://www.ncbi.nlm.nih.gov/geo/query/acc.cgi?acc). The mRNA expression of HOXA10 and the key genes of ESC and OESC were analyzed (**Supplementary Table S2**).

ESC Isolation, Purification, and Identification

ESC used in our study were respectively isolated from five eutopic endometrium tissues from patients with non-endometriosis-related diseases. Tissues were digested with 1 mg/ml type IV collagenases (Solarbio, Beijing, China) and 150 U/ml DNase I (Tiangen Biotech, Beijing, China) in 37°C for 30 min and homogenized into single-cell suspension. Then, cells, which were filtered through a 40-μm filter (Solarbio, CHN), were collected and resuspended in Dulbecco's modified Eagle's medium (DMEM)/F12 complete medium (HyClone, Logan, UT, USA) containing 10% fetal bovine serum (FBS) (GIBCO, Grand Island, NY, USA). ESC with high purity were cultured by differential adherent and identified by using Alexa Flour 488 anti-human vimentin antibody (BD Biosciences, USA) and Alexa Flour 647 anti-human cytokeratin antibody (BD Biosciences, Franklin Lakes, NJ, USA). The flow cytometry data and gating strategies are provided in **Supplementary Data 1**.

Over-Expression and Silence of HOXA10 in Cultured ESC

For HOXA10 over-expression, the pHBLV-ZsGreen-HOXA10 plasmid (Han Bio, Shanghai, China) and packaging plasmid (PSPAX2, pCMV-VSVG) (Han Bio, Shanghai, China) were transfected into 293T (Procell, Wuhan, China) to package the recombinant lentivirus. The plasmid pHBLV-ZsGreen was set as control. Virus was collected by ultracentrifugation, and the final

concentration was 2×10^7 virus/ml. ESC cells of HOXA10 overexpression group (HOXA10OE) and control group (ZsGreen) were treated with 0.8 μg/μl polybrene for 30 min, respectively. Then, ESC cells in both groups were infected with corresponding viruses, respectively [multiplicity of infection (MOI) ratio = 10]. For HOXA10 silence, ESC cells of HOXA10 silence group (siHOXA10) and control group (siNC) were transfected with 50 nM of HOXA10 siRNA (RIBOBIO, Guangzhou, China) and 50 nM of NC siRNA (RIBOBIO, Guangzhou, China), respectively, by Lipofectamine 3000 Transfection Reagent lipo3000 (Thermo Fisher Scientific, Waltham, MA, USA). Total mRNAs of all treatment groups and control groups were extracted with an RNeasy Mini kit (Qiagen, Hilden, Germary) and subjected to RNA sequencing (Berry Genomic, Illumina Nova 6000). The fragments per kilobase million (FPKM) of RNA-seq data are provided in **Supplementary Table S3**. The sequence of HOXA10 siRNA was 5′-GAGCTCACAGCCAACTTTA -3′.

Differentially Expressed Genes Screening

Two groups of differentially expressed genes were screened respectively in both HOXA10-overexpresed ESC and HOXA10-RNAi ESC by comparing with their control group *via* the "limma" R package, according to the criteria of adj.P.Val <0.05 and |logFC| > 2 (20). By merging the two sets of different genes and removing duplicate genes, a set of genes was screened as DEGs.

Weighted Gene Co-Expression Network Analysis

WGCNA is used to cluster highly coordinated gene sets and determine phenotype-related genes based on their correlation (21). To identify the related genes of HOXA10, we used WGCNA R package to analyze the mRNA expression data of HOXA10OE group, siHOXA10 group, and control groups. The soft-thresholding power was determined based on a scale-free $R^2 = 0.85$. Similar dynamic modules were merged by setting 0.2 as the dissimilarity threshold. Pearson correlation analysis was used to selected the model related to HOXA10 expression. HOXA10-associated genes were identified when the gene significance (GS) is >0.8 and module membership (MM) is >0.8 in the selected model.

PPI and Cystoscope

Protein–protein interactions (PPIs) are a vital mechanism for the regulation and coordination of most biological processes within the cell (22). Intersection genes were selected as candidate genes between the DEGs and HOXA10-associated genes screened by WGCNA. To investigate the key genes that were related to HOXA10, PPIs were constructed in the database (https://www.string-db.org) and visualized by Cytoscape software (version 3.2.1) based on the intersection genes. Then, key genes were selected by MCODE APP in Cytoscape software.

Function Enrichment Analysis and Correlation Analysis Between HOXA10 and the Key Genes

To identify the significant biological functions and pathways in which the key genes were involved, Gene Ontology (GO) functional annotation and Kyoto Encyclopedia of Genes and Genomes (KEGG) analysis with the "clusterProfiler" R package were applied. p-value < 0.05 was chosen as the criteria. The correlation between HOXA10 and the key genes were analyzed.

Validation of mRNA Expression of Six Key Genes in Both HOXA10-Overexpresed ESC and HOXA10-RNAi ESC

We detected the mRNA expression levels of these six genes in HOXA10-overexpressing ESC and HOXA10-knockout ESC by quantitative PCR (qPCR). The total RNA of ectopic and eutopic tissue was extracted according to the RNeasy Plus Mini Kit protocol (Qiagen, Hilden, Germary). According to the Iscript cDNA Synthesis Kit protocol (Bio-Rad, Hercules, CA, USA), cDNA sample were synthesized. qPCR reactions were carried out by the iTaq Univer SYBR Green Supermix Kit protocol (Bio-Rad, Hercules, CA, USA) by repeating each reaction at least three times. The information about the primers is provided in **Supplementary Table S4**.

Detection of Methylation Rate of HOXA10 CpG Site

According to the reported research (19), we selected three adjacent CpG sites in the third islands, which have only been methylation modified in endometriosis patients. Genomic DNA of both OC and EU tissues were extracted with the QIAamp DNA Mini Kit according to the manufacturer's instructions (Qiagen, Hilden, Germany). Then, each genomic DNA was converted into bis-DNA with the EZ DNA Methylation-Lightning Kit in accordance with the manufacturer's protocol (Zymo Research, Irvine, CA, USA). The specific methylation and non-methylation probes for CpGs of interest were designed, and the methylation rates of these CpGs sites were detected by droplet digital PCR (ddPCR). Primers and probes were designed on the basis of the above CpG sites (13). Digital droplet PCR was conducted, and the methylation rate (MR) of each CpGs was calculated. MR (%) = CMS/(CMS + CNMS) × 100% (CMS and CNMS represent the copies for the methylation and non-methylation sites, respectively). The total RNA were extracted, and cDNA was synthesized. qPCR reactions were carried out by the iTaq Univer SYBR Green Supermix Kit protocol (Bio-Rad, Hercules, CA, USA) by repeating each reaction at least three times. To investigate the correlation between the MR of HOXA10 and HOXA10 mRNA expression (**Supplementary Table S5**), the correlation matrix was generated. The primers and probes were listed below:

HOXA10 primer: forward: 5′- TCCGAGAGCAGCAAAGCCT-3′, reverse: 5′-TCCGAGAGCAGCAAAGCCT-3′.

HOXA10 methylation primer: forward: 5′-ATGTTA GGTAATTTTAAAGGTGAA-3′, reverse: 5′-CTTCTCCAAC TCCAATATCTAAT-3′, HOXA10 methylation probes: M: 5′-FAM/TGGTCGGAAGAAGCGTTGTTTTTATAC/BHQ1-3′, NM: 5′-HEX/TGGTTGGAAGAAGTGTTGTTTTTATAT/BHQ1-3′. (M, methylation; NM, non-methylation).

Data Analysis

The statistical analyses performed in this study were conducted in the R environment (version 4.0.3) and GraphPad Prism

(version 8.0). The comparison of FPKM of HOXA10 in ESC and OESC was analyzed with t-test. The comparison of mRNA expressions and MRs of HOXA10 in tissue samples was analyzed by GraphPad Prism with non-parametric t-test. The comparison of key genes mRNA expressions was analyzed by t-test. $p<0.05$ was considered a significant difference. The correlation of Dct and MRs of HOXA10 in tissue samples was analyzed by "corrplor" R package. All R scripts were provided in **Supplementary Data 2**.

RESULTS

HOXA10 mRNA Expression in ESC and OESC

To compare the expression of HOXA10 in ESC and OESC, we analyzed the download data (GSE136412). The mRNA expression of HOXA10 in ESC was significantly higher than that in OESC no matter in 2D or 3D culture system ($p<0.0001$ and $p<0.0001$, respectively) (**Figure 1**).

The Effects of HOXA10 Over-Expression or Silence in Cultured ESC

The cultured cells were verified as ESC by flow cytometry, which positively expressed vimentin and negatively expressed cytokeratin (**Figures 2A, B**). mRNA sequencing was conducted in HOXA10-OE ESC (**Figure 2C**) and HOXA10 RNAi ESC (**Figure 2D**). There were 341 DEGs including 103 upregulated genes and 238 downregulated genes in HOXA10 over-expression group (**Figure 2E**). In HOXA10 RNAi group, there were 418 DEGs including 132 upregulated genes and 286 downregulated genes (**Figure 2F**). A union of 636 DEGs that associated with HOXA10 expression were selected after removing the repeated genes (**Figure 2G**).

Weighted Gene Co-Expression Network Analysis

For screening the HOXA10-associated genes, WGCNA was used to analyze the expression values of 19,225 genes in 20 samples of 4 groups. The soft-thresholding power was 5, which was determined based on a scale-free R^2 (R^2 = 0.85) (**Figure 3A**). Therefore, we identified 37 modules when the Diss Thres was set as 0.2 after merging dynamic modules, as shown in the clustering dendrograms (**Figure 3B**). Then, to identify the most HOXA10-related module, we calculated the correlation coefficients between modules and HOXA10 expression. As shown in **Figure 3C**, the salmon4 module exhibited the strongest correlation, with the Pearson correlation of 0.94 and the p-value of 4E−10. **Figure 3D** also indicated that the salmon4 module was most correlated to the HOXA10. Key genes are indicated in the upper-right corner with the threshold of gene significance (GS) > 0.8 and module membership (MM) > 0.8. Finally, for the subsequent analysis, we set the thresholds of GS > 0.8 and MM > 0.8, which allowed us to screen out the final 180 HOXA10-associated genes (**Figure 3E**).

Screening and Pathway Enrich of Key Gene

We selected the 42 intersection genes between the 636 DEGs and 180 HOXA10-associated genes (**Figure 4A**). To investigate the key genes that were related to HOXA10, PPIs were constructed in the database (https://www.string-db.org) and visualized by Cytoscape software (version 3.2.1) based on the 42-candidate gene (**Figure 4B**). HMGCR, MSMO1, ACAT2, HMGCS1, EBP, and SQLE were selected by MCODE APP as key genes (**Figure 4C**). The correlation analysis indicated that all these key genes showed significantly negative relationship with HOXA10 (**Figure 4D**). As shown in **Figure 4E**, the six key genes were markedly enriched in the biological process (BP) of

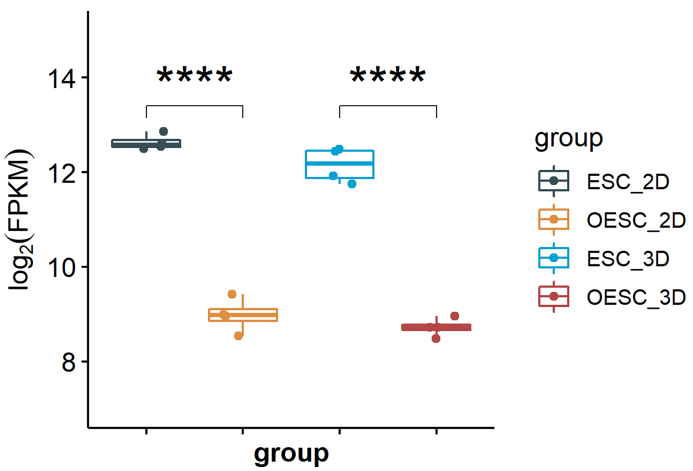

FIGURE 1 | The mRNA expression of HOXA10 in ESC and OESC (ESC_2D, ESC cultured in 2D system; OESC_2D, OESC cultured in 2D system; ESC_3D, ESC cultured in 3D system; OESC_3D, OESC cultured in 3D system. ****p<0.0001).

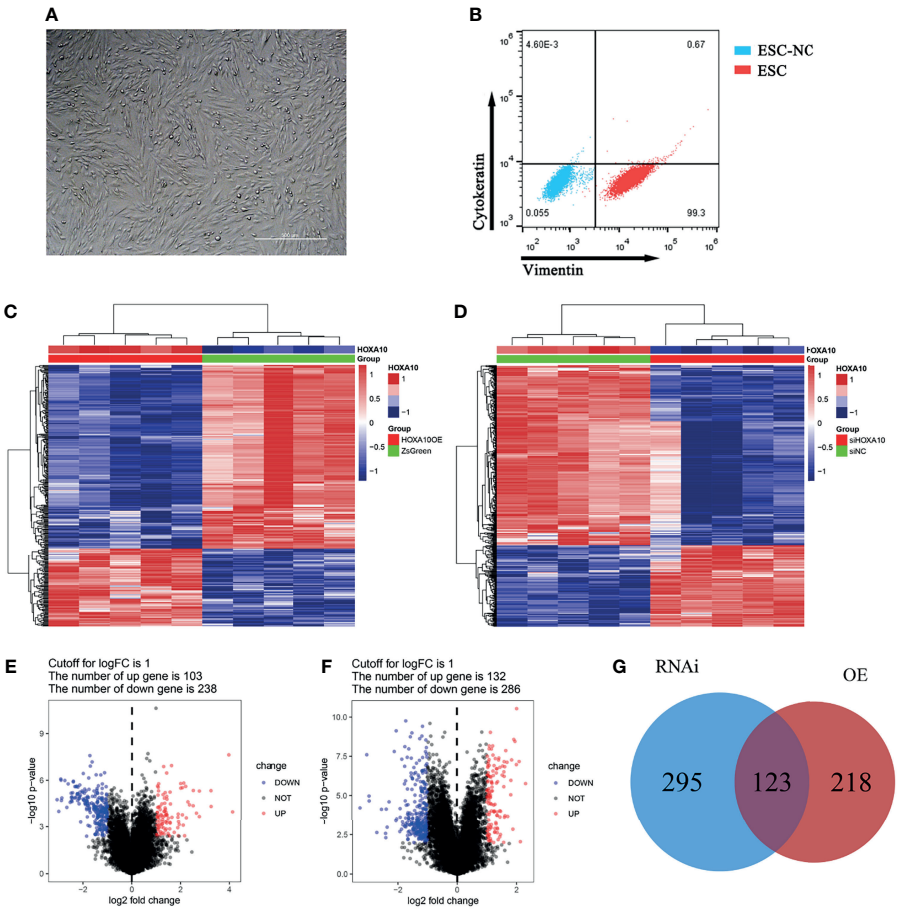

FIGURE 2 | DEGs screening between HOXA10 over-expression and HOXA10 silence ESC. **(A)** ESC culturation. **(B)** ESC identification. **(C)** Heatmap of DEGs between HOXA10OE group and ZsGreen group. **(D)** Heatmap of DEGs between siHOXA10 group and siNC group. **(E)** Volcano plot of DEGs between HOXA10OE group and ZsGreen group. **(F)** DEGs between siHOXA10 group and siNC group. **(G)** The union of two sets of DEGs (HOXA10OE, HOXA10 over-expression ESC; ZsGreen, control for over-expression group; siHOXA10, HOXA10 silence ESC; siNC, control for silence group).

cholesterol synthesis pathway by GO analysis; the main related molecular function (MF) terms was oxidoreductase activity, and the main cellular component (CC) was peroxisomal membrane. KEGG analysis demonstrated that the most significantly enriched pathway was steroid biosynthesis and terpenoid backbone biosynthesis (**Figure 4F**).

The Regulation of HOXA10 on Key Genes

To figure out the details of the HOXA10 regulation effect on key genes, we analyzed the gene expression [log2(fpkm+1)] of both HOXA10 and key genes in four groups (**Figure 5A**). HOXA10 over-expression downregulated all the key genes (**Figure 5B**), and interfering with HOXA10 expression by siRNA up-regulated the expression of ACAT2, EBP, and SQLE (**Figure 5C**).

Validation of mRNA Expression of Six Key Genes

We verified the mRNA expression levels of key genes in the above four groups of ESC by qPCR. As shown in **Figure 6**, all six genes were down-regulated in HOXA10-overexpresed ESC (**Figure 6A**). In addition, five of the six key genes were upregulated in HOXA10-RNAi ESC except for HMGCR (**Figure 6B**). The qPCR results confirmed the results of mRNA sequencing.

Comparation of the Methylation Rate of HOXA10 in EU and OC Tissues

We collected surgical endometrial tissue samples from patients with non-endometriosis-related disease [negative control (NC); n = 24], surgical eutopic endometrial tissue samples from patients with OEMs (EU; n = 16), and ovarian cyst (the chocolate-colored part of the tissue) (OC; n = 24). We further verified the MR of the selected CpGs in both OC and EU tissue. As shown in **Figure 7**, the MR of the representative sites in OC was remarkably higher than that in EU ($p<0.0001$) (**Figure 7A**), while the expression of HOXA10 in OC was notably lower than that in EU ($p<0.0001$) (**Figure 7B**). The methylation rates of the representative CpGs were positively correlated with ΔCt values HOXA10 mRNA expressions ($R=0.708$) (**Figure 7C**). Results of

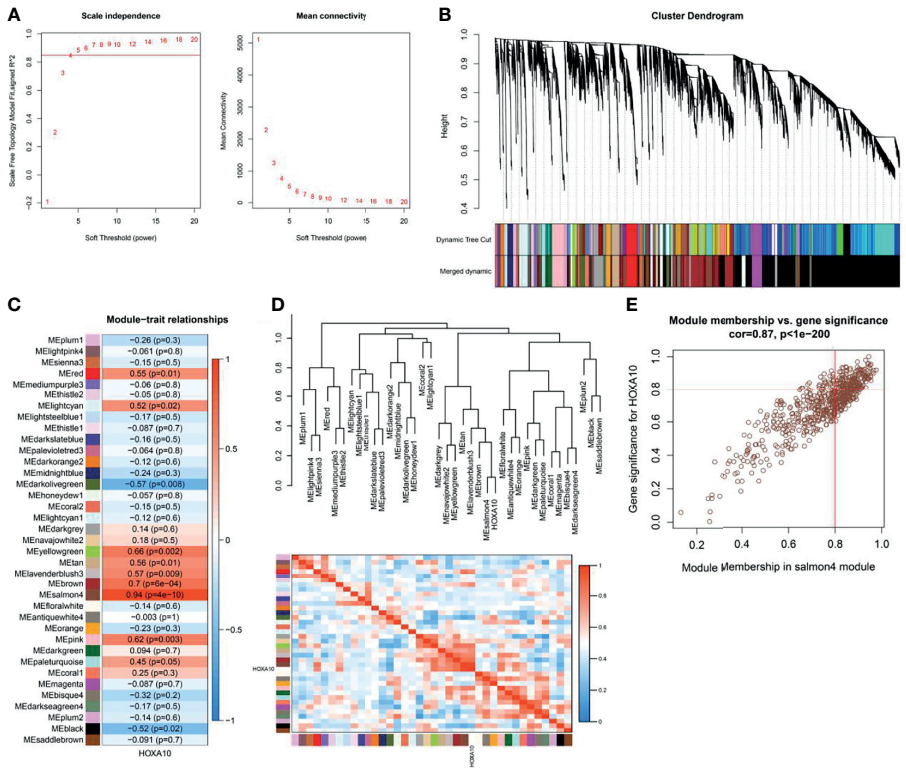

FIGURE 3 | Weighted gene co-expression network analysis. **(A)** Selection of the optimal soft-thresholding power for the scale-free network. **(B)** Module clustering dendrograms. **(C)** Correlation analysis of the module most associated with HOXA10 (Pearson's correlation coefficient and the corresponding p-value are shown in the horizonal bars). **(D)** Cluster plot of the relationship between HOXA10 and the 37 modules. **(E)** Scatter plot of the genes in salmon4 module showing the relationship between GS and MM (GS, gene significance; MM, module membership).

EU and OC from the same patient showed that the MR of the representative sites in OC was also remarkably higher than that in EU ($p<0.0001$) (**Figure 7D**), the expression of HOXA10 in OC was also notably lower than that in EU ($p<0.0001$) (**Figure 7E**). The methylation rates of the representative CpGs were positively correlated with ΔCt values HOXA10 mRNA expressions ($R=0.716$) (**Figure 7F**).

DISCUSSION

HOXA10 is highly expressed in endometrial stromal cells and plays a key role in the proliferation and differentiation of the endometrium (23). However, the expression of HOXA10 is significantly diminished in ectopic lesions of OEMs (24). What is more, patients with endometriosis have a significantly increased risk of diseases, which is probably due to the lipids (total cholesterol, LDL-C) (25). It is reported that the expression of HOXA10 in patients with polycystic ovary is positively correlated with the concentrations of blood HDL and is negatively correlated with the concentrations of blood TG, TC, and LDL (11). Therefore, HOXA10 may play a regulatory role in the steroid hormone–cholesterol synthesis pathway of endometrial stromal cells. The expression of HOXA10 in ESC is regulated by the level of steroid hormones (10, 26), but the regulation mechanism is still unclear. In patients with OEMs, the expression of HOXA10 in ectopic lesions is diminished or significantly downregulated (24, 27). In patients with OEMs, it is accompanied by abnormal cholesterol metabolism. As cholesterol is the parent molecule of sterol hormones, HOXA10 may play a regulatory role in the steroid hormone–cholesterol synthesis pathway of endometrial stromal cells. The expression of HOXA10 is diminished in ectopic endometrium. Abnormal cholesterol metabolism in patients with ovarian endometriosis may be related to the abnormal low expression of HOXA10.

In our study, we found that HOXA10 mRNA expression in ESC was significantly lower than that in OESC. Six genes (HMGCOR, MSMO1, ACAT2, HMGCS1, EBP, and SQLE) were screened and markedly enriched in cholesterol and secondary alcohol synthesis pathway (**Figures 4C–F**). HMG-CoA reductase (HMGCR), as the rate-limiting enzyme for cholesterol synthesis, catalyzes the formation of mevalonate, which is a key intermediate for sterol synthesis (28, 29). The 3-hydroxy-3-methylglutaryl-CoA synthase 1 (HMGCS1) works as a potential gatekeeper in the mevalonate pathway (30). Squalene epoxidase (SQLE) is also one of the rate-limiting enzymes in the cholesterol biosynthesis (31). MSMO1 is the oxidase-encoding gene, catalyzing demethylation of C4-methylsterols, which was named as meiosis activating and stimulated cell over proliferation (32). The protein encoded by

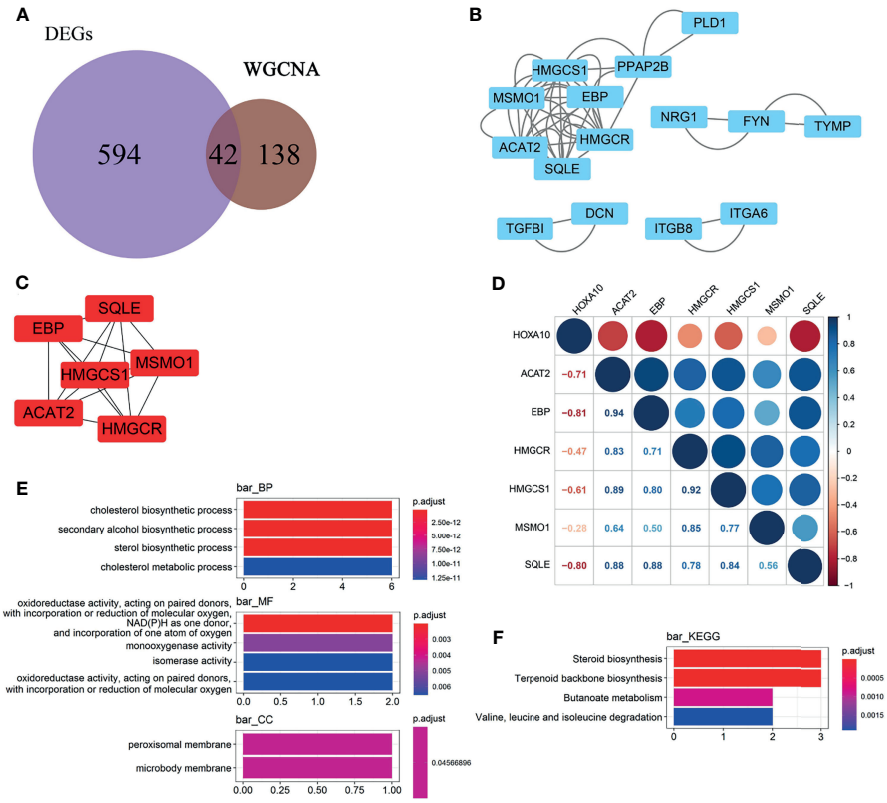

FIGURE 4 | Selection and enrichment analysis of the key genes. **(A)** Venn diagrams showing the candidate genes between the 636 DEGs and 180 HOXA10-associated genes. **(B)** PPI network of the candidate genes. **(C)** Key genes selected by MCODE APP. **(D)** Correlation between the HOXA10 and the six selected key genes. **(E)** GO enrichment analysis of the key genes. **(F)** KEGG enrichment analysis of the key genes (BP, biological process; CC, cellular component; MF, molecular function).

gene EBP is an ER-localized protein, which is also a 3-beta hydroxysteroid-delta (8) and delta (7)-isomerase and essential for sterol biosynthesis in eukaryotic cells (33). ACAT1 encodes an enzyme that synthesizes cholesterol and long-chain fatty acids into cholesterol esters, which is transported to the circulatory system through cholesterol ester transfer protein (34). Therefore, we proposed that HOXA10 may regulate cholesterol synthesis in endometrial stromal cells.

All key genes were downregulated by HOXA10 overexpression, and at least three key genes (ACAT2, EBP, and SQLE) were upregulated by HOXA10 silence. Compared with the cholesterol synthesis promoted by HOXA10 downregulation, the upregulation of HOXA10 inhibited the synthesis of cholesterol more significantly. Hence, we proposed that HOXA10 acts as an inhibitor of cholesterol synthesis, and the low expression of HOXA10 in ectopic lesions loses its regulatory effect on cholesterol synthesis. Additionally, we also found that MRs of the representative CpGs was significantly related to HOXA10 mRNA expression in endometrial tissue. Therefore, HOXA10 DNA methylation modification be involved in regulating its mRNA expression. As one of the epigenetic modification, DNA methylation modification is the early event of diseases (35), indicating that HOXA10 methylation may be the early indicator of endometriosis. It should be noted that chocolate cysts contain very few endometriotic tissues (36), so further purification of the ovarian ectopic endometrial tissue is required to illustrate the relationship between HOXA10 mRNA and methylation rates.

It was reported that steroid hormone regulates the expression of HOXA10 *in vivo* and *in vitro* (37). After binding to estradiol, the estrogen receptor binds to the estrogen response elements (EREs) of HOXA10 to upregulate its expression (10). In the primary endometrial cell from healthy volunteers, the expression of HOXA10 is significantly upregulated after being treated with 17β-estradiol (9). Considering that cholesterol is the parent molecule of estrogen and HOXA10 regulated the synthesis of cholesterol in ESC, we speculated that HOXA10 plays an important negative feedback regulation role in the pathway of cholesterol and estrogen metabolism. After estrogen upregulated the expression of HOXA10, the synthesis of cholesterol was inhibited by downregulating the six key genes of cholesterol synthesis, thereby reducing the synthesis of estrogen parent molecules. Therefore, for patients with OEMs, the abnormal expression of HOXA10 in OESC reduced the inhibitory effect on the cholesterol synthesis pathway, leading to an increased risk of sterol metabolism diseases. The cholesterol abnormal

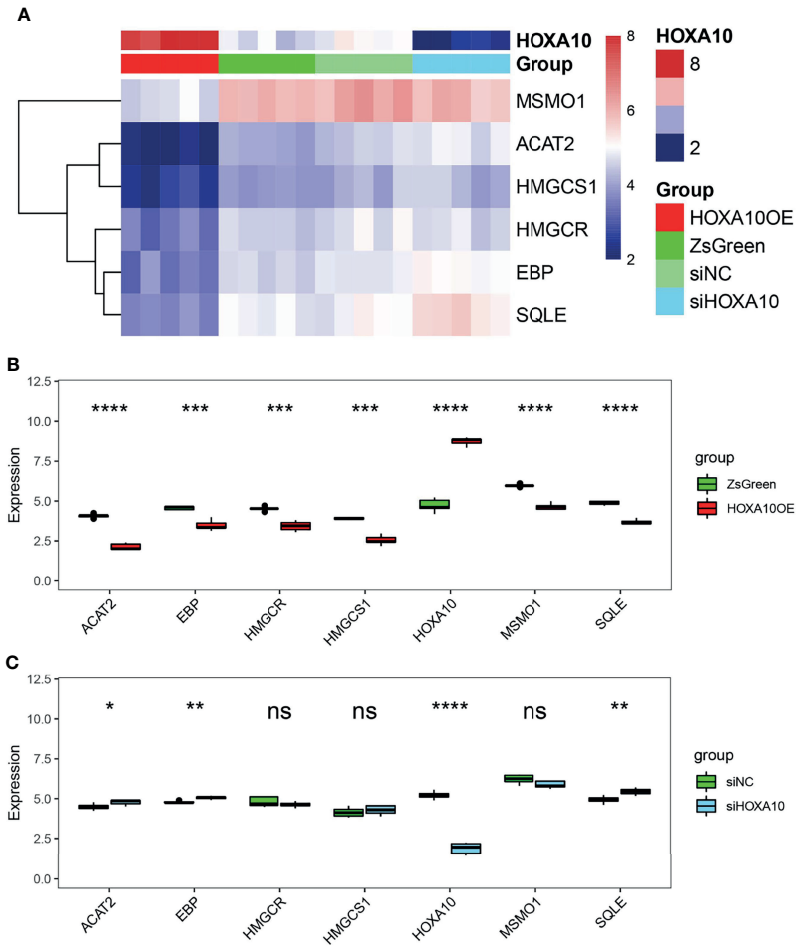

FIGURE 5 | The regulatory effect of HOXA10 on key genes. **(A)** Heatmap of key genes in HOXA10OE, ZsGreen, siHOXA10, and siNC groups. **(B)** The comparison of key genes mRNA expression in HOXA10OE and ZsGreen groups. **(C)** The comparison of key genes mRNA expression in siHOXA10 and siNC groups (HOXA10OE, HOXA10 over expression ESC; ZsGreen, control for over-expression group; siHOXA10, HOXA10 silence ESC; siNC, control for silence group. *p<0.05, **p<0.01, ***p<0.001, ****p<0.0001; ns, no significant difference).

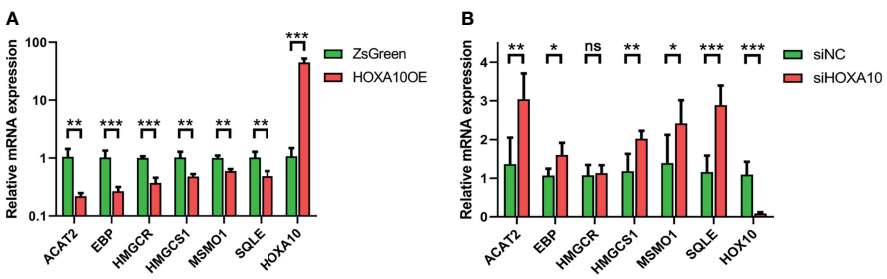

FIGURE 6 | Validation of mRNA expression of six key genes by qPCR. **(A)** The relative mRNA expressions of the six key genes in HOXA10OE and ZsGreen groups. **(B)** The relative mRNA expressions of the six key genes in siHOXA10 and siNC groups (HOXA10OE, HOXA10 over expression ESC; ZsGreen, control for HOXA10OE; siHOXA10, HOXA10 silence ESC; siNC, control for silence group; *p<0.05, **p<0.01, ***p<0.001. ns, no significant difference).

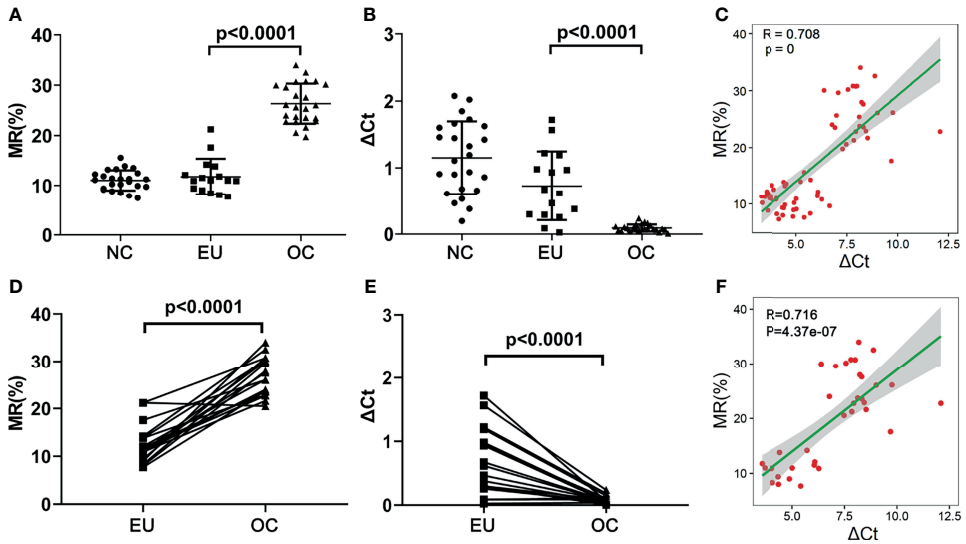

FIGURE 7 | The MRs and mRNA expression of HOXA10 in NC, EU and OC. **(A)** The MRs of representative CpGs detected by ddPCR. **(B)** The mRNA expression of HOXA10 in EU and OC. **(C)** The correlation between MRs and HOXA10 mRNA expression. **(D)** The comparisons of MR in EU and OC from the same patients. **(E)** The comparisons of HOXA10 mRNA expression in EU and OC from the same patients. **(F)** The correlation between MRs and HOXA10 mRNA expressions in EU and OC from the same patients (MR, methylation rate; EU, eutopic endometrial tissues; OC, ovarian cyst; NC, normal control).

metabolism has been observed to be correlated with the endometriosis (16). Mu et al. reported a strong association between confirmed EMs and hypercholesterolemia and hypertension in a large prospective cohort study (17). We also proposed that patients treated with GnRH antagonist may also need to consider the use of drugs that inhibit cholesterol accumulation. HOXA10 and its methylation modification sites may become one of the potential therapeutic targets for OEMs.

However, our study was not without its shortcomings. We have not verified the regulatory effect of HOXA10 on the six key genes in ectopic endometrial stromal cells because we have not obtained target cells that can be passaged stably. Additionally, whether HOXA10 directly or indirectly affects these six key genes needs to be verified by Hi-C or Chip-seq. The correlation between methylation and HOXA10 expression needs to be verified by methylation editing in our future study.

In summary, we found that HOXA10 regulates the cholesterol synthesis in ESC through the six key genes. We speculated that the relatively high expression of HOXA10 in normal endometrium inhibits the excessive synthesis of cholesterol. On the contrary, the relatively low expression of HOXA10 in ectopic lesions may lead to the loss of proper inhibition of cholesterol synthesis in the patients with OEMS. In addition, the expression of HOXA10 may be regulated by the methylation modification on HOXA10 CpGs.

DATA AVAILABILITY STATEMENT

The datasets presented in this study can be found in online repositories. The names of the repository/repositories and accession number(s) can be found in the article/**Supplementary Material**.

ETHICS STATEMENT

The studies involving human participants were reviewed and approved by the Ethics Committee of Guangzhou Women and Children's Medical Center, Guangzhou, China (Permit Approval No. 2017102709). The patients/participants provided their written informed consent to participate in this study.

AUTHOR CONTRIBUTIONS

MY designed the research and revised the language of the paper. JT, CG, PD, and NL collected the research data. YH sorted the patients' information. QL analyzed the data and wrote the draft. All authors contributed to the article and approved the submitted version.

SUPPLEMENTARY MATERIAL

The Supplementary Material for this article can be found online at: https://www.frontiersin.org/articles/10.3389/fendo.2022.852671/full#supplementary-material

Supplementary Table 1 | Clinical characteristics of the study participants.

Supplementary Table 2 | HOXA10 mRNA expression level in ESC and OESC.

Supplementary Table 3 | The FPKM of HOXA10 over-expression and HOXA10 silence in ESC.

Supplementary Table 4 | The qPCR primers for mRNA expression of the six genes.

Supplementary Table 5 | The data of MR and mRNA expression of HOXA10 in tissue samples.

Supplementary Data Sheet 1 | The flow cytometry data and gating strategies.

Supplementary Data Sheet 2 | The R script.

REFERENCES

1. Giudice L. Clinical Practice. Endometriosis. *N Engl J Med* (2010) 362:2389–98. doi: 10.1056/NEJMcp1000274
2. Andersson KL, Bussani C, Fambrini M, Polverino V, Taddei GL, Gemzell-Danielsson K, et al. DNA Methylation of HOXA10 in Eutopic and Ectopic Endometrium. *Hum Reprod* (2014) 29:1906–11. doi: 10.1093/humrep/deu161
3. Fuldeore MJ, Soliman AM. Prevalence and Symptomatic Burden of Diagnosed Endometriosis in the United States: National Estimates From a Cross-Sectional Survey of 59,411 Women. *Gynecol Obstet Invest* (2017) 82:453–61. doi: 10.1159/000452660
4. Taylor HS, Giudice LC, Lessey BA, Abrao MS, Kotarski J, Archer DF, et al. Treatment of Endometriosis-Associated Pain With Elagolix, an Oral GnRH Antagonist. *N Engl J Med* (2017) 377:28–40. doi: 10.1056/NEJMoa1700089
5. Bulun S. Endometriosis. *EN Engl J Med* (2009) 360:268–79. doi: 10.1056/NEJMra0804690
6. Mandalà M. Influence of Estrogens on Uterine Vascular Adaptation in Normal and Preeclamptic Pregnancies. *Int J Mol Sci* (2020) 21:2592. doi: 10.3390/ijms21072592
7. Benson GV, Lim H, Paria BC, Satokata I, Dey SK, Maas RL. Mechanisms of Reduced Fertility in Hoxa-10 Mutant Mice: Uterine Homeosis and Loss of Maternal Hoxa-10 Expression. *Development* (1996) 122:2687-2696. doi: 10.1242/dev.122.9.2687
8. Kim JJ, Taylor HS, Lu Z, Ladhani O, J M Hastings JM, Jackson KS, et al. Altered Expression of HOXA10 in Endometriosis: Potential Role in Decidualization. *Mol Hum Reprod* (2007) 13:323-332. doi: 10.1093/molehr/gam005
9. Taylor HS, Arici A, Olive D, Igarashi P. HOXA10 is Expressed in Response to Sex Steroids at the Time of Implantation in the Human Endometrium. *J Clin Invest* (1998) 101:1379–84. doi: 10.1172/JCI1057
10. Akbas GE, Song J, Taylor HS. A HOXA10 Estrogen Response Element (ERE) is Differentially Regulated by 17 Beta-Estradiol and Diethylstilbestrol (DES). *J Mol Biol* (2004) 340:1013–23. doi: 10.1016/j.jmb.2004.05.052
11. Liu Z, Guo Y, Lian F, Wang K, Sun Z, Wang Y, et al. Expression of HOXA10 Gene in Women With Polycystic Ovarian Syndrome and its Correlation Analysis With Lipid Metabolism. *Minerva Endocrinol* (2019) 44:413–5. doi: 10.23736/S0391-1977.19.03064-5
12. Huhtinen K, Desai R, Ståhle M, Salminen A, Handelsman DJ, Perheentupa A, et al. Endometrial and Endometriotic Concentrations of Estrone and Estradiol Are Determined by Local Metabolism Rather Than Circulating Levels. *J Clin Endocrinol Metab* (2012) 97:4228–35. doi: 10.1210/jc.2012-1154
13. Huhtinen K, Saloniemi-Heinonen T, Keski-Rahkonen P, Desai R, Laajala D, Ståhle M, et al. Intra-Tissue Steroid Profiling Indicates Differential Progesterone and Testosterone Metabolism in the Endometrium and Endometriosis Lesions. *J Clin Endocrinol Metab* (2014) 99:E2188–97. doi: 10.1210/jc.2014-1913
14. Attar E, Bulun SE. Aromatase and Other Steroidogenic Genes in Endometriosis: Translational Aspects. *Hum Reprod Update* (2006) 12:49–56. doi: 10.1093/humupd/dmi034
15. Davydov R, Gilep AA, Strushkevich NV, Usanov SA, Hoffman BM. Compound I is the Reactive Intermediate in the First Monooxygenation Step During Conversion of Cholesterol to Pregnenolone by Cytochrome P450scc: EPR/ENDOR/cryoreduction/annealing Studies. *J Am Chem Soc* (2012) 134:17149–56. doi: 10.1021/ja3067226
16. Melo AS, Rosa-e-Silva JC, Japur de Sá Rosa-e-Silva AC, Poli-Neto OB, Ferriani RA, Vieira CS. Unfavorable Lipid Profile in Women With Endometriosis. *Fertil Steril* (2010) 93:2433–6. doi: 10.1016/j.fertnstert.2009.08.043
17. Mu F, Rich-Edwards J, Rimm EB, Spiegelman D, Missmer SA. Endometriosis and Risk of Coronary Heart Disease. *Circ Cardiovasc Qual Outcomes* (2016) 9:257–64. doi: 10.1161/CIRCOUTCOMES.115.002224
18. Hughes E, Brown J, Collins JJ, Farquhar C, Fedorkow DM, Vandekerckhove P. Ovulation Suppression for Endometriosis. *Cochrane Database Syst Rev* (2007) 3):CD000155. doi: 10.1002/14651858.CD000155.pub2
19. Wu Y, Halverson G, Basir Z, Strawn E, Yan P, Guo S-W. Aberrant Methylation at HOXA10 may be Responsible for its Aberrant Expression in the Endometrium of Patients With Endometriosis. *Am J Obstet Gynecol* (2005) 193:371–80. doi: 10.1016/j.ajog.2005.01.034
20. Yu G, Wang LG, Han Y, He QY. Clusterprofiler: An R Package for Comparing Biological Themes Among Gene Clusters. *OMICS* (2012) 6:284–7. doi: 10.1089/omi.2011.0118
21. Langfelder P, Horvath S. WGCNA: An R Package for Weighted Correlation Network Analysis. *BMC Bioinf* (2008) 9:559. doi: 10.1186/1471-2105-9-559
22. Szklarczyk D, Gable AL, Lyon D, Alexander J, Stefan W, Huerta-Cepas J, et al. STRING V11: Protein-Protein Association Networks With Increased Coverage, Supporting Functional Discovery in Genome-Wide Experimental Datasets. *Nucleic Acids Res* (2019) 47:D607–13. doi: 10.1093/nar/gky1131
23. Wang Y, Hu S, Yao G, Sun Y. Identification of HOXA10 Target Genes in Human Endometrial Stromal Cells by RNA-Seq Analysis. *Acta Biochim Biophys Sin (Shanghai)* (2021) 53:365–71. doi: 10.1093/abbs/gmaa173
24. Browne H, Taylor H. HOXA10 Expression in Ectopic Endometrial Tissue. *Fertil Steril* (2006) 85:1386–90. doi: 10.1016/j.fertnstert.2005.10.072
25. Cirillo M, Coccia ME, Petraglia F, Fatini C. Role of Endometriosis in Defining Cardiovascular Risk: A Gender Medicine Approach for Women's Health. *Hum Fertil (Camb)* (2021) 30:1–9. doi: 10.1080/14647273.2021.1919764
26. Varayoud J, Ramos JG, Bosquiazzo VL, Muñoz-de-Toro M, Luque EH. Developmental Exposure to Bisphenol a Impairs the Uterine Response to Ovarian Steroids in the Adult. *Endocrinology* (2008) 149:5848–60. doi: 10.1210/en.2008-0651
27. Özcan C, Özdamar Ö., Gökbayrak M, Doğer E, Çakıroğlu Y, Çine N. HOXA-10 Gene Expression in Ectopic and Eutopic Endometrium Tissues: Does it Differ Between Fertile and Infertile Women With Endometriosis? *Eur J Obstet Gynecol Reprod Biol* (2018) 233:43–8. doi: 10.1016/j.ejogrb.2018.11.027
28. Espenshade PJ, Hughes AL. Regulation of Sterol Synthesis in Eukaryotes. *Annu Rev Genet* (2007) 41:401–27. doi: 10.1146/annurev.genet.41.110306.130315
29. Wang DQH. Regulation of Intestinal Cholesterol Absorption. *Annu Rev Physiol* (2007) 69:221–48. doi: 10.1146/annurev.physiol.69.031905.160725
30. Wang IH, Huang TT, Chen JL, Chu LW, Ping YH, Hsu KW, et al. Mevalonate Pathway Enzyme HMGCS1 Contributes to Gastric Cancer Progression. *Cancers (Basel)* (2020) 12:1088. doi: 10.3390/cancers12051088
31. Tan JME, Cook ECL, van den Berg M, Scheij S, Zelcer N, Loregger A, et al. Differential Use of E2 Ubiquitin Conjugating Enzymes for Regulated Degradation of the Rate-Limiting Enzymes HMGCR and SQLE in Cholesterol Biosynthesis. *Atherosclerosis* (2019) 281:137–42. doi: 10.1016/j.atherosclerosis.2018.12.008
32. He M, Kratz LE, Michel JJ, Vallejo AN, Ferris L, Kelley RI, et al. Mutations in the Human SC4MOL Gene Encoding a Methyl Sterol Oxidase Cause Psoriasiform Dermatitis, Microcephaly, and Developmental Delay. *J Clin Invest* (2011) 121:976–84. doi: 10.1172/JCI42650
33. Hsu CC, Lu CW, Huang BM, Wu MH, Tsai SJ. Cyclic Adenosine 3',5'-Monophosphate Response Element-Binding Protein and CCAAT/enhancer-Binding Protein Mediate Prostaglandin E2-Induced Steroidogenic Acute Regulatory Protein Expression in Endometriotic Stromal Cells. *Am J Pathol* (2018) 173:433–41. doi: 10.2353/ajpath.2008.080199
34. Long T, Sun Y, Hassan A, Qi X, Li X. Structure of Nevanimibe-Bound Tetrameric Human ACAT1. *Nature* (2020) 581:339–43. doi: 10.1038/s41586-020-2295-8
35. Xu RH, Wei W, Krawczyk M, Wang W, Luo H, Flagg K, et al. Circulating Tumour DNA Methylation Markers for Diagnosis and Prognosis of Hepatocellular Carcinoma. *Nat Mater* (2017) 16:1155–61. doi: 10.1038/nmat4997
36. Bulun SE, Yilmaz BD, Sison C, Miyazaki K, Bernardi L, Liu S, et al. Endometriosis. *Endocr Rev* (2019) 40:1048–79. doi: 10.1210/er.2018-00242
37. Paria BC, Reese J, Das SK, Dey SK. Deciphering the Cross-Talk of Implantation: Advances and Challenges. *Science* (2002) 296:2185–8. doi: 10.1126/science.1071601

Conflict of Interest: The authors declare that the research was conducted in the absence of any commercial or financial relationships that could be construed as a potential conflict of interest.

Publisher's Note: All claims expressed in this article are solely those of the authors and do not necessarily represent those of their affiliated organizations, or those of the publisher, the editors and the reviewers. Any product that may be evaluated in

this article, or claim that may be made by its manufacturer, is not guaranteed or endorsed by the publisher.

Copyright © 2022 Yu, Tang, Huang, Guo, Du, Li and Quan. This is an open-access article distributed under the terms of the Creative Commons Attribution License (CC BY). The use, distribution or reproduction in other forums is permitted, provided the original author(s) and the copyright owner(s) are credited and that the original publication in this journal is cited, in accordance with accepted academic practice. No use, distribution or reproduction is permitted which does not comply with these terms.

frontiers | Frontiers in Endocrinology

ORIGINAL RESEARCH
published: 10 June 2022
doi: 10.3389/fendo.2022.859332

Decreased Ovarian Reserves With an Increasing Number of Previous Early Miscarriages: A Retrospective Analysis

Jifan Tan[1,2†], *Lu Luo*[1,2†], *Jiaxin Jiang*[1,2], *Niwei Yan*[1,2] *and Qiong Wang*[1,2*]

[1] Reproductive Medicine Center, The First Affiliated Hospital, Sun Yat-sen University, Guangzhou, China,
[2] Guangdong Provincial Key Laboratory of Reproductive Medicine, Guangzhou, China

OPEN ACCESS

Edited by:
Ihtisham Bukhari,
Fifth Affiliated Hospital of Zhengzhou University, China

Reviewed by:
Jian Xu,
Chongqing Medical University, China
Long Zhang,
Xi'an Jiaotong University, China

***Correspondence:**
Qiong Wang
wqiong@mail.sysu.edu.cn

[†]These authors have contributed equally to this work and share first authorship

Specialty section:
This article was submitted to Reproduction, a section of the journal Frontiers in Endocrinology

Received: 21 January 2022
Accepted: 11 May 2022
Published: 10 June 2022

Citation:
Tan J, Luo L, Jiang J, Yan N and Wang Q (2022) Decreased Ovarian Reserves With an Increasing Number of Previous Early Miscarriages: A Retrospective Analysis. Front. Endocrinol. 13:859332. doi: 10.3389/fendo.2022.859332

The fact of ovarian reserve (OR) decreased in women with recurrent miscarriage has been well known. However, Whether OR would decrease with increasing numbers of previous miscarriages (PMs) is still unclear. To address this, OR parameters of following four groups' patients were evaluated: 99 women with one previous miscarriage (PM1), 46 women with two previous miscarriages (PM2) and 35 women with three or more previous miscarriages (PM3). The control group included 213 women without a history of miscarriage (PM0). The correlation of OR parameters and the proportion of diminished ovarian reserve (DOR) patients between the four groups were analyzed using Kendall's Tau-B coefficients. The results showed the median anti-Müllerian hormone (AMH) levels were 4.04, 3.40, 3.14 and 2.55 respectively in the PM0, PM1, PM2 and PM3 groups, respectively (H=15.99, $P = 0.001$); the median antral follicle counts (AFCs) were 10, 8, 8 and 6, respectively (H=24.53, $P < 0.001$); and the proportions of DOR patients were 10.8%, 15.2%, 23.9% and 31.4% ($\chi 2 = 13.01$, $P = 0.005$). In addition, AMH level and AFC correlated negatively with the number of PMs (correlation coefficients -0.154, $P < 0.001$; -0.205, $P < 0.001$ respectively), the proportion of DOR patients correlated positively with the number of PMs (correlation coefficients 0.156, $P = 0.001$). After stratification by age, AMH and AFC levels were still significantly lower in the PM3 group than the PM0 group ($P < 0.05$). The proportion of DOR patients between the PM0 and PM3 groups was statistically significant ($P < 0.001$). This study showed that AMH levels and AFCs decreased as well as the proportion of DOR patients increased significantly as the number of PMs increased. In conclusion, our study indicates decreased AMH levels and AFCs might be one of the factors contributing to early miscarriage.

Keywords: previous miscarriages, ovarian reserve, anti-Müllerian hormone, antral follicle count, recurrent miscarriage

INTRODUCTION

Miscarriage is defined as spontaneous loss of a pregnancy before 22 weeks of gestational age (1), which is recognized as a relatively common event, occurring in 15-20% of pregnancies. Most miscarriages are early, occur before 12 weeks of gestational age (1, 2).

Approximately 1–2% of the women face three or more consecutive spontaneous miscarriages with the same partner, termed recurrent miscarriage (RM). Even after a detailed evaluation of the etiology of early miscarriage, 50% of RM cases remained unexplained, idiopathic, or unknown (1–3).

Abnormal or low-quality oocytes could be a potential factor contributing spontaneous pregnancy losses in these women (4, 5). Ovarian reserve (OR) demonstrates reproductive potential as the number and quality of remaining oocytes. The basal serum levels of basal follicle-stimulating hormone (FSH), luteinizing hormone (LH), estradiol (E_2), and FSH : LH ratio, inhibit B, anti-Müllerian hormone (AMH) and antral follicle count (AFC) are parameters of OR, which have been proven to be predictors of oocyte quantity (6–10). Although still be controversial, they are also thought to be possible predictors of oocyte quantity (9–12). Diminished ovarian reserve (DOR) is a common phrase for evaluating the value of OR, which is important to provide the clinical counseling for women with the previous miscarriages (PMs) (4, 9, 13, 14).

Recent studies have documented an association between RM and decreased OR, using AMH levels and AFCs as markers of OR (9, 14, 15). In addition, many of these studies showed that the proportion of DOR patients in the RM group was significantly higher than that in the control group (9, 14). However, whether OR would decrease with the number of PMs is still unclear. As an approach to address this problem, we conducted a cohort study to explore the association between OR parameters and the proportion of DOR patients with increasing numbers of PMs.

MATERIALS AND METHODS

Patients

All patients who had undergone assisted reproductive technology (ART) therapy because of female pelvic or fallopian tube factor infertility at the Center for Reproductive Medicine of the First Affiliated Hospital of Sun Yat-sen University from October 2016 to May 2018 were retrospectively included. The study was performed after receiving approval from the Medical Ethics Committee of the First Affiliated Hospital of Sun Yat-sen University (No. 2016115), and informed consent was obtained from all patients.

All patients were classified into the following study groups according to their medical records: 99 women with one previous early miscarriage (PM1), 46 with two previous early miscarriages (PM2) and 35 with three or more previous early miscarriages (PM3). Additionally, the control group included 213 women without a history of miscarriage (PM0). All patients underwent routine investigations of infertility and examinations to exclude factors known to interfere with OR, including parental chromosomal abnormalities, a history of ovarian surgery, endometriosis, structural uterine abnormalities (e.g., unicornuate uterus, uterine septum) and endocrine abnormalities (e.g., thyroid dysfunction, polycystic ovary syndrome). Women in the PM2 and PM3 groups were further investigated to exclude possibly known causes of miscarriage, including autoimmune disease, antiphospholipid syndrome, lipidemia, hemolysis and thrombophilia. The exclusion criterion was abnormal results during any of the aforementioned investigations or hemolysis. Finally, 393 women who underwent IVF-ET because of pelvic or fallopian tubal factors met the eligibility criteria.

Measurements of Ovarian Reserve Parameters

We used the following six OR tests: AMH, AFC, follicle-stimulating hormone FSH, LH, E_2, and FSH : LH ratio. The serum levels of FSH, LH and E2 were measured during the early follicular phase (Days 3-5) of the menstrual cycle within 6 months before the initiation of IVF cycles. An ultrasound assessment of the number of AFCs measuring 2–10 mm in diameter between the second and the fifth days of the menstrual cycle was performed by a single skilled physician who was blinded to the patients' conditions. All women involved in the study were administered a long-term or short-term gonadotropin releasing hormone agonist (GnRH-a) for pituitary downregulation during the mid-luteal phase, according to the protocol. Before initiating gonadotropin injections, blood samples were collected from a peripheral vein on the 3rd to the 5th day of a menstrual cycle and then centrifuged at 3000 r/min for 15 mins at room temperature. Then the serum was separated and stored in a refrigerator at –80°C.

The serum levels of FSH (normal range: 2.00-138.00 IU/L), LH (normal range: 0.40-105.00 IU/L) and E2 (normal range: 0.00-300.00 pg/ml) were measured using the chemiluminescence method (Architect Alinity, Abbott, Longford, Ireland). The serum level of AMH (normal range: 0.24-11.78 ng/ml) was measured using an enzyme-linked immunosorbent assay (ELISA) (Diagnostic Kits for the Quantitative Detection of AMH; GK Biological Technology Ltd).

Statistical Analyses

The Kolmogorov–Smirnov test was used to assess the distribution of data. Nonnormally distributed data were analyzed using the Kruskal–Wallis test for comparisons between multiple groups and the Mann–Whitney U test for comparisons of two groups. The chi-square test was used to compare categorical data and Bonferroni comparisons were performed for two groups. Kendall's Tau-B correlation coefficients were calculated to describe the correlations between variables. Significance was defined as a P value <0.05.

Abbreviations: PM1, one previous miscarriage; PM2, two previous miscarriages; PM3, three or more previous miscarriages; PMs, previous miscarriages; RM, recurrent miscarriage; OR, ovarian reserve; DOR, diminished ovarian reserve; AMH, Serum levels of anti-Mullerian hormone; AFC, antral follicle count; FSH, follicle-stimulating hormone; LH, luteinizing hormone.

RESULTS

The Baseline Characteristics and Variables Indicating of the OR Between Groups

The baseline characteristics and variables indicating of the OR are presented in **Table 1**. The mean age of the 393 included women was 33.86 years (range: 25–45 years). The numbers of PMs ranged from 0 to 10. The mean age, proportions of women aged <35 years and ≥35 years and body mass index (BMI) values did not differ significantly among the groups (P>0.05).

The Relationship Between AMH Levels and AFCs Numbers With an Increasing Number of PMs

Regarding the variables indicating of OR (**Table 1**), the median AMH levels were 4.04, 3.40, 3.14 and 2.55 in the PM0, PM1, PM2 and PM3 groups, respectively, and the differences were statistically significant (H= 15.99, P = 0.001). The median AFCs values were 10, 8, 8 and 6 in the PM0, PM1, PM2 and PM3 groups, respectively, and the differences were statistically significant (H= 24.53, $P < 0.001$). According to the Mann–Whitney U test for comparisons of pairs of groups, the differences in the AMH level and AFC between the PM0 and PM3 groups were statistically significant ($P < 0.001$), while the differences between other groups were not statistically significant. In contrast, the comparisons of basal FSH and E2 levels and FSH/LH ratios did not yield significant differences.

The Correlations Between the PM Number and Age With OR

Regarding the variables indicative of OR, AMH and AFC showed a decreasing trend (**Figure 1**). Kendall's Tau-B correlation was subsequently used in this study to evaluate the correlations between OR markers (AMH concentration, AFC), and age with the number of PMs (**Table 2**). The AMH level, as a marker of OR function, exhibited significant negative correlations with both age and the number of PMs (Kendall's Tau-$B_{\text{the numbers of PMs}}$= -0.154, $P < 0.001$; Kendall's Tau-B_{age}=-0.340, $P < 0.001$). Similar results were also observed when the AFC was used as a marker of OR function. Age and the number of PMs were negatively correlated with AFC (Kendall's Tau-$B_{\text{the numbers of PMs}}$= -0.205, $P < 0.001$; Kendall's Tau-B_{age}=-0.339, $P < 0.001$). The comparison of other OR functions (basic FSH and E2 levels and the FSH/LH ratio) showed no significant differences.

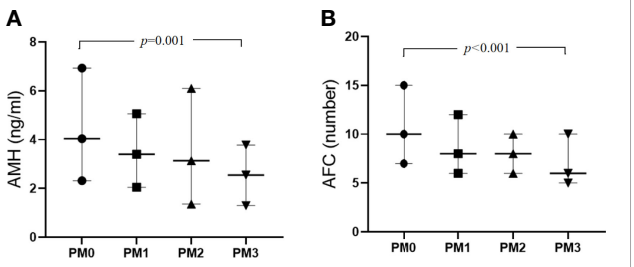

FIGURE 1 | Comparisons of AMH level **(A)** and AFC **(B)** numbers show a decreasing trend from PM0 to PM3.

TABLE 2 | Correlation analyses of PM number and age with AMH levels and AFCs levels (by Kendall's Tau-B correlation).

parameters	AMH		AFC	
	correlation coefficient	*P* -value	correlation coefficient	*P*- value
Age	-0.340	<0.001	-0.339	<0.001
Number of PM	-0.154	0.001	-0.205	<0.001

PM, previous miscarriage; AMH, anti-Müllerian hormone; AFC, antral follicle count.

The Relationship Between the PM0 and PM3 Groups and OR

As maternal age was identified as a prominent confounding factor affecting AMH levels and AFC, we further compared the PM0 and PM3 groups after stratification by age (**Table 3**). Among participants aged <35 years, AMH and AFC levels were both significantly higher in the PM0 group (median 4.96 ng/ml, IQR [2.99-8.00] and median 11 number, IQR [8-15], respectively) than in the PM3 group (median 3.62 ng/ml, IQR [1.71-5.49], $P =$

TABLE 1 | Comparison of baseline characteristics and parameters of the ovarian reserve between groups.

Variables	PM 0 (n = 213)	PM 1(n = 99)	PM 2 (n = 46)	PM 3 (n = 35)	*P*-value
<35 years	138 (64.00%)	49 (49.49%)	25 (54.35%)	19 (54.29%)	0.061
≥35 years	75 (35.21%)	50 (50.51%)	21 (45.65%)	16 (45.71%)	
BMI (kg/m2)	20.83 (19.48, 23.01)	21.08 (19.29, 23.23)	21.01 (19.42, 23.46)	21.64 (20.03, 24.03)	0.340
AMH (ng/ml)	4.04 (2.32, 6.93)	3.40 (2.05, 5.06)	3.14 (1.36, 6.10)	2.55 (1.30, 3.78)	0.001
AFC (number)	10 (7, 15)	8 (6, 12)	8 (6, 10)	6 (5, 10)	<0.001
FSH (IU/L)	5.55 (4.67, 6.67)	5.79 (4.79, 6.96)	5.20 (4.53, 6.92)	5.83 (4.52, 7.58)	0.641
E2 (pg/ml)	34.00 (26.25, 45.75)	36.00 (27.00, 44.00)	35.00 (27.00, 46.00)	36.00 (29.00, 55.00)	0.636
LH (IU/L)	3.48 (2.66, 4.45)	3.21 (2.49, 4.18)	3.58 (2.25, 4.35)	3.28 (2.58, 4.16)	0.745
FSH/LH(value)	1.63 (1.21, 2.27)	1.75 (1.38, 2.35)	1.77 (1.33, 2.28)	1.74 (1.21,2.60)	0.598

Nonnormally distributed data were presented as numbers (%) or as medians (interquartile ranges).

OR, ovarian reserve; PM0, no previous miscarriages; PM1, one previous miscarriage; PM2, two previous miscarriages; PM3, three or more previous miscarriages; BMI, body mass index; AMH, anti-Müllerian hormone; AFC, antrum follicle count; FSH, follicle-stimulating hormone; E2, estradiol; LH, luteinizing hormone.

TABLE 3 | Comparisons of parameters of OR between the PM0 and PM3 groups with age stratification.

Age	<35years			≥35years		
parameters	**PM 0**	**PM 3**	***p*-value**	**PM 0**	**PM 3**	***p*-value**
Age (years)	30.49±2.39	31.26±2.53	0.19	38.13±2.73	39.19±2.54	0.16
AMH (ng/ml)	4.78 (2.96,8.35)	3.70 (1.76.5.37)	0.01	2.81 (1.48,4.82)	2.00 (1.13,2.96)	0.03
AFC (ug/L)	11.00 (8.00,15.00)	6.00 (5.00,8.50)	<0.001	8.00 (6.00,11.50)	6.00 (4.00,10.50)	0.25
FSH (ug/L)	5.42 (4.55.6.39)	5.06 (4.27,7.02)	0.50	5.86 (5.00,7.43)	7.27 (5.37,7.73)	0.14
E2 (ug/L)	34.00 (26.75,44.00)	36.00 (27.00,55.00)	0.29	34.50 (25.75,48.00)	36.50 (29.00,59.50)	0.52
LH (ug/L)	3.59 (2.68,4.49)	3.39 (2.87,4.30)	0.86	3.35 (2.51,4.45)	2.72 (2.53,4.16)	0.71
FSH/LH (value)	1.53 (1.13,2.09)	1.51 (0.95,2.39)	0.78	1.88 (1.45,2.42)	2.23 (1.52,2.81)	0.32

Data are presented as medians (interquartile ranges).
OR, ovarian reserve; PM0, no previous miscarriages; PM3, three or more previous miscarriages; AMH, anti-Müllerian hormone; AFC, antrum follicle count; FSH, follicle-stimulating hormone; E2, estradiol; LH, luteinizing hormone.

0.01 and median 6 number, IQR [5-8.5], respectively; $P < 0.05$). Among women aged >35 years, the AMH level was also significantly higher in the PM0 group than in the PM3 group (median, [IQR]: 2.81[1.48-4.82] *vs.* 2.00[1.19-2.82], $P = 0.03$); however, the AFCs did not differ significantly (median, [IQR]: 8 [6-11.75] *vs.* 6[4-10.5], $P = 0.25$). The AFC was still lower in the PM3 groups than in the PM0 groups but was not different.

The Relationship and Correlations Between the PM Number and Age With DOR

Thus far, the definition of DOR remains controversial. In the present study, the DOR was defined as an FSH level ≥10 mIU/mL and/or AMH level < 1.1 ng/mL and/or AFC< 5 by referring to a large number of studies and conference reports (9, 14–16). Using chi-square values from PM0 patients, the proportions of DOR were 10.8%, 15.2%, 23.9% and 31.4% in the groups PM0, PM1, PM2 and PM3 groups, respectively, with statistically significant differences ($\chi 2 = 13.01$, $P = 0.005$). According to the Bonferroni pairwise comparison, the difference in the proportion of DOR patients between the PM0 and PM3 groups was statistically significant ($P<0.001$), while the comparisons between other groups showed no significant differences (**Table 4**). In addition, the proportion of DOR patients showed significant positive correlations with both age and the number of PMs (Kendall's Tau-B $_{\text{the numbers of PMs}} = 0.156$, $P = 0.001$; Kendall's Tau-B_{age}=0.277, $P < 0.001$) (**Table 5**).

TABLE 5 | Correlation analyses of PM number and age with DOR (by Kendall's Tau-B).

parameters	DOR	
	correlation coefficient	***p*- value**
Age	0.277	<0.001
Number of PM	0.156	0.001

PM, previous miscarriage; DOR, diminished ovarian reserve.

DISCUSSION

Our study revealed a significant negative correlation between the number of PMs and OR after adjusting for maternal age, as measured by AMH levels and AFCs. To the best of our knowledge, the present study is the first to report a possible relationship between OR parameters and the proportion of DOR patients with the number of PMs. Previous studies mainly explored the potential association between the OR and RM, not including the PM1 or PM2 groups. We also verified that low AMH levels and AFCs in women with RM in both women aged <35 years and those aged >35 years. In addition, the percentages of women with DOR in the RM group were significantly higher than those in the PM0 group, consistent with recently reported observations (9, 14).

TABLE 4 | Comparison of the proportion of DOR patients among groups.

	PM0	PM1	PM2	PM3	*p*
DOR	23 (10.8%)	15 (15.2%)	11 (23.9%)	11 (31.4%)	0.005
Non-DOR	190 (89.2%)	84 (84.8%)	35 (76.1%)	24 (68.6%)	

PM, previous miscarriage; DOR, diminished ovarian reserve.

In our study, only the PM3 group had a significantly lower AMH levels and AFCs than the PM0 group. The respective comparisons of the PM0 group with the PM1 and PM2 groups did not yield statistically significant results. In addition, we conducted the Kendall's Tau-B correlation analyses and confirmed a significant negative correlation of AMH levels and AFCs with the number of PM after adjusting for maternal age. Therefore, in women with advanced maternal age or DOR who are predisposed to a greater risk of more miscarriages, and adverse effects become apparent and only then does OR decrease to a sufficient extent. It is well known that OR are thought to be possible markers of oocyte quality (6, 7). Besides, it is assumed that quality of oocytes could be one of the potential factors related to aberrant embryo quality or embryo aneuploidy which may lead to subsequent early miscarriage (17, 18). Our study also supported the hypothesis that a decreased OR might be a potential contributing factor to the etiology of the PM.

OR represents the quality and quantity of the remaining oocytes. The basal serum levels of basal FSH, E2, LH, FSH/LH, inhibin B and AMH, as well as the AFC, ovarian stromal vascularization and ovary volume, are commonly used to assess OR (4, 13), However, the value of these OR tests to predict the quality and quantity of the ovarian primordial

follicular pool remains controversial (9, 14, 18, 19). Hormone levels fluctuate with the menstrual cycle and vary between laboratories to laboratories (19, 20), but they are still used in most units as a baseline test for ovarian function. The present study showed no statistically significant differences in the levels of FSH and E2 between women with RM and PM0, which was consistent with numerous studies (21–23). However, studies by Atasever, et al. (14) and Trout, et al. (24) reported statistically significant differences in the levels of FSH and E_2 between the RM and explained RM groups. In addition, similar to our study, Tow studies (14, 21) showed no statistically significant differences in the FSH : LH ratio between women with RM compared with the non-RM group.

In contrast, the serum AMH level, a novel marker of OR, is a dimeric glycoprotein produced solely by the ovarian follicles and is not affected by the menstrual cycle. Recently, an increasing number of studies have verified that lower AMH levels in women with RM than in non-RM groups (9, 14, 15, 25); Similarly, our results also showed that women with three or more previous unexplained miscarriages had lower AMH levels. However, one study by Prakash et al. (26) suggested that AMH levels were not significantly different between RM and non-RM groups.

The AFC has a better value in predicting a poor response and OR than the basal FSH level. In the present study, we found that women with RM had lower AFC levels, suggesting an association with decreased OR, but no statistically significant differences were observed between the PM1, PM2 and PM0 groups. A systematic (9) review also supported the hypothesis that low AFCs predict a higher odds of miscarriages. However, Atasever, et al. (14)found that the AFC level in the RM group was not significantly different from that in the non-RM group, but the results may have been affected by difficulties in obtaining an accurate AFC, such as intraobserver variability and anatomic variations.

Accordingly, AMH levels and AFCs are closely related, and they are considered the most reliable and accurate markers of OR (4, 13, 18, 19). Based on our results, these two markers might also be considered to have the best prognostic value. Recently, Sophie Pils et al. (27) confirmed the effect of the number of PMs, which predicted the outcome of further pregnancies in women with RM through a multivariate analysis. In our study, we found that AMH levels and AFCs decreased with increasing numbers of PMs. We suggest that a decreased quantitative OR may predict poor oocyte quality which affects the next pregnancy. Blood samples were analyzed under the same conditions, and previous studies have reported that different ovulation stimulation protocols, including GnRH-a, have no effect on the results of AMH analyses (28). Therefore, we propose that the AMH measurements in our study are stable and reliable and therefore did not affect the final conclusions.

In recent decades, DOR has gradually become a challenge for women of reproductive age and those using reproductive medicine (9, 14, 29). However, the criteria for defining DOR remains controversial, including the selection of various OR functional markers and the specific ranges. AMH levels and AFCs have been widely used OR markers. However, the detected values of AMH levels are quite different because of the diversities of testing methods, laboratory conditions, the absence of international unified standards and quality control systems, and other factors. Similarly, AFC measurements are highly subjective. Research has shown that AMH levels and AFCs combined with FSH levels jointly predict DOR, which is an overall assessment of egg quantity and quality and is conducive to the prediction of embryo quality and pregnancy outcomes (29, 30).

In this study, the DOR patients were defined as an FSH level ≥10 mIU/mL and/or an AMH level <1 ng/mL and/or AFC<5, based on a previous expert consensus, academic conferences and related studies (9, 16, 29–31). In contrast, previous studies reporting on DOR with RM used cutoff values of FSH levels, E_2 levels, AMH levels and AFC that had not been updated as the definition of DOR. Our study found the similar higher odds of DOR in the RM group, consistent with the aforementioned studies (9, 14, 32). We previously knew that patients with DOR had high miscarriage rates, and many patients with DOR were of advanced age. Thus, for many years, we were unable to differentiate whether high miscarriage rates in patients with DOR were associated with advanced age. Recently, Morin SJ et al. (33) reported that an aneuploidy rate less than 38 in patients with DOR was similar to that in controls, even in patients with higher FSH levels and lower AMH levels and AFCs. In our study, we found that the association of miscarriage women associated with DOR was evenly balanced with age.

Our study explored the number of PM groups and multiple parameters of OR which is in different with previous studies. However, one limitation of present study is that our sample size is still limited, especially in the PM2 and PM3 groups. In future, large prospective cohort studies are warranted and mechanism of OR decreased on spontaneous miscarriage should be explored. Similar to advanced age women, Patients with RM also have high embryo aneuploidy and decreased OR (8, 34, 35), but it is still unknown whether their mechanism was similar or not. The other limitation of present study is the absence of chromosome information in no PM group patients because of its retrospective approach.

In conclusion, our study found that AMH levels and AFCs decreased as well as the proportion of DOR patients increased significantly as the number of PMs increased. Decreased AMH levels and AFCs might be a contributing factor to early miscarriage. We believe that these new insights could be useful in counseling for couples with PM. DOR should be predicted in multiple PMs patients and early interference should be conducted to achieve the better pregnancy outcomes in the future.

DATA AVAILABILITY STATEMENT

The raw data supporting the conclusions of this article will be made available by the authors, without undue reservation.

ETHICS STATEMENT

The studies involving human participants were reviewed and approved by The First Affiliated Hospital of Sun Yat-sen University on 22 Jun 2016 (No. 2016115). The patients/

participants provided their written informed consent to participate in this study.

AUTHOR CONTRIBUTIONS

JT and QW contributed to the design of the work. JT and LL contributed to manuscript written and statistical analyses. Data acquisition and analysis were carried out by JJ and NY. JT and LL carried out the statistical analyses. QW critically reviewed the paper. All authors contributed to the article and approved the submitted version.

FUNDING

The study was supported by Natural Science Foundation of Guangdong Province (2021A1515010290) and National Natural Science Foundation of China (81871159).

ACKNOWLEDGMENTS

The authors thank Professor Qian Zhao for the support of statistical analyses.

REFERENCES

1. Stirrat GM. Recurrent Miscarriage. II: Clinical Associations, Causes, and Management. *Lancet* (1990) 336(8717):728–33. doi: 10.1016/0140-6736(90)92215-4
2. Wang X, Chen C, Wang L, Chen D, Guang W, French J. Conception, Early Pregnancy Loss, and Time to Clinical Pregnancy: A Population-Based Prospective Study. *Fertil Steril* (2003) 79(3):577–84. doi: 10.1016/S0015-0282(02)04694-0
3. El Hachem H, Crepaux V, May-Panloup P, Descamps P, Legendre G, Bouet PE. Recurrent Pregnancy Loss: Current Perspectives. *Int J Womens Health* (2017) 9:331–45. doi: 10.2147/IJWH.S100817
4. Coomarasamy A, Dhillon-Smith RK, Papadopoulou A, Al-Memar M, Brewin J, Abrahams VM, et al. Recurrent Miscarriage: Evidence to Accelerate Action. *Lancet* (2021) 397(10285):1675–82. doi: 10.1016/S0140-6736(21)00681-4
5. Saravelos SH, Li TC. Unexplained Recurrent Miscarriage: How can We Explain it? *Hum Reprod* (2012) 27(7):1882–6. doi: 10.1093/humrep/des102
6. Wiweko B, Prawesti DM, Hestiantoro A, Sumapraja K, Natadisastra M, Baziad A. Chronological Age vs Biological Age: An Age-Related Normogram for Antral Follicle Count, FSH and Anti-Mullerian Hormone. *J Assist Reprod Genet* (2013) 30(12):1563–7. doi: 10.1007/s10815-013-0083-1
7. La Marca A, Sighinolfi G, Radi D, Argento C, Baraldi E, Artenisio AC, et al. Anti-Mullerian Hormone (AMH) as a Predictive Marker in Assisted Reproductive Technology (ART). *Hum Reprod Update* (2010) 16(2):113–30. doi: 10.1093/humupd/dmp036
8. Jaswa EG, McCulloch CE, Simbulan R, Cedars MI, Rosen MP. Diminished Ovarian Reserve is Associated With Reduced Euploid Rates *via* Preimplantation Genetic Testing for Aneuploidy Independently From Age: Evidence for Concomitant Reduction in Oocyte Quality With Quantity. *Fertil Steril* (2021) 115(4):966–73. doi: 10.1016/j.fertnstert.2020.10.051
9. Bunnewell SJ, Honess ER, Karia AM, Keay SD, Al Wattar BH, Quenby S. Diminished Ovarian Reserve in Recurrent Pregnancy Loss: A Systematic Review and Meta-Analysis. *Fertil Steril* (2020) 113(4):818–27.e3. doi: 10.1016/j.fertnstert.2019.11.014
10. Seifer DB. Connecting the Dots Between Oocyte Quantity and Quality in Diminished Ovarian Reserve. *Fertil Steril* (2021) 115(4):890. doi: 10.1016/j.fertnstert.2021.01.020
11. Tarasconi B, Tadros T, Ayoubi JM, Belloc S, de Ziegler D, Fanchin R. Serum Antimullerian Hormone Levels are Independently Related to Miscarriage Rates After *In Vitro* Fertilization-Embryo Transfer. *Fertil Steril* (2017) 108(3):518–24. doi: 10.1016/j.fertnstert.2017.07.001
12. Lyttle Schumacher BM, Jukic AMZ, Steiner AZ. Antimullerian Hormone as a Risk Factor for Miscarriage in Naturally Conceived Pregnancies. *Fertil Steril* (2018) 109(6):1065–71.e1. doi: 10.1016/j.fertnstert.2018.01.039
13. Pils S, Promberger R, Springer S, Joura E, Ott J. Decreased Ovarian Reserve Predicts Inexplicability of Recurrent Miscarriage? A Retrospective Analysis. *PLoS One* (2016) 11(9):e0161606. doi: 10.1371/journal.pone.0161606
14. Atasever M, Soyman Z, Demirel E, Gencdal S, Kelekci S. Diminished Ovarian Reserve: Is it a Neglected Cause in the Assessment of Recurrent Miscarriage? A Cohort Study. *Fertil Steril* (2016) 105(5):1236–40. doi: 10.1016/j.fertnstert.2016.01.001
15. Leclercq E, de Saint Martin L, Bohec C, Le Martelot MT, Roche S, Alavi Z, et al. Blood Anti-Mullerian Hormone is a Possible Determinant of Recurrent Early Miscarriage, Yet Not Conclusive in Predicting a Further Miscarriage. *Reprod BioMed Online* (2019) 39(2):304–11. doi: 10.1016/j.rbmo.2019.04.004
16. Practice Committee of the American Society for Reproductive M. Testing and Interpreting Measures of Ovarian Reserve: A Committee Opinion. *Fertil Steril* (2015) 103:e9–e17. doi: 10.1016/j.fertnstert.2014.12.093
17. Shahine LK, Marshall L, Lamb JD, Hickok LR. Higher Rates of Aneuploidy in Blastocysts and Higher Risk of No Embryo Transfer in Recurrent Pregnancy Loss Patients With Diminished Ovarian Reserve Undergoing *In Vitro* Fertilization. *Fertil Steril* (2016) 106(5):1124–8. doi: 10.1016/j.fertnstert.2016.06.016
18. Tal R, Seifer DB. Ovarian Reserve Testing: A User's Guide. *Am J Obstet Gynecol* (2017) 217(2):129–40. doi: 10.1016/j.ajog.2017.02.027
19. ACOG Committee Opinion No. 773 Summary: The Use of Antimullerian Hormone in Women Not Seeking Fertility Care. *Obstet Gynecol* (2019) 133(4):840–1. doi: 10.1097/AOG.0000000000003163
20. Kotlyar A, Seifer DB. Anti-Mullerian Hormone as a Qualitative Marker - or Just Quantity? *Curr Opin Obstet Gynecol* (2020) 32(3):219–26. doi: 10.1097/GCO.0000000000000623
21. Gonca Yetkin Yildirim HGC, Nadiye K, Esra K. Do Ovarian Reserve Markers Predict the Subsequent Pregnancy Outcomes in Women With Recurrent Pregnancy Loss? *Turk J Biochem* (2018) 43(5):481–6. doi: 10.1515/tjb-2017-0238
22. Mahdavipour M, Zarei S, Fatemi R, Edalatkhah H, Heidari-Vala H, Jeddi-Tehrani M, et al. Polymorphisms in the Estrogen Receptor Beta Gene and the Risk of Unexplained Recurrent Spontaneous Abortion. *Avicenna J Med Biotechnol* (2017) 9(3):150–4.
23. Liu S, Wei H, Li Y, Huang C, Lian R, Xu J, et al. Downregulation of ILT4 + Dendritic Cells in Recurrent Miscarriage and Recurrent Implantation Failure. *Am J Reprod Immunol* (2018) 80(4):e12998. doi: 10.1111/aji.12998
24. Trout SW SD. Do Women With Unexplained Recurrent Pregnancy Loss Have Higher Day 3 Serum FSH and Estradiol Values? *Fertil Steril* (2000) 74(2):335–7. doi: 10.1016/S0015-0282(00)00625-7
25. McCormack CD, Leemaqz SY, Furness DL, Dekker GA, Roberts CT. Anti-Mullerian Hormone Levels in Recurrent Embryonic Miscarriage Patients are Frequently Abnormal, and may Affect Pregnancy Outcomes. *J Obstet Gynaecol* (2019) 39(5):623–7. doi: 10.1080/01443615.2018.1552669
26. Prakash A, Li TC, Laird S, Nargund G, Ledger WL. Absence of Follicular Phase Defect in Women With Recurrent Miscarriage. *Fertil Steril* (2006) 85(6):1784–90. doi: 10.1016/j.fertnstert.2005.11.045
27. Pils S, Stepien N, Kurz C, Nouri K, Springer S, Hager M, et al. Does Anti-Mullerian Hormone Predict the Outcome of Further Pregnancies in Idiopathic Recurrent Miscarriage? A Retrospective Cohort Study. *Arch Gynecol Obstet* (2019) 299(1):259–65. doi: 10.1007/s00404-018-4946-7
28. Kaya A, Atabekoglu CS, Kahraman K, Taskin S, Ozmen B, Berker B, et al. Follicular Fluid 406 Concentrations of IGF-I, IGF-II, IGFBP-3, VEGF, AMH, and Inhibin-B in Women Undergoing 407 Controlled Ovarian Hyperstimulation Using GnRH Agonist or GnRH Antagonist. *Eur J Obstet Gynecol 408 Reprod Biol* (2012) 164(2):167–71. doi: 10.1016/j.ejogrb.2012.06.010
29. Cohen J, Chabbert-Buffet N, Darai E. Diminished Ovarian Reserve, Premature Ovarian Failure, Poor Ovarian Responder–a Plea for Universal Definitions. *J Assist Reprod Genet* (2015) 32(12):1709–12. doi: 10.1007/s10815-015-0595-y
30. Bishop LA, Richter KS, Patounakis G, Andriani L, Moon K, Devine K. Diminished Ovarian Reserve as Measured by Means of Baseline Follicle-

Stimulating Hormone and Antral Follicle Count is Not Associated With Pregnancy Loss in Younger *In Vitro* Fertilization Patients. *Fertil Steril* (2017) 108(6):980–7. doi: 10.1016/j.fertnstert.2017.09.011
31. Broer SL, Mol BW, Hendriks D, Broekmans FJ. The Role of Antimullerian Hormone in Prediction of Outcome After IVF: Comparison With the Antral Follicle Count. *Fertil Steril* (2009) 91(3):705–14. doi: 10.1016/j.fertnstert.2007.12.013
32. Wald KA, Shahine LK, Lamb JD, Marshall LA, Hickok LR. High Incidence of Diminished Ovarian Reserve in Young Unexplained Recurrent Pregnancy Loss Patients. *Gynecol Endocrinol* (2020) 36(12):1079–81. doi: 10.1080/09513590.2020.1750001
33. Morin SJ, Patounakis G, Juneau CR, Neal SA, Scott RT, Seli E. Diminished Ovarian Reserve and Poor Response to Stimulation in Patients <38 Years Old: A Quantitative But Not Qualitative Reduction in Performance. *Hum Reprod* (2018) 33(8):1489–98. doi: 10.1093/humrep/dey238
34. Ata B, Seyhan A, Seli E. Diminished Ovarian Reserve Versus Ovarian Aging: Overlaps and Differences. *Curr Opin Obstet Gynecol* (2019) 31(3):139–47. doi: 10.1097/GCO.0000000000000536
35. Sato T, Sugiura-Ogasawara M, Ozawa F, Yamamoto T, Kato T, Kurahashi H, et al. Preimplantation Genetic Testing for Aneuploidy: A Comparison of Live Birth Rates in Patients With Recurrent Pregnancy Loss Due to Embryonic Aneuploidy or Recurrent Implantation Failure. *Hum Reprod* (2019) 34 (12):2340–8. doi: 10.1093/humrep/dez229

Conflict of Interest: The authors declare that the research was conducted in the absence of any commercial or financial relationships that could be construed as a potential conflict of interest.

Publisher's Note: All claims expressed in this article are solely those of the authors and do not necessarily represent those of their affiliated organizations, or those of the publisher, the editors and the reviewers. Any product that may be evaluated in this article, or claim that may be made by its manufacturer, is not guaranteed or endorsed by the publisher.

Copyright © 2022 Tan, Luo, Jiang, Yan and Wang. This is an open-access article distributed under the terms of the Creative Commons Attribution License (CC BY). The use, distribution or reproduction in other forums is permitted, provided the original author(s) and the copyright owner(s) are credited and that the original publication in this journal is cited, in accordance with accepted academic practice. No use, distribution or reproduction is permitted which does not comply with these terms.

frontiers | Frontiers in Endocrinology

TYPE Original Research
PUBLISHED 28 September 2022
DOI 10.3389/fendo.2022.1002279

Check for updates

OPEN ACCESS

EDITED BY
Rick Francis Thorne,
The University of Newcastle, Australia

REVIEWED BY
Yi Zheng,
Northwest A&F University, China
Peter Schlegel,
NewYork-Presbyterian, United States

*CORRESPONDENCE
Hooman Sadri-Ardekani
hsadri@wakehealth.edu

SPECIALTY SECTION
This article was submitted to Reproduction, a section of the journal Frontiers in Endocrinology

RECEIVED 25 July 2022
ACCEPTED 05 September 2022
PUBLISHED 28 September 2022

CITATION
Galdon G, Deebel NA, Zarandi NP, Teramoto D, Lue Y, Wang C, Swerdloff R, Pettenati MJ, Kearns WG, Howards S, Kogan S, Atala A and Sadri-Ardekani H (2022) *In vitro* propagation of XXY human Klinefelter spermatogonial stem cells: A step towards new fertility opportunities. *Front. Endocrinol.* 13:1002279. doi: 10.3389/fendo.2022.1002279

COPYRIGHT
© 2022 Galdon, Deebel, Zarandi, Teramoto, Lue, Wang, Swerdloff, Pettenati, Kearns, Howards, Kogan, Atala and Sadri-Ardekani. This is an open-access article distributed under the terms of the Creative Commons Attribution License (CC BY). The use, distribution or reproduction in other forums is permitted, provided the original author(s) and the copyright owner(s) are credited and that the original publication in this journal is cited, in accordance with accepted academic practice. No use, distribution or reproduction is permitted which does not comply with these terms.

In vitro propagation of XXY human Klinefelter spermatogonial stem cells: A step towards new fertility opportunities

Guillermo Galdon[1,2], Nicholas A. Deebel[1,3], Nima Pourhabibi Zarandi[1], Darren Teramoto[4], YanHe Lue[4], Christina Wang[4], Ronald Swerdloff[4], Mark J. Pettenati[5], William G. Kearns[6], Stuart Howards[3], Stanley Kogan[1,3], Anthony Atala[1,3] and Hooman Sadri-Ardekani[1,3]*

[1]Wake Forest Institute for Regenerative Medicine (WFIRM), Winston-Salem, NC, United States, [2]Facultad de Medicina, Escuela de doctorado, Universidad de Barcelona, Barcelona, Spain, [3]Department of Urology, Wake Forest School of Medicine, Winston-Salem, NC, United States, [4]Division of Endocrinology, The Lundquist Institute at Harbor-University of California, Los Angeles (UCLA) Medical Center, Los Angeles, CA, United States, [5]Section of Medical Genetics, Department of Pathology, Wake Forest School of Medicine, Winston-Salem, NC, United States, [6]AdvaGenix and Johns Hopkins Medicine, Baltimore and Rockville, MD, United States

Klinefelter Syndrome (KS) is characterized by a masculine phenotype, supernumerary sex chromosomes (47, XXY), and impaired fertility due to loss of spermatogonial stem cells (SSCs). Early testicular cryopreservation could be an option for future fertility treatments in these patients, including SSCs transplantation or *in vitro* spermatogenesis. It is critically essential to adapt current *in vitro* SSCs propagation systems as a fertility option for KS patients. KS human testicular samples (13,15- and 17-year-old non-mosaic KS boys) were donated by patients enrolled in an experimental testicular tissue banking program. Testicular cells were isolated from cryopreserved tissue and propagated in long-term culture for 110 days. Cell-specific gene expression confirmed the presence of all four main cell types found in testes: Spermatogonia, Sertoli, Leydig, and Peritubular cells. A population of $ZBTB16^{+}$ undifferentiated spermatogonia was identified throughout the culture using digital PCR. Flow cytometric analysis also detected an HLA^{-}/$CD9^{+}$/$CD49f^{+}$ population, indicating maintenance of a stem cell subpopulation among the spermatogonial cells. FISH staining for chromosomes X and Y showed most cells containing an XXY karyotype with a smaller number containing either XY or XX. Both XY and XX populations were able to be enriched by magnetic sorting for CD9 as a spermatogonia marker. Molecular karyotyping demonstrated genomic stability of the cultured cells, over time. Finally, single-cell RNAseq analysis confirmed transcription of ID4, TCN2, and

NANOS 3 within a population of putative SSCs population. This is the first study showing successful isolation and long-term *in vitro* propagation of human KS testicular cells. These findings could inform the development of therapeutic fertility options for KS patients, either through *in vitro* spermatogenesis or transplantation of SSC, *in vivo*.

KEYWORDS

spermatogonia, stem cell, germ cell transplantation, fertility preservation, Klinefelter Syndrome, male infertility, cell culture

Introduction

Klinefelter Syndrome (KS) is a classically underdiagnosed cause of male infertility characterized by a male phenotype and altered karyotype, usually presenting as non-mosaic 47 XXY (1). However, variants have been described with additional X chromosomes and different degrees of mosaicism. Recent studies using non-invasive genetic diagnostic technology estimated KS may affect one of every 600-1000 males born (2, 3). Hence, KS is now considered the most common chromosomal cause of male infertility.

The pathophysiological mechanisms underlying male infertility in KS patients are not yet entirely understood. However, several studies have attempted to describe KS testicular morphology from the fetus into adulthood (4–6). Testicular morphology remains largely unaffected in prepubertal patients. During puberty, when testicular fibrosis accelerates, distortion of the tubular architecture was seen (7). By the end of puberty, over 95% of KS patients are azoospermic (8). Leydig cell hyperplasia occurs in the interstitial space in response to elevated LH. Despite Leydig cell hyperplasia, KS patients commonly present with low or low normal range serum testosterone levels. Nevertheless, the degree of testicular fibrosis differs from patient to patient. Foci of active spermatogenesis have been found in KS patients with testicular fibrosis. Current literature shows that only 8% of KS patients have sperm present in the ejaculate (9). These KS patients with adequate sperm in the ejaculate can achieve natural conception with euploid offspring suggesting that cells that complete meiosis may develop into normal gametes (10). The current gold standard of care for treatment of infertility in KS patients is micro-TESE (microscopic testicular sperm extraction) with a reported 44% success rate in testicular sperm retrieval (11, 12), 43% pregnancy rate, and 43% birth rate from *in vitro* fertilization (IVF) or intracytoplasmatic sperm injection (ICSI). No other fertility options for KS patients are currently available.

Since the development of prenatal genetic diagnostic techniques (e.g. Amniocentesis, Chorion Villus Sample, Cell-Free-Fetal DNA determination, Quantitative Fluorescence PCR, Multiplex Ligation Dependent Probe Amplification, Preimplantation Genetic Screening), it is now possible to diagnose and follow KS patients in the prepubertal period, providing social support and enhanced education for preservation of occult sperm that would provide fertility options, should infertility develop. Several reports showed that in patients from whom no spermatozoa could be retrieved by microTESE, viable spermatogonia, including SSCs, may be found in testicular biopsies (13, 14). SSCs are a subpopulation of undifferentiated spermatogonia present in the testis. Their primary function is both continuous self-renewal and differentiation into germ cells committed to undergo spermatogenesis (15). It has been hypothesized that SSCs should be capable of complete restoration of spermatogenesis following transplantation into infertile patients (16). This hypothesis has been supported by several different animal studies (17–22). However, successful SSCs transplantation in humans has yet to be accomplished (23). Experimental SSCs-based therapies may potentially treat KS patients' infertility, even in those patients with unsuccessful TESE. Testicular tissue banking has been implemented in KS patients to provide a source of spermatogonia for new fertility treatments (24, 25). As previously mentioned, germ cell loss in KS accelerates with the onset of puberty. Therefore, retrieval of viable spermatogonia in testicular biopsy is higher in peripubertal than in adult KS patients (8). About 25% of KS patients are diagnosed before puberty (1), and storing testicular tissue from these patients is not a standard practice. Our Wake Forest Baptist School of Medicine group has established an experimental testicular tissue banking for boys and men with a high risk of infertility. KS is one of the approved indications (26). Participating patients are given the option to donate a portion of their testicular samples for research voluntarily.

Our setting provides a unique opportunity to explore the ability to isolate and propagate KS testicular cells from testicular biopsy performed before puberty. Expanding the number of KS

Abbreviations: KS, Klinefelter Syndrome; SSCs, Spermatogonial Stem Cell; SSC, Sodium Chloride-Sodium; dPCR, Digital PCR; MACS, Magnetic Activated Cell Sorting; FISH, Fluorescent *In Situ* Hybridization; PGM, Personal Genome Machine.

testicular cells *in vitro* would be critically important when considering autologous cell-based fertility treatments. It would also provide material for research to preserve and enhance fertility in KS patients, and improve our understanding of why XXY males lose germ cells at puberty. Our previous work tested SSC isolation and culture on 41 XXY KS mice (27–30). Cells were successfully propagated in culture for up to 120 days while expanding 650,000-fold in number. Moreover, characteristic phenotypes of all four common cell types were maintained in culture, including a population of putative SSCs (30). Similar findings are now confirmed using human frozen testicular tissue from KS patients.

Material and methods

Patients

Selected Klinefelter adolescent patients eligible for micro-Testicular Sperm Extraction (mTESE) were offered the opportunity to store their testicular tissue for potential stem cell therapy at Wake Forest Baptist experimental testicular tissue bank under IRB approved protocols at Wake Forest School of Medicine (IRB00021686 and IRB00061265). Surgery was performed by experienced pediatric and adult reproductive urologists (26). Intraoperative testicular tissue examination to evaluate the presence of sperm was performed by the clinical embryologist. The protocol included several rinses, microbiology testing, and histology tissue processing. Testicular samples were dissected into 2-4mm^3 portions and cryopreserved in 1ml cryovials using cryoprotectant solution: Hank Balances Saline Solution 5% Human Serum Albumin (CSL Behring LLC) 5% DMSO (Mylan Institutional). A controlled rate freezing machine was used to freeze the samples following the in house validated protocol (26, 31). Cryovials were transferred into vapor nitrogen tanks at the Manufacturing and Development Center (MDC) of Wake Forest Institute for Regenerative Medicine (WFIRM) for long-term storage. A maximum of 20% of stored tissue was used in this study. The remaining portion (80%) was kept for future clinical use.

A portion of the testicular biopsies was fixed in 4% Formalin, 4% Paraformaldehyde, and Bouin fixatives. Tissue was then processed, paraffinized, and mounted by a clinical pathology lab for staining and histology.

Hematoxylin-Eosin staining and immunohistochemical staining with PGP 9.5 (UCHL1) as a spermatogonia marker were performed on 5 micron thick tissue sections using an automated stainer. Immunostaining was performed using the Leica Microsystems Bond 3 autostainer at the Wake Forest University clinical pathology laboratory. After 20 minutes of antigen retrieval using Bond Epitope Retrieval Solution 2 (ER2), the primary antibody (PA0286; mouse monoclonal PGP9.5 (UCHL1)) was incubated for 15 minutes at room temperature. To detect and visualize the antigen, a Bond Polymer Refine Detection kit (peroxide block, post-primary, polymer reagent, DAB chromogen/Leica, DS9800, followed by hematoxylin counterstain) was used. Counterstaining of hematoxylin identified the nucleus of cells. Isotype control (mouse IgG) was used as a negative control for the primary antibody. Age-matched controls (testes biopsies from 46 XY patients *via* National Disease Research Interchange, NDRI) were used to compare testicular morphology. Microscopic images were acquired using LEICA DM4000B microscope, Olympus camera DP73, and Olympus Cellsens software.

Cell isolation, culture, and cryopreservation

Testicular cells were isolated from cryopreserved testicular tissue. The process was performed under pre-clinical Good Laboratory Practice (GLP)-conditions following a protocol previously described by our group (30, 32, 33) with some modifications for potential clinical application of human SSCs isolation and culture. Selected cryovials were thawed uniformly by immersion in warm water. Immediately after, DMSO was washed out from the tissue using 1x MEM 8µg/ml DNAse (Roche). External connective tissue was removed, and single seminiferous tubules were dissected apart using a dissecting microscope (Leica S6D) and jeweler tweezers.

Tissue was transferred into a 1.5 ml Eppendorf tube due to the small sample size and resuspended in an enzymatic digestion solution made of: 1x MEM; 12µg/ml DNAse (Roche); 0.4 PZU/ml Collagenase NB4 Standard Grade (SERVA); 0.02 DMCU/ml Natural Protease NB (SERVA). Samples were incubated in a shaking water bath at 120 rpm and 32°C. The enzyme mix was exchanged after every hour of incubation. Tubules and cells were pelleted by centrifugation at 16g for 5 min. A sample of the pellet was examined under the microscope, and the process was repeated with fresh enzymatic solution until disassociation of the tubules was confirmed by these examinations.

Once the enzymatic digestion disrupted the seminiferous tubules and many single floating cells were visible floating, the sample was pipetted up and down energetically to help release the remaining cells. The tube was then centrifuged for 5 min at 350g (1500 rpm) with a brake. The resultant supernatant was discarded, and pellets containing released cells were used for culture.

During the isolation process released tubular cells might form tight clumps. In these cases, it was helpful to additionally incubate the sample in 0.25% Trypsin-EDTA (FisherScientific-Gibco) at 37°C for 5-30 minutes, checking every 5 minutes until a single cell suspension was observed again. Then the sample was

10.3389/fendo.2022.1002279

TABLE 1 Stempro Complete culture media composition.

Reagent	Company	Catalog #	Final concentration
Stem Pro-34 SFM	Invitrogren	10639-011	–
Stem Pro Supplement	Invitrogren	10639-011	–
Bovine Albumine	Roche	1.07E+10	5 mg/ml
D(+) Glucose	Sigma	G7021	6 mg/ml
Ascorbic acid	Sigma	A4544	1x 10-4
Transferrin	Sigma	T1147	100 µg/
Pyruvic acid	Sigma	P2256	30 mg/ml
d-Biotin	Sigma	B4501	10 µg/ml
2-beta Mercatoethanol	Sigma	M7522	5x 10-5
DL-lactic acid	Sigma	L4263	1 µl/ml
MEM-non essential	Invitrogen	11140-035	10 µl/ml
Stem Pro Supplement	Invitrogen	10639-011	26 µl/ml
Insulin	Sigma	I1882	25 µg/ml
Sodium Selenite	Sigma	S1382	30 nM
Putrescine	Sigma	P7505	60 µM
L-Glutamine	Invitrogen	25030-024	2 mM
MEM Vitamine	Invitrogen	11120-037	10 µl/ml
b-Estradiol	Sigma	E2758	30 ng/ml
Progesterone	Sigma	P8783	60 ng/ml
Human EGF	Sigma	E9644	20 ng/ml
Human bFGF	Sigma	F0291	10 ng/ml
Human LIF	Chemicon	LIF1010	10 ng/ml
GDNF	Sigma	G1777	10 ng/ml
FCS	Invitrogen	10106-169	1%
Pen/Strep	Invitrogen	15140122	0,5%

centrifuged again for 5 min at 350g (1500 rpm) with brake, trypsin supernatant was removed, and the pellet containing released cells was used for culture.

The final pellet of cells was resuspended on MEM 10% FBS for culture. This culture media was used to improve the initial attachment of cells. Hematocytometer should be used to assess cell numbers in the final sample and all the previously removed supernatants to ensure no cell is wasted. Viable cells were seeded at 10.000 cells/cm^2 on plastic plates (Falcon) and kept in an incubator constant 37°C 5% CO2 in a room with positive air pressure GLP conditions. The next day, culture media was switched from MEM 10% FBS into an enriched StemPro medium, Table 1 (32, 33), previously reported to support testicular cell propagation *in vitro*.

During the culture, samples were checked every other day. The media was refreshed every 2-3 days. Cells were passaged and split when cell confluency approached 80% using 0.25% Trypsin-EDTA (FisherScientific-Gibco).

After every passage, when possible, a portion of cells were cryopreserved for backup in a 2ml cryotube (Sigma Aldrich). Cryopreservation media used was MEM 20% FBS and 8% DMSO, and Mr.Frosty (Nalgene) at -80˚C was used for slow freezing overnight. The next day, cryotubes were transferred into liquid nitrogen tanks for long-term storage.

Quantitative reverse transcriptase polymerase chain reaction

RNA was extracted using RNEasy Minikit (Qiagen) from Snap Frozen tissue or cells. The quality and quantity of extracted RNAs were tested with a spectrophotometer (Nanodrop 2000, ThermoFisher). RNA was then converted to cDNA using Reverse Transcriptase Kit (Life Technologies) and through the following thermocycler (Simpli amp thermal cycler, life technologies) conditions: 25°C for 10min, 37°C for 120min, 85°C for 5 min, and 4°C hold.

The cDNA samples underwent PCR amplification using Taqman primers (Table 2) and applied Biosystems 7300 Real Time PCR system. The cycling conditions followed were 95˚C for 10 minutes, then 40 cycles of 95˚C for 15 seconds, and 60˚C for 1 minute.

All primers were chosen intron spanning and previously tested for not amplifying genomic DNA. A minus RT (water)

TABLE 2 Taqman assay primers used for PCR.

Gene	Catalog #	Primer length
UCHL1	Hs00985157 m1	80
ZBTB16	Hs00957433 m1	65
THY1 (CD90)	Hs00174816 m1	60
PRM1	Hs00358158 g1	99
GATA4	Hs00171403 m1	68
Clusterin	Hs00971656 m1	93
CD34	Hs02576480_m1	63
STAR	Hs00264912 m1	85
TSPO	Hs00559362 m1	57
CYP11A1	Hs00897320 m1	81
POLR2A	Hs00172187 m1	61

control has been used to rule out any contamination in PCR mixtures (not shown in the gel picture, Figure 4). POLR2A was selected as a housekeeping gene, and the expression of genes were normalized to this gene; relative expression was determined with the Delta CT method.

Amplified cDNA from RT qPCR was later used for an Electrophoresis study on a gel to visualize the specific product bands. A 2% Agarose gel was used, given that our target primers were between 50-120 bp in length (Table 2). Ethidium Bromide was included in the gel formulation at a concentration of 5ul/100ml. After the Samples and DNA ladder were loaded, a 140V Voltage (Enduro power supply, Labnet) was applied for 20 mins when the DNA dye reached 2/3 of the total gel size. Images of the gel were taken using a UV light Camera system (Gel logic 200 imaging system).

Digital reverse transcriptase polymerase chain reaction

Digital PCR is a molecular biology tool that evenly distributes sample cDNA along with RT PCR mix into independent microchip wells. Then independent thermocycling reactions are conducted separately in each well prior to fluorescent signal reading. Digital PCR is especially useful for small population assessment or rare events analysis. This system has been validated by both manufacturer and independent researchers (34), even in a clinical setting (35, 36).

To estimate the percentage of undifferentiated spermatogonia during the culture, we used a Digital PCR system (Quant Studio, Life Technologies) and Taqman assays labeled with VIC (for POLR2A as housekeeping gene) and FAM for target gene (ZBTB16). As each mammalian cell has a range of 10–30 pg of total RNA, we used the cDNA made from 50 ng of total RNA in 20 000 wells of a digital PCR chip for each assay.

The chips were loaded following the manufacturer's protocol with commercially available dPCR Master Mix (Life Technologies), water, cDNA, and Taqman primers. cDNA for this project was obtained using retrotranscriptase reaction on RNA extracted from Snap Frozen cells. Cycling conditions were: 95˚C for 10 minutes, then 40 cycles of 95˚C for 15 seconds and 60˚C for 1 minute.

Flow cytometry analysis and MACS-sorting

The population of putative spermatogonial stem cells in culture was estimated as HLA-ABC-/CD9+/CD49f+ population (37–41) using BD Accuri C6 Flow cytometry system without sorting. BD antibodies were used (Table 3) at a concentration of 5ul of antibody per 50.000 cells in 100ul Flow Cytometry buffer (PBS 1% FBS). Cells were incubated with the antibody for 30 minutes at room temperature and then washed with flow cytometry buffer. Obtained data were analyzed using BD Accuri software. Unstained cells and cells incubated with isotypes control antibodies (Table 3) were used to optimize channel compensation and negative control. In every condition, 10,000 events were evaluated.

The same staining method was used in separate experiments to perform Fluorescence Activated Cell Sorting using BD FACS ARIA. Cells expressing HLA-ABC-/CD9+/CD49f+ were sorted and used for FISH analysis.

TABLE 3 Antibodies used for Flow cytometry and Magnetic-activated cell sorting (MACS).

Antigen	Reactive species	Raised in	Flourochrome	Company	Catalog #
HLA-ABC	Anti-Human	Mouse	FITC	BD Biosciences	555552
CD9	Anti-Human	Mouse	PE	BD Biosciences	341637
CD49f (Integrin alpha 6)	Anti-Human	Mouse	APC	Thermofisher	17-0495-80
Mouse IgG			FITC	BD Biosciences	340755
Mouse IgG			PE	BD Biosciences	340756
Mouse IgG			APC	BD Biosciences	340754
FcR Blocking Reagent	Anti-Human		MACS Microbeads	Miltenyl Biotec	120-000-442
Anti-PE	Anti-Human		MACS Microbeads	Miltenyl Biotec	120-000-294

Single-cell RNA sequencing

Cultured and cryopreserved testicular cells from XXY and XY adolescent individuals were sent from WFIRM to UCLA. Upon arriving at the Lundquist Institute of Harbor-UCLA Medical Center, testicular cells were revived and cultured in a 25 cm^2 flask with 4 ml of enriched StemPro-34 medium/flask for five days. Cells were harvested, washed, resuspended in 0.04% BSA in PBS, and delivered to UCLA Technology Center for Genomics and Bioinformatics (TCGB). The cell concentration and viability were determined at TCGB using a countess II automated cell count. Per manufacturer recommendations, a single cell suspension (1000 cells/μL) from each sample was loaded onto the 10x Chromium chip and controller. Ten thousand cells were targeted for capture per sample. Cell capture and 10X single cell 3' gene expression sequence library preparation were performed. The resultant library was sequenced using a NovaSeq 6000 SP (100 Cycles). Mapping, cell identification, and clustering analysis were performed using 10x Cell Ranger software at the UCLA-TCGB.

For the data analysis, raw count matrices generated from 10X Genomics and Cell Ranger were imported to the Seurat package in R, where cells were screened based on QC metrics (42). An object of class Seurat 19618 features across 9580 cells of XY testicular sample and 19284 features across 11845 cells of XXY sample were subject to data analysis. Data normalization, scaling, and feature selection was performed as described in the SeuratV3 procedure. These were followed by unsupervised cell clustering and a UMAP analysis (43, 44). Differential gene expression among clusters was determined in Seurat using a Wilcoxon rank sum test, and gene expression probability across clusters was visualized with VlnPot and FeaturePlot.

X and Y chromosome fluorescent *in situ* hybridization

After cells in culture had been trypsinized, fifty thousand cells were cytospin for 10 min at 1000 RPM on glass poly-l-lysine slides (Cytopro, ELI Tech Biomedical Systems) using the cytopro 7620 cytocentrifuge system (Wescor). The slides were left to dry at room temperature overnight. In parallel, testicular tissue samples from the same patients archived in pathology were processed by for the same X and Y hybridization.

Slides were soaked in 2X saline sodium citrate (made from stock 20xSSC from ABBOTT/VYSIS Company) at 37°C for 35 minutes. Subsequently, cells were incubated in Pepsin (AVANTOR PERFORMANCE MATERIALS, INC 2629, company) 0.5mg/ml solution of HCl 0.1M at 37 degrees C for 35 minutes. Slides were then washed at room temperature in 1XPBS for 5 minutes, and Post-Fixation Solution (0.9% formaldehyde W/V; 4.5 mg/ml MgCl2 in PBS) was added for 5 minutes incubation at room temperature. Slides were re-washed at room temperature 1XPBS for 5 minutes, and the dehydration process was performed by submerging slides in increasing concentrations of ethanol (70%, 80%, 100%) for 1 minute each at room temperature.

A working solution of X and Y chromosome probes (EMPIRE GENOMICS Company kit 1:1:4 probe buffer dilution) was added to the sample, and slides were kept at 75°C for 5 minutes, followed by overnight incubation at 40°C (16 Hours minimum). The following day, slides were washed in 0.3% IGEPAL/solution (SCI-GENE) on 0.4X saline sodium citrate/for 2 minutes at 73° C and 0.1% IGEPAL (SCI-GENE) solution on 2X saline sodium citrate for 1 minute at room temperature.

Slides were finally mounted with ABBOTT/VYSIS DAPI II and coverslipped.

Imaging of the slides was performed using a Zeiss Axiophot microscope and Applied Spectral Imaging Software.

Molecular karyotyping with next generation sequencing

The cryopreserved cultured cells were transported from WFIRM to AdvaGenix and Johns Hopkins Medicine lab. After DNA extraction, fifty to 100 ng of amplified DNA underwent library preparation (Thermo Fisher Scientific, Waltham, MA). First, the pooled DNA samples underwent enzymatic shearing to produce fragment sizes of approximately 200 bp. The DNA fragments were purified using an AMPure Bead (Beckman Coulter, Sharon Il) wash, stabilized by the ligation of adapters and barcodes at either end of each fragment, and size selected using a second AMPure Bead wash. Each DNA fragment was bound to one ion sphere particle (ISP) and amplified thousands of times using an emulsion PCR reaction. The positive template ISPs were recovered using Dynabeads MyOne Streptavidin CI bead washes (Invitrogen, Carlsbad, CA). Following recovery, sequencing primers and Ion Hi-Q sequencing polymerase were added to the samples, and the samples were loaded onto a sequencing chip and analyzed at a depth of 1X across the entire genome by a Personal Genome Machine (PGM) or S5 (Thermo Fisher Scientific, Waltham, MA). Sequencing data were processed by a Torrent Browser Server (Thermo Fisher Scientific, Waltham, MA) to provide initial sequencing information and ensure adherence to our required quality assurance metrics. The data was then transferred to an Ion Reporter Server (Thermo Fisher Scientific, Waltham, MA) for comprehensive data analysis and interpretation. The PGM or S5 sequencing provided a minimum of over 3.5 million reads with a median sequencing fragment length of 181 bp.

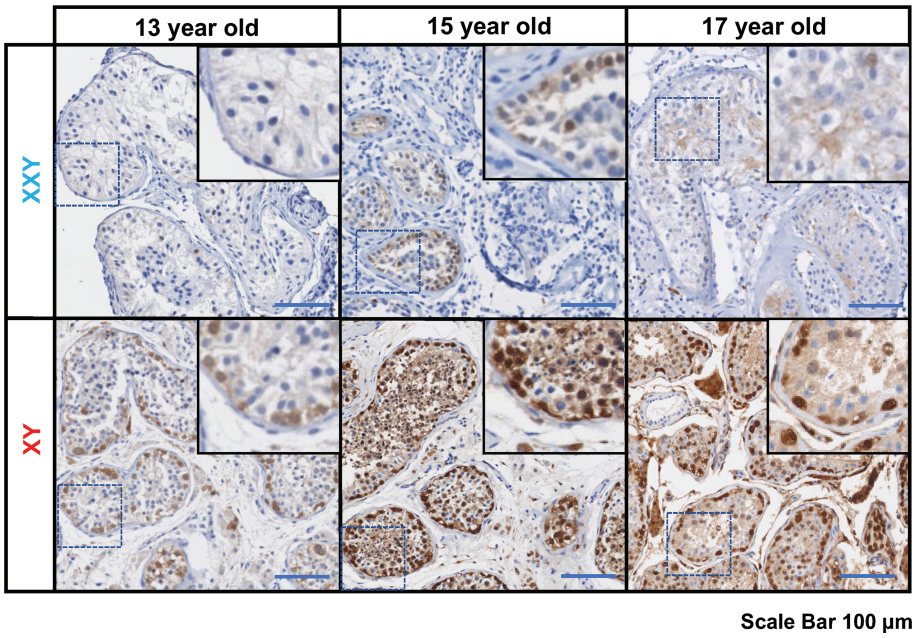

FIGURE 1
Immunostaining for undifferentiated spermatogonia marker UCHL1 (PGP 9.5), subjects' ages: 13, 15 and 17 years old. On the top panel, three Klinefelter patients included in the study. On the bottom panel, three aged-matched controls. Scale bar 100µm.

Results

Presence of undifferentiated spermatogonia in TESE negative KS patients' testes

Standard of care at Wake Forest testicular tissue bank includes histologic analysis and pathology review of all samples. Every KS patient case is discussed and compared with age-matched controls from our archives. Three KS patients enrolled in the testicular tissue bank were selected for this study (13 years old, 15 years old, and 17 years old). Pathology slides from testicular biopsy stained immunohistochemically for PGP 9.5 (UCHL1) and Hematoxylin-Eosin and compared with age-matched controls (Figure 1).

In all KS subjects, most seminiferous tubules were either hyalinized or only contained Sertoli cells. Rarely, some tubules contained the cells expressing the PGP 9.5, a marker for undifferentiated spermatogonia, with no further spermatogenic cells such as spermatocytes and spermatid. Leydig cell hyperplasia was prominent between tubules. No evidence of germ cell neoplasia or carcinoma *in situ* was observed. In contrast, age-matched controls presented a well-organized tubular architecture containing spermatogonia at different stages of differentiation into elongated spermatids.

Given that sperm were not found using micro TESE in any of the three patients (TESE negative), they were considered ideal candidates to benefit from SSCs isolation and culture strategy.

Long term *in vitro* propagation of KS testicular cells

Compared to previous experiences by our group in isolating cells from human testes, KS samples presented as a different consistency. Tubules were thickly packed and more difficult to dissect. In our hands, pieces took between 2-2.5 h of enzymatic digestion to release cells, but it varied from sample to sample. Once the isolation method was tuned and optimized for KS tissue, cell isolation yield was comparable to XY age matched controls. Similarly, the morphology of cells in short- and long-term cultures was similar to previous testicular cells cultured from euploidy patients (Figure 2).

Isolated testicular cells from KS patients remained viable in culture for more than 90 days. For the first eight days in culture, the number of cells did not significantly increase. Cells then started growing exponentially until the end of the study. The number of cells expanded more than 100 million fold within 90 days (Figure 3). Cell viability was always ≥ 95%, as determined by trypan blue staining at each passage. These findings are

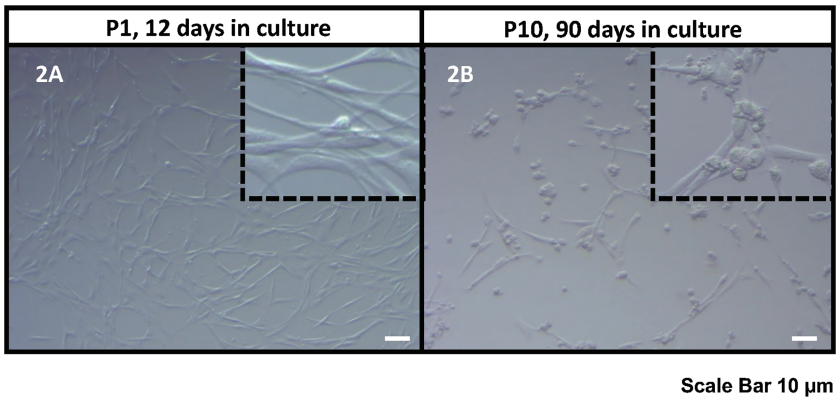

FIGURE 2
Bright field microscope images of the human KS testicular cells in culture at passage 1, 12 days in culture **(A)** and passage 10, 90 days in culture **(B)**. As it was also reported previously (30, 32, 33), the current culture system includes both spermatogonia and testicular somatic cells. Somatic cells usually attach earlier forming an extensive network of plain elongated cells. Then round spermatogonia cells attach forming clusters on top of somatic cell feeder layer (showed in inserts). Scale Bar 10 µm.

comparable to previous data from our group in propagating testicular cells from peripubertal euploid patients (32).

Presence of undifferentiated spermatogonia and somatic cells in culture

After testicular cell isolation, a heterogeneous mixture of cells is expected in this culture system. Somatic cells are expected to quickly attach to the culture surface and form a feeding layer that provides an excellent environment for spermatogonia propagation. It is critically important to confirm the presence of all significant testicular cell types during the culture period, as a misbalance could prevent the other cell types from expanding.

qPCR analysis was used to confirm the presence of characteristic gene expression from the main four testicular cell types expected in culture: undifferentiated spermatogonia (UCHL1, ZBTB16, and THY1), Leydig (TSPO, STAR, CYP11A1), Sertoli (GATA4, Clusterin) and peritubular cells (CD34) (Figure 4). A

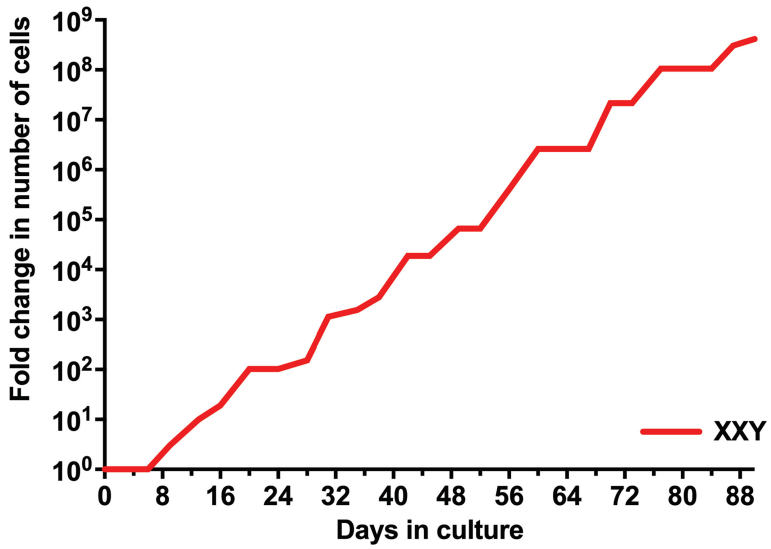

FIGURE 3
Evolution of the number of isolated human KS testicular cells in culture. Results show the average from KS subjects' testicular tissue. The initial number of cells was standardized to 1 to better assess growth along time in the graph and compare subjects with different initial cell numbers.

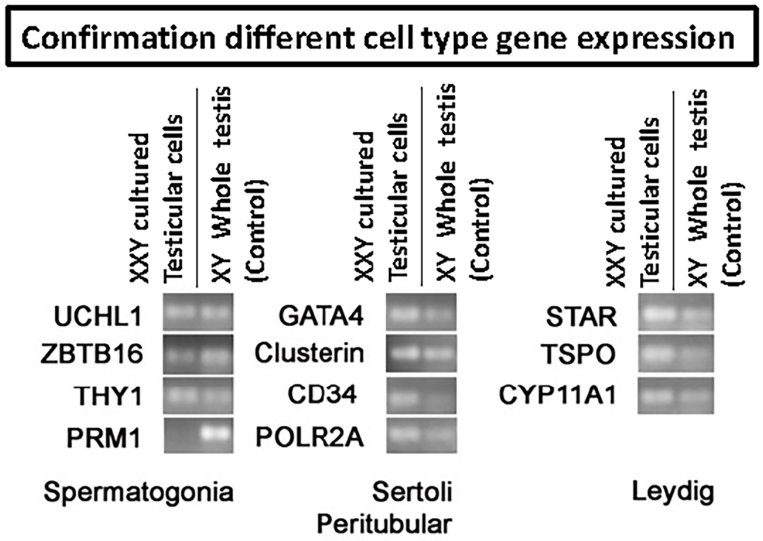

FIGURE 4
RT-PCR to confirm the presence of the four main testicular cells in culture based on cell-specific gene expression: spermatogonia (UCHL1, ZBTB16, THY1, PRM1), Sertoli (Gata4, Clusterin), peritubular (CD34) and Leydig (STAR, TSPO, CYP11A1). POLR2A was used as a housekeeping gene for internal control. Results confirmed the presence of all four common cell types. However, differentiated germ cell marker PRM1 remained negative, indicating the undifferentiated status of the germ cells in culture.

positive signal for all of these was obtained from cultured cells. Conversely, the expression of differentiated germ cell marker PRM1 remained negative (Figure 4). This demonstrated that spermatogonia remained undifferentiated and capable of maintaining a putative SSCs population suitable for transplantation.

After confirming the phenotypes of cells present in the culture, the focus moved to determining the percentage of spermatogonia throughout the culture period. Digital PCR analysis was performed (Figure 5) on isolated testicular cells from frozen tissue with 2.3% of cells shown to be ZTBTB16^{+}. This population grew during the initial stages of culture, climbing from 20- 37% between days 13-66. In the culture's late stages, the percentage of undifferentiated spermatogonia dropped to 14% but remained present throughout the entire culture period (Figure 5). Therefore, our culture system for Klinefelter testicular cells propagated every cell type expected

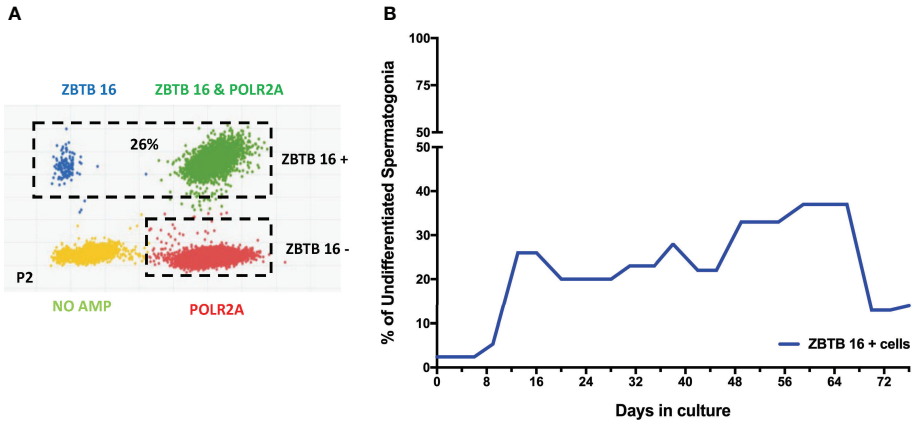

FIGURE 5
Digital PCR analysis was used to assess the population of undifferentiated spermatogonia expressing ZBTB16 (PLZF) marker and housekeeping gene POLR2A in testicular cells in culture: After 2nd passage from 15-year-old KS patient **(A)**. The same analysis was repeated at different time points. The graph shows the average undifferentiated spermatogonia population during the culture of testicular cells from KS patients **(B)**.

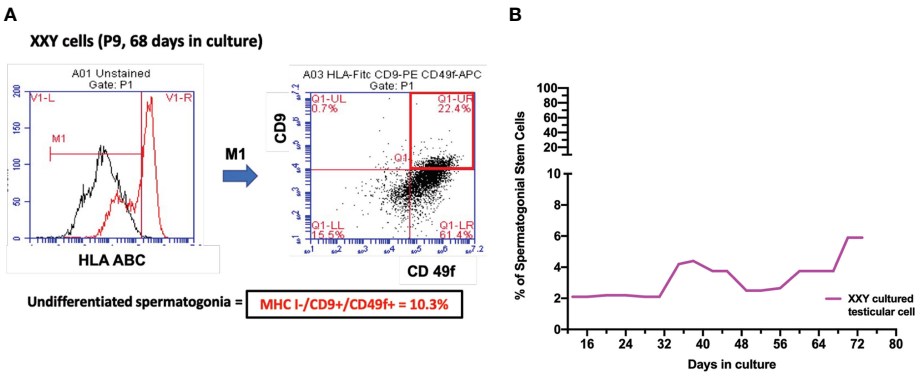

FIGURE 6
(A) Spermatogonial stem cells (SSC) population was estimated by combining HLA-/CD9+/CD49f+ markers on Flow Cytometry analysis. After 68 days in culture and nine passages, the percentage of putative SSC was 10.1% of a 17-year-old KS patient **(B)**. Several time points were analyzed to evaluate the evolution of this population over time in all subject samples in culture. The graph shows the average of the SSCs population during the culture in KS patients **(B)**.

while maintaining a significant population of undifferentiated spermatogonia throughout the 90 days culture.

The constant presence of SSCs during the culture

At the time of transplantation, only SSCs are expected to migrate to the basal membrane of the seminiferous tubules and restore spermatogenesis in azoospermic patients. So far, the scientific community has struggled to identify a single marker that could fully characterize this population of cells. Meanwhile, a combination of HLA-ABC -/CD9 +/CD49f + has been postulated as markers for the enrichment of SSCs and predicting therapeutic success following transplantation (38–41, 45).To assess putative SSCs in culture, flow cytometry analysis was utilized.

Successfully propagated testicular cells from KS patients presented putative SSCs at every analyzed time point (Figure 6). Quantitative analysis suggested a consistent population in culture, representing between 2-10% of cells in the culture. This indicates that our culture system not only promotes cell propagation, but also provides an excellent environment for maintaining SSCs phenotype, *in vitro*. These results align with prior data using dPCR that identified viable undifferentiated spermatogonia within the culture.

ID4 positive cells in culture as an SSCs sub-population

To further characterize the cells in culture, ScRNA Seq analysis was carried out. Cell partitioning *via* UMAP identified 6 clusters in cultured XY and 7 clusters in cultured XXY testicular cells. As shown in Figure 7, the ID4, TCN2, and NANOS 3 positive SSCs (46–48) are predominately located within clusters 0 and 1. The data showed that ID4 positive SSCs were more abundant in the XY testicular cell culture than in the XXY culture. The number of TCN2 and NANOS 3 positive SSCs was similar between XY and XXY testicular cell cultures. This data demonstrated that our human testicular cell culture system could provide a favorable environment for SSCs to grow and support survival, *in vitro*.

The stable genotype of SSCs in culture

NGS technology has been successfully established to assess chromosome copy number and integrity by applying linear regression to the amplification of chromosome-specific sequences for 24-chromosome aneuploidy screening (49). In this study, chromosome copy number analysis was essential to address the concern of genotype instability of cells in culture.

Fluorescence-activated cell sorting (FACS) was used to isolate putative SSCs using the markers HLA^{-}ABC. $^{-}$/CD9 $_{+}$/CD49f $^{+}$ and compared to peripheral blood XX and XY controls. Results showed no significant difference in the number of somatic chromosomes using up to a 10% confidence filter (Figure 8). Sexual chromosome analysis identified an XXY sample compared to XX and XY controls. The sample was finally characterized as non-mosaic 47XXY.

These data suggested that cells in culture remained karyotypically stable. These findings are interpreted as a favorable indication of clinical application potential. The same experiment was conducted on non-sorted cells with equivalent results (data not shown).

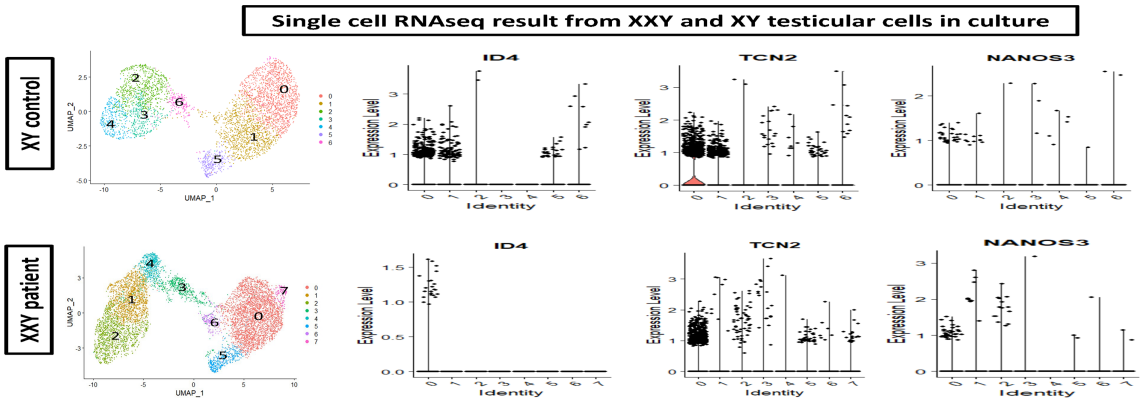

FIGURE 7
Single cell RNAseq analysis of cultured human XY (upper panel) and XXY (lower panel) testicular cells. Cell partitioning *via* UMAP identified 6 clusters in cultured XY and 7 clusters in cultured XXY testicular cells. Expression patterns of ID4, TCN2 and NANOS 3 (violin plot) supported the presence of SSCs during the culture.

Fluorescent *in situ* hybridization

Fluorescent *in situ* hybridization (FISH) staining for X and Y chromosomes was performed to demonstrate the presence of KS XXY cells in culture. The probes used for this study marked the X chromosome with a red signal (5-ROX) and the Y chromosome with a green signal (5-Fluorescein).

The initial goal of this analysis was to confirm the aneuploidy of the cells in culture. Cytospun slides were systematically examined, XXY cells were identified. Additionally, XY and XX and their dividing counter partners were also seen (Figure 9A).

After these findings were confirmed, we hypothesized that although all of the patients included in this study had been clinically diagnosed as non-mosaic 47XXY Klinefelter, we might have some mosaicism in the testicular cell culture. An experiment was designed to analyze FISH slides in consecutive passages to identify different mosaic populations and describe their evolution in culture over time. Moreover, when the total cell number was sufficient, FISH staining was performed in parallel in CD9+ Magnetic Activated Cell Sorter (MACS) cells and non-sorted controls.

Results showed that even at the earliest time point at four days, there was a small population of both XY (1.4%) and XX

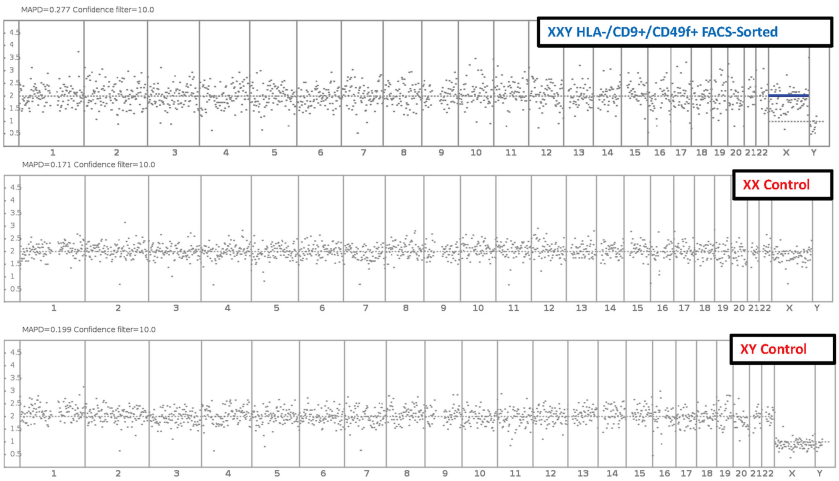

FIGURE 8
Molecular Karyotyping by next-generation sequencing. After 47 days and 6 passages, Klinefelter cells in culture were FAC Sorted for putative SSC markers HLA-/CD9+/CD49f+. Then cells were analyzed with next generation sequencing and compared to XX and XY controls. Results identified cells in culture as 47 XXY with a 10% confidence filter.

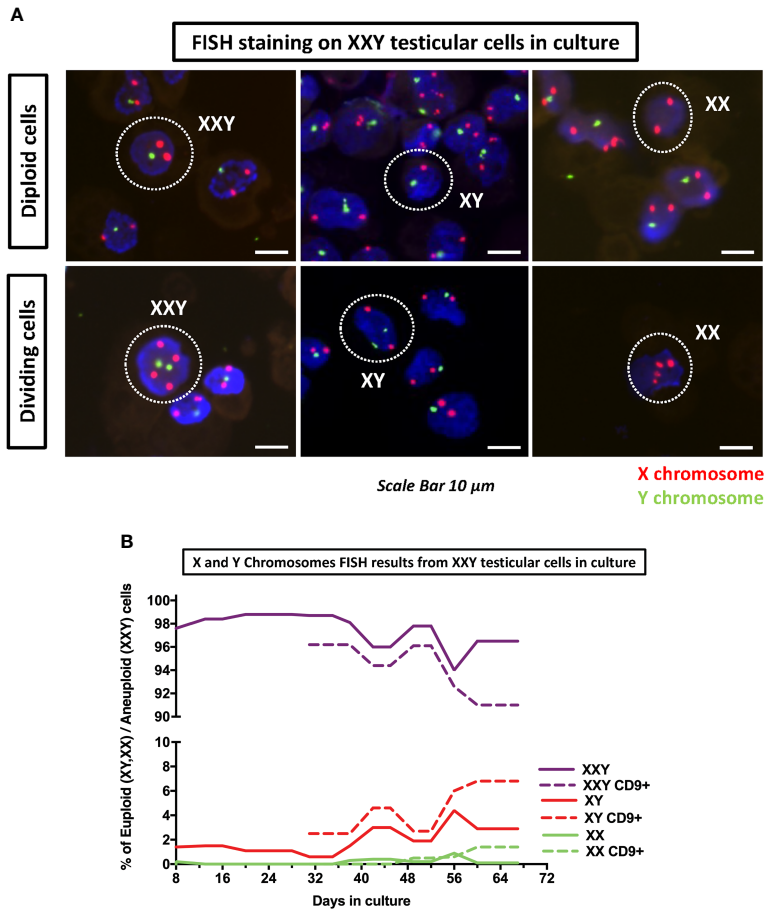

FIGURE 9
DNA FISH analyses of cultured cells was used to assess the number of copies of X (red probe) and Y (green probe) chromosomes on KS testicular cells in culture. **(A)** Detection of XXY, XY and XX in culture as well as their respective dividing counterparts. **(B)** Quantification of XXY, XY and XX populations in consecutive passages during the culture. The results showed a consistent mosaic population (solid lines). Moreover, when cells in culture were enriched for undifferentiated spermatogonia marker CD9+ using MACS, both XY and XX population increased (dot lines) suggesting that higher number of euploid cells in spermatogonia population.

(0.2%) (Figure 9A). As time passed, both populations thrived and came to represent (4.4%) and (0.9%) respectively. Furthermore, when cells were MACS sorted using CD9 to enrich spermatogonia, XY and XX populations were enriched up to 6.8% and 1.4%, respectively (Figure 9B). These findings confirmed that small populations of XY and XX cell mosaicism among XXY cells in culture and suggested XX and XY cells were preferably spermatogonia. This is critical, as euploid spermatogonia may impact the product of spermatogenesis and might, at some level, provide an explanation for the presence of healthy offspring produced from azoospermic KS patients with intratesticular sperm available.

A question was raised about the possibility of KS patients presenting some congenital testicular mosaicism that had remained undiagnosed with standard clinical Karyotype techniques. FISH staining was then performed in testicular tissue histology slides from the same patients. The results showed most cells presenting XXY signal. However, few XX and XY cells were found inside the few preserved seminiferous tubules (Figure 10). In the basal membrane from one of the tubules, few XY cells were found to be dividing. These findings strongly support some mosaicism in the testes of non-Mosaic 47 XXY KS patients diagnosed by karyotyping.

Discussion

Although testicular morphology was severely affected by fibrosis in all KS subjects, PGP 9.5 positive spermatogonia cells were still found inside several seminiferous tubules (Figure 1). Following isolation and culture of testicular cells from all three subjects, undifferentiated spermatogonia cells were positive for PGP 9.5 ZBTB16 and THY1. These findings suggest that even in patients with negative IHC for spermatogonia, viable

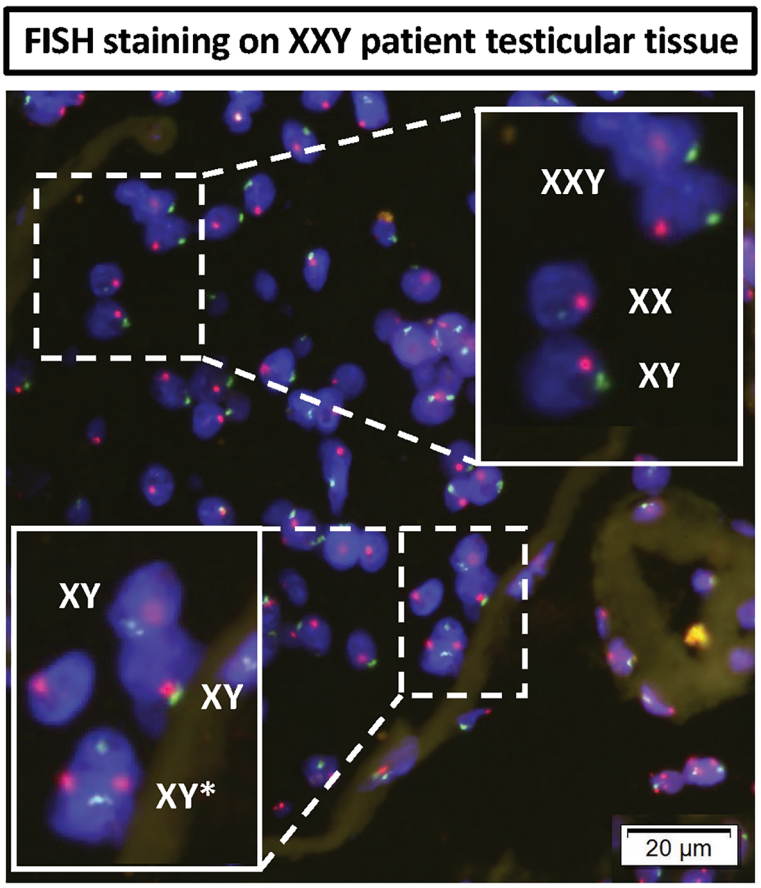

FIGURE 10
DNA FISH analyses of KS testicular tissue was used to assess any mosaicism in KS testes: X (red probe) and Y (green probe) chromosomes. The top magnified region showed all three XXY, XY and XX cells in non-mosaic KS subject. The bottom magnified region shows an XY cell actively dividing in the basal membrane of seminiferous tubules of non-mosaic KS subject.

spermatogonia are likely present in the cryopreserved samples. Cell isolation and culture under optimal conditions may be able to selectively expand these spermatogonia for fertility treatments. The age of the subjects and other developmental factors may be vital in predicting the success of spermatogonia retrieval and optimizing cell culture.

SSC transplantation is the definitive test for SSCs identification. However, regulatory limitations do not allow for human SSC transplantation. The connection between HLA-/CD9+/CD49f+ enriched cells and SSC transplantation success has long been characterized in autologous animal models and xenotransplantation (37–41). The presence of SSC in our culture system has previous already been tested using xenotransplantation into nude mice (32). We feel that SSC characterization using FACS and RNAseq can reasonably assess the SSC population and may predict SSC transplantation efficacy without the economic costs, ethical challenges, and time associated with low efficient xenotransplantation.

By reaching a 20 million-fold increase in the number of cells in culture, the goal of *in vitro* propagation of spermatogonia cells was achieved. The number of cells isolated per biopsy varied between subjects from 275,000 to 400,000, and the propagation culture system could provide around 5.5 and 8 trillion cells. Conservatively estimating the enriched population of SSCs (HLA-ABC-/CD9 +/CD49f+ or ID4 +) as 2% of propagated testicular cells, 110 billion SSCs could be provided after 50 days of culture. Based on previous studies in non-human primates (19, 21, 22), these numbers of cells might potentially enable SSC transplantation. An even lower number of cells might be needed for *in vitro* spermatogenesis (45, 50). Another advantage to this strategy is that only XY SSCs from KS subjects (1% of all propagated SSCs) are likely to go through complete spermatogenesis. Also worth mentioning is that a maximum of 20% of the original testicular biopsy sample was used for this project, as 80% remained untouched for future clinical applications. When the full samples are used, the starting number of cells in culture will increase, and the duration of culture reduced.

Due to characterization challenges, it has been difficult to quantify the SSC population *in vivo*. However, recent reports by Brinster and Kubota (15) in different mammals estimated this population to be somewhere between 0.01-12.5% of spermatogonia. Using HLA-/CD9+/CD49f+ markers, a population of 2-10% putative SSC was identified in culture. RNAseq data provided confirmation of SSC presence, identifying ID4, TCN2, and NANOS 3 positive clusters of cells. These findings correlate with current literature describing SSC dynamics and their cellular niche, which could indicate an *in vitro* system mimicking *in vivo* physiology (38, 40, 41, 46, 47, 51). Although further research is required on this topic, we expect these data to help optimize the timing between testicular cell culture and SSC transplantation.

Different hypotheses may explain the fluctuation in the number of undifferentiated spermatogonia in culture. It is possible that somatic cells, although able to be maintained in culture long term, do not have the ability to propagate indefinitely. Therefore, somatic testicular cells become less proliferative and efficient in supporting the SSCs population.

FISH and NGS analyses were combined to better characterize the chromosomal stability of cells in culture. Molecular Karyotyping by NGS gave a broad overview of chromosomal integrity across hundreds of thousands of cells using a high number of specific gene loci, very reproducible technology, increased statistical power. The technical limitations of statistical analysis provided a 10% confidence filter, meaning that mosaicisms representing less than 10% of the cells could not be detected.

The limitation of detecting mosaicism in cultured cells was overcome using FISH staining for X and Y chromosomes and manually counting over 5000 cells per subject. Using this method, XY and XX cells were identified within the predominantly XXY population, and the ratio of these karyotypes were characterized during the time in culture. Consistent with NGS data, mosaicism never reached 10%, meaning at least 90% of the cells in culture presented a 47XXY karyotype. Up to 10% might present some mosaicism, including XX and XY karyotypes. Therefore, looking to potential clinical fertility applications, preimplantation genetic screening (PGS) should be recommended for these patients. However, our data support a reasonable level of genetic stability and safety in the cells in culture.

Previous studies have shown sex chromosome mosaicism in cultured iPSCs (52). Similar mosaicism was also described by Hirota et al. (45) using iPSC derived from both XXY mouse and human fibroblasts. Cells in our culture system were not immortalized and achieved long-term culture, up to 100 days. Future studies should compare different cell sources in parallel to verify which options presents the greatest chromosomal stability in culture.

Another interesting finding was that observation of XY and XX cells, even at the earliest timepoint (day four) in our culture system. Similar FISH staining was performed on testis tissue from the same patients before isolation to validate this data. A general review of the slides identifed both XX and XY cells. This fact contradicted previous clinical genetics reports that diagnosed these subjects as non-mosaic Klinefelter 47 XXY. Standard clinical karyotyping usually analyzes no more than 20 cells in peripheral blood smear and cannot rule out organ-specific mosaicism. Although these procedures are beneficial for diagnosing minor defects on the chromosomes constantly present in cells, it lacks the sensitivity to detect small mosaic populations. Further studies are needed to systematically analyze the histology and establish a better quantification method for testicular mosaicism of the KS patient testis, *in vivo*, and its fertility repercussions.

To assess the impact of this finding for future KS fertility treatments, the suitability of KS testis for transplantation should be evaluated. Previous reports by Lue et al. (29) successfully demonstrated SSC transplantation from XY mice into the seminiferous tubules of azoospermic young adult XXY mice. This study suggests that azoospermic KS adult testis, although severely fibrotic, may still retain the basic seminiferous architecture required to perform SSC transplantation. Subsequent studies have shown SSC transplant efficacy in structurally defective seminiferous tubules (53), even without prior germ cell ablation (54) Nevertheless, more studies are needed to confirm that these animal model results are reproducible in humans.

On the other hand, Hirota et al. (45) successfully transplanted primordial iPSC derived germ cell-like cells from XXY mouse fibroblasts into the seminiferous tubules of azoospermic KS mice. Donor XXY SSCs successfully migrated into the basal membrane and restored spermatogenesis. Fertilization and healthy offspring were achieved by ICSI using testicular sperm (45). Our current study suggests that the use of primary human SSCs may provide a better strategy for clinical fertility applications.

Conclusions

To the best of our knowledge, this is the first report of *in vitro* propagation of human SSCs in long-term culture. This study describes the dynamic chromosomal changes in primary testicular cells from KS subjects in culture. This is a critical step forward in utilizing SSC technology to preserve fertility in KS patients.

Data availability statement

The datasets presented in this study can be found in online repositories. The names of the repository/repositories and accession number(s) can be found in the article/supplementary material.

Ethics statement

This study was reviewed and approved by Wake Forest School of Medicine, IRB00021686 and IRB00061265. Written informed consent to participate in this study was provided by the participants' legal guardian/next of kin.

Author Contributions

Conceptualization, GG, SK, CW, RS, YL and HS-A. Methodology, GG, YL and HS-A. Software, GG and HS-A. Validation, GG, MP, WK, YL and HS. Formal analysis, GG,ND, WK, YL and HS-A. Investigation, GG,ND, NZ, YL and HS-A. Resources, GG,YL and HS. Data curation, GG,YL and HS-A. Writing—original draft preparation, GG, YL and HS-A. Writing—review and editing, GG, ND, NZ, MP, SK, CW, RS, WK, SH, AA, YL and HS-A. Visualization, GG,YL and HS-A. Supervision, YL and HS-A. Project administration, HS-A. Funding acquisition, AA, YL and HS-A. All authors contributed to the article and approved the submitted version.

Funding

This work was supported by the Urology Care Foundation Research Scholar Award Program and American Urological Association Southeastern Section. Single cell experiment supported in part by The Lundquist Institute and the UCLA CTSI (ULITR001881-01).

Acknowledgments

We would like to acknowledge Bethy Jackle, Angela Caviness, Martha ward. Kristine Ali, and Brandi Bickford (Wake Forest diagnostic pathology laboratory) for their technical assistance on FISH staining, automotive immunohistochemistry, and virtual microscopy. We acknowledge the use of tissues procured by the National Disease Research Interchange (NDRI) with support from the NIH grant 5 U42 RR006042". We also thank Dr Thomas Shupe for editing the manuscript.

Conflict of interest

The authors declare that the research was conducted in the absence of any commercial or financial relationships that could be construed as a potential conflict of interest.

Publisher's note

All claims expressed in this article are solely those of the authors and do not necessarily represent those of their affiliated organizations, or those of the publisher, the editors and the reviewers. Any product that may be evaluated in this article, or claim that may be made by its manufacturer, is not guaranteed or endorsed by the publisher.

References

1. Bonomi M, Rochira V, Pasquali D, Balercia G, Jannini EA, Ferlin A, et al. Klinefelter syndrome (KS): Genetics, clinical phenotype and hypogonadism. *J Endocrinol Invest* (2017) 40(2):123–34. doi: 10.1007/s40618-016-0541-6

2. Nielsen J, Wohlert M. Sex chromosome abnormalities found among 34,910 newborn children: results from a 13-year incidence study in arhus, Denmark. *Birth Defects Orig Artic Ser* (1990) 26(4):209–23.

3. Bojesen A, Juul S, Gravholt CH. Prenatal and postnatal prevalence of klinefelter syndrome: A national registry study. *J Clin Endocrinol Metab* (2003) 88(2):622–6. doi: 10.1210/jc.2002-021491

4. Aksglaede L, Wikstrom AM, Rajpert-De Meyts E, Dunkel L, Skakkebaek NE, Juul A. Natural history of seminiferous tubule degeneration in klinefelter syndrome. *Hum Reprod Update* (2006) 12(1):39–48. doi: 10.1093/humupd/dmi039

5. Wikstrom AM, Hoei-Hansen CE, Dunkel L, Rajpert-De Meyts E. Immunoexpression of androgen receptor and nine markers of maturation in the testes of adolescent boys with klinefelter syndrome: evidence for degeneration of germ cells at the onset of meiosis. *J Clin Endocrinol Metab* (2007) 92(2):714–9. doi: 10.1210/jc.2006-1892

6. Shiraishi K, Matsuyama H. Klinefelter syndrome: From pediatrics to geriatrics. *Reprod Med Biol* (2019) 18(2):140–50. doi: 10.1002/rmb2.12261

7. Wikstrom AM, Raivio T, Hadziselimovic F, Wikstrom S, Tuuri T, Dunkel L. Klinefelter syndrome in adolescence: onset of puberty is associated with accelerated germ cell depletion. *J Clin Endocrinol Metab* (2004) 89(5):2263–70. doi: 10.1210/jc.2003-031725

8. Groth KA, Skakkebaek A, Host C, Gravholt CH, Bojesen A. Clinical review: Klinefelter syndrome–a clinical update. *J Clin Endocrinol Metab* (2013) 98(1):20–30. doi: 10.1210/jc.2012-2382

9. Lanfranco F, Kamischke A, Zitzmann M, Nieschlag E. Klinefelter's syndrome. *Lancet* (2004) 364(9430):273–83. doi: 10.1016/S0140-6736(04)16678-6

10. Gonsalves J, Turek PJ, Schlegel PN, Hopps CV, Weier JF, Pera RA. Recombination in men with klinefelter syndrome. *Reproduction* (2005) 130(2):223–9. doi: 10.1530/rep.1.00641

11. Vicdan K, Akarsu C, Sozen E, Buluc B, Vicdan A, Yilmaz Y, et al. Outcome of intracytoplasmic sperm injection using fresh and cryopreserved-thawed testicular spermatozoa in 83 azoospermic men with klinefelter syndrome. *J Obstet Gynaecol Res* (2016) 42(11):1558–66. doi: 10.1111/jog.13090

12. Corona G, Pizzocaro A, Lanfranco F, Garolla A, Pelliccione F, Vignozzi L, et al. Sperm recovery and ICSI outcomes in klinefelter syndrome: A systematic review and meta-analysis. *Hum Reprod Update* (2017) 23(3):265–75. doi: 10.1093/humupd/dmx008

13. Van Saen D, Tournaye H, Goossens E. Presence of spermatogonia in 47, XXY men with no spermatozoa recovered after testicular sperm extraction. *Fertil Steril* (2012) 97(2):319–23. doi: 10.1016/j.fertnstert.2011.11.009

14. Deebel NA, Galdon G, Zarandi NP, Stogner-Underwood K, Howards S, Lovato J, et al. Age-related presence of spermatogonia in patients with klinefelter syndrome: A systematic review and meta-analysis. *Hum Reprod Update* (2020) 26 (1):58–72. doi: 10.1093/humupd/dmz038

15. Kubota H, Brinster RL. Spermatogonial stem cells. *Biol Reprod* (2018) 99 (1):52–74. doi: 10.1093/biolre/ioy077

16. Sinha N, Whelan EC, Brinster RL. Isolation, cryopreservation, and transplantation of spermatogonial stem cells. *Methods Mol Biol* (2019) 2005:205–20. doi: 10.1007/978-1-4939-9524-0_14

17. Brinster RL, Zimmermann JW. Spermatogenesis following male germ-cell transplantation. *Proc Natl Acad Sci U S A* (1994) 91(24):11298–302. doi: 10.1073/pnas.91.24.11298

18. Joerg H, Janett F, Schlatt S, Mueller S, Graphodatskaya D, Suwattana D, et al. Germ cell transplantation in an azoospermic klinefelter bull. *Biol Reprod* (2003) 69 (6):1940–4. doi: 10.1095/biolreprod.103.020297

19. Hermann BP, Sukhwani M, Winkler F, Pascarella JN, Peters KA, Sheng Y, et al. Spermatogonial stem cell transplantation into rhesus testes regenerates spermatogenesis producing functional sperm. *Cell Stem Cell* (2012) 11(5):715–26. doi: 10.1016/j.stem.2012.07.017

20. Harkey MA, Asano A, Zoulas ME, Torok-Storb B, Nagashima J, Travis A. Isolation, genetic manipulation, and transplantation of canine spermatogonial stem cells: progress toward transgenesis through the male germ-line. *Reproduction* (2013) 146(1):75–90. doi: 10.1530/REP-13-0086

21. Shetty G, Mitchell JM, Meyer JM, Wu Z, Lam TNA, Phan TT, et al. Restoration of functional sperm production in irradiated pubertal rhesus monkeys by spermatogonial stem cell transplantation. *Andrology* (2020) 8(5):1428–41. doi: 10.1111/andr.12807

22. Shetty G, Mitchell JM, Lam TNA, Phan TT, Zhang J, Tailor RC, et al. Postpubertal spermatogonial stem cell transplantation restores functional sperm production in rhesus monkeys irradiated before and after puberty. *Andrology* (2021) 9(5):1603–16. doi: 10.1111/andr.13033

23. Sadri-Ardekani H, Atala A. Testicular tissue cryopreservation and spermatogonial stem cell transplantation to restore fertility: From bench to bedside. *Stem Cell Res Ther* (2014) 5(3):68. doi: 10.1186/scrt457

24. Gies I, Oates R, De Schepper J, Tournaye H. Testicular biopsy and cryopreservation for fertility preservation of prepubertal boys with klinefelter syndrome: a pro/con debate. *Fertil Steril* (2016) 105(2):249–55. doi: 10.1016/j.fertnstert.2015.12.011

25. Gies I, Tournaye H, De Schepper J. Attitudes of parents of klinefelter boys and pediatricians towards neonatal screening and fertility preservation techniques in klinefelter syndrome. *Eur J Pediatr* (2016) 175(3):399–404. doi: 10.1007/s00431-015-2657-7

26. Sadri-Ardekani H, McLean TW, Kogan S, Sirintrapun J, Crowell K, Yousif MQ, et al. Experimental testicular tissue banking to generate spermatogenesis in the future: A multidisciplinary team approach. *Methods* (2016) 99:120–7. doi: 10.1016/j.ymeth.2016.02.013

27. Lue Y, Rao PN, Sinha Hikim AP, Im M, Salameh WA, Yen PH, et al. XXY male mice: an experimental model for klinefelter syndrome. *Endocrinology* (2001) 142(4):1461–70. doi: 10.1210/endo.142.4.8086

28. Lue Y, Jentsch JD, Wang C, Rao PN, Hikim AP, Salameh W, et al. XXY mice exhibit gonadal and behavioral phenotypes similar to klinefelter syndrome. *Endocrinology* (2005) 146(9):4148–54. doi: 10.1210/en.2005-0278

29. Lue Y, Liu PY, Erkkila K, Ma K, Schwarcz M, Wang C, et al. Transplanted XY germ cells produce spermatozoa in testes of XXY mice. *Int J Androl* (2010) 33(4):581–7. doi: 10.1111/j.1365-2605.2009.00979.x

30. Galdon G, Deebel NA, Zarandi NP, Pettenati MJ, Kogan S, Wang C, et al. *In vitro* propagation of XXY undifferentiated mouse spermatogonia: Model for fertility preservation in klinefelter syndrome patients. *Int J Mol Sci* (2021) 23 (1):173. doi: 10.3390/ijms23010173

31. Zarandi NP, Galdon G, Kogan S, Atala A, Sadri-Ardekani H. Cryostorage of immature and mature human testis tissue to preserve spermatogonial stem cells (SSCs): a systematic review of current experiences toward clinical applications. *Stem Cells Cloning Adv Appl* (2018) 11:23–38. doi: 10.2147/SCCAA.S137873

32. Sadri-Ardekani H, Akhondi MA, van der Veen F, Repping S, van Pelt AM. *In vitro* propagation of human prepubertal spermatogonial stem cells. *JAMA* (2011) 305(23):2416–8. doi: 10.1001/jama.2011.791

33. Sadri-Ardekani H, Mizrak SC, van Daalen SK, Korver CM, Roepers-Gajadien HL, Koruji M, et al. Propagation of human spermatogonial stem cells in vitro. *JAMA* (2009) 302(19):2127–34. doi: 10.1001/jama.2009.1689

34. Taylor SC, Nadeau K, Abbasi M, Lachance C, Nguyen M, Fenrich J. The ultimate qPCR experiment: Producing publication quality, reproducible data the first time. *Trends Biotechnol* (2019) 37(7):761–74. doi: 10.1016/j.tibtech.2018.12.002

35. Fehse B, Badbaran A, Berger C, Sonntag T, Riecken K, Geffken M, et al. Digital PCR assays for precise quantification of CD19-CAR-T cells after treatment with axicabtagene ciloleucel. *Mol Ther Methods Clin Dev* (2020) 16:172–8. doi: 10.1095/biolreprod.112.098913

36. Nykel A, Woźniak R, Gach A. Clinical validation of novel chip-based digital PCR platform for fetal aneuploidies screening. *Diagn Basel Switz* (2021) 11(7):1131. doi: 10.3390/diagnostics11071131

37. Nickkholgh B, Mizrak SC, Korver CM, van Daalen SK, Meissner A, Repping S, et al. Enrichment of spermatogonial stem cells from long-term cultured human testicular cells. *Fertil Steril* (2014) 102(2):558–565.e5. doi: 10.1016/j.fertnstert.2014.04.022

38. Zohni K, Zhang X, Tan SL, Chan P, Nagano M. CD9 is expressed on human male germ cells that have a long-term repopulation potential after transplantation into mouse testes. *Biol Reprod* (2012) 87(2):27.

39. Guo Y, Hai Y, Gong Y, Li Z, He Z. Characterization, isolation, and culture of mouse and human spermatogonial stem cells. *J Cell Physiol* (2014) 229(4):407–13. doi: 10.1002/jcp.24471

40. Harichandan A, Sivasubramaniyan K, Hennenlotter J, Poths S, Bedke J, Kruck S, et al. Molecular signatures of primary human spermatogonial progenitors and its neighboring peritubular stromal compartment. *Stem Cells Dev* (2017) 26 (4):263–73. doi: 10.1089/scd.2016.0042

41. Hutter H, Dohr G. HLA expression on immature and mature human germ cells. *J Reprod Immunol* (1998) 38(2):101–22. doi: 10.1016/S0165-0378(98)00032-1

42. Butler A, Hoffman P, Smibert P, Papalexi E, Satija R. Integrating single-cell transcriptomic data across different conditions, technologies, and species. *Nat Biotechnol* (2018) 36(5):411–20. doi: 10.1038/nbt.4096

43. Satija R, Farrell JA, Gennert D, Schier AF, Regev A. Spatial reconstruction of single-cell gene expression data. *Nat Biotechnol* (2015) 33(5):495–502. doi: 10.1038/nbt.3192

44. Stuart T, Butler A, Hoffman P, Hafemeister C, Papalexi E, Mauck WM, et al. Comprehensive integration of single-cell data. *Cell* (2019) 177(7):1888–902. doi: 10.1016/j.celrep.2018.10.026

45. Hirota T, Ohta H, Powell BE, Mahadevaiah SK, Ojarikre OA, Saitou M, et al. Fertile offspring from sterile sex chromosome trisomic mice. *Science* (2017) 357 (6354):932–5. doi: 10.1126/science.aam9046

46. Sohni A, Tan K, Song HW, Burow D, de Rooij DG, Laurent L, et al. The neonatal and adult human testis defined at the single-cell level. *Cell Rep* (2019) 26 (6):1501–17. doi: 10.1016/j.celrep.2019.01.045

47. Hermann BP, Cheng K, Singh A, Roa-De La Cruz L, Mutoji KN, Chen IC, et al. The mammalian spermatogenesis single-cell transcriptome, from spermatogonial stem cells to spermatids. *Cell Rep* (2018) 25(6):1650–67. doi: 10.1016/j.celrep.2018.10.026

48. Di Persio S, Tekath T, Siebert-Kuss LM, Cremers JF, Wistuba J, Li X, et al. Single-cell RNA-seq unravels alterations of the human spermatogonial stem cell compartment in patients with impaired spermatogenesis. *Cell Rep Med* (2021) 2 (9):100395. doi: 10.1016/j.xcrm.2021.100395

49. Fiorentino F, Biricik A, Bono S, Spizzichino L, Cotroneo E, Cottone G, et al. Development and validation of a next-generation sequencing-based protocol for 24-chromosome aneuploidy screening of embryos. *Fertil Steril* (2014) 101(5):1375–82. doi: 10.1016/j.fertnstert.2014.01.051

50. Pendergraft SS, Sadri-Ardekani H, Atala A, Bishop CE. Three-dimensional testicular organoid: A novel tool for the study of human spermatogenesis and gonadotoxicity *in vitro*. *Biol Reprod* (2017) 96(3):720–32. doi: 10.1095/biolreprod.116.143446

51. Guo J, Grow EJ, Mlcochova H, Maher GJ, Lindskog C, Nie X, et al. The adult human testis transcriptional cell atlas. *Cell Res* (2018) 28(12):1141–57. doi: 10.1038/s41422-018-0099-2

52. Robertson EJ, Evans MJ, Kaufman MH. X-Chromosome instability in pluripotential stem cell lines derived from parthenogenetic embryos. *J Embryol Exp Morphol* (1983) 74:297–309. doi: 10.1242/dev.74.1.297

53. Kanatsu-Shinohara M, Ogonuki N, Matoba S, Ogura A, Shinohara T. Autologous transplantation of spermatogonial stem cells restores fertility in congenitally infertile mice. *Proc Natl Acad Sci U S A* (2020) 117(14):7837–44. doi: 10.1073/pnas.1914963117

54. Morimoto H, Ogonuki N, Kanatsu-Shinohara M, Matoba S, Ogura A, Shinohara T. Spermatogonial stem cell transplantation into nonablated mouse recipient testes. *Stem Cell Rep* (2021) 16(7):1832–44. doi: 10.1016/j.stemcr.2021.05.013

Frontiers in Endocrinology

Explores the endocrine system to find new therapies for key health issues

The second most-cited endocrinology and metabolism journal, which advances our understanding of the endocrine system. It uncovers new therapies for prevalent health issues such as obesity, diabetes, reproduction, and aging.

Discover the latest Research Topics

See more →

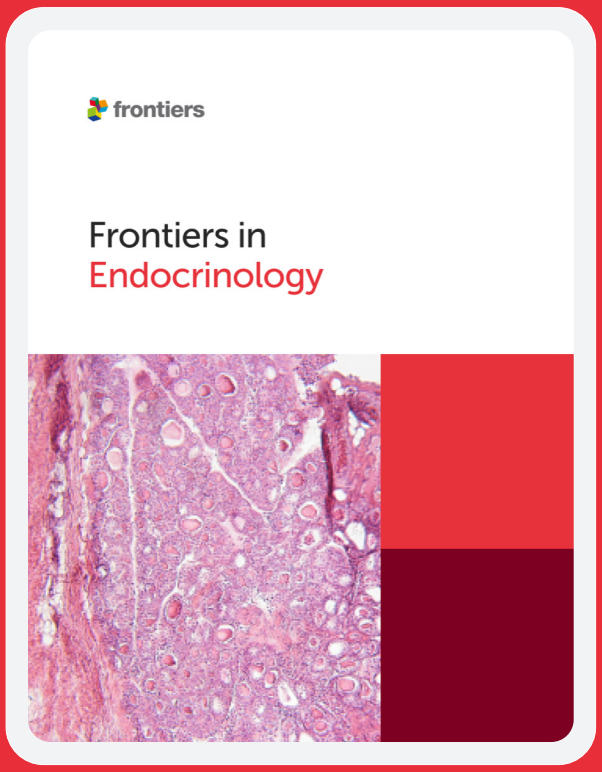

Frontiers

Avenue du Tribunal-Fédéral 34
1005 Lausanne, Switzerland
frontiersin.org

Contact us

+41 (0)21 510 17 00
frontiersin.org/about/contact